Flood Analysis

in the Wei River Basin, China

Lingtong Gai

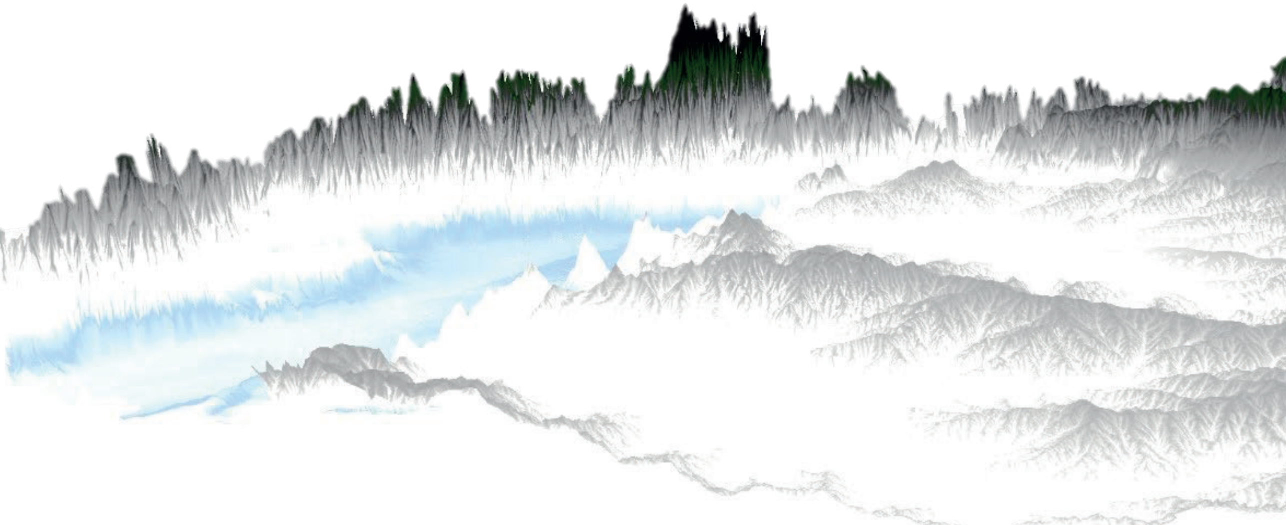

PROPOSITIONS

1. Due to the dynamics of the anthroposphere, past discharge patterns and flood events cannot be extrapolated to the future.
   (this thesis)

2. Contrary to common practice, most regional climate model projections are not accurate enough for modelling flood discharge.
   (this thesis)

3. Dissemination of scientific knowledge should be a criterion to evaluate the performance of a scientist.

4. People working with "Big data" should focus more on data quality instead of only data quantity.

5. Non-experts talk about yes or no, while experts talk about trends and possibilities.

6. Both started from passion, the honesty, the traits and communication determine how far your PhD and your relationship goes.

Propositions belonging to the thesis, entitled:

"Flood analysis in the Wei River Basin, China"

Lingtong Gai

Wageningen, 3rd July 2019

Flood analysis in the Wei River Basin, China

Lingtong Gai

Thesis committee

Promotors
Prof. Dr C.J. Ritsema
Professor of Soil Physics and Land Management
Wageningen University & Research

Prof. Dr V. Geissen
Personal chair at the Soil Physics and Land Management
Wageningen University & Research

Co-promotors
Dr J. P. C. Nunes
Assistant Researcher at Faculty of Sciences
University of Lisbon

Dr J. E.M. Baartman
Assistant Professor of Soil Physics and Land Management
Wageningen University & Research

Other members
Prof. Dr C. Kroeze, Wageningen University & Research
Dr. R. van Beek, University of Utrecht, Utrecht, The Netherlands
Dr. Z. Bai, ISRIC, Wageningen, The Netherlands
Dr. J. Mendes de Jesus, Geocat, Bennekom, The Netherlands

This research was conducted under the auspices of the Research School for Socio-Economic and Natural Sciences of the Environment (SENSE)

Flood analysis in the Wei River Basin, China

Lingtong Gai

Thesis
submitted in fulfilment of the requirements for the degree of doctor
at Wageningen University
by the authority of the Rector Magnificus
Prof. Dr A.P.J. Mol
in the presence of the
Thesis Committee appointed by the Academic Board
to be defended in public
on Wednesday 03 July 2019
at time 1.30 p.m. in the Aula.

Lingtong Gai
Flood analysis in the Wei River Basin, China, 168 pages.

PhD thesis, Wageningen University, Wageningen, the Netherlands (2019)
With references, with summaries in English and Dutch

ISBN: 978-94-6343-986-2
DOI: https://doi.org/10.18174/477522

Table of contents

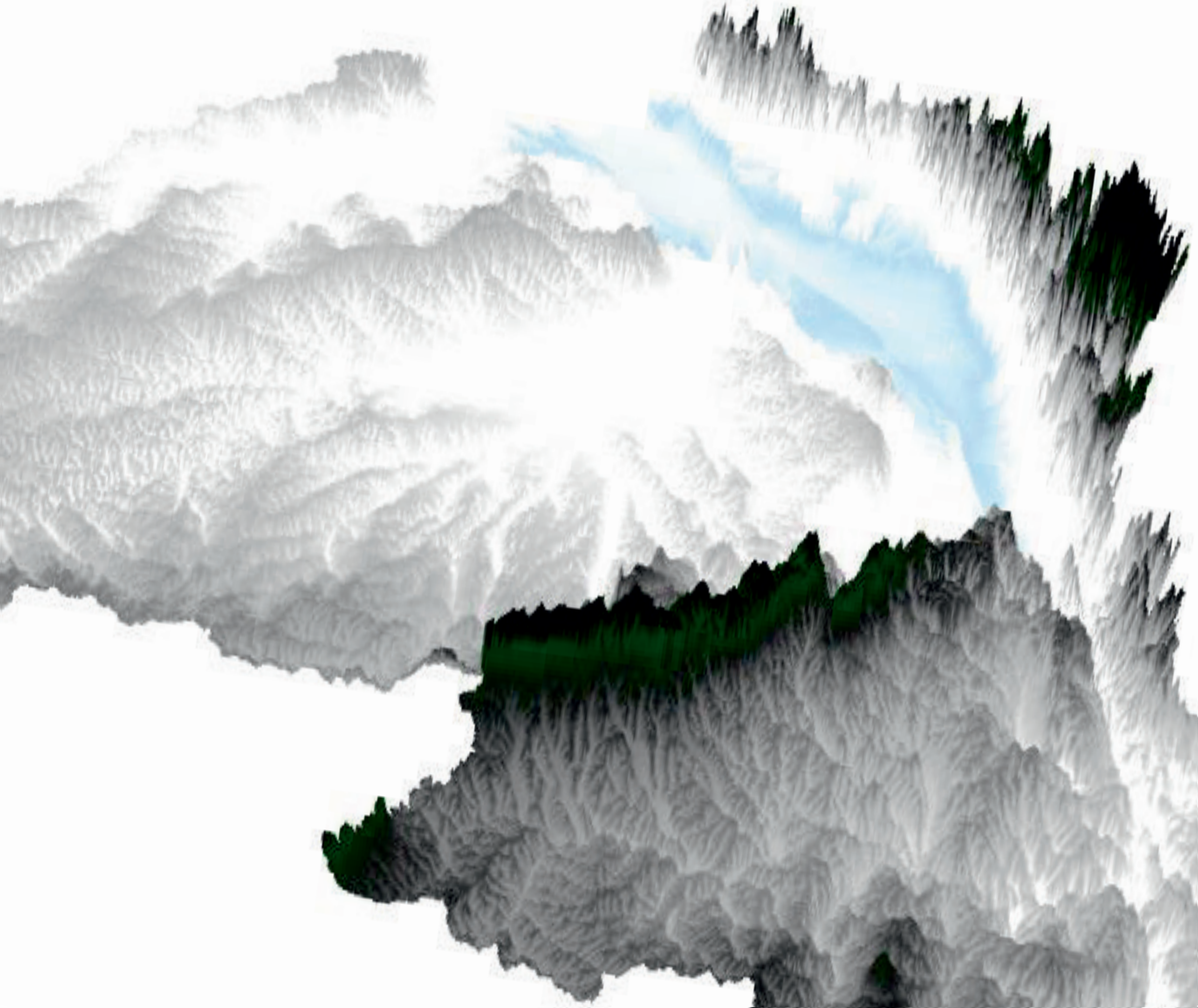

1. General introduction

1.1 General Introduction

1.1.1 Floods

Floods are recognized among Earth's most common and destructive natural hazards (Hirabayashi et al., 2013; Winsemius et al., 2015). A flood is defined as a large amount of water that overflows onto normally dry land (Merriam-Webster dictionary). Depending on the location and triggers of the flood occurrence, there is the distinction among coastal floods, flash floods and river floods (Berz et al., 2001; Jonkman, 2005; Kron, 2005). Coastal floods are usually led by strong tides and winds from the sea or big lakes, occasionally triggered by earthquakes in the ocean (Blöschl et al., 2015). Flash floods can be initiated by excessive rainfall, dam breach or glacier lake outburst that generally happens in relatively small areas (Hapuarachchi et al., 2011). A river flood, however, can involve multiple factors, occur in small or big catchments, and evolve more slowly than e.g. flash floods (Blöschl et al., 2015; Kron, 2005). This thesis focus on better understanding of typical river floods.

Three types of factors influence flood occurrence: meteorological factors, biophysical factors and anthropogenic factors. Meteorological conditions might cause intensive rainfall, leading to surface runoff, which can be partially offset by evaporation depending on the temperature, wind and solar radiation conditions (Beven, 2012; Lindsey and Farnsworth, 1997; Nkemdirim, 1991). Biophysical factors, such as elevation, slope, vegetation and soil conditions will determine whether intensive rainfall and runoff will result in the development of a flood. Soil saturation and high intensity rainfall enhance runoff and flood development (Brocca et al., 2008; Chifflard et al., 2018; Saini et al., 2016). Channel formation of the flood plain and sedimentation-induced river bed elevation can also cause floodings (Chen et al., 2016; Reisenbüchler et al., 2019; Wyzga, 2001). Anthropogenic factors like expansion of built-up areas and increasing arable land at the expense of nature reserves and forested areas impact the hydrological processes in watersheds distinctly, often increasing risks and frequency of floods at the end (BRADSHAW et al., 2007; Brown et al., 2013; de la Paix et al., 2013; Kavian et al., 2014; Khaleghi, 2017; Du et al., 2015; Hsu et al., 2015; Khaleghi, 2017).

In addition, flood magnitude and frequency are also influenced by climate change (Arnell and Gosling, 2016; Eisner et al., 2017), and impacts might differ geographically (Alfieri et al., 2017; Best, 2019; Braatne et al., 2008; Milly et al., 2008; Shaw et al., 2014; Winsemius et al., 2015). Furthermore, efforts have been undertaken to regulate and optimize river system functioning by implementation all kinds of related infrastructure, like dams, reservoirs, water withdrawal and transfer systems and diking. Especially the construction of large dams dramatically alters the hydrological, morphological and ecological conditions of watersheds, like what happened for instance in the Yellow River basin in China (Best, 2019; Kong et al., 2017; Wang et al., 2015). It is widely admitted that China, which is much affected by floods due to monsoon rains and snowmelt, faces large amounts of river flooding every year and is extremely vulnerable (WWAP, 2006 Zhang et al., 2018; IPCC, 2013; Ni et al., 2010). Around 50% of the population and 70% of the properties are threatened by flooding in the country (Chen et al., 2003). The 1998 and 1996 floods caused about 30 and 26 billion US$ losses, respectively, ranking these two floods as the largest and most damaging ever in the history of the world (Jiang et al., 2008). Therefore, it is of vital importance to better understand the river hydrological regime, in particular in relation to flood development and management.

1.1.2 Methods to assess flooding

Large efforts have been made globally to understand flood occurrence with the ultimate goal of an effective flood forecasting and warning scheme to protect our assets and lives. The first effort to predict the peak discharge of a river can be traced back to around 150 years ago with the development of the Rational Method (Beven, 2012). Since then, hydrologists have continued in their efforts to understand the principals, interactions and functioning of complex river systems and related flooding events. In particular, statistical and modelling techniques have been used to unravel and simulate flooding events. The statistical approach usually refers to flood frequency analysis based on different distribution functions and intensity-duration-frequency curves constructed from hydrological or meteorological data (Ewea et al., 2017; Javelle et al., 2002; Khelfi et al., 2017; Mantegna et al., 2017; Requena et al., 2016; Saad et al., 2015; Wang et al., 2017; Xu et al., 2015; Zhang and Singh, 2006; Zhang et al., 2013). However, it is not always possible to apply such distribution functions for frequency analysis in many regions directly due to data scarcity and the non-linearity between meteorological characteristics and hydrological responses.

In general, modelling approaches aim to generate discharge time-series, ranging from minutes for event-based simulation to years for water resources analysis. The first hydrological model was introduced by Thornthwaite and Mather (1955) with the purpose to simulate the overall water balance. Nowadays, hydrological modelling is capable of simulating interactive processes including but not limited to infiltration, interception, snow melting, groundwater recharge, soil moisture redistribution, channel routing and others. One of the first semi-distributed hydrological models was developed by Beven and Kirky (1979), nowadays capable to simulate soil moisture dynamics (Peng et al., 2016). The Swedish Hydrologiska Byrans Vattenbalansmodel (HBV) model is a distributed model with applications to simulate the water balance and assess effects of climate change (Beldring et al., 2003; Beldring et al., 2008; Lindström et al., 1997), however lacking a component to simulate impacts of human activities. The Soil and Water Assessment Tool (SWAT) has been used widely around the world, as it is able to simulate impacts of soil and water conservation measures on discharge (Ahn et al., 2015; Arnold et al., 1998; Awotwi et al., 2015; Bieger et al., 2012; Cheng et al., 2016; Neupane et al., 2015). The Variable Infiltration Capacity (VIC) model is a distributed model for macro-scale hydrological processes simulation, however not yet taking into account human water use, or reservoirs (Bierkens, 2015; Liang et al., 1994; Lohmann et al., 1998; Zhang et al., 2014). The LISFLOOD model, on the other hand, integrates processes included in all the previous models with the special purpose to be applied in large and trans-national catchments for assessing the impacts of river regulation measures, land use change and climate change on flood discharge (Burek et al., 2013; De Roo et al., 2001; van der Knijff et al., 2010). The application of a hydrological model is to generate the discharge time-series in a watershed to provide intial conditions of a flood analysis. With the discharge time-series, the quantity of the peak discharge as well as the return peiod of a certain destrcutive discharge can be calculated for flood occurrence prediction (Abdulkareem et al., 2018). Therefore, in this study, the LISFLOOD model was chosen to be applied because of its ability to take into consideration human interventions on the water cycle in large river catchments.

1.2 Wei River Basin, China

The study area of this thesis, the Wei River Basin (138,000 km^2, 103–111˚E, 33–38˚N), is located on the Loess Plateau in the centre of China (Fig. 1.1). The Wei River is the largest tributary of the Yellow River, which is the second largest river in China and the sixth in the world. The Yellow River is well known for its high quantities of sediment transport and deposition in the river channel as it incise through one of the world's largest loess deposit region: The Loess Plateau in China. The Wei River catchment covers three provinces: Gansu Province (44.1%), Ningxia Province (6.1%) and Shaanxi Province (49.8%), with 84 counties and around 33 million inhabitants and is a major region for agriculture, industry and commerce in north-western China. Originated in Weiyuan County in Gansu Province, the Wei River flows East through the Loess Plateau into the Yellow River at Tongguan City in Shaanxi Province with a total length of 818 km.

The main stream of the Wei River divides the basin into two distinctive parts. The southern part of the basin is characterized by steep slopes and an earth-rock mountain landscape due to the Qinling Mountain range. The geology of the mountainous area varies from granitic to metamorphic bedrock type. The northern part of the basin form part of the Loess Plateau with gentler slopes. Channels and caves have formed in the thick, highly erodible loess deposits. The largest two tributaries of the Wei River - Jing River and Beiluo River – are located on the northern side of the Wei River and comprise 34% and 20% of the total catchment area of the Wei River Basin, respectively. The Guanzhong Plain, of which part is the floodplain of the Wei River, starts from Baoji City all the way East to the outlet of the Wei River which is Tongguan City. The land use in the catchments is mainly farmland and grassland. The “Grain for Green” project was conducted in 1999 in the Loess Plateau (Deng et al., 2014), which resulted in an increase of the forest area from 4.8% to 14.4% in the year 2005 compared to 1980. Residential areas contributed only 0.8% to the total catchment area in the 1980s, but had increased to 2.2% by 1996. This change in residential area is negligible compared to that of other land-use types, but the increase within a time span of 10 years is significant. In the Wei River basin, 302 large/medium-sized reservoirs and dams with total storage capacities of 2.73 km^3 were constructed for floods mitigation, irrigation and water supply purposes (Su et al., 2007).

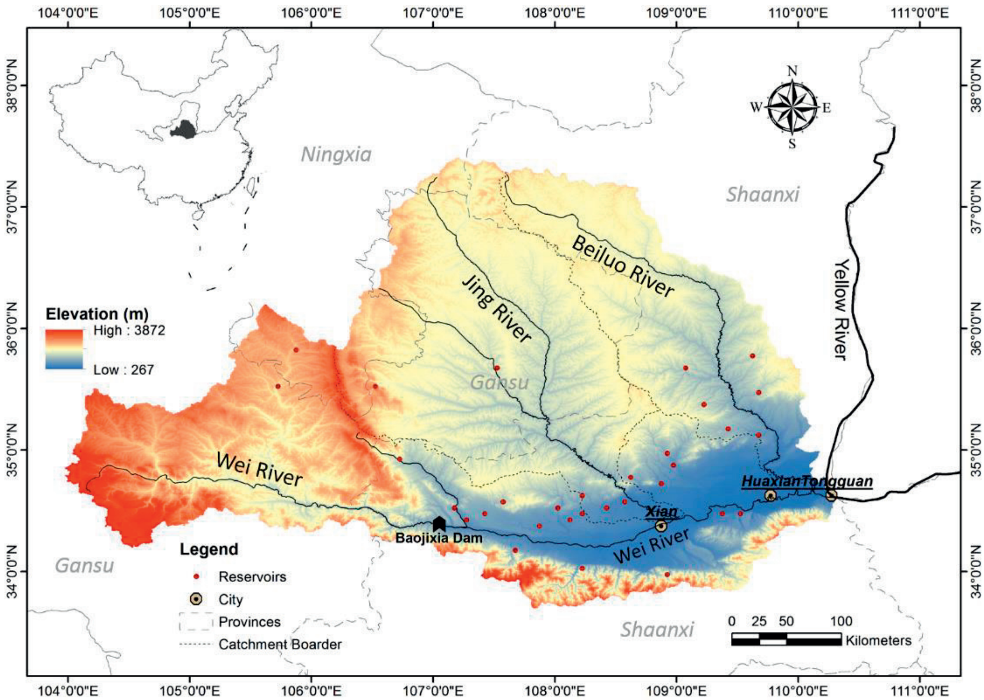

Figure 1.1 *Study area Wei River Basin.*

Like other regions in China, the Wei River Basin is controlled by the continental monsoon, which brings an average annual precipitation of approximately 570 mm. Precipitation is concentrated on the South Bank of the basin in the Qinling Mountains, with an average annual precipitation of 800 mm. A yearly average of 540 mm falls North of the river. Wei River Basin has suffered from the effects of flooding through many years, threatening both the livelihood and fragile environment of the region, particularly in the areas of the downstream floodplain (Jiang et al., 2004; Liang, 2006; Pang, 2007b; Tao and Dang, 2011; Tian et al., 2010; Xing et al., 2004; Zhao et al., 2010). Between 1950 and 2005, more than 60 floods occurred in the Wei river catchment, causing destruction of direct properties costing 17.1 billion RMBs (about 2.75 billion US Dollars) affecting a total population of 70.67 million, a death toll of 5300 people and inundation of 9.68 million ha of agriculture areas (Yan, 2008). Besides the pressure of climate change, with the rapid growth of the economy, the concomitant increase of the population density, the rapid development of urbanization and infrastructure, Wei River is becoming more vulnerable to flood hazards (Liu et al., 2013; Wohlfart et al., 2016). Better understanding of flood occurrence and dynamics is required to improve flood management and to reduce the damage of flooding. Within the Wei River, most studies focused on analysing and obtaining the flood characteristics of the basin based on individual historical events (Huo et al., 2004; Jiang et al., 2004; Liang, 2006; Pang, 2007a; Tao and Dang, 2011; Wang et al., 2007; Xing et al., 2004; Yin et al., 2010); while some other studies focussed more on palaeo-floods and floods detected by sediment analysis (Zha et al., 2007; Zha et al., 2009; Wan et al., 2010; Huang et al., 2012). Seasonal and monthly streamflow have also been studied for the Wei River Basin (Chang et al., 2015; Gao et al., 2013; Li et al., 2007; Peng et al., 2014; Shao et al., 2013; Wei and Zhang, 2010; Zhao et al., 2013). However, the flood regime has not yet been studied in relation and connection to deployed human activities in the basin, like construction of dams and water transfer pathways.

1.3 Research objectives

This PhD thesis aims at improving and advancing scientific understanding of flooding under the pressure of climate change and human intervention in the Wei River Basin in China. From this respect, it is important to account for spatio-temporal dynamics and related effects across the watershed. A comprehensive study to understand the flood regime of the basin will therefore help to develop future flood management and related sustainable use of land and water resources in the region.

The following research objectives will be addressed:

1. Investigate past catchment flooding that has caused inundation on the floodplain of the Wei River Basin.
2. Calibrate and validate the LISFLOOD model for flood discharge simulation in the Wei River Basin.
3. Evaluate the feasibility to use globally freely available meteorological datasets as input for the LISFLOOD model to simulate flood discharge in the Wei River Basin.

4. Execute an analysis to assess impacts of different water management and land use scenarios on the flood regime of the Wei River Basin.

Fig. 1.1 shows an overview of the outlined research steps taken in this thesis to address the research objectives. This thesis combines large-scale data collection, factor analysis and modelling to achieve the research objectives as presented in the different research chapters.

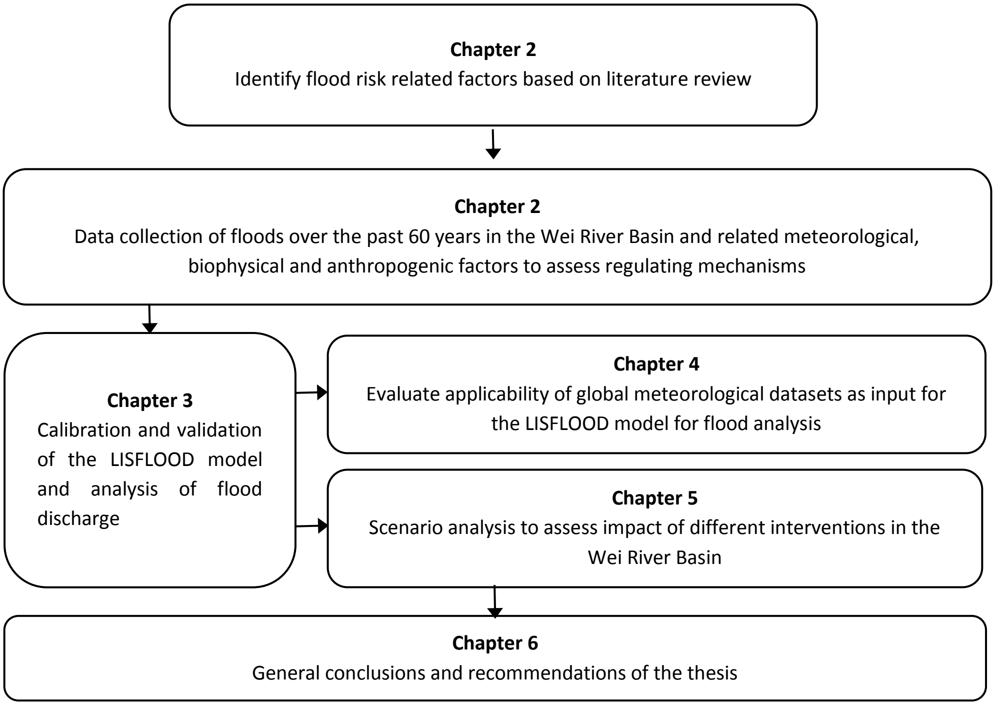

Figure 1.1 *Schematic structure of research activities and objectives of the thesis.*

1.4 LISFLOOD model

The LISFLOOD model is a physically-based rainfall-runoff model, specifically developed for flood simulation in large and transnational catchments. So far, the model has been used for flood forecasting, assessing the effects of river regulation measures, assessing the effects of land-use change, and assessing the effects of climate change (Dankers et al., 2007; De Roo et al., 2001; Mo et al., 2005; Revilla-Romero et al. 2015; Siqueira et al., 2018).

The model is grid-based and designed to be applied across a wide range of spatial resolutions varying from 100 metres for medium sized catchments up to 0.1° for modelling global water resources. The detailed processes included in the most recent version of the LISFLOOD model are snow melt, infiltration, interception of rainfall, leaf drainage, evaporation and water uptake by vegetation, surface runoff, preferential flow, exchange of soil moisture between the two soil layers and drainage to the groundwater, sub-surface and groundwater flow, and flow through river channels, as shown in Fig. 1.2 .

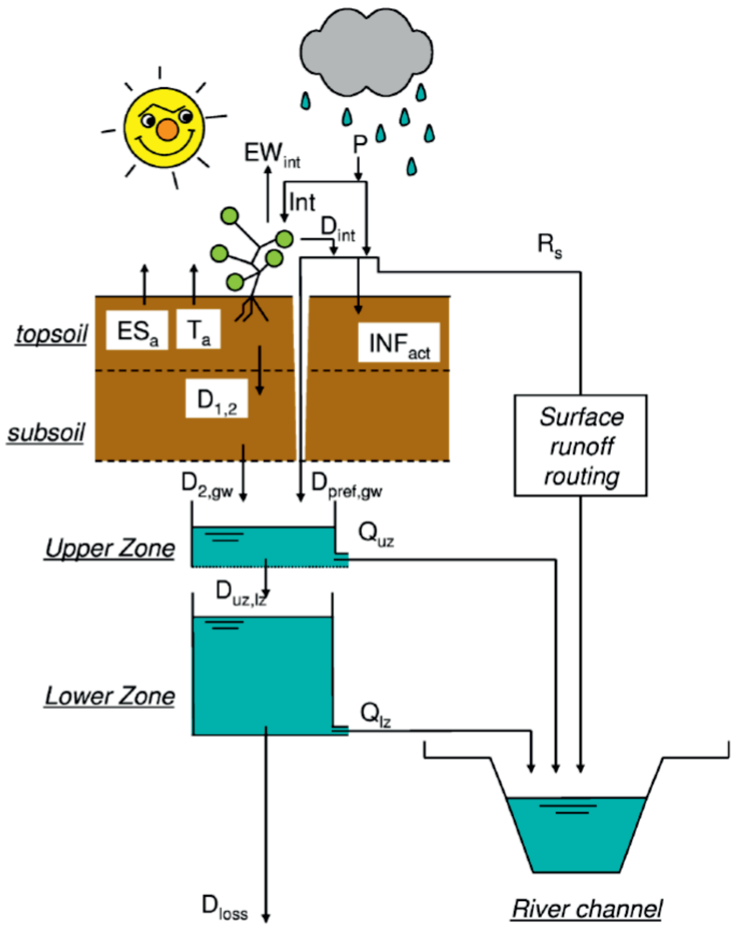

Figure 1.2 *Overview of the LISFLOOD model. P = precipitation; Int = interception;* EW_{int} *= evaporation of intercepted water;* D_{int} *= leaf drainage;* ES_a *= evaporation from soil surface;* T_a *= transpiration (water uptake by plant roots);* INF_{act} *= infiltration;* R_s *= surface runoff;* $D_{1,2}$ *= drainage from top- to subsoil;* $D_{2,gw}$ *= drainage from subsoil to upper groundwater zone;* $D_{pref,gw}$ *= preferential flow to upper groundwater zone;* $D_{uz,lz}$ *= drainage from upper- to lower groundwater zone;* Q_{uz} *= outflow from upper groundwater zone;* Q_l *= outflow from lower groundwater zone;* D_{loss} *= loss from lower groundwater zone. (Burek et al., 2013)*

The LISFLOOD model is basically composed of the following four elements:

- A 2-layer soil water balance sub-model

- Sub-models for the simulation of groudwater and subsurface flow (using 2 parallel interconnected linear reservoirs)
- A sub-model for the routing of surface runoff to the nearest river channel
- A sub-model for the routing of channel flow.

1.5 Thesis outline

This thesis comprises 6 chapters in total. Chapter 1 provides a general introduction on flooding events, details of the study region, the research objectives, and information on the LISFLOOD model used in this study.

Chapter 2 analyses the characteristics of floods in the Wei River Basin over the last 60 years to understand the impacts of various factors on flooding and discharge using a new framework approach that is capable of analysing the multitude of potentially contributing factors on the flood events over multiple years.

Chapter 3 assesses the possibility to calibrate and validate the LISFLOOD model for flood discharge simulation in several sub-basins as well as the main outlet of the river using observed meteorological data.

Chapter 4 investigates the feasibility of using global freely available meteorological datasets as input for the LISFLOOD model to simulate flood discharge in the Wei River Basin.

Chapter 5 evaluates the impact of different scenarios on flood discharge of the Wei River Basin.

At last, Chapter 6 summarizes the general conclusions of this thesis, discusses the implications of the research, and provides recommendations for scientists and policy makers.

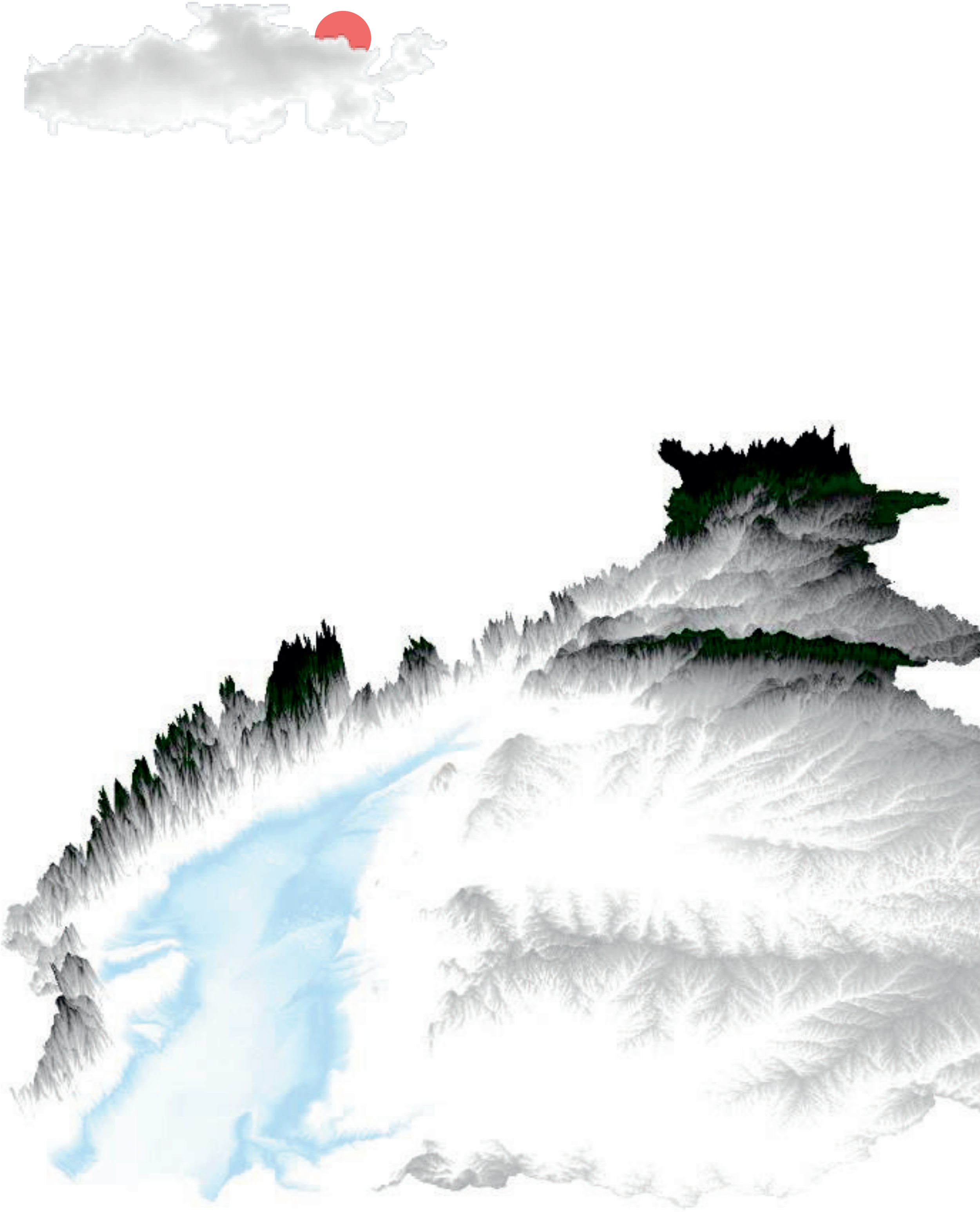

2. A framework approach for unravelling the impact of multiple factors influencing flooding

To achieve a better understanding of the influence of biophysical, climatic and especially anthropogenic factors on hydrological discharge and flooding, this study proposes a new framework approach using a set of methods to answer the questions why, where, when, and how flooding occurs. Including conditional inference tree (CIT), cross correlation and double mass curves analysis, the approach is demonstrated in an application to the Wei River Basin, China. From the CIT analysis, dam construction period was identified as the most important factor (why), and the subcatchment farthest upstream contributed the most to the flooding of the downstream floodplain (where). We then analysed the effect of the periods of dam construction on the time lag change (when) and the precipitation-discharge relationship (how) using cross-correlation analysis and double mass curves analysis, respectively. The results suggested that the dam construction delayed the precipitation for 0.4 days on average compared to before the dam construction period, and the discharge at the outlet of the basin was reduced by around 44%. This framework approach is promising as it can quantitatively evaluate the importance of multiple factors on multiple years of flooding, while many studies evaluate single flooding events only.

Based on:

L. Gai, J.E.M. Baartman, M. Mendoza-Carranza, F. Wang, C.J. Ritsema, V. Geissen. 2018. A framework approach for unravelling the impact of multiple factors influencing flooding. Journal of Flood Risk Management, 11 (2), 111-126.

2.1 Introduction

Flood hazard has become a growing concern due to an increasing number of extreme meteorological events and human intervention in the hydrological cycle (IPCC 2013). Studies of the causes and characteristics of different kinds of floods, ranging from coastal regions, urban areas, and large river catchments to flash floods have been undertaken worldwide (Cançado et al., 2008; Islam and Sado, 2000; Thumerer et al., 2000). The assessment of flood risk on different scales has also been studied worldwide (Delgado et al., 2010; Gao et al., 2007; Islam and Sado, 2000; Mohamed Elmoustafa, 2012). Studies of palaeofloods have suggested that extreme floods are usually associated with unique atmospheric patterns (Huang et al., 2007; Li et al., 2014). The interaction between precipitation and stream flow has thus been the main focus for flood prediction and studies of risk assessment (Huang et al., 2015a,b; Peng et al., 2014). These and other studies worldwide have concluded that the causes of flooding can be categorised into three groups: i) Biophysical factors; ii) Meteorological factors, and iii) Anthropogenic factors. A comprehensive and accurate evaluation of flood analysis requires knowledge of the factors that have triggered a flood and how these indicators influence the flood discharge.

Precipitation has a direct impact on flooding, and the biophysical condition of catchments has an influence on the spatial distribution of soil moisture and thus evapotranspiration and surface and subsurface runoff (Berger and Entekhabi, 2001; Wilson et al., 2005; Hardie et al., 2011; Neupane et al., 2015; Peng et al., 2015). The stationary theory of flood risk on a fluvial system has been challenged due to the effect of sediment deposition and the influence of water infrastructure, channel modifications, and changes in land cover and use (Plate, 2002; Milly et al., 2008). The diversion of water, construction of reservoirs, and even the installation of small dams can dramatically alter the hydrological characteristics of a drainage basin (Braatne, et al. 2008; Shaw et al., 2014). Gao et al. (2010) have identified water diversions for irrigation and urban and industrial use, measures of soil and water conservation, and the construction of water-control projects as some of the human interventions that led to the trend of decreasing discharge in the Yellow River. The construction of the Sanmenxia Dam on the Yellow River was the most influential project. The dam has changed the processes and morphology of the Wei River (Wang et al., 2007) because the outlet of the Wei River is controlled by the elevation and discharge of the Yellow River. The Sanmenxia Dam has increased sediment deposition in both rivers, and the raised bed of the Wei River has reduced the drainage capacity of the river and has even led to water drawback. The number of floods has thus increased since the construction of this dam.

Urbanisation decreases the cover of vegetation and increases direct runoff, which increases discharge. Urbanisation also decreases the time lag between the effective precipitation and peak discharge (Islam and Sado, 2000; Wen Liu et al. 2014). The large Grain to Green project implemented in 1999 is an example of land-use change in which farmers are compensated for converting cultivated areas to green land (Jian et al., 2015). Urbanisation developed rapidly, but also the conversion of cropland to woodland and grassland increased substantially between 2000-2010 on the central Loess Plateau (Liu et al., 2014). The impact of these dramatic changes on discharge, however, has been poorly studied.

Many methodologies have been applied to evaluate the impact of distinctive factors on flooding or the associated hydrological processes. Models are often used to explore the effect of unique factors on river discharge or water yield (Braud et al., 2001; Schreider et al., 2002; Brath et al., 2003; Bormann et al., 2005; Bormann et al., 2007; Yihdego and Webb, 2013). Double mass curve analyses are widely used to understand the precipitation-discharge relationships in hydrological studies and for filling gaps in gauge records (Kliment and Matoušková, 2006; Abedini et al., 2013; Gao et al., 2013; Choi et al., 2015). Double mass curves are also used to test long-term discharge trends and together with Mann-Kendall tests are thus suitable for examining the impact of human activities over a certain time period (Kliment and Matoušková, 2009; Matoušková et al., 2011; Zhang et al., 2012). Cross-correlation is able to identify the time lag between precipitation and its correlated discharge measured at the hydrological station for a single event (Talei and Chua, 2012; Löwe et al., 2014) but has not been used for exploring the precipitation-discharge relationship over a long period.

The effect of climate change and human activities on hydrological processes has been studied in a variety of Chinese catchments (Ma et al., 2010; Wang et al., 2010; Ye et al., 2013). The Wei River Basin is one of the most important sites for studying the influence of all factors on hydrological processes due to its delicate environment and large-scale human intervention. The causes and characteristics of individual floods in the basin have been extensively analysed (Jiang et al., 2004; Xing et al., 2004; Pang, 2007; Tao and Dang, 2011). Human activities have contributed up to an estimated 80% of the change in discharge of the Wei River (Gao et al., 2013; Zhao et al., 2013). A large range of studies has begun to address the flood hazard of the Wei River Basin (Jiang et al., 2004; Li and Wu, 2011; Yin et al., 2012; Peng et al., 2014). However, a comprehensive study or an integrated approach to identify the most influential factors causing flooding in the Wei River over multiple years (as opposed to individual floods) at both spatial and temporal scales is still lacking. Especially in the multitude of impacts from multiple factors, it is difficult to explore the importance and the contribution of each factor in comparison to others.

The objective of this study was therefore to analyse the characteristics of floods in the Wei River Basin over the last 60 years and to understand the impacts of various factors on flooding and discharges using a new framework approach that is capable to analyse this multitude of potentially contributing factors over multiple years. Using this framework, we specifically focused on the following questions. (1) Why: what are the most important factors influencing flooding of the catchment on a monthly and yearly basis? (2) Where: what is the most influential location (subcatchment) to the downstream flood regarding the discharge? (3) When: what is the effect of the identified factor on the time lag between precipitation and discharge? And (4) How: how does the identified factor affect the precipitation-discharge relationship? The new framework approach includes a set of methods to answer the above four questions in a systematic way.

2.2 Methods

2.2.1 Introduction of the framework approach for unravelling the impact of multiple factors on flooding at the catchment scale

In order to answer the questions of why, where, when and how flooding occurred in a catchment in a systematic way, a framework approach was proposed in this study with a suggested set of methods listed in Fig. 2.1. The methods included in the framework approach are conditional inference tree analysis (CIT), cross-correlation analysis and double mass curves, which are able to qualitatively and quantitatively assess the impact of multiple factors on flooding occurrence using either qualitative or quantitative data. The result on flood occurrence of this framework is able to identify the driving factor(s), or sub-catchment(s), and also give the ranking among all factors or sub-catchments leading to flood occurrence by applying the CIT. Based on the factors that are identifed by the CIT, the dataset should then be reorganized for conducting the cross correlation analysis and the double mass curves analysis. These two analyses are able to give more detailed insight into the impact of the identifed driving factor on the time-lag effect and the quantitative change of the relation between precipitation and discharge. The detailed explanation of each method and its application regarding the questions and the interpretation of the result are demonstrated in a case study of the Wei River Basin, China.

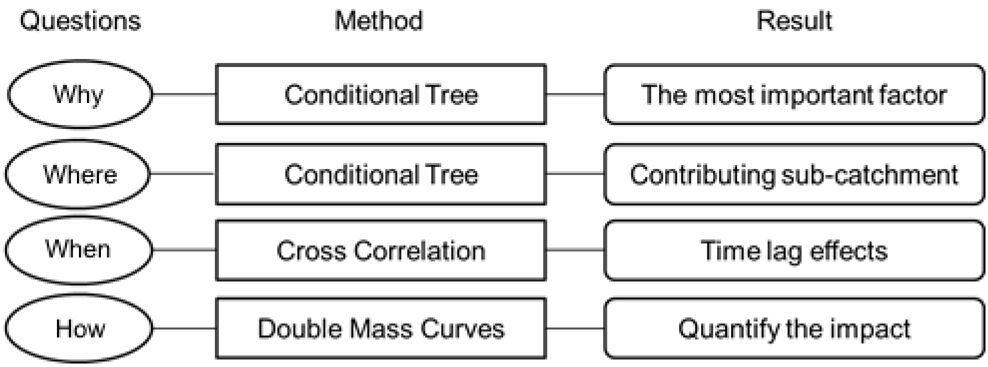

Figure. 2.1 *The structure of the framework approach for analysing the impact of multiple factors on flooding.*

2.2.2 Application of the framework approach to the Wei River Basin, China

2.2.2.1 Study area

The Wei River in China is the largest tributary of the Yellow River and is regarded as the "Mother River" of the Guanzhong Plain with a total catchment area of 134 800 km^2 (Fig. 2.2a). The river originates in the Niaoshu Mountains in Gansu province and flows east through Ningxia and Shaanxi provinces to the Yellow River, with a total length of 818 km. Two important tributaries, Jing River and Beiluo River, comprise 34% and 20% of the total catchment area of the Wei River Basin, respectively.

The climate of the basin is controlled by the continental summer monsoon, which brings an average annual precipitation of approximately 570 mm, over 60% of which falls in summer (July-September) in the flood season (Gao et al., 2013). Precipitation is concentrated on the South Bank of the Wei River in the Qinling Mountains, with an average annual precipitation of 800 mm. A yearly average of 540 mm falls north of the river. The catchment can be divided into four subcatchments (Fig. 2.2a): Jing River (J), Beiluo River (B), upstream along the Wei River (U), and the South Bank (S). Jing River and Beiluo River are the two largest tributaries of the Wei River, with Zhangjiashan (J1) and Zhuangtou (B1) hydrological stations located at their respective outlets. Linjiacun (U1) is a control station of the upstream Wei River subcatchment, and Huaxian is the most downstream control station in the Wei River Basin, although the Beiluo River flows into the Wei River below the Huaxian station. The corresponding meteorological and hydrological stations with data for the various subcatchments are listed in Table 2.1. Daily discharge data were unfortunately not available for the hydrological stations for the period 1990-1999.

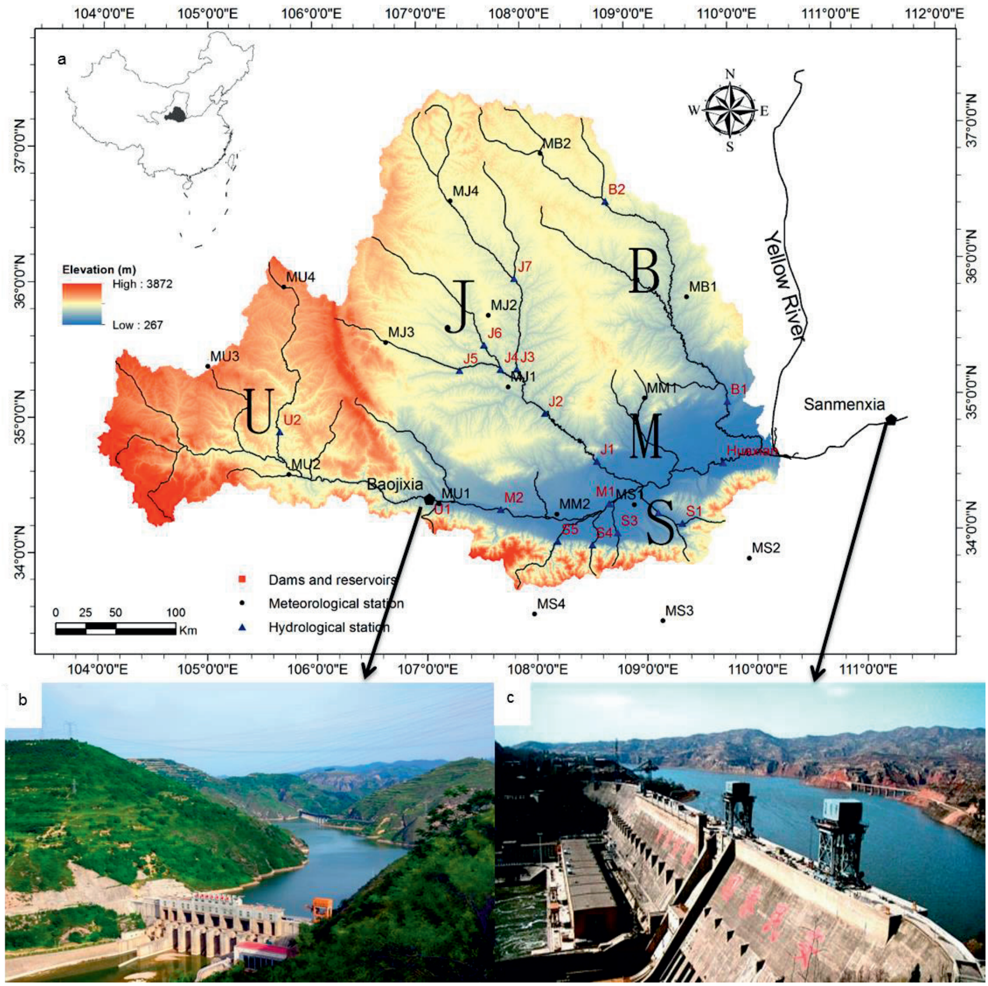

Figure 2.2 *a) Location of the study area and distribution of the hydrological and meteorological stations (abbreviations as in Table 2.1), dams and reservoirs, subcatchments, and example pictures of b) the Baojixia Dam, and c) the Sanmenxia Dam.*

Land use in the catchment consists mainly of farmland (~38%) and grassland (~50%). After the Grain for Green project conducted in 1999 (Deng et al., 2014), the forest area of the basin was raised from 4.8% to 14.4% in the year 2005, while the grass land area decreased from 58.7% to 44.0% in the same time span. Residential areas contributed only 0.8% to the total catchment area in the 1980s but had increased to 2.2% by 1996. This change in residential area is negligible compared to that of other land-use types, but the increase within a time span of 10 years is significant. Other land uses, however, generally did not change significantly between 1980 and 2005 (Gao et al., 2013).

***Table 2.1**. Hydrological and meteorological stations in the subcatchments.*

Subcatchments	J Jing River	B Beiluo River	U Upstream of Wei River	S South Bank of Wei River	M Wei + Jing Rivers
Corresponding hydrological-stations	J1 (Zhangjiashan)	B1 (Zhuangtou)	U1 (Linjiacun)		Huaxian
Catchment area (km^2)	43216	25154	30661	106498	105350
Hydrological stations*	J2 (Jingcun) J3 (Yuluoping) J4 (Yangjiaping) J5 (Jingchuan) J6 (Maojiahe) J7 (Qingyang)	B2 (Liujiahe)	U2 (Qin'an)	S1 (Luolicun) S2 (Maduwang) S3 (Qinduzhen) S4 (Laoyukou) S5 (Heiyukou)	M1 (Weijiabao) M2 (Xianyang)
Meteorological stations*	MJ1 (Changwu) MJ2 (Xifengzhen) MJ3 (Pingliang) MJ4 (Huanxian)	MB1 (Luochuan) MB2 (Wuqi)	MU1 (Baoji) MU2 (Tianshui) MU3 (Huajialing) MU4 (Xiji)	MS1 (Xi'an) MS2 (Shangzhou) MS3 (Zhen'an) MS4 (Fuping)	MM1 (Tongchuan) MM2 (Wugong)

* increasing numbers indicate increasing distances from the hydrological station at the outlet.

Soils in the Wei River Basin vary but have developed from the dominant loess deposits that are widely distributed in the Jing and Beiluo River Basins, with an average thickness of approximately 100 m (Zhang et al., 2014). The South Bank subcatchment, with a total area of about 15200 km^2, is sharply defined by the abrupt cliff-like northern face of the Qinling Mountains, with steep slopes that accelerate surface discharge.

The Tongguan elevation, defined as the water table corresponding to a discharge of 1000 m^3/s at the Tongguan hydrological station on the Yellow River, is the base level of erosion of the lower Wei River. The Tongguan elevation is negatively correlated with the bankfull discharge at Huaxian (Li and Wu, 2010) and has been raised by approximately 5 meters since the construction of the Sanmenxia Dam in the 1960s (Wang et al., 2007).

Flooding, defined as water overflowing the riverbanks onto the floodplain, occurred in the Wei River Basin on average 1.3 times per year in the last 60 years. The floodplain of the catchment covers the lower reaches of the Wei River Basin where the elevation is relatively low, especially where most of the South Bank tributaries join the main river. The floodplain of the Wei River begins at the Baojixia Dam midway along the main river (Fig. 2.2b), but most floods occur east of the city of Xi'an (meteorological station MS1 in Fig. 2.2a). Sedimentation upstream of the Sanmenxia Dam on the Yellow River (Fig. 2.2a and 2.2c) has raised the lower sections of most of the tributaries in the South Bank above the level of the ground surface. These raised rivers are the main cause of flooding in the floodplain. Numerous dams and reservoirs have been constructed in the catchment both for controlling flooding and for water and soil conservation. Thirty-one large-scale (storage $>10^6$ m^3) reservoirs (Fig. 2.2a) in the catchment with a total storage capacity of approximately 1.4 billion m^3, twenty-one of which were built between 1970 and 1983 and the rest were built before 1970, have been included in this study.

2.2.2.2 Collection of flooding records

An extensive literature and internet search was performed to collect information of flooding records onto the floodplains at the Wei River Basin during 1956-2010. The characteristics of each flood were extracted from the Table of Flooding Elements in the Annual Hydrological Report of the P. R. China – Hydrological Data of the Yellow River Basin, including the date and amount of peak discharge, level of the water table at peak discharge, and peak sedimentation at Huaxian.

2.2.2.3 Datasets

To apply the framework approach, a wide range of datasets regarding the factors possibly affecting flooding were collected and organized based on the CIT model requirements (Table 2.2). Slope data was derived from the Digital Elevation Model of the basin using ArcMap 10.0. Land use was calculated from land use datasets of the years 1980, 1985, 2000 and 2005, and we assumed the land use for 1956-1984 to be the same as that in 1980 (no earlier records of land use were available), 1985-1990 the same as that in 1985, 2000-2004 the same as that in 2000 and 2005-2010 the same as that in 2005. Both the DEM and land use data were provided by the Environmental and Ecological Science Data Center for West China, National Natural Science Foundation of China (http://westdc.westgis.ac.cn) and the International Scientific Data Mirror Website of Computer Network Information Center of Chinese Academy of Science (http://datamirror.csdb.cn). Meteorological data was obtained from The National Meteorological Information Centre. Data of the elevation of the outlet was obtained from the Shaanxi Administration Bureau of Sanmenxia Reservoir. Three periods were analysed based on the time of dam construction: (i) before extensive dam construction (1956-1969), (ii) during the construction of most of the dams (1970-1983), and (iii) after most of the dams had been constructed (1984-2010). The factors were classified into three groups corresponding to the influencing factors identified in the introduction:

biophysical, meteorological, and anthropogenic factors listed in Table 2.2. All analyses excluded 1991-1999 due to the lack of daily discharge data for all hydrological stations.

Table 2.2. *Description of the datasets used in the framework approach.*

Variable	Variable name	Description
	Biophysical factors	
Slope	Average slope of the catchment (°)	J subcatchment: 14.10 B subcatchment: 13.51 U subcatchment: 12.50 S subcatchment: 16.80
	Meteorological factors	
Temperature	Average monthly temperature (°C)	Continuous value
Precipitation	Average monthly precipitation (mm)	Continuous value
Humidity	Average monthly humidity (%)	Continuous value
Sunshine hours	Total monthly hours of sunshine (h)	Continuous value
Sunshine percentage	Average monthly sunshine percentage (%)	Continuous value
Season	Rainy or dry season	Rainy season: Jun-Oct Dry season: Nov-May
Month		Continuous value
Year		Continuous value
	Anthropogenic factors	
Grass	Grassland area (% of total area)	
Water	Water area (% of total area)	
Cultivation	Cultivated area (% of total area)	
Residence	Residential area (% of total area)	
Forest	Forested area (% of total area)	
Elevation of the outlet	The water table at the Tongguan hydrological station* (m)	Water table corresponding to a discharge of 1000 m^3/s at the Tongguan hydrological station, continuous value
Period of dam construction		Before: 1956-1969 During: 1970-1983 After: 1984-2010

* The Tongguan water table is influenced by the accumulated sedimentation because of the downstream Sanmenxia Dam. Tongguan is considered as the outlet and erosion base of the Wei River.

2.2.2.4 Why – CIT analysis for identifying the most influential factor causing flooding

A CIT analysis was constructed to identify the driving factor and the contribution of each factor associated with flooding occurrence on both a monthly and yearly basis by recursive binary partitioning in a conditional inference framework (Hothorn et al., 2006). This non-parametric class of regression trees supports all types of variables, including nominal, ordinal, numeric, and multivariate response variables (Hothorn et al., 2006). The statistics–based approach of CIT uses non-parametric tests as splitting criteria, corrected for multiple testing to avoid overfitting. This approach results in unbiased predictor selection and does not require pruning. Stopping criteria based on multiple test procedures are implemented and it is shown that the predictive performance of the resulting trees is as good as the performance of established exhaustive search procedures (Hothorn et al., 2006). We assumed that the distribution of the responding variables depended on a function of the variables. Flooding was the responding variable, and the influencing factors were the variables. Flooding was defined as "Yes" or "No", with "Yes" indicating an occurrence of flood in a certain month or year. A subset of available factors possibly affecting flooding was included in the model (Table 2.2). The model generated a tree-shaped graph, with each node of the tree representing the case weights of the observations of the responding variable. The P value represents the result of multiple significance tests under a permutation test algorithm. The covariate with the minimum P value was selected among all covariates for further splitting. The P value shown in the tree indicates the level of significance of the selected covariate (Hothorn et al., 2006).

2.2.2.5 Where – CIT analysis to identify the subcatchments contributing to flooding

CIT was constructed to analyse the most important hydrological stations and subcatchments contributing to flooding downstream. Monthly averaged discharge data from 18 hydrological stations (Table 2.1, the Huaxian station was excluded because it was the control station for the entire basin and did not represent a subcatchment) were the input variables, and monthly and yearly flood occurrence were the responding variables. In this analysis, we assumed the distribution of the flood occurrence on a monthly or yearly basis is based on a function of the discharge of the 18 hydrological stations.

2.2.2.6 When – Cross-correlation analysis for time-lag investigation

Cross-correlation analysis investigated and quantified a possible time lag between precipitation and discharge (or flood) (Bieger et al., 2012; Talei and Chua, 2012; Löwe et al., 2014). We analysed the time lags between the precipitation at the meteorological stations (Table 2.1) and the measured discharge at the control (Huaxian) hydrological station at the outlet of the Wei River Basin. Precipitation data for 122 days in the rainy season (from 1 June to 30 September) of each year of a recorded flood were extracted from the data set of daily precipitation. Based on the most influential factor identified by the CIT analysis done in section 2.2.2.4 and 2.2.2.5, the datasets can be divided into subsets accordingly to be used as comparison with each other. The precipitation data from each meteorological station are then cross-correlated with the discharge data at Huaxian within each subgroup using the ccf function of R version 2.14.0 (Venables and Ripley, 2002). This result is aiming at explaining the impact of the most influential factor (or any factor of interest) on the time lag effect between precipitation and discharge.

2.2.2.7 How – Double mass curves to analyse the effect of dam construction on the precipitation-discharge relationship

Double mass curves are widely used in hydrology to test the consistency and long-term trends of hydro-meteorological data (Abedini et al., 2013; Gao et al., 2013; Choi et al., 2015).

A straight line between cumulative precipitation and discharge indicates that the proportionality between the two remains unchanged. This method is able to smooth and show the main trends of time series. However, a change in the regression slope (proportionality) of the plotted curve indicates the change of trends, which is usually caused by external factors. In order to investigate the impact of the most influential factor or subcatchment identified by the CIT analysis in section 2.2.2.4 and 2.2.2.5, in this study we divided the precipitation and discharge data into contrastive subsets according to the identified factor. Double mass curves are then plotted regarding each subgroup to quantify the overall influence of the factor on the change between cumulative average precipitation from all meteorological stations in the catchment and discharge at Huaxian hydrological station. The significance in differences amongst the changes in the regression slopes were compared using analysis of covariance (ANCOVA) using R version 3.1.2.

2.3 Results

2.3.1 Floods

Thirty one floods occurred between 1956 and 2010 on the floodplain of the Wei River Basin were identified with relevant flood information (Table 2.3), with an average frequency of 0.6 per year. All floods occurred between May and October, with more than half in July and August. The peak discharge at Huaxian (control station) averaged 3912 m^3/s, and the depth of the water table averaged 339.8 m. The peak discharges are constant over time while the level of the water table shows an increasing trend (Table 2.3).

Table 2.3 *Characteristics of the floods at the Huaxian hydrological station with the highest peak discharge for each year with a flood.*

Year	Month	Day	Peak-discharge depth (m)	Peak discharge (m^3/s)	Peak sedimentation (kg/m^3)
1958	8	21	338.46	6040	213
1959	7	16	336.77	3920	438
1960	8	4	337.23	2900	605
1961	10	20	337.48	2700	25.9
1962	7	28	338.07	3540	65.4
1963	5	25	338.45	4570	59
1964	9	15	338.78	5130	85.7
1965	7	9	337.48	3200	357
1966	7	28	339.47	5160	636
1967	5	19	338.27	2110	80.6
1968	9	12	340.54	5000	76
1970	8	31	340.55	4320	235
1973	9	1	341.57	5010	428
1974	7	14	340.13	3150	47.8

1975	10	2	340.97	4010	96
1976	8	29	340.15	4900	117
1977	7	7	340.43	4470	795
1980	7	4	340.35	3770	33.3
1981	8	23	341.05	5380	68.7
1983	9	28	339.37	4160	38.3
1984	9	10	339.16	3900	50.6
1985	9	16	339.24	2660	31.1
1986	6	28	339.02	2980	485
1990	7	8	339.24	3210	55.4
1992	8	14	340.95	3950	528
1994	7	9	338.54	2000	765
1996	7	29	342.25	3500	565
1998	8	23	340.06	1620	130
2003	9	1	342.76	3570	598
2005	10	4	342.32	4820	31.4
2010	7	26	341.15	2040	459

2.3.2 Why – factors influencing flooding

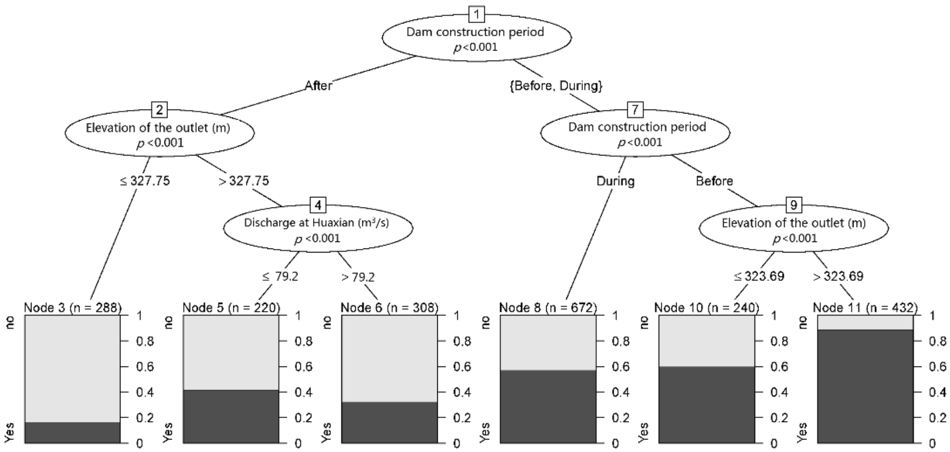

Figure 2.3 *Results of CIT analysis of yearly flooding with all factors listed in Table 2.3. The dark areas indicate the ratio of the number of flooding cases to the total number of the cases (n) in the node. (Total number of cases in all categories is 2160, P value represents the significance level of the variable chose at each split).*

CIT analysis was first constructed to identify the driving factor and the contribution of each factor to the occurrence of flooding on a yearly basis. As “Yes” (shown as dark area in Fig. 2.3) indicating the occurrence of flood, the node of the tree represents the case weights of the “Yes” observations of the total responding variable (Fig. 2.3). The period of dam construction was identified as the most important factor for flooding occurrence on a yearly basis. The number of floods was significantly higher before and during the period of dam construction than after the period of dam construction (Node 8, 10 and 11 compared to Node 3, 5 and 6 in Fig. 2.3). A further division (Node 7) shows that more flooding occurred before than during the period of dam construction (Node 10 and 11 compared to Node 8). Elevation of the outlet was subsequently identified as the second most important factor after the dam construction period. Before the dam construction period, there were more floods when the elevation of the outlet is higher than 323.69 m (Node 9 in Fig. 2.3). After the dam construction period, there is a clear division for the occurrence of flood when the elevation of the outlet reached 327.75 m (Node 2 in Fig. 2.3). Floods were much more common before dam construction even though the identified elevation of the outlet was lower (323.69 m compared to 327.75 m) than in the period after dam construction (compare Nodes 3 and 11 in Fig. 2.3).

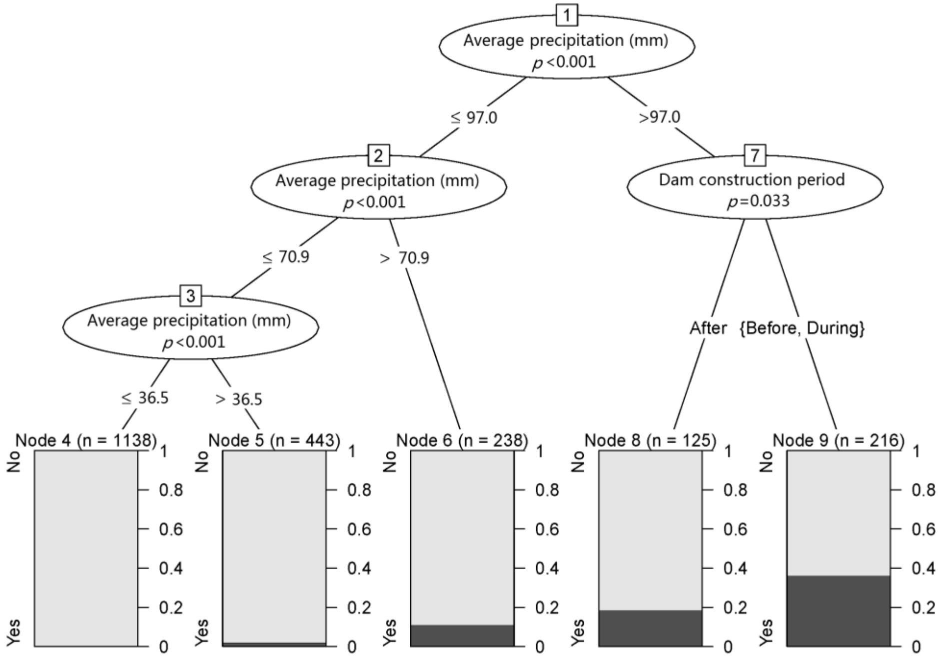

__Figure 2.4__ Results of CIT analysis of monthly flooding with all factors listed in Table 2.3. The dark areas indicate the ratio of the number of flooding cases to the total number of the cases (n) in the node. (Total number of cases in all categories is 2160, P value represents the significance level of the variables chose at each split).

CIT analysis was also applied to analyse the factors influencing flood occurrence on a monthly basis. Similar to the yearly analysis, the corresponding factor is the "Yes" case (shown as dark area in Fig. 2.4) indicating the occurrence of a flood in the month. Average monthly precipitation appeared to be the dominant factor for flooding on a monthly basis (Node 1, 2 and 3 in Fig. 2.4). There is a significant difference between the number of occurrence of floods from precipitation more and less than 97 mm (Node 8 and 9 compared to Node 4, 5 and 6 in Fig. 2.4). In the category of precipitation more than 97 mm, which is the condition leading to more flooding, the dam construction period appeared to be the second most important factor causing flooding. It can be clearly seen that even with the same precipitation condition, less floods occurred after the dam construction period than before and during.

2.3.3 Where – effect of discharge of subcatchments on flooding

Fig. 2.5 shows the results of the CIT analysis conducted based on the variables being the discharge of the control hydrological stations of each subcatchment and the responding variable being the occurrence of flooding on a monthly basis. Only the control hydrological stations in subcatchments U, J, and B (U1, J1, and B1 in Table 2.2) and the hydrological stations in subcatchment S (S1, S2, S3, S4, and S5 in Table 2.2) were included in the model to identify the most influential subcatchment, i.e. the most important control station of the tributaries. The most upstream subcatchment (U) was identified as the dominant contributor (Node 1 in Fig. 2.5). Additionally, the South Bank discharge was the second most important factor contributing to the flooding downstream. Especially when the discharge of U1 station is above 131 m^3/s and the discharge of S5 station is higher than 19.4 m^3/s (Node 7 in Fig. 2.5), the flooding occurrence is significantly higher than for all the other cases (Node 9 compared to Node 4, 5, 6 and 8 in Fig. 2.5). When the discharge of the S2 station is higher than 53 m^3/s, more floods occurred (Nodes 6 compared to Node 4 and 5 in Fig. 2.5). The results highlightthe importance of the South Bank and upstream discharge on the flooding of the floodplain.

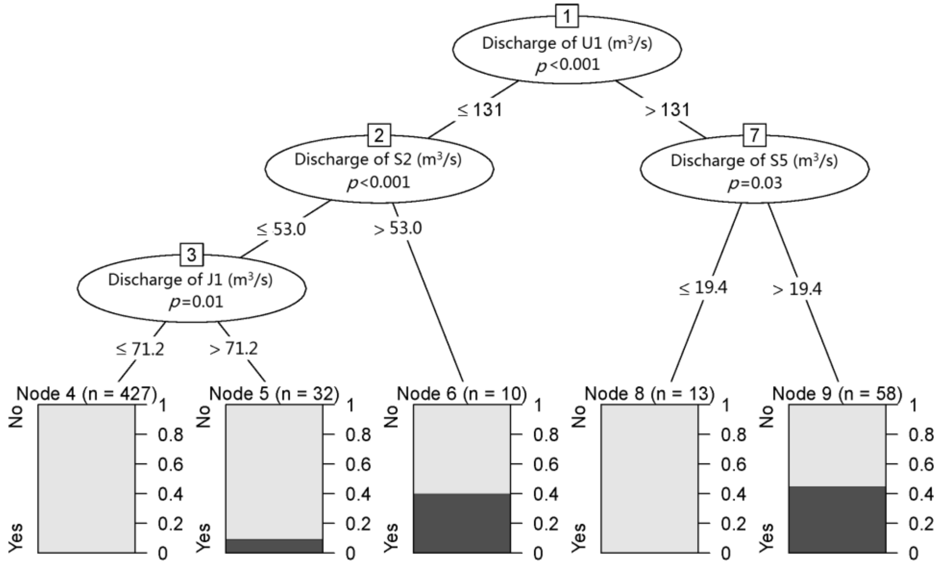

Figure 2.5 *Results of CIT analysis of monthly flooding with discharge of the hydrological stations of subcatchment S and the control stations of subcatchments J, U, and B. The dark areas indicate the ratio of the number of flooding cases to the total number of the cases (n) in the node. (Total number of cases in all categories is 540, P value represents the significance level of the variables chose at each split).*

3.3.4 When – effect of dam construction on time lag with respect to precipitation to discharge

The period of the dam construction was identified as the most important factor causing the flood occurrence downstream in section 2.3.2. Therefore, as a next step, we analysed the time lags between the precipitation at the meteorological stations (Table 2.2) and the measured discharge at the control hydrological station (Huaxian) at the outlet of the basin for the three periods subsequently. Meteorological and hydrological datasets were subdivided into the three groups regarding the periods described in section 2.2.2.3 based on the dam construction periods.

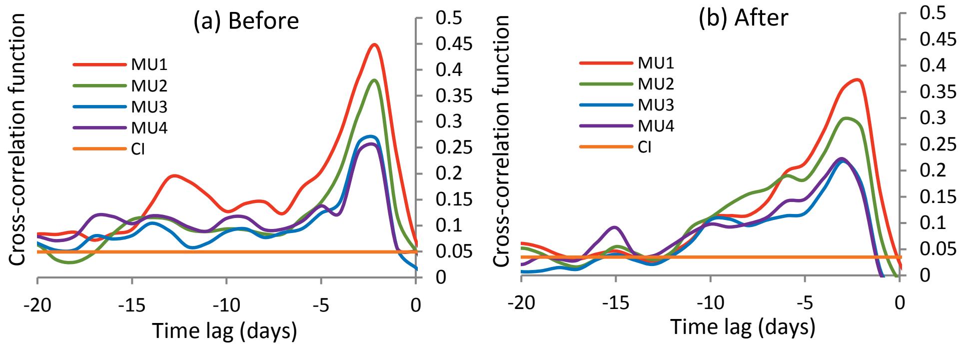

Figure 2.6 *Cross-correlations between precipitation measured at meteorological stations and discharge at the Huaxian station for the U subcatchment before (a) and after (b) dam construction (abbreviations as in Table 2.2; CI, 95% confidence interval).*

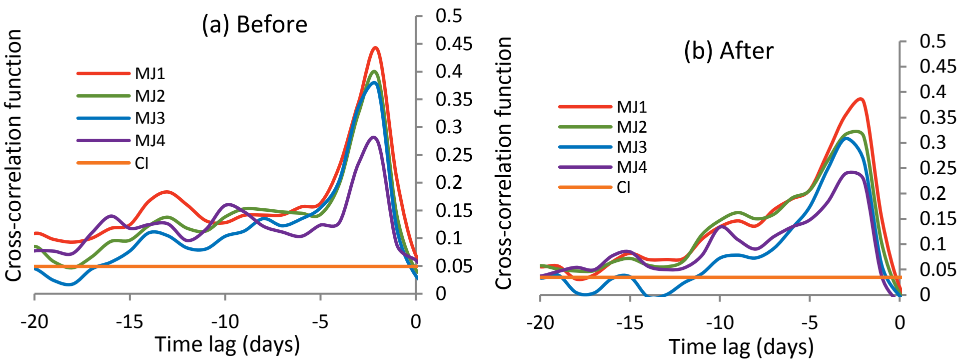

Figure 2.7 *Cross-correlations between precipitation measured at meteorological stations and discharge at the Huaxian station for the J subcatchment before (a) and after (b) dam construction (abbreviations as in Table 2.2; CI, 95% confidence interval).*

Figs. 2.6 – 2.9 show the results of the cross-correlation between precipitation, as measured at the meteorological stations in Table 2.2, and discharge, as measured at the main river outlet (Huaxian) for the four subcatchments and two periods (before and after dam construction). In general, for all subcatchments, the highest cross-correlation indicates the highest correlated time lags, i.e. the highest correlated discharge of all meteorological stations occurred within five days after precipitation. In addition, the strength of the correlation decreased with increasing distance to the outlet for all meteorological stations located in the catchment (the ascending number of the meteorological stations indicates the increasing distance to the outlet, for instance, MU1 is located closer to the outlet compared to MU2), except for subcatchment M. The detailed time lag effects of meteorological stations of different subcatchments regarding the periods are listed in Table 2.5.

Table 2.5 *Time lags (days) between precipitation measured at meteorological stations and the discharge at the Huaxian station before and after dam construction based on the cross-correlations in Figs. 6 - 9.*

	U subcatchment				J subcatchment				S subcatchment			
	MU1	MU2	MU3	MU4	MJ1	MJ2	MJ3	MJ4	MS1	MS2	MS3	MS4
Before	2	2	2.5	2.5	2	2	2	2	2	1.5	2	2
After	2	3	3	3	2	3	3	3	2	2	2	2
Change	0	1	0.5	0.5	0	1	1	1	0	0.5	0	0

	M subcatchment		
	MM1	MM2	Average
Before	2	2	2.0
After	2	2	2.4
Change	0	0	0.4

The time lags between precipitation in the Wei River Basin and discharge at Huaxian increased after the period of dam construction by an average of 0.4 days (Table 2.5). The delay was most pronounced in subcatchment J (0.75 days), while subcatchment M had no time lag change. The fact that the construction of the dams has the most impact in subcatchment J is consistent with the result obtained from the CIT analysis in section 2.3.3. As the dam construction successfully delayed the precipitation, the discharge in subcatchment J appeared to be not important for the flood occurrence. Moreover, the time lag increased with distance from Huaxian. The construction of the dams and reservoirs thus had a large effect on the time lags for subcatchments U and J.

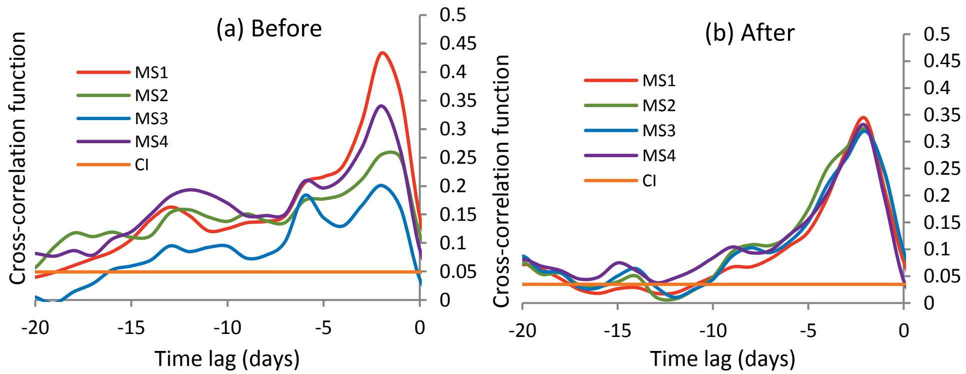

Figure 2.8 *Cross-correlations between precipitation measured at meteorological stations and discharge at the Huaxian station for the S subcatchment before (a) and after (b) dam construction (abbreviations as in Table 2.2; CI, 95% confidence interval).*

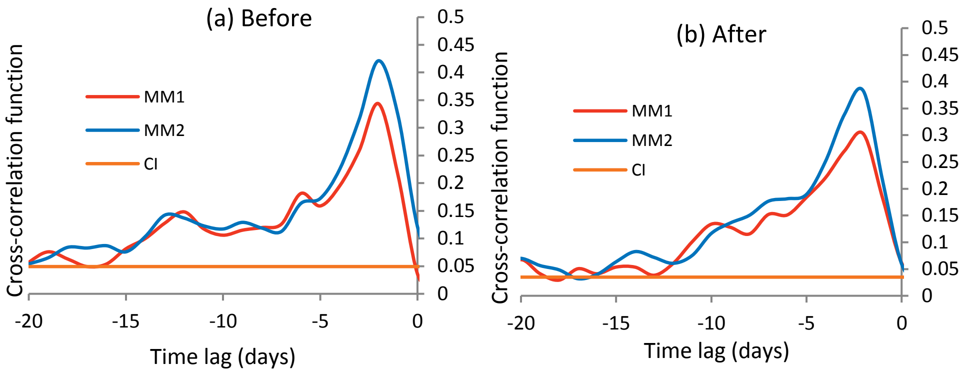

Figure 2.9 *Cross-correlations between precipitation measured at meteorological stations and discharge at the Huaxian station for the M subcatchment before (a) and after (b) dam construction (abbreviations as in Table 2.2; CI, 95% confidence interval).*

2.3.5 How – effect of dam construction on the precipitation-discharge relationship

In order to investigate how much the dam construction period affects the precipitation-discharge relationship, we plotted double mass curves for the three periods mentioned in section 2.2.2.3, i.e. before, during and after construction of most of the large dams. Fig. 2.10 shows the results of the double mass curve analysis of the precipitation-discharge relationship at Huaxian for the three periods. The slope of the regression lines decreased over time (ANCOVA, $p < 0.0001$); it was highest for the period before dam construction and was lowest after construction. This decline indicates that the discharge decreased with the same amount of precipitation, which may have been due to the construction of the dams and reservoirs. Compared with the accumulative discharge for the period before dam construction, the accumulative discharge for the period after dam constructions was reduced by 44%.

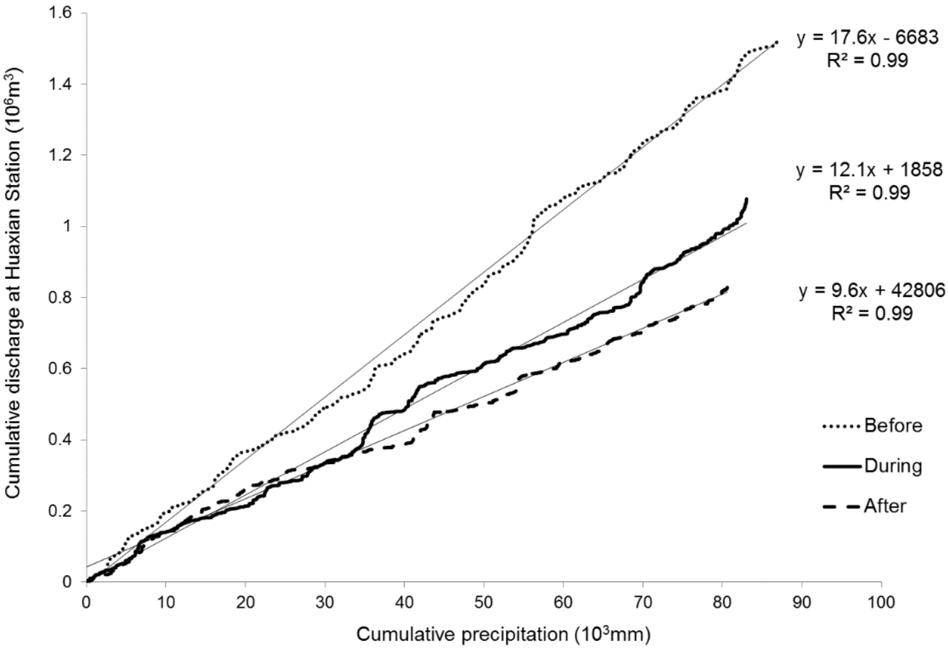

Figure 2.10 *Double mass curves of precipitation-discharge at the Huaxian station. The straight lines are the regression lines for the cumulative data before, during, and after the construction of dams.*

2.4 Discussion

This study presented and evaluated a framework approach consisting of a set of methods to answer the questions why, where, when and how flooding occurs in a catchment with complex conditions, multiple potential contributing factors and including multiple years. CIT analysis is a relatively new method used mainly in biological and medical studies to identify the factors and primary components of phenomena (Blank and Blaustein, 2014; Johnstone et al., 2014; Zeng et al., 2015). It has not often been applied in hydrological studies. Many studies of flooding in the Wei River Basin have focused on one or two factors, mainly those involved in the precipitation-discharge or sediment load relationships. We introduced CIT analysis in this study to determine the most important factors, amongst all climatic and anthropogenic factors, and their impacts on flooding. The result from this study was able to present statistical evidence to the fact that the dam construction period has the most important impact on flooding occurrence in a catchment. Together with the cross-correlation analysis and double mass curves analysis, we were able to identify the quantitative influence of the identified factors. The results of the three methods were consistent among themselves, highlighting the importance of dams effects on flooding control in the catchment. However, the framework method can be applied in any catchment flooding analysis where many factors need to be considered.

The cross-correlations indicated that dam construction had a more pronounced effect on the discharge than on the time lag after precipitation. The operation of the reservoirs can account for this result. We assume that reservoirs store the runoff from upstream precipitation. The reservoirs in our study, however, only stored the amount of runoff sufficient to prevent flooding downstream and passed along most of the runoff generated from the upstream precipitation (RDRSMPRC, 1991; LFPPRC, 1998). The effect of the time lag was thus not very pronounced. With the amount of the runoff stored in the reservoir, infiltration and water diversions led to the decrease in the total discharge at the outlet gauging station, accounting for the results of the double mass curve analysis.

Changes in land use are assumed to be extensive in the study area due to the Grain to Green project (Liu et al., 2014; Jian et al., 2015). Land-use changes are also an important factor influencing the infiltration and interception of rainwater (Fohrer et al., 2001; Costa et al., 2003), which were responsible for the change in discharge downstream. Our study did include land use change as factors in the analysis, however, they were not identified as an important factor for flooding occurrence. This is consistent with Gao et al. (2014), who also suggested a low impact of land-use change on streamflow and sediment load in the Wei River Basin. We further investigated the effect of land use on flooding by changing the criteria of the CIT analysis to generate another level of separation based on the current result of Fig. 2.3. Residential area was a branch of Node 5 below the discharge at Huaxian, indicating the influence of built-up areas on river discharge. Pfister et al. (2004) and Yang et al. (2015) suggested that land-use changes may have a more significant impact on local and small catchments than on regional or mesoscale catchments, consistent with the results of our study.

Xia et al. (2014) found that discharge and sediment load were the two dominant factors determining the bankfull channel dimensions in an alluvial river, but sediment load was not identified as an important factor in our study. Sediment load was not correlated with either flood-peak discharge or flood-peak water table (Table 2.3). Sediment loads may affect the morphology of riverbeds, which affects flooding, especially associated with downstream dams (Batalla and Vericat, 2009; Magilligan et al., 2013; Opere, 2013). The effect of sediment load on channel morphology and flooding should thus be studied further.

The slope of subcatchment S (South Bank) was higher than those in the other three subcatchments (Table 2.2), but slope was not identified as an important factor affecting flooding (Fig. 2.3), which was unexpected and perhaps due to the averaged slope. The slopes of the Qinling Mountains in subcatchment S are very steep, but nearly half of the area of this subcatchment is floodplain, which decreases the average slope. The steeper slopes, combined with the different geology of subcatchment S compared to the other three subcatchments, produced a larger discharge from this subcatchment. The effect of discharge from subcatchment S was successfully identified in the spatial analysis using CIT (Fig. 2.5). The discharge from subcatchment S was responsible for most of the flooding in the Wei River Basin on a monthly basis (Nodes 6 and 9 in Fig. 2.5).

Factors that lead to flooding can be identified by analysing the characteristics of individual floods but are difficult to include in our type of analysis. For example, cultivation on the floodplain affects the retreat of flood water. The small dikes and roads for protecting cultivated areas also increase the vulnerability of the floodplain to flooding. These factors were difficult to include in our analysis because they were unregulated, temporal, and small in scale (Jiang et al., 2004). Dike failure or exceeding the designed threshold of the dikes, as occurred with the flooding on the Yangtze River in 1998 (Plate, 2002), were difficult to be included for the same reasons.

As the dams in the study area were constructed mainly for flood control and irrigation purposes, the discharge generated from precipitation of the upper stream of the river are collected and stored in the reservoirs. The propagation time from precipitation to the discharge at the outlet of the catchment is thus extended. This process is consistent with the observation of the CIT analysis that dam construction period is the most important factor explaining the occurrence of flood. The time lag between precipitation and discharge on average increased from the cross correlation analysis. It can be concluded that the dam constructions successfully delayed the precipitation.

Factors other than dam construction not included in the double mass curve analysis may also have played a role in lowering the slope of the regression line of the precipitation-discharge relationship, so determining the exact contribution of each factor was not possible. The CIT analysis (Figs. 2.3 and 2.4), however, suggested that the period of dam construction was the most influential factor for flooding. The analysis was thus constructed based on the division of the dam construction period.

Further studies are required to quantify the effects on flooding of the factors we have identified. A model including all the above factors as input that is able to simulate the hydrology of a large-scale catchment will be applied by changing the input data according to their changes in the past and to scenarios of the future. The main focus will be the influence on flooding of the construction of dams and reservoirs, water-diversion projects, precipitation, and land-use changes.

2.5 Conclusions

A new framework approach for flood analysis capable of including multiple potential factors and multiple years of data was proposed by this research with a demonstration of a case study of the Wei River Basin, China. The study revealed that the dam construction and the most upstream subcatchment of the Wei River Basin were the most important factors influencing flooding, highlighting the importance of the effects of dams on flooding control in the basin and the effect of precipitation of the most upstream subcatchment on the discharge downstream. This upstream subcatchment contained the fewest dams and land-use changes and was important for managing soil and water to avoid flooding in the Wei River Basin. The approach can be used in any large spatial and temporal scale analysis of multiple factors affecting flooding.

Acknowledgements
This study was part of the China-Netherlands Joint Scientific Thematic Research Programme (JSTP) supported by the External Cooperation Program of the Chinese Academy of Sciences (GJHZ1018) and Netherlands Organization for Scientific Research (NWO, OND1339291). The authors would like to thank the Institute of Soil and Water Conservation, Northwest A&F University/Chinese Academy of Sciences and the Ministry of Water Resources for their help and support and the National Natural Science Foundation of China (Grant Nos.: 41371277) and the Data Sharing Infrastructure of Earth System Science – Data Sharing Service Centre for the Loess Plateau for their help with the data collection. Dr. William Blackhall is also highly appreciated for language editing.

3. Application of the LISFLOOD model for flood discharge simulation in the Wei River Basin, China

An increasing number of residents living on floodplains are being exposed to flood hazards due to climate change and city expansions. There is an urgent need for the development of an integrated approach to evaluate the impact of climate change, land use change as well as river alteration on the occurrence of hydrological extreme events. The LISFLOOD model is a physically based rainfall-runoff model that simulates the hydrological processes in a catchment taking into account human induced changes in the catchment. Using globally available land cover, soil, and vegetation as well as meteorological and geographical datasets as input, the LISFLOOD model has the potential to be applied worldwide, even for regions where data are scarce. This study is the first application of the LISFLOOD model for a semi-arid region in China for flood discharge analysis. The LISFLOOD model was first calibrated and validated in the Wei River Basin in China for the years between 2000 and 2010 at 0.05° resolution with a monthly Nash-Sutcliffe model efficiency coefficient of 0.79 and a daily score of 0.69 at the Huaxian station located at the catchment outlet. The outlets of 17 tributaries draining into the main river were then analysed in order to assess the contribution of each tributary to flood and occurrence and discharge. In conclusion, the LISFLOOD model is applicable for simulating discharge in the Wei River Basin for flood analysis.

Based on:

L. Gai, J.P. Nunes, J.E.M. Baartman, H. Zhang, F. Wang, A. de Roo, C.J. Ritsema, V. Geissen. 2019. Assessing the impact of human interventions on floods and low flows in the Wei River Basin in China using the LISFLOOD model. Science of The Total Environment 653: 1077-1094.

3.1 Introduction

Floods are extreme hydroclimatic events that threaten societies and ecosystems. The effects of these events are greatly influenced by the changes that humans have imposed on the environment (Montanari et al., 2013). Pronounced and extreme events are occurring more and more frequently on the global scale due to climate and environmental changes (van Dijk et al., 2013; Huang et al., 2015b). Current flood assessments are mostly based on the statistical analysis of gauge station meteorological or discharge data (Archfield et al., 2013; Ewea et al., 2017; Feng et al., 2017; Khelfi et al., 2017; Martínez-Graña et al, 2016; Yang et al., 2016). As the direct driving force for a meteorological flood, precipitation is often used for flood prediction fitting in different distributions (Seiler et al., 2002; Huang et al., 2015a; Ewea et al. ,2017; Khelfi et al., 2017; Mantegna et al., 2017; Simonovic, 2017). Daily streamflow is also used for flood magnitude and frequency analysis (Yue, 2001; Zhang and Singh, 2006). Developed from single factor analysis, double factor or multivariate analysis have been applied to both meteorological records and streamflow data to get a more comprehensive understanding of flood characteristics (Dalrymple, 1960; Mediero et al., 2011; Ma et al., 2013; Haslinger et al., 2014; Saad et al., 2015; Xu et al., 2015; Viglione et al., 2016; Feng et al., 2017). Recent statistical analysis has explored the possibilities of predicting streamflow for ungauged catchments (Parajka et al., 2013; Requena et al., 2017). However, none of the above methods is able to simulate all of the processes including climate, land use and river channel changes on a catchment scale.

Meanwhile, modelling approaches are beginning to be applied because they provide the possibility of stimulating the relevant parameters under different scenarios and thus allow for the exploration of future hydrological responses (Zhang et al., 2006; Brocca et al., 2011; Wu et al., 2011; Zou and Zhou, 2013; Massari et al., 2014; Apurv et al., 2015; Aich et al., 2016; Zou and Zhou, 2013; Park et al., 2016; Roudier et al., 2016). Some studies have tried to simulate catchment streamflow using a regionalization method (Archfield et al., 2013; Hundecha and Bárdossy, 2004; Khelfi et al., 2017). However, regionalization can only be done in geographically identical catchments, which makes it difficult to take land use changes and water diversions into account. Tan et al. (2015) indicated that the lack of simulation of the lake/reservoir is usually a limitation for a modelling approach aiming to obtain the proper hydrological characteristics. The result of Zhang et al. (2015) has clearly suggested that simple hydrological models no longer satisfy the need for simulating hydrological responses under land use changes and construction of reservoirs since dam construction has a significant effect on the reduction of the flood magnitude, especially on the daily scale (Batalla et al., 2004; Lv et al., 2016). Therefore, recent hydrological models make the effort to take into account the reservoir simulations, such as Distributed Hydrology Soil-Vegetation Model-Res (DHSVM-RES) (Zhao et al, 2016), the Soil and Water

Assessment Tool (SWAT) (Arnold and Fohrer, 2005), the Variable Infiltration Capacity (VIC) model (Haddeland et al., 2006), global water resources model H08 (Hanasaki et al., 2006), and the LISFLOOD model (Van der Kniff 2008).

To tackle the aforementioned difficulties and satisfy the demands for an accurate daily streamflow simulation for flood analysis, and thereupon the flood prediction, this study chose the LISFLOOD model to test for flood management. The LISFLOOD model is a spatially distributed and physically-based rainfall-runoff model, which was specifically created for flood forecasting as well as assessing the effects of river regulation measures, land-use changes and climate changes in large and trans-national catchments (Pappenberger et al., 2011; Thielen et al., 2009; Thiemig et al., 2015). The increasing number of globally available datasets that can be directly used as input to the LISFLOOD model has meant that even regions that are poorly gauged can be simulated without needing to develop a site-specific model.

This study intended to be the first application of the LISFLOOD model in China to investigate the feasibility of using LISFLOOD model for flood analysis. The model was calibrated and validated for the Wei River Basin in China with the application of the reservoir module. Then the spatial and temporal flood characteristics were analysed based on the simulation results of the model.

3.2 Methodology

3.2.1 Study Area

Originating from Niaoshu Mountains in Gansu province, the Wei River flows east across the Loess Plateau into the Yellow River at Tongguan and has a total length of 818 km. The Wei River Basin (103–111˚E, 33–38˚N) covers three provinces and has a total catchment area of 134, 800 km^2 (Fig. 3.1). The average annual precipitation in the basin is about 570 mm and influenced by the continental summer monsoon. Over 60% of the annual precipitation falls during the flood season (July-September) (Gao et al., 2013), which has caused more than 40 floods on the floodplain since 1956 (Gai et al., 2017).

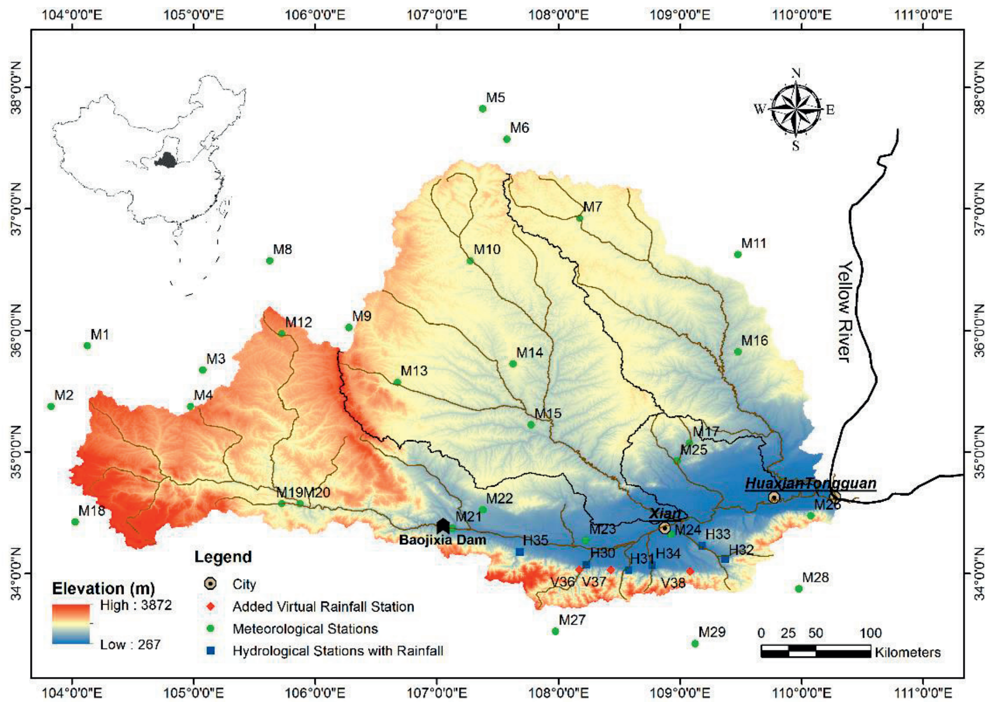

Figure 3.1 *Study area and distribution of the monitoring stations (M: Meteorological station, H: hydrological stations with rainfall data, V: Added virtual stations. 1-29 are meteorological stations with temperature data. 30-35 are hydrological stations with rainfall record, 36, 37 and 38 are virtual rainfall stations corrected by orographic factor).*

The main stream of Wei River divided the whole basin into two distinctive parts. The southern part of the Wei River are characterized by steep slopes and an earth-rock mountain landscape due to the Qinling Mountain range. The Qinling Mountain range is the highest east-west trending mountain range and the dividing line between the northern warm-temperate and southern subtropical zones in central China (Jun-ping and Yan-sui, 2001). The southern catchments of the Wei River are on the northern side of the Qinling Mountains, and have an average annual precipitation of 800 mm. The geology of the mountainous area varies from granitic to metamorphic bedrock type. Numerous short tributaries with swift flows originate from the mountains. The northern part of the Wei River Basin form part of the Loess Plateau with gentler slopes. The thick deposition of the loess layer (80-120 m in general) has masked the detailed underlying relief and has led to the formation of channels and caves due to its high erodibility (Shi and Shao, 2000, Yan et al., 2014). The largest two tributaries of the Wei River - Jing River and Beiluo River – are located on the northern side of the Wei River and comprise 34% and 20% of the total catchment area of the Wei River Basin, respectively. The land use in the catchments is mainly farmland (~38%) and grassland (~50%), located on the northern loess area. For soil and water conservation purposes, around 130 reservoirs and thousands of check dams have been built since 1949 (Chang et al., 2015).

3.2.2 LISFLOOD model

The LISFLOOD model was initially developed specifically for flood forecasting as well as to assess the effects of river regulation measures, land-use changes and climate changes in large and trans-national catchments (De Roo et al., 2001; van der Knijff et al., 2010). As the operational basis for both the European Flood Awareness System (EFAS), the Global Flood Alert System (GloFAS) and the European Drought Observatory (EDO), the LISFLOOD model is a spatially distributed and physically-based rainfall-runoff model (Pappenberger et al., 2011; Thielen et al., 2009; Thiemig et al., 2015). The fact of it being a grid-based model makes it possible to be applied to a wide range of spatial and temporal scales. The spatial resolution of the LISFLOOD can range from 10 m to 5 km depending on the input data resolution and the computational capability. The long-term water balance spanning several decades can be simulated as well as individual flood events by using a user-defined time step. The LISFLOOD model input includes topographic, soil, land use, river channel, meteorology and reservoir information as listed in Supplementary material Table S.1.

The application of the LISFLOOD model consists of three parts: the LISVAP model (Van der Kniff 2008), the LISFLOOD model (Burek et al., 2013) and the LISFLOOD calibration model. LISVAP model is a pre-processor used to calculate potential evapo(transpi)ration grids which are then used as input to LISFLOOD. The processes included in the LISFLOOD model are snow melt, infiltration, interception of rainfall, leaf drainage, evaporation and water uptake by vegetation, surface runoff, preferential flow, soil moisture distribution, drainage to the groundwater, sub-surface as well as groundwater flow, reservoirs and river channel routing. The Xinanjiang model is used for simulating the infiltration capacity of the soil (Ren-Jun, 1992). The simulation of the sub-surface storage and transport is done by using a two parallel linear reservoirs model, where the upper zone is considered as a quick runoff component and the lower zone as the slow groundwater component that generates the base flow. Kinematic wave equations are used for the surface runoff and channel routing processes. Reservoirs are simulated as points in the channel network and their inflow equals the channel flow upstream of the reservoir, while the outflow of the reservoirs are calculated as follows (Burek et al., 2013; van der Knijff et al., 2010):

$$
\begin{aligned}
&O_{res} = min\left(O_{min}, \frac{1}{\Delta t} F \cdot S\right) && F \leq 2L_c \\
&O_{res} = O_{min} + (O_{norm} - O_{min}) \frac{(F - 2L_c)}{(L_n - 2L_c)} && L_n \geq F > 2L_c \\
&O_{res} = O_{norm} + \frac{(F - L_n)}{(L_f - L_n)} \cdot max\{(O_{res} - O_{norm}), (O_{nd} - O_{norm})\} && L_f \geq F > L_n \\
&O_{res} = \max\left(\frac{(F - L_f)}{\Delta t} S, O_{nd}\right) && F > L_f
\end{aligned}
\tag{3.1}
$$

Where:
S: Reservoir storage capacity (m^3)
F: Reservoir fill (fraction, 1 at total storage capacity)
L_c: Conservative storage limit (-)
L_n: Normal storage limit (-)
L_f: Flood storage limit (-)
O_{min}: Minimum outflow (m^3/s)
O_{norm}: Normal outflow (m^3/s)
O_{nd}: Non-damaging outflow (m^3/s)
I_{res}: Reservoir inflow (m^3/s)

The LISFLOOD calibration tool uses a multi-objective generic algorithm to calibrate the simulated streamflow against the observations from the hydrological stations for multiple catchments scripted in Python programming language. In our study, we calibrated the simulated daily discharge with the reservoir module in the LISFLOOD model against the observed discharge from seven hydrological stations. A Pareto optimal solution was obtained after the automated calibration using the Nash–Sutcliffe model efficiency coefficient (NSE) (optimal value =1) as the objective function (Supplementary Material S.5). Along with the NSE, the Kling-Gupta Efficiency (KGE) (Supplementary Material S.6-8), the percent bias (Pbias) (Supplementary Material S.9) and the Pearson linear correlation coefficient (r) (Supplementary Material S.10) were also used for the model performance evaluation. Criteria given by Moriasi et al. (2007) were used to evaluate the performance of the model based on the NSE coefficient as listed in Table 3.1.

Table 3.1 *General performance evaluation criteria for recommended statistics for a monthly time step regarding hydrological modelling result.*

Performance rating	Very good	Good	Satisfactory	Unsatisfactory
NSE	0.75<NSE≤1.00	0.65<NSE≤0.75	0.50<NSE≤0.65	NSE≤0.50
Pbias	Pbias<±15	±15≤Pbias<±30	±30≤Pbias<±55	Pbias≥±55

Based on the sensitivity analysis of the LISFLOOD model, this study calibrated 10 parameters of the model involved in 4 modules. All other parameters are empirical ones that remain the same as the base run of the model. Considering the computational time and capability, this study chose a spatial resolution of 0.05° (about 5km) based on the catchment size (138, 000 km^2). The temporal resolution of daily time step was determined based on the need for flood assessment and the availability of data for validation.

***Table 3.2** Division of sub-catchments across the Wei River watershed.*

	Southern catchments					Northern catchments		Main River
Catchment Code	S1	S2	S3	S4	S5	N1	N2	M1
Control Station	Heiyukou (HS1)	Laoyukou (HS2)	Qinduzhen (HS3)	Luolicun (HS4)	Maduwang (HS5)	Zhangjiashan (HN1)	Zhuangtou (HN2)	Huaxian (HM1)
Name of the tributary	Heiyu River	Laoyu River	Feng River	Ba River	Ba River	Jing River	Beiluo River	Wei River

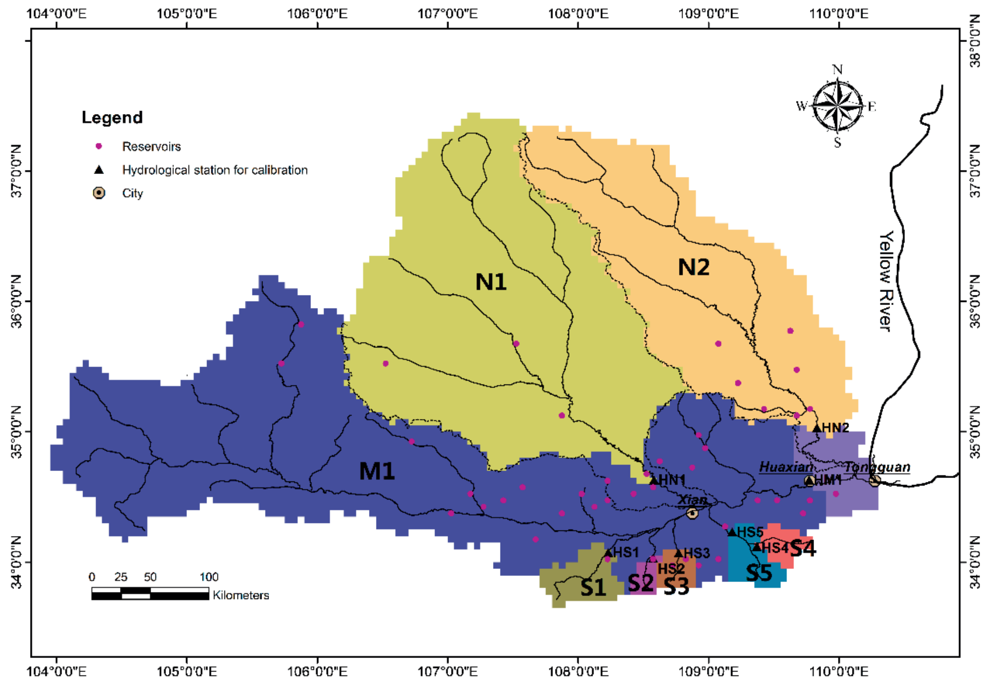

***Figure 3.2** Sub-catchments (indicated by number and color) calibrated in the LISFLOOD model with the location of the outlets of each sub-catchment and the location of the existing reservoirs used for calibration in the model.*

3.2.3 Data Processing

The Digital Elevation Model (DEM) of the study area was obtained based on the ASTER Global Digital Elevation Model (GDEM) data provided by the International Scientific & Technical Data Mirror Site, Computer Network Information Centre of Chinese Academy of Sciences (http://www.gscloud.cn/). Land use data from the Chinese land use data set were provided by the National Science and Technology Infrastructure Centre, Data-Sharing Network of China Earth System Science (www.geodata.cn). Leaf Area Index (LAI) data were extracted from the MODIS Leaf Area Index - Fraction of Photosynthetically Active Radiation 8-Day L4 Global 1km dataset from the NASA Land Processes Distributed Active Archive Centre. In this study we used the LAI data of the year 2005 for the whole simulation period assuming that the year 2005 represent the average. Soil hydraulic properties were processed based on the SoilGrid1km datasets (Hengl et al., 2014). River Channel Network maps were created based on the DEM, and this was visually compared with the river channel network data provided by the Institute of Soil and Water Conservation China. The visual comparison showed a very good match between the two datasets. The DEM based River Channel Network was used in the LISFLOOD model because the local drainage direction (LDD) which indicates the flow direction of each grid cell is an essential part of the model simulation and is only able to be derived based on the DEM based river channel network. All other topographic and channel map were generated based on DEM using a PCRaster programming language. Daily precipitation (p), maximum (tx), minimum (tn) and averaged temperature (ta) data of 29 meteorological stations located in and around the study area for the years 1995 to 2010 were obtained from The Dataset of Daily Values of Climate Data from Chinese Surface Stations from the China Meteorological Data Service Centre. Daily precipitation data from seven hydrological gauge stations in the southern catchments and daily discharge data from seven gauging stations in the whole river basin were acquired from the Annual Hydrological Report of the P. R. China – Hydrological Data of the Yellow River Basin.

The mountainous nature of the southern catchments leads to different morphological conditions, with hydrological impacts on streamflow flow concentration, and also to different climatic conditions due to orographic impacts on rainfall and temperature. The precipitation was expected to increase with altitude due to orographic effects (Kloos and Legesse, 2010). An orographic correction factor of 1.7 was used to obtain more representative distributed precipitation data in the mountainous area of the catchment. This factor was calculated based on the correlation between the elevation (m) and averaged annual precipitation (mm) of the eight hydrological gauge stations in the southern catchments for the years with recorded data from 1960 to 2010 (Fig. 3.1). Three virtual rainfall points were added in addition to the existing stations on the same contour line in the mountainous area. The orographic factor of 1.7 was used for estimating the precipitation in this three virtual points based on the observed precipitation of the closest hydrological gauges with available precipitation data (Fig. 3.3).

With the 31 reservoirs identified and simulated in this study, the total storage capacity S (m^3) for each reservoir was collected from a literature review. The relative filling of a reservoir, F, is a fraction between 0 and 1. Three filling levels are considered in the simulation: 1) the dead storage which is the conservative storage limit (defined as 10% of the total storage capacity); 2) the flood storage limit which is the maximum allowed storage (defined as 97% of the total storage capacity); 3) the normal storage (initial value defined as 40% of the total storage capacity). The actual fraction of the normal storage is calibrated as the parameter Adjusted Normal Flood. Three outflow parameters were also defined to regulate the reservoirs. For ecological reasons, the minimum outflow was defined as the 5th percentile of the flow at each of the reservoirs' point calculated for the 50 years' period (1960-2010) without the reservoir module. The 'non-damaging outflow' is defined as the 97th percentile of the flow at each of the reservoirs' point. The normal outflow is valid once the reservoir reaches its normal storage filling level. The initial values of the normal outflow are the 80% of the average inflow over the 50 years period for each reservoir point. The actual normal outflow was calibrated in the model presented as the parameter the RnormqMultiplier.

Daily precipitation and temperature map stacks were generated using the Inverse Distance Weighting (IDW) interpolation method. All input maps of the model were resampled to a 0.05° resolution. Based on observed hydrological data quality and availability, the calibration period of the model was 1-1-2000 to 31-12-2007, the validation period was from 1-1-2008 to 31-12-2010. The model was run and calibrated both at a daily time step. The goodness of fit between the modelled and measured discharge data were evaluated using the objective functions for both the calibration and validation period as well as for the whole period. The whole catchment was divided into seven sub-basins in the calibration model, with the discharge in the outlet of each sub-basin as input into the downstream sub-basin (Fig. 3.2). The calibration script loops through the seven sub-basins in ascending order of catchment rea and calibrates LISFLOOD for each interstation region using a genetic algorithm. Due to the lack of data for the HS1 station in the S1 catchment, parameters for the S1 catchment was not calibrated. Instead, the same parameter set calibrated for S2 catchment was applied to S1 catchment for the simulating the discharge as inflow into the downstream catchment.

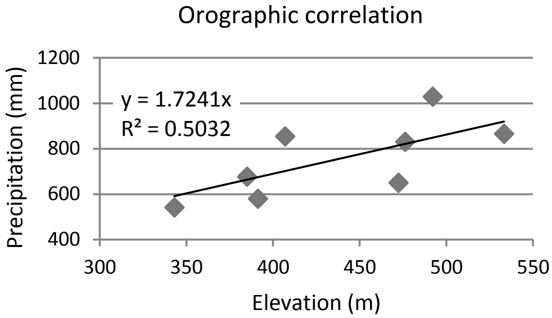

Figure 3.3 *Orographic correlation used for determining the orographic factor for the virtual rainfall stations added in the southern catchments.*

3.2.4 Data Analysis

3.2.4.1 Identifying the contribution of all tributaries

The discharge of the outlets of the five northern tributaries and nine southern tributaries and one point on the main river (Fig. 3.4) were analysed in terms of their contribution to the total discharge. The contribution of each outlet was calculated as the percentage of the total discharge. Southern outlets were grouped together as Sum South. The contribution of different tributaries regarding the two largest floods on 22nd September 2003 and 4th October 2005 were analysed in detail.

3.2.4.2 Flood Analysis

Flow duration curves (FDC) were constructed and the flood return period was calculated for all discharge time series. The exceedance probability (P) and reoccurrence period were calculated based on the 11 years of observation and simulation results. The flood return period was calculated based on the Gumbel Distribution (Onen and Bagatur, 2017) following the instruction of (Rajib, 2018).

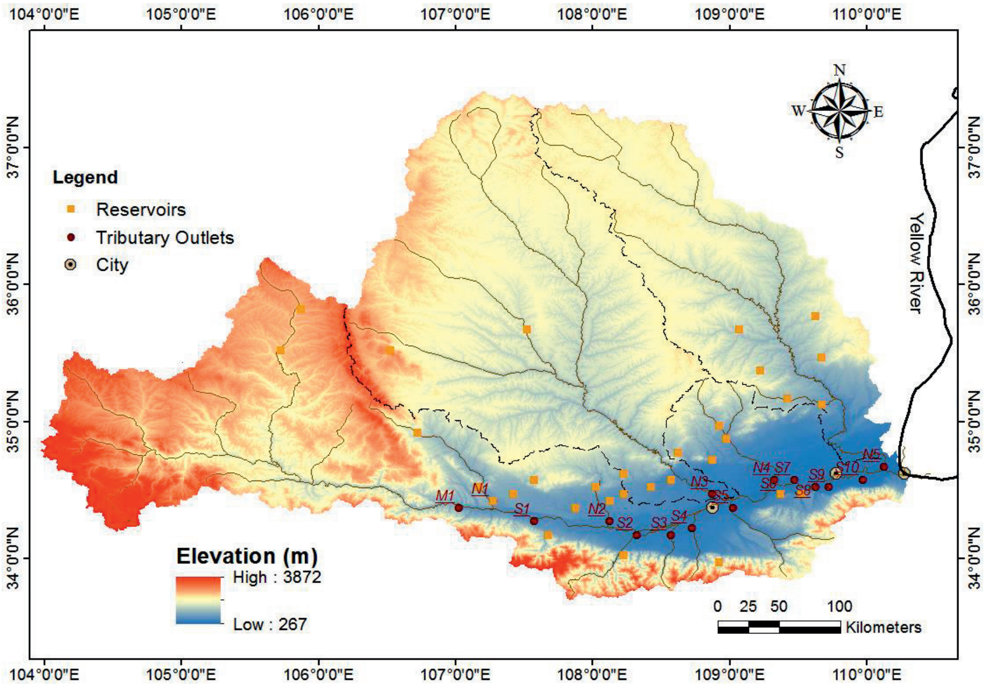

Figure 3.4 *Location of the 1) outlets of all tributaries (dark red dots); 2) the simulated 31 reservoirs (yellow squares).*

3.3 Results

3.3.1 Model calibration results

Table 3.3 summarizes the calibration and validation results of the model (Location of the Hydro-Stations in Fig. 3.2). The calibration result of the model on the outlet of the whole catchment (HM1) shows a very good result with the monthly streamflow NSE>0.75 (daily NSE>0.65) for both the calibration period and the whole period, while the result of the validation period is satisfactory (monthly streamflow 0.50<NSE≤0.65). The calibration results of the southern catchments HS2, HS5 and northern catchment HN2 are good (monthly streamflow 0.65<NSE≤0.75), but the results for catchments HS4 and HN1 were only satisfactory (monthly streamflow 0.50<NSE≤0.65) for the calibration period. The result of the catchment HS3 is unsatisfactory. The daily NSE values are in general relatively lower than the monthly values. The daily NSE of the main outlet NM1 is good in the calibration period (NSE=0.73) and the whole period (NSE=0.69) but not in the validation period. The daily NSE value for all other stations are satisfactory in the calibration period, but unsatisfactory in both the validation and the whole period. The overall dissatisfaction of the

calibration and validation result for the whole period can be explained from the different model performance in wet and dry years, as illustrated by the yearly statistics shown in Table 3.4. The daily NSE values for the flood years 2003 and 2005 in the calibration period are in most stations very good except for that of HS3 and the northern stations. However, the daily NSE value for the dry years are rather poor. Besides the temporal differences, the spatial differences among the stations are also worth mentioning. The daily performance of the model for the southern stations are lower than the HM1, probably due to the virtual rainfall stations that were created for the southern mountains. In particular, the method used to generate synthetic precipitation from recorded rainfall does not increase the number of rain days, leading to larger peak rainfall rates than expected. Daily NSE values are more sensitive to this day to day difference than monthly NSE values and are therefore lower. The hydrographs of the calibration period and validation period for all stations are shown in Fig. 3.4. The visual check of the hydrographs shows that the model simulations are able to grab the peaks and the recession curves very well especially for the calibration period. The simulation of the base flows for HS2, HS5 and both northern catchments are not idea. In general, the calibration results of the larger catchments and monthly scores are better than the results for the smaller catchments and daily scores.

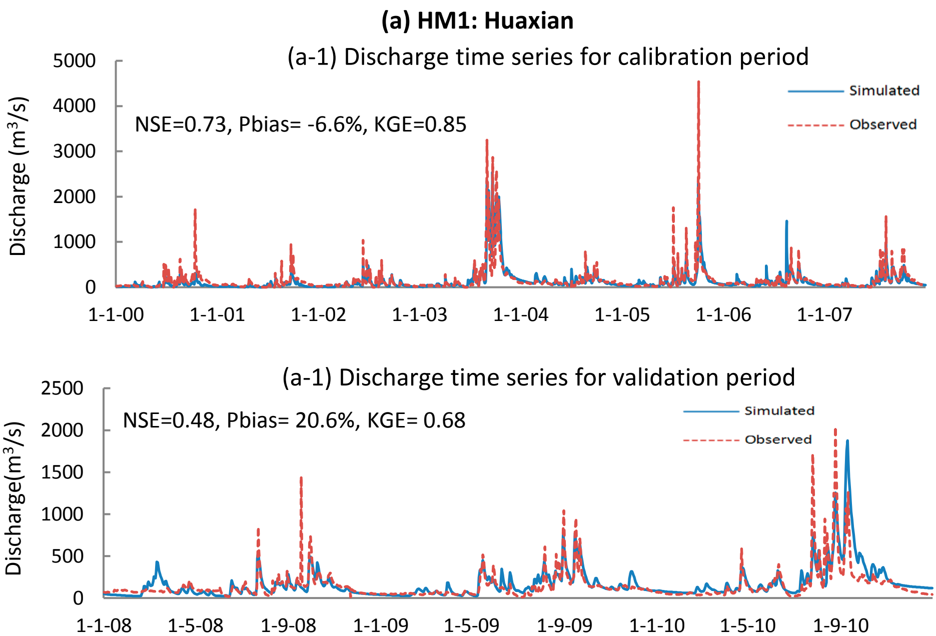

Figure 3.4 *To be continued on next page.*

(b) HS2: Laoyukou

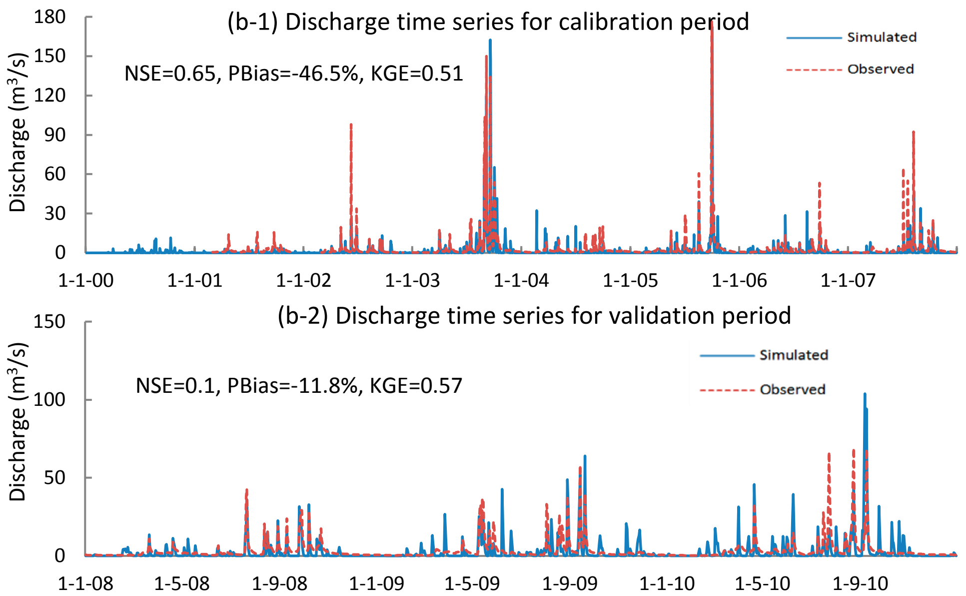

(c) HS3: Qinduzhen

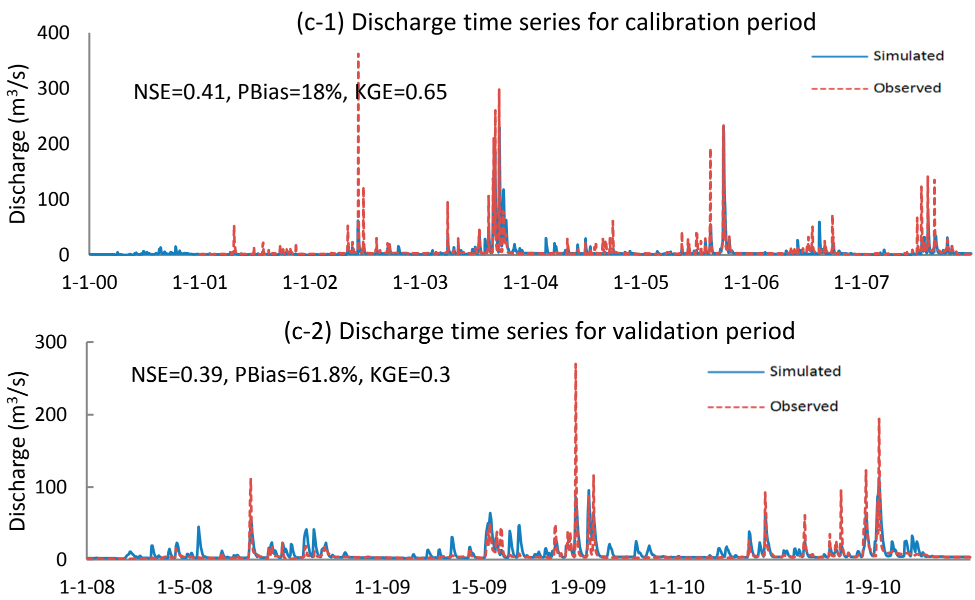

Figure 3.4 *To be continued on next page.*

(d) HS4: Luolicun

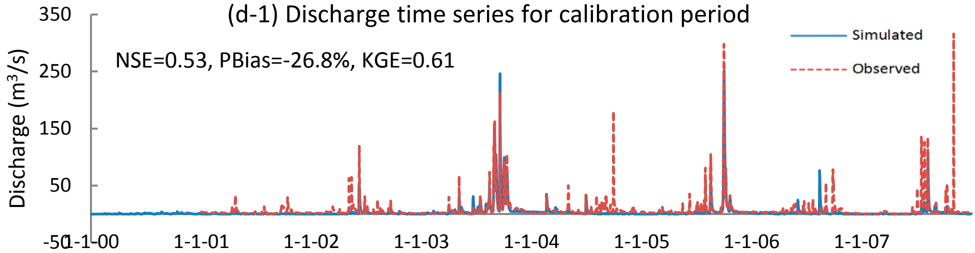

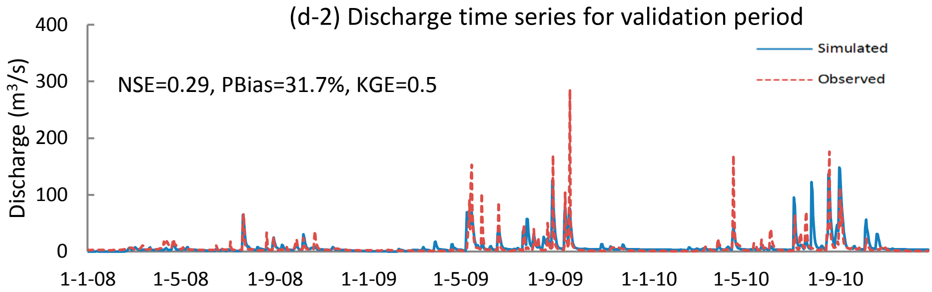

(e) HS5: Weijiabao

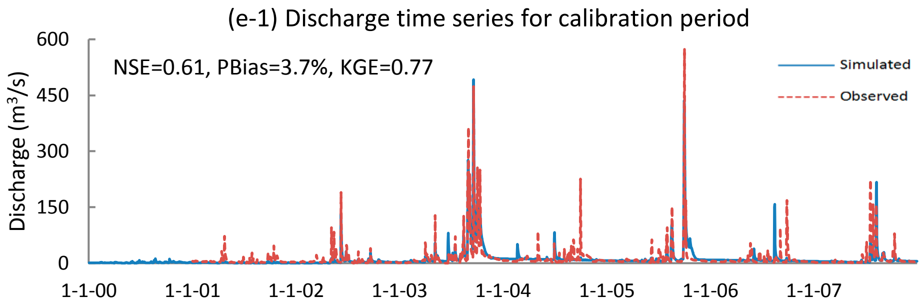

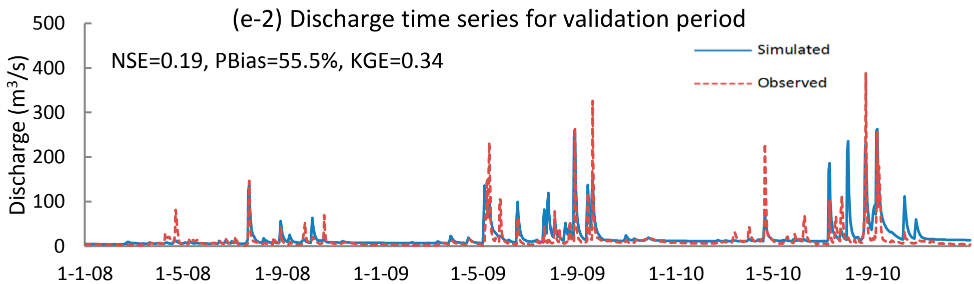

Figure 3.4 *To be continued on next page.*

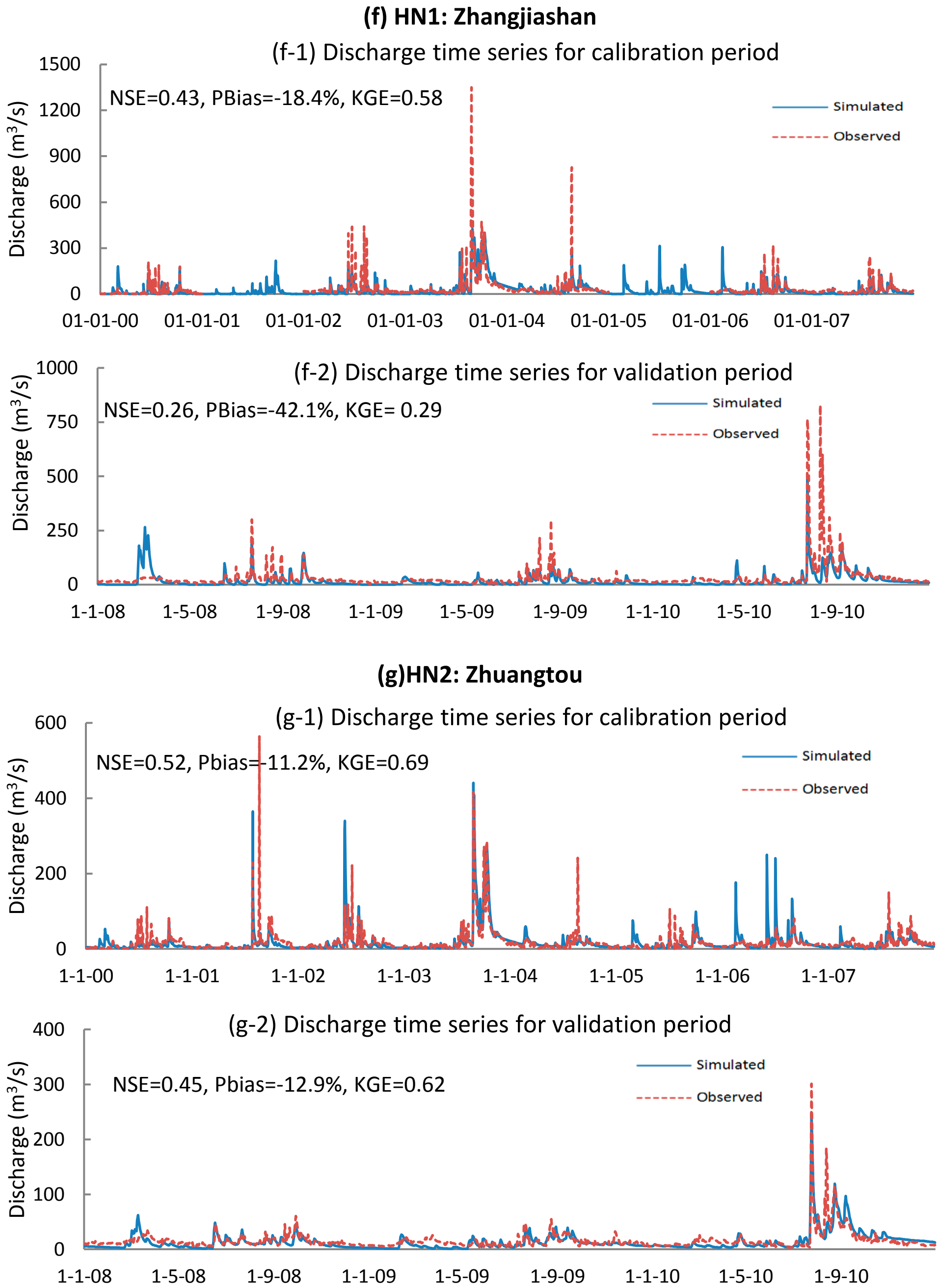

Figure 3.4 *Hydrographs of the simulated and observed discharge at the outlet station of all calibration sub-basins in the (1) calibration (2000-2007) and (2) validation (2008-2010) period respectively with performance scores (In station names, N: northern catchments, S: southern catchments, M: main stream of the Wei River).*

Table 3.3 *The NSE, KGE, Pbias and r scores for the Calibration Period (CP), Validation Period (VP) and Whole Period (WP) of the simulations against observations of the seven calibrated hydrological stations in LISFLOOD model (Location of the Hydro-stations please refer to Figure 3.2. H: Hydro-stations, S: Southern catchment, N: Northern catchment, M: main stream).*

Hydro-Stations	NSE score			KGE score			Pbias score			r score		
	Daily Statistics											
	CP	VP	WP	CP	VP	WP	CP	VP	WP	CP	VP	WP
HS2	0.65	0.1	0.55	0.51	0.57	0.59	-46.5	-11.8	-34.6	0.83	0.67	0.79
HS3	0.41	0.39	0.41	0.65	0.3	0.56	18	61.8	31.9	0.7	0.7	0.7
HM1	0.73	0.48	0.69	0.85	0.68	0.84	-6.6	20.6	0.9	0.87	0.79	0.86
HS4	0.53	0.29	0.46	0.61	0.5	0.68	-26.8	31.7	-8.8	0.75	0.62	0.7
HS5	0.61	0.19	0.5	0.77	0.34	0.67	3.7	55.5	20.9	0.79	0.64	0.74
HN1	0.43	0.26	0.38	0.58	0.29	0.51	-18.4	-42.1	-25.9	0.67	0.56	0.65
HN2	0.52	0.45	0.51	0.69	0.62	0.69	-11.2	-12.9	-11.7	0.74	0.69	0.73
	Monthly Statistics											
	CP	VP	WP	CP	VP	WP	CP	VP	WP	CP	VP	WP
HS2	0.67	0.36	0.6	0.51	0.68	0.61	-46.3	-11.7	-34.3	0.91	0.74	0.86
HS3	0.31	0.19	0.28	0.37	0.32	0.36	18.1	62.6	32.1	0.9	0.87	0.88
HM1	0.83	0.51	0.79	0.76	0.57	0.75	-6.6	19.8	0.9	0.95	0.89	0.94
HS4	0.62	0.41	0.57	0.66	0.55	0.72	-26.7	30.4	-8.8	0.87	0.84	0.85
HS5	0.68	-0.32	0.5	0.71	0.17	0.56	3.9	55.4	21	0.9	0.84	0.88
HN1	0.6	0.38	0.54	0.7	0.39	0.68	-17.8	-42.7	-25.4	0.86	0.75	0.82
HN2	0.7	0.6	0.69	0.8	0.78	0.8	-10.9	-13.1	-11.4	0.88	0.83	0.87

Flood return periods were calculated for both the observed discharge and the simulated discharge for Huaxian city (Fig. 3.5). The maximum annual peak flow of the observed data (4540 m^3/s) is higher than the simulated discharge (3323 m^3/s). Therefore, for instance, a 2000 m^3/s discharge is equivalent to a 2.5-year-return-period flood in the observation but a 5-year-return-period flood in the simulated result.

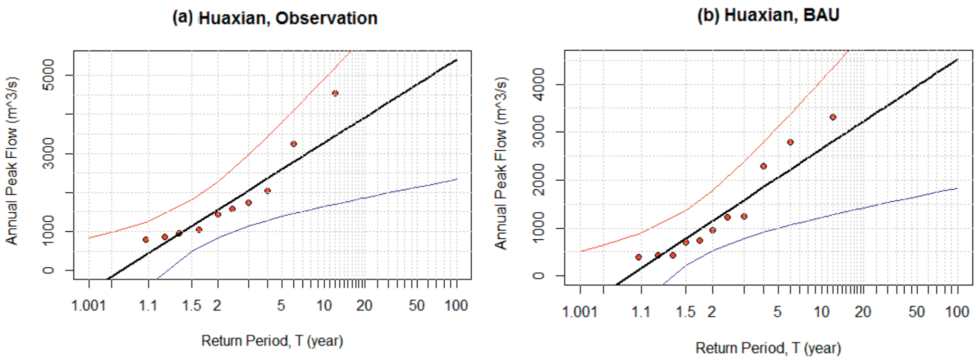

Figure 3.5 *Return periods of annual peak discharge at Huaxian city calculated based on (a) observed data and (b) simulated result (Red dots: the actual annual peak discharge values. Black line: the calculated probability distribution. The red and blue lines: the 95% confidence band).*

3.3.2 Contribution to flooding from tributaries

Tributaries M1, N3 and all of the southern tributaries (summed together, but especially S6) are the main contributors to the total discharge (Fig. 3.6 and Fig. 3.7a). The contribution of

M1, which is located upstream of the main Wei River, is higher during the wet periods (March to October). From Fig. 3.7b, it can be concluded that the flood that occurred in September 2003 is mainly owed to the discharge of N3, S5, N5, S2, and S4 (in that order), while the flood of October 2005 occurred mainly because of high discharge of S2, S5, N3, S4, and N5 listed in order of contribution (Fig. 3.7c). Although the catchment areas of S2, S4 and S5 are on average not even 5% of the average catchment area of the two northern catchments, the contribution of these three southern tributaries is comparable with that of the northern tributaries (Fig. 3.7). N5 is one of the two largest tributaries of the Wei River Basin, however, the average contribution by N5 is relatively small due to the high coverage of forest in the catchment which leads to low streamflow. The contribution of the southern catchments is also pronounced in the low flows, which can be concluded from the dry seasons in Fig. 3.6.

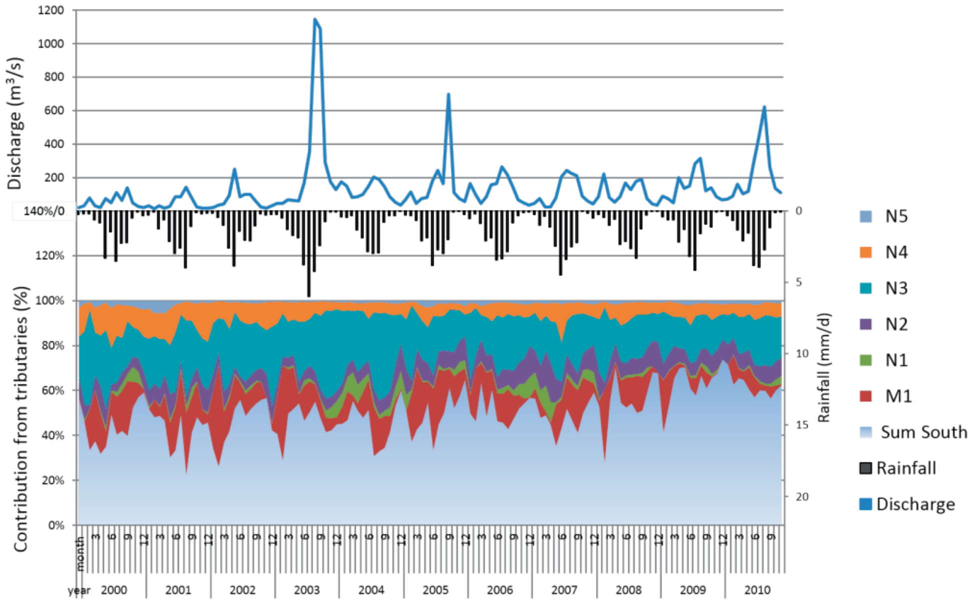

Figure 3.6 *Monthly averaged percentage contribution of all tributaries to the total discharge and monthly average rainfall and discharge of the whole catchment over the 10 years.*

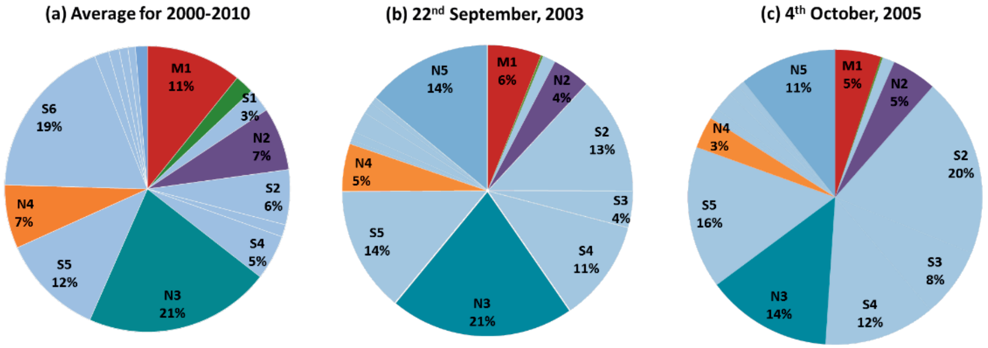

Figure 3.7 *Pie chart of contribution of different tributaries for the entire period (2000-2010), and for the floods on 22nd September, 2003 and 4th October, 2005 respectively.*

3.4 Discussion

3.4.1 Model performance

In this study, the LISFLOOD model was applied for the first time to the Wei River Basin in China in order to analyse the flood and low flow characteristics with the simulation of 31 existing big reservoirs. The limited data availability is a drawback for the analysis which is the cause of uncertainty of the results. To overcome the data availability limitation, several globally available datasets (e.g. soils, topography, river and reservoir parameters) were used.

With the model calibration and validation results, we concluded that the monthly averaged performance of the model is better than the daily performances. On the one hand, this fact is well acknowledged mainly due to the mistiming of the daily peaks in the simulations vs the observations, and also specifically due to the poor quality of the observation data used in this study. On the other hand, the LISFLOOD model was designed and simulated with a special emphasis on flood (high peak) simulation. Therefore, although the overall statistics seem low, the statistics for the flood years (2003 and 2005 in the calibration period and 2010 in the validation period) are in general much better even by looking only at the daily scores (Table 3.4). Besides these three years, the other years in the study period are rather dry which lead to a worse performance of the model. Criteria given by Moriasi et al. (2007) is only applicable for the monthly NSE score. The processes that contribute to discharge are averaged for bigger catchments, as water storage in soils, groundwater etc. contributes to decrease the variability of rainfall-runoff response observed in smaller catchments (Blöschl and Sivapalan, 1995), making larger catchments easier to simulate.

Table 3.4 *Single year statistics based on the daily simulated discharge against observed discharge at different stations (years in red meaning years with flood (wet year), years in grey meaning years without flood (dry year)).*

		NSE	Pbias	R^2	NSE	Pbias	R^2	NSE	Pbias	R^2	NSE	Pbias	R^2
Calibration Period		2000			2001			2002			2003		
	HM1	0.41	-53.5%	0.7	0.5	-47.4%	0.64	0.42	-12.2%	0.54	0.8	25.2%	0.88
	HS2	-	-	-	-0.59	-97.5%	0.23	0.13	-81.4%	0.49	0.75	-2.3%	0.8
	HS3	-	-	-	0.19	-27.4%	0.36	0.27	-21.0%	0.31	0.44	58.1%	0.61
	HS4	-	-	-	-0.33	-87.3%	0.38	0.29	-46.0%	0.35	0.76	18.6%	0.81
	HS5	-	-	-	-0.3	-83.5%	0.34	0.41	-20.2%	0.46	0.73	22.7%	0.74
	HN1	-0.19	-19.5%	0.13	-	-	-	0.17	-48.1%	0.26	0.51	4.2%	0.52
	HN2	-0.15	-36.8%	0.09	0.2	-59.7%	0.29	0.12	-31.6%	0.25	0.86	5.9%	0.86
		2004			2005			2006			2007		
	HM1	-0.22	8.7%	0.28	0.76	-11.5%	0.78	-0.27	4.9%	0.4	0.65	-22.7%	0.69
	HS2	-0.7	-70.7%	0.01	0.81	-32.9%	0.84	-0.13	-59.3%	0.07	0.31	-72.0%	0.45
	HS3	-0.35	30.4%	0.02	0.58	25.5%	0.65	-0.77	8.2%	0.05	0.43	-7.0%	0.44
	HS4	-0.04	-38.6%	0.03	0.85	-21.0%	0.86	-0.72	-40.5%	0	0.2	-51.0%	0.23
	HS5	-0.1	1.5%	0.02	0.8	23.2%	0.81	-1.12	15.0%	0	0.35	-14.3%	0.37
	HN1	0.42	-10.9%	0.47	-	-	-	-0.49	-22.2%	0.17	0.24	-46.0%	0.44
	HN2	0.01	24.7%	0.09	-0.29	2.3%	0.2	-2.89	19.5%	0.27	0.4	-26.5%	0.49

Validation Period		2008			2009			2010		
	HM1	0.17	-3.0%	0.36	0.53	26.7%	0.68	0.51	31.7%	0.67
	HS2	0.59	-44.7%	0.67	0.32	-1.1%	0.52	-0.24	2.8%	0.4
	HS3	-0.09	98.1%	0.41	0.33	70.5%	0.43	0.55	36.9%	0.58
	HS4	0.48	-7.1%	0.59	0.38	34.4%	0.4	0.08	54.3%	0.42
	HS5	0.39	28.5%	0.49	0.31	59.6%	0.45	0.04	65.1%	0.36
	HN1	-1.08	-25.7%	0.17	0.08	-50.5%	0.28	0.37	-46.7%	0.48
	HN2	-0.7	-14.5%	0.29	-0.12	-24.5%	0.3	0.56	-4.1%	0.57

Concerning the data uncertainties, it has been studied that both the rain gauge density/distribution and the interpolation method can affect the result of hydrological modelling (Zeng et al., 2018; Younger et al., 2009). However, Johansson and Chen (2003) has found that the relationships between the precipitation and some covariates for interpolation, such as topography indexes or terrain elevation, are less clear on a daily time scale. Therefore, the limitation of precipitation data is an unavoidable factor for the uncertainty in hydrological data. In this study, since the southern part of the catchment lies mostly in mountain ranges, the orographic effect is strong. Because there was no meteorological gauging station in the whole mountain region, the hydrological gauging stations which keep records of precipitation had to be used. However, even these gauging stations are mainly located on the floodplain at the mountain footslopes, which does not represent the orographic effect either. Johansson and Chen (2003) suggested that among all variables that can be used to describe precipitation patterns, the most important variable is the orographic factor. To present the catchment in a more realistic way, three virtual rainfall points were created to simulate the precipitation from the mountains. To a certain extent, the data from the virtual rainfall points are synthetic and therefore of limited data quality. In particular, the rainy days are not able to be simulate correctly, since the synthetic precipitation that are created only happens on the days when the correlated hydrological gauging station recorded a precipitation; however in reality, the precipitation at the virtual points might happen one day before or after the neighbour stations, or even in additional rainy days. Nevertheless, the calculation of the precipitation by correlating the neighbour hydrological gauging stations with orographic factor represent better the reality than no data at all. This is also the reason why southern stations all have a relatively low daily NSE value. The HS3 station is particularly bad because the virtual rainfall points have a bigger impact on this station than on the others. Therefore the model results of this study need to be carefully interpreted taking this low performance into account.

In terms of the interpolation of the point data, as it is suggested that the Inverse Distance Weighted (IDW) method is a relatively better interpolation method in many cases (Ruelland et al., 2008), this study applied the IDW method to interpolate the spatial pattern of the daily precipitation. However, the performance for daily data by IDW interpolation can be limited by the low density of the gauging station and the big climatic gradient. Nonetheless, the calibration result of the model is generally good meaning this study have limited the impacts of rainfall data uncertainty to an acceptable level.

With respect to the better performance in the calibration period than in the validation, several reasons can explain this. First, the validation period is much drier than the calibration period, as can be seen from the hydrograph of HM1 station (Fig. 3.4; maximum discharge around 2000 m^3/s compared to 5000 m^3/s). Also, the land use map used in this study is from the year 2000, and the land use are expected to have changed a lot in 10 years, especially considering that the study area is in China with fast development and change. The further it is from 2000, the more bias we could get from the land use changes. Moreover, although the reservoirs are simulated in the model, the actual reservoir functionality is unknown, and particular decisions (e.g. larger flow release during some of the drier years in the second period) can lead to a large uncertainty which cannot be addressed in the reservoir simulation module. Nevertheless, this model application was designed for flood simulation; the daily scores for each individual year of all stations (Table 3.4) clearly showed that the daily score for the wet years (2003, 2005, 2010 in which a flood occurred in the catchment) are good, except for some small bias. Therefore, while the dry years might compromise the overall performance of the model, the performance for flood assessment is noticeably better. And since in our calibration period (2000-2007), there are more wet years (2003 and 2005) than in the validation period (2010), the overall performance of the calibration is also better than the validation.

This study included the reservoir functionality to a certain extent, some general parameters were applied to all reservoirs and only two sets of parameters were applied to each catchment representing the average performance of the reservoirs for each catchment. However, without the actual functionality data of each reservoir, and considering the lack of any surface area or the volume data of the reservoirs, it is not easy to evaluate or validate each reservoirs functionality regarding their contributions to the reduction of the floods. The reservoirs are presented in the model as points due to the design of the model, which compromised the simulation with surface area related processes, such as evaporation. This is, however, simulated by the land use type of open water by regarding the reservoir point as open water land use, which is a valid simplified solution to this problem.

3.4.2 Application of the LISFLOOD model

As an important step in understanding the cause of the flood in the floodplain, this study started a contribution analysis from the tributaries to the flood discharge to a) identify the contribution of the tributaries for proposing the locations of the new dams in the scenario analysis; b) be used as model evaluation tool to see if the result is identical with the flood records; and c) set as an example for the application of the LISFLOOD model. The result of the contribution analysis of the two largest floods that occurred in 2003 and 2005 are identical with the previous findings (Jiang et al., 2004; Liang, 2006; Pang, 2007). In our study, the contribution of tributaries was calculated as the discharge from each tributary divided by the sum of all the tributaries. In this way, the contribution to the flood at a certain point is not completely accurate due to the propagation of the flood process along the stream.

The area upstream of the main river was identified as the most important factor for flood occurrence in the past 60 years (Gai et al., 2017), and it was shown again in the contribution analysis (Fig. 3.5) that the upstream station contributed 11% to the total discharge during the wet period (March to October). However, it was not identified as the biggest contributor to the floods that occurred in 2003 and 2005. In these flood events, the contribution of the southern catchments to the flooding was higher because of the steep slopes and fast drainage towards the floodplain. Especially when the rain falls into the southern mountain area, most of the southern tributaries contribute simultaneously to the flood discharge. Therefore, it highlights the necessity of separating the flood analysis from the normal streamflow analysis of any of the catchments (Merz et al., 2006; Ravazzani et al., 2015).

Hydrological modelling is usually more challenging than statistical methods due to its high demand for data and long computing time as well as the associated uncertainties (Requena et al., 2016). With the development of remote sensing technologies, an increasing number of globally available high quality datasets are used in hydrological modelling (Alfieri et al., 2015; Massari et al., 2014). This study has shown the possibility of using global datasets for the LISFLOOD model, which is designed as a generalistic model applicable anywhere, taking the computation time and representative resolution into account. Although the local meteorological and hydrological gauge station data were used in the present study, testing model performance using global precipitation datasets is ongoing. In conclusion, we applied the LISFLOOD model as a generalistic physically-based model with global datasets, which is opposed to empirical regionalized hydrological models.

By applying the LISFLOOD model to simulate the discharge at all 19 tributary outlets, we conducted a contribution analysis. The identified contributing tributaries in our study for the whole period and the two single flood events are the same as from the study of Gai et al. (2017). This indicates that the LISFLOOD model can be used for flood event identification or flood discharge forecasting with decent data inputs.

3.5 Conclusions

The calibration and validation results of the application of the LISFLOOD model in the Wei River Basin are very good (monthly NSE =0.79) for the whole catchment. With the simulated daily streamflow from the model, the contribution of the tributaries to the total discharge were analysed, showing that the mainstream and the northern tributaries are the largest contributors to the overall discharge. Meanwhile, the contribution of the flood events may differ from the northern tributaries to the southern ones. With access to the increasing number of global datasets and the development of computing power, including the possibility to define spatial and temporal resolution, LISFLOOD has proven to be an sophisticated model for flood discharge simulation at the catchment scale.

Acknowledgements
This study was part of the China-Netherlands Joint Scientific Thematic Research Programme (JSTP) supported by the External Cooperation Program of the Chinese Academy of Sciences (GJHZ1018) and Netherlands Organization for Scientific Research (NWO, OND1339291). The authors would like to thank the Institute of Soil and Water Conservation, Northwest A&F University/Chinese Academy of Sciences and the Ministry of Water Resources for their help and support and the National Natural Science Foundation of China. J.P. Nunes and Hongming Zhang was supported by a research grant from the Fundação para a Ciência e a Tecnologia (IF/00586/2015) and the National Natural Science Foundation of China (Grant No.: 41771315) respectively. Our thanks also goes to Hylke Beck for his help with the LISFLOOD calibration model and the Data Sharing Infrastructure of Earth System Science – Data Sharing Service Centre for the Loess Plateau for their help with the data collection.

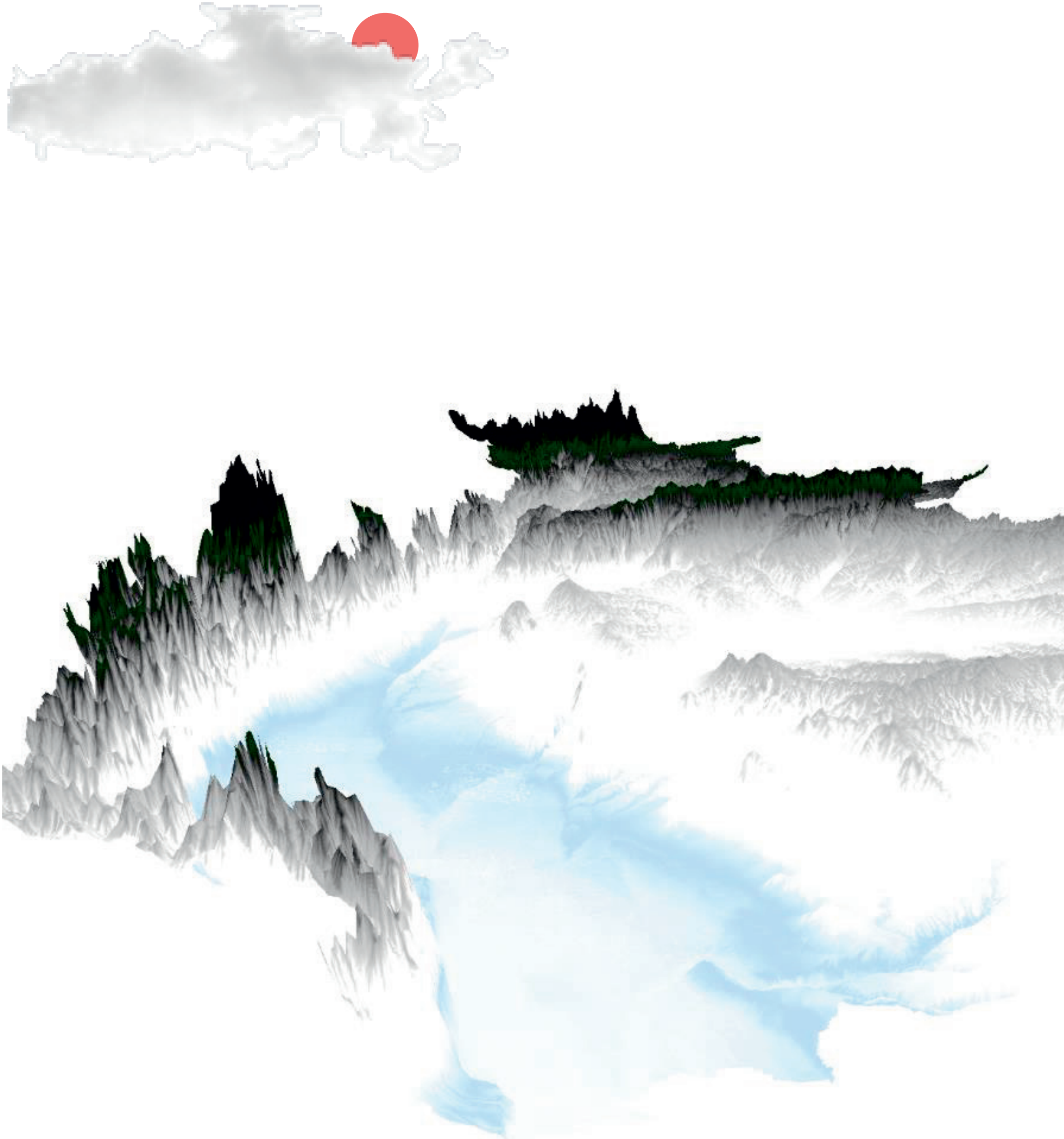

4. Evaluation of different meteorological datasets for flood discharge simulation with the LISFLOOD model

The quality of the meteorological data inputs into the hydrological model is of vital importance for understanding the hydrological cycle as well as for hydrological extreme analysis and prediction. Many efforts have been made to develop global freely available meteorological reanalyses data especially aiming at being applied for data scarce regions. With the Coordinated Regional Climate Downscaling Experiment (CORDEX) frame, regional specific climate models were developed for future climate change projections. This study evaluated ten global freely available datasets, including The Global Meteorological Forcing Dataset for land surface modelling, the National Centres for Environmental Prediction (NCEP) Climate Forecast System Reanalysis (CFSR) and CORDEX-East Asia, for discharge simulation by the physically distributed hydrological model LISFLOOD in the Wei River Basin in China. The results reveal that none of the evaluated datasets can be applied directly for daily discharge simulation with the LISFLOOD model, being an essential modelling tool for flood analysis. An in-depth analysis of precipitation and temperature data against observations showed large differences and accuracy between the ten different meteorological datasets.

Based on:

L. Gai, J. P. Nunes, J. E.M. Baartman, H. Zhang, F. Wang, A. de Roo, C. J. Ritsema, V. Geissen. Evaluation of different meteorological datasets for flood discharge simulation with the LISFLOOD model, submitted to Hydrology and Earth System Sciences.

4.1 Introduction

The increasing application of hydrological models to improve understanding of the hydrological cycle, assessing the anthropogenic impact on water resources, flood and drought predictions as well as regional management planning requires a very large amount of data (Silberstein, 2006). Future flood risk analysis based on hydrological modelling is highly dependent on the accuracy of meteorological projections. Global climate models (GCMs) are useful tools for climate change projections; however, they are often criticized because of their limitation to produce a regional specific high-resolution prediction, and the uncertainties in GCMs are well recognized as a limitation for accurate future projections (Park et al., 2016). Therefore, climate scenarios with meteorological data downscaled to regions of interest are often the solution. Nevertheless, the quality of the outputs of regional models is essential for the uncertainty of the hydrological modelling results. As the key components of the water balance, the simulation of precipitation and evapotranspiration have a substantial impact on modelling results (Andréassian et al., 2004; Michaelides et al., 2009; Masih et al., 2011; Dan Li et al., 2018). Different from the precipitation data, evapotranspiration is difficult to be either directly measured or derive from the water balance. Although studies have explored different methods to estimate evapotranspiration (Jung et al., 2016; Zhenzhong et al., 2012), temperature data are generally needed for calculating evapotranspiration. Therefore, the spatial and temporal accuracy of the precipitation and temperature datasets are of paramount importance for hydrological modelling especially to estimate and predict hydrological extremes (Oudin, 2006; Koutsouris et al., 2017).

In general, there are three ways to obtain precipitation and temperature data: gauge data, remote sensing (radar and satellite) and “reanalysis” data (Beck et al., 2017, Michaelides et al., 2009). Surface gauge stations are often too sparse to represent the meteorological pattern over large watersheds (Fuka et al., 2014), and many areas even lack monitoring stations. Remote sensing data usually has a good simulation for temperature (Benali et al., 2012; Stisen et al., 2007) while having the disadvantage of the systematic error mostly related with snow detection and the orographic effect of the topography (Duan et al., 2016; Kimani et al., 2017; Milewski et al., 2015; Sharifi et al., 2016; Bai et al., 2018; Changming Li et al., 2018). Recent efforts have been putting on generating globally available meteorological datasets with a combination of weather forecasting models and assimilation of observations, which is called “reanalysis” (Essou et al., 2017). Due to the complete temporal resolution and spatial representation of the meteorological pattern, reanalyses are recognized currently as the potentially best driving force for hydrological models (Essou et al., 2017; Essou et al., 2016; Lauri et al., 2014).

The most commonly used reanalyses include the Modern-Era Retrospective Analysis for Research Applications (MERRA) from the US National Aeronautics and Space Administration (NASA) (Rienecker et al., 2011), the interim Reanalysis (ERA-Interim) from the European Centre for Medium-Range Weather Forecasts (ECMWF) (Dee et al., 2011), and the Climate Forecast System Reanalysis (CFSR) from the US National Centres for Environmental Prediction (Saha et al., 2010). Studies have found that the above-mentioned reanalyses pattern are able to capture the seasonal or annual cycle of the meteorology in many regions of the world on a large spatial scale (Smith and Kummerow, 2013; Worqlul et al., 2014; Chen et al., 2014; Auger et al., 2018; Gao et al., 2014; Zhang et al., 2018), and they have been widely applied to drive hydrological models to compare simulated streamflow with observation records (Dile and Srinivasan, 2014; Essou et al., 2016; Fuka et al., 2014; Gao et al., 2012; Hu et al., 2017; Lauri et al. 2014). In contrast to the lack of terrestrial observations, the relative wealth of observations of the atmosphere and sea surface has also allowed the emergence of a number of other global long-term reanalysis datasets, such as the National Centers for Environmental Prediction–National Center for Atmospheric Research (NCEP–NCAR, Kalnay et al., 1996; Kistler et al., 2001), the 40- and 15-yr European Centre for Medium-Range Weather Forecasts (ECMWF- ERA-40 and ERA-15; Gibson et al., 1997), the NCEP– Department of Energy (DOE; Kanamitsu et al., 2002), and the National Aeronautics and Space Administration Data Assimilation Office (NASA DAO; Schubert et al., 1993) reanalyses (Sheffield et al., 2006).

The Coordinated Regional Climate Downscaling Experiment (CORDEX) was launched in 2009 to improve regional climate change projections, enabling the possibility to evaluate the performance of different Regional Climate Models (RCMs) with the current situation for predefined regions worldwide (Giorgi et al., 2009). Different regions conducted their own regional climate models. The recent generation of regional climate models dedicated to China is presented in CORDEX-East Asia (CORDEX-EA). A few studies have evaluated the consistency between the dataset and the meteorological observations for the Eastern Asia region (Myoung-Jin et al., 2017, Wang et al., 2018) with variable results; however, this dataset has not yet been applied to evaluate its impact on the hydrological modelling results.

This study aimed to evaluate if current freely available global reanalysis and CORDEX datasets can be used as direct input for the physically based rainfall-runoff LISFLOOD model to analyse floods in the Wei River basin, a semi-arid catchment in China.

4.2 Methodology

4.2.1 Application of the LISFLOOD model in the Wei River Basin

The Wei River in China originates from the Niaoshu Mountains in Gansu province and runs through the Loess Plateau east into the Yellow River. With a total length of 818 km, the Wei River Basin covers three provinces and has a total catchment area of 134,800 km^2 (Fig. 4.1).

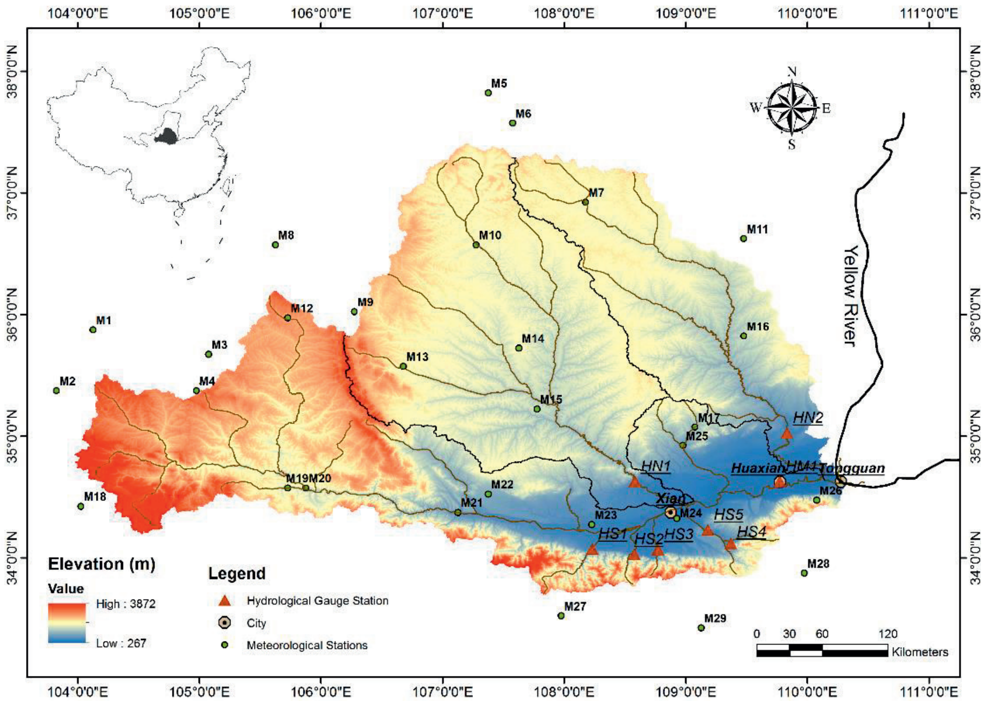

Figure 4.1 *Study area and distribution of the meteorological and hydrological stations (M: meteorological station, 1-29 are meteorological stations with temperature data, H: hydrological gauge stations with observed discharge data; S: southern catchments; N: northern catchments; M: main river).*

Under the control of the continental summer monsoon, the average annual precipitation of the whole basin is about 570 mm. Over 60% of the annual precipitation falls in the flood season from July to September (Gao et al., 2013). The southern catchments of the Wei River Basin are located on the northern side of the Qinling Mountain rainge characterized by steep slopes and an earth-rock mountain landscape, with an average annual precipitation of around 800 mm. The Qinling Mountain range is the highest east-west trending mountain range and the dividing line between the northern warm-temperate and southern subtropical zones in central China (Jun-ping and Yan-sui, 2001). The northern catchments of the Wei River form part of the Loess Plateau with gentler slopes. The largest two tributaries of the Wei River - Jing River and Beiluo River – are located on the northern side of the Wei River and comprise 34% and 20% of the total catchment area of the Wei River Basin, respectively.

The LISFLOOD model is a spatially distributed and physically-based rainfall-runoff model (De Roo et al., 2001; van der Knijff et al., 2010). Model application consists of three parts: the LISVAP model, the LISFLOOD model and the LISFLOOD calibration model. The simulation of the evapotranspiration is conducted with the LISVAP model involving the calculation of a 'potential reference' evapotranspiration rate - *ET*0 (Allen et al., 1998), a potential soil evaporation rate - *ES*0, and potential evaporation of an open water surface, *EW*0. The detailed calculation of the evaporation in LISVAP model is shown in Supplementary Material S.1.

In the calculation of the evapotranspiration, only maximum, minimum and average daily temperature is needed (Van der Kniff, 2008). The processes included in the LISFLOOD model are snowmelt, infiltration, interception of rainfall, leaf drainage, evaporation and water uptake by vegetation, surface runoff, preferential flow, soil moisture distribution, drainage to the groundwater, sub-surface and groundwater flow, reservoirs and river channel routing (Thielen et al., 2009; van der Knijff et al., 2010; Pappenberger et al, 2011; Burek et al., 2013; Thiemig et al., 2015). The detailed model description and equations can be found in (Burek et al., 2013).

In order to set up the baseline run of the discharge and potential evapotranspiration of the Wei River Basin, the LISFLOOD model was firstly calibrated and validated with the gauge station data for the period of 2000-2010. The detailed application of the LISFLOOD model in the Wei River Basin can be found in Gai et al. (2019). Only the description with respect to the application of the forcing datasets are given in this paper. In total 29 meteorological gauge stations located in and around the study area were selected to obtain the daily precipitation(p), maximum (tx), minimum (tn) and averaged temperature (ta) data (Fig. 4.1). In addition, the daily precipitation data from six hydrological gauge stations in the southern catchments and three virtual precipitation points generated based on an orographic correction factor of 1.7 from the closest hydrological gauge station records, were used as the observation forcing dataset to drive the LISFLOOD model (Gai et al., 2019). Daily precipitation and temperature maps were generated using the Inverse Distance Weighting (IDW) interpolation at a spatial resolution of 0.05˚ as input to the LISFLOOD model. A multi-objective generic algorithm was used to calibrate the simulated streamflow against observations of the hydrological stations, aiming at obtaining a Pareto optimal solution by using the Nash–Sutcliffe model efficiency coefficient (NSE) as the objective function.

4.2.2 Evaluation of the forcing datasets using LISFLOOD model

To test the effect of different reanalysis datasets on the simulated hydrological response, this study chose the Global Land Surface Forcing Datasets developed by Princeton University, the Global Weather Data for SWAT and a subsample of the CORDEX-EA datasets based on the following criteria: a) globally and freely available and including precipitation and minimum and maximum temperature variables; b) spatial resolution not larger than 0.5˚; c) temporal range covering the records for as much as possible the period of 2000-2010 for calibration and validation which is consistent with the available observed discharge data, with a temporal resolution of one day. The CORDEX-EA dataset was chosen specifically due to the preference of having future projections for the purpose of assessing the flood risks under future climate change prediction.

4.2.2.1 Princeton Dataset (hereafter Princeton)

The Global Meteorological Forcing Dataset for land surface modelling (the Princeton Dataset) provides near-surface meteorological data for driving land surface models and other terrestrial modelling systems. It is based on the National Centres for Environmental Prediction–National Centre for Atmospheric Research (NCEP-NCAR) reanalysis, in combination with a suite of global, observation–based datasets of precipitation, temperature, and radiation (Sheffield et al., 2006). The dataset combines both reanalysis data and observations. The data used for this study is under a spatial resolution of 0.25˚ and temporal resolution of one day for the period of 2000-2010.

4.2.2.2 Global Weather Data for SWAT (hereafter CFSR)

The National Centres for Environmental Prediction (NCEP) Climate Forecast System Reanalysis (CFSR) was designed and executed as a high resolution global dataset to provide the best estimation of the atmosphere-ocean-land surface-sea ice system for the application of The Soil & Water Assessment Tool. The current CFSR dataset covered the period of 1979-2014. The resolution of the CFSR is 0.33˚ (about 38km). The daily precipitation, minimum and maximum temperature data were downloaded from the website https://globalweather.tamu.edu/#pubs. This study used the data for the period of 2000-2010.

4.2.2.3 CORDEX-EA

Three RCMs of the CORDEX-EA project were evaluated in this study: The Regional Climate Model version 4 (RegCM4), the Hadley Centre Global Environmental Model version 3-Regional climate model (HadGEM3-RA) and the Yonsei University Regional Spectral Model

(YSU-RSM). The model domain follows a protocol of the Coordinated Regional climate Downscaling Experiment (CORDEX) for Asia, East Asia, India, the Western Pacific Ocean, and the northern part of Australia (Giorgi et al., 2009). All models were conducted with two experiments for the past, including two evaluation (hereafter EVA) experiment, except for HadGEM3-RA, and one historical (hereafter HIS) experiment. Table 4.1 details the RCMs in the CORDEX-EA dataset.

4.2.2.4 Driving LISFLOOD model with the forcing datasets

The ten forcing datasets from the three sources mentioned above were used directly to drive the LISFLOOD model with the best Pareto front parameterization found in the calibration driven by the observation data (the baseline run of Gai et al, 2019). Then the simulated discharge under different forcing datasets was compared with the discharge records from the seven hydrological gauges (hereafter OBS) as well as the baseline run of the model (hereafter BAU). The seven hydrological gauge stations with the observation discharge data are located in the southern catchments (S1, S2, S3, S4), the northern catchments (N1, N2) and the main river (M1), respectively (Fig. 4.1). The comparison between the simulation under different forcing datasets and the model baseline run were demonstrated with the results for Xi'an, Huaxian and Tongguan cities, which are located in the floodplain. In order to better understand the impact of different reanalyses with respect to their precipitation and temperature simulation, the precipitation and temperature data of 29 points from each dataset was compared with nearby observation records from 29 meteorological gauges.

***Table 4.1**. RCMs used in this study*

Name	RegCM4 (KNU)	HadGEM3-RA (NIMR)	YSU-RSM
Horizontal resolution	50km	0.44˚	50km
Number of grid points (west-east x north-south)	243 x 197	220 x 183	241 x 198
Available temporal resolution	3-hourly, day, month	3-hourly, 6-hourly, day, month	3-hourly, day, month
Land Surface model	NCAR CLM 3.5	MOSES-II	NOAH LSM
Reference	(Giorgi et al., 2012)	(Davies et al., 2005)	(Hong et al., 2013)
Initial and boundary conditions	Evaluation (EVA): EVA1: ERA-Interim reanalysis EVA2: NCEP-DOE reanalysis (except for HadGEM3-RA) Historical (HIS): HadGEM2-AO historical simulation		
Simulation of Evaluation period	1989-2008 (RegCM4(KNU) model only run until 2007)		
Simulation of Historical period	1979-2005	1950-2005	1980-2005

The efficiency coefficients which are used to evaluate the goodness of fit between the simulation and the OBS/BAU run include the Nash-Sutcliffe model efficiency coefficient

(NSE) (Supplementary Material S.5), Percent bias (Pbias) (Supplementary Material S.9) and Pearson linear correlation coefficient (r) (Supplementary Material S.10).

4.2.3 Using bias corrected datasets to drive the LISFLOOD model

After evaluating the impact of different forcing datasets on the simulated hydrological response, the datasets that represent the best simulation result were selected for a bias correction in order to tackle the bias in the reanalyses (Bastola and Misra, 2014; Boé et al., 2007; Casanueva et al., 2016; Ngai et al., 2017). The bias correction method used in this study was quantile mapping (QM) as introduced by Gudmundsson (2016). The data points from each forcing dataset were firstly correlated with the closest meteorological gauge station for a quantile distribution, then all the data in each quantile were corrected based on the quantile factors obtained from the distribution. The bias correction procedure was conducted using the "QUANT" bias correction function in the "Qmap" package in R version 3.4.0. The bias corrected datasets were then applied to drive the LISFLOOD model for the discharge evaluation, which was done as explained in section 2. The datasets that has the best performance will then be calibrated with the LISFLOOD calibration tool. The calibration process is automated in Python programming language by using the Nash-Sutcliffe model efficiency coefficient as the objective function in a generic algorithm to calibrate the simulated discharge against the observations from the hydrological stations (Gai et al., 2019). A Pareto optimal solution including all the parameters was then obtained after the calibration.

4.3 Results

In order to examine the accuracy of the forcing datasets for driving LISFLOOD model, the result part of the study is organized in the following way: we first compared the observed and the simulated results from the model by using the ten different datasets. Then, the three best-performing datasets were chosen for the quantile mapping bias correction and further calibration. Again, the results between the simulated and observed discharge were shown before and after bias correction and calibration. Finally, we explore the reasons of differences in performance by an in-depth analysis of the precipitation and temperature (and resultant evaporation) data.

4.3.1 Discharge analysis

4.3 1.1 Simulation vs Observation

With the same parameter set as the baseline run (model), the simulated discharge driven by different forcing datasets were compared with the observed discharge at seven hydrological gauge stations. Statistical results of the daily and monthly discharge are shown in Fig. 4.2 and Fig. 4.3, respectively. Almost all datasets except for the Princeton dataset overestimated the discharge (Pbias>0) in the northern catchments (N1 and N2). In the southern catchments, discharge were underestimated by Princeton, CFSR and NIMR-2 datasets for all the four stations. Overall the performance of the forcing datasets regarding the simulated discharge from LISFLOOD model, as judged from the NSE values, was rather bad (NSE < 0). The performance of Princeton, KNU-3 and NIMR-1 datasets are slightly better than all other datasets with a higher NSE, especially in the southern catchments. With regards to the CORDEX-EA RCMs, the RegCM4 (KNU) model remarkably overestimated the discharge in the whole basin for all the two evaluations and one historical simulation.

4.3.1.2 Discharge simulated from the bias corrected datasets

Based on the daily and monthly statistics from the previous section, the Princeton, KNU-3 and NIMR-1 datasets were chosen for bias correction due to their relatively good performance. The simulation of the discharge by the LISFLOOD model using bias corrected datasets only showed an improvement at the main station (Fig. 4.4 and Fig. 4.5). Especially with the KNU-3 and NIMR-1 model, for both the southern and northern stations, the bias corrected forcing datasets decreased the discharge by reducing the peak precipitation. Therefore, the good monthly simulation at the main outlet of the catchment is probably achieved by compromising the good performance of the southern catchments to decrease the discharge from the northern catchments, which are the largest contributor to the main river discharge. Therefore, the southern catchments and the northern catchments need to be corrected separately.

		Princeton	SWAT	KNU_1	KNU_2	KNU_3	NIMR_1	NIMR_2	YSU_1	YSU_2	YSU_3	Model
S1	NSE	-0.25	-0.11	-1.54	-1.74	-0.29	0.06	-0.15	-1.00	-1.07	-1.68	0.55
	Pbias	-40%	-94%	184%	91%	88%	22%	-55%	4.4%	-22%	46%	-35%
	R^2	0.05	0.01	0.18	0.00	0.26	0.16	0.00	0.01	0.00	0.02	0.79
S2	NSE	0.03	-0.09	-0.28	-0.48	0.19	0.12	-0.06	-0.23	-0.33	-0.47	0.41
	Pbias	-52%	-87%	149%	60%	58%	8.3%	-60%	-0.7%	-29%	38%	32%
	R^2	0.06	0.02	0.18	0.00	0.24	0.12	0.00	0.01	0.00	0.02	0.70
S3	NSE	-0.19	-0.14	-1.39	-1.24	-0.01	0.09	-0.14	-1.21	-1.74	-1.35	0.46
	Pbias	-63%	-95%	190%	52%	71%	-29%	-89%	50%	51%	86%	-8.8%
	R^2	0.02	0.00	0.17	0.00	0.27	0.10	0.01	0.01	0.00	0.02	0.70
S4	NSE	-0.05	-0.15	-0.27	-0.42	0.27	0.12	-0.12	-0.49	-0.55	-0.50	0.50
	Pbias	-60%	-92%	156%	55%	59%	-8.1%	-77%	38%	20%	77%	21%
	R^2	0.05	0.01	0.22	0.00	0.33	0.14	0.01	0.01	0.00	0.02	0.74
N1	NSE	0.07	-0.48	-220	-39.1	-61.1	-4.87	-1.55	-12.6	-3.94	-36.7	0.38
	Pbias	-43%	85%	2489%	1108%	1384%	356%	53%	498%	81%	941%	-26%
	R^2	0.13	0.07	0.13	0.00	0.14	0.19	0.02	0.05	0.00	0.09	0.65
N2	NSE	-0.36	-1.90	-626	-102	-140	-6.89	-3.95	-141	-46.8	-234	0.51
	Pbias	-51%	95%	3444%	1545%	1719%	325%	26%	1120%	565%	1746%	-12%
	R^2	0.03	0.01	0.21	0.00	0.26	0.27	0.00	0.05	0.01	0.10	0.73
M1	NSE	0.17	-0.03	-99.2	-24.0	-25.1	-2.45	-1.17	-12.7	-4.84	-25.1	0.69
	P bias	-30%	69%	1453%	737%	793%	260%	95%	371%	111%	599%	0.9%
	R^2	0.21	0.24	0.31	0.00	0.44	0.37	0.02	0.06	0.01	0.10	0.86

Figure 4.2. *Efficiency coefficients of the daily observation discharge against the simulated discharge from the model runs using different forcing datasets at seven hydrological gauging stations. (RCMs and the initial and boundary conditions: KNU-1: RegCM4-EVA1; KNU-2: RegCM4-EVA2; KNU-3:RegCM4-HIS; NIMR-1: HadGEM3-RA-EVA1; NIMR-2: HadGEM3-RA-HIS; YSU-1: YSU-RSM-EVA1; YSU-2: YSU-RSM-EVA2; YSU-3: YSU-RSM-HIS. Model: The calibrated model run by using meteorological observation data, from Gai (2019). : negative NSE score : 0<NSE <0.5 : NSE >0.5).*

		Princeton	SWAT	KNU-1	KNU-2	KNU-3	NIMR-1	NIMR-2	YSU-1	YSU-2	YSU-3	Model
S1	NSE	0.52	-0.55	-2.81	-3.69	-0.38	0.30	-0.49	-0.78	-2.10	-1.57	0.60
	Pbias	-40%	-94%	183%	114%	88%	22%	-50%	4.8%	-12%	46%	-34%
	R^2	0.62	0.01	0.34	0.04	0.41	0.38	0.04	0.10	0.02	0.10	0.86
S2	NSE	0.17	-0.50	-1.29	-1.51	0.37	0.33	-0.28	-0.27	-0.99	-0.70	0.28
	Pbias	-52%	-87%	150%	72%	58%	8.4%	-57%	-0.6%	-24%	39%	32%
	R^2	0.45	0.08	0.49	0.02	0.58	0.38	0.02	0.07	0.00	0.09	0.88
S3	NSE	0.08	-0.69	-3.61	-2.28	0.09	0.21	-0.61	-1.80	-4.57	-2.77	0.57
	Pbias	-63%	-95%	190%	66%	71%	-29%	-88%	50%	64%	87%	-8.8%
	R^2	0.39	0.00	0.41	0.01	0.59	0.28	0.04	0.05	0.01	0.07	0.85
S4	NSE	0.13	-0.61	-1.24	-1.06	0.44	0.30	-0.41	-0.78	-1.42	-1.13	0.50
	Pbias	-60%	-92%	157%	68%	59%	-8.3%	-75%	38%	29%	78%	21%
	R^2	0.44	0.01	0.49	0.00	0.64	0.37	0.10	0.04	0.01	0.07	0.88
N1	NSE	0.32	-1.37	-698	-119	-194	-15.5	-3.31	-35.2	-8.48	-110	0.54
	Pbias	-42%	86%	2476%	1098%	1369%	350%	50%	496%	80%	937%	-25%
	R^2	0.47	0.12	0.31	0.02	0.36	0.41	0.07	0.20	0.01	0.26	0.82
N2	NSE	-0.28	-3.47	-1458	-230	-326	-15.0	-4.34	-258	-98.8	-486	0.69
	Pbias	-50%	96%	3438%	1553%	1712%	319%	29%	1120%	567%	1746%	-11%
	R^2	0.12	0.01	0.33	0.00	0.40	0.56	0.03	0.11	0.02	0.21	0.87
M1	NSE	0.47	-0.22	-184	-51.4	-46.8	-4.68	-2.38	-20.9	-9.76	-41.7	0.79
	Pbias	-30%	69%	1450%	795%	790%	258%	107%	371%	126%	600%	0.9%
	R^2	0.55	0.35	0.48	0.01	0.68	0.57	0.04	0.11	0.02	0.18	0.94

Figure 4.3. *Efficiency coefficients of the monthly observation discharge against the simulated discharge from the model runs using different forcing datasets at seven hydrological gauging stations. (RCMs and the initial and boundary conditions: KNU-1: RegCM4-EVA1; KNU-2: RegCM4-EVA2; KNU-3:RegCM4-HIS; NIMR-1: HadGEM3-RA-EVA1; NIMR-2: HadGEM3-RA-HIS; YSU-1: YSU-RSM-EVA1; YSU-2: YSU-RSM-EVA2; YSU-3: YSU-RSM-HIS. Model: The calibrated model run by using meteorological observation data, from Gai (2019).* *: negative NSE score* *: 0<NSE <0.5* *: NSE >0.5).*

The LISFLOOD model was calibrated using the bias corrected datasets, namely KNU-3, NIMR-1 and Princeton. The efficiency coefficients of the daily and monthly discharge simulated against the observations are shown in Fig. 4.4 and Fig. 4.5, respectively. The bias corrected KNU-3 and NIMR-1 datasets have increased the NSE value of all stations after calibration, especially at the main station (Huaxian). The bias correction decreased the discharge of all stations and the calibration processes modified the distribution of the peak and base flows. The hydrographs of the discharge driven by the before-bias-corrected, after-bias-corrected and after calibrated three datasets are shown in Fig. 4.6. From the hydrograph and the NSE value, we can conclude that the bias corrected NIMR-1 datasets and the bias corrected KNU-3 datasets after calibration best simulated the discharge at the main station. Although the calibration has increased the general score of the main station and the southern catchments, the performance of the northern catchments remains rather poor.

		Before bias correction			After bias correction			After bias correction & calibration		
		KNU_3	NIMR_1	Princeton	KNU-3	NIMR-1	Princeton	KNU-3	NIMR-1	Princeton
M1	NSE	-25.06	-2.45	0.17	-1.00	0.35	0.16	-6.33	-0.39	-3.15
	Pbias	793%	260%	-30%	197%	25%	34%	258%	9.2%	179%
	R^2	0.44	0.37	0.21	0.42	0.37	0.21	0.15	0.29	0.19
S1	NSE	-0.29	0.06	-0.25	-0.04	-0.07	-0.14	0.45	0.37	0.22
	Pbias	88%	22%	-40%	-95%	-94%	-90%	9.4%	-0.2%	-3.1%
	R^2	0.26	0.16	0.05	0.26	0.08	0.02	0.49	0.44	0.22
S2	NSE	0.19	0.12	0.03	-0.04	-0.07	-0.07	0.14	0.10	0.08
	Pbias	58%	8.3%	-52%	-90%	-88%	-85%	-64%	-33%	-39%
	R^2	0.24	0.12	0.06	0.26	0.06	0.04	0.21	0.12	0.10
S3	NSE	-0.01	0.09	-0.19	-0.08	-0.11	-0.15	0.17	0.05	0.06
	Pbias	71%	-29%	-63%	-91%	-91%	-87%	-66%	-46%	-44%
	R^2	0.27	0.10	0.02	0.08	0.03	0.01	0.26	0.09	0.09
S4	NSE	0.27	0.12	-0.05	-0.05	-0.09	-0.12	0.19	0.05	0.08
	Pbias	59%	-8.1%	-60%	-88%	-88%	-86%	-42%	-48%	-18%
	R^2	0.33	0.14	0.05	0.19	0.06	0.02	0.22	0.09	0.09
N1	NSE	-61.10	-4.87	0.07	-1.65	-4.14	-3.90	0.22	0.04	0.11
	Pbias	1384%	356%	-43%	218%	286%	337%	-2.4%	-6.0%	-19%
	R^2	0.14	0.19	0.13	0.17	0.17	0.15	0.30	0.11	0.12
N2	NSE	-139.79	-6.89	-0.36	-16.04	-2.31	-16.35	-1.19	-2.26	-2.18
	Pbias	1719%	325%	-51%	4901%	64%	449%	120%	118%	191%
	R^2	0.26	0.27	0.03	0.22	0.23	0.11	0.21	0.16	0.13

Figure 4.4. *Efficiency coefficients of the daily discharge simulated by using different forcing datasets compared to the observed discharge. (RCMs and the initial and boundary conditions: KNU-3:RegCM4-HIS; NIMR-1: HadGEM3-RA-EVA1. : NSE<0 : 0≤NSE<0.5 : NSE ≥0.5).*

		Before bias correction			After bias correction			After bias correction & calibration		
		KNU-3	NIMR-1	Princeton	KNU-3	NIMR-1	Princeton	KNU-3	NIMR-1	Princeton
M1	NSE	-46.79	-4.68	0.47	-2.16	0.60	0.35	0.59	0.58	0.44
	Pbias	790%	258%	-30%	198%	25%	34%	9.2%	-0.3%	-3.1%
	R^2	0.68	0.57	0.55	0.64	0.64	0.44	0.64	0.68	0.45
S1	NSE	-0.38	0.30	0.52	-0.36	-0.44	-0.36	0.23	0.32	0.36
	Pbias	88%	22%	-40%	-95%	-94%	-90%	-64%	-34%	-40%
	R^2	0.41	0.38	0.62	0.55	0.22	0.16	0.53	0.38	0.46
S2	NSE	0.37	0.33	0.17	-0.37	-0.4	-0.37	0.14	0.23	0.31
	Pbias	58%	8.4%	-52%	-90%	-88%	-85%	-67%	-47%	-44%
	R^2	0.58	0.38	0.45	0.6	0.26	0.24	0.56	0.37	0.47
S3	NSE	0.09	0.21	0.08	-0.44	-0.51	-0.33	0.48	0.14	0.37
	Pbias	71%	-29%	-63%	-91%	-91%	-87%	-42%	-48%	-19%
	R^2	0.59	0.28	0.39	0.31	0.11	0.37	0.61	0.3	0.4
S4	NSE	0.44	0.3	0.13	-0.34	-0.4	-0.28	0.49	0.07	0.38
	Pbias	59%	-8.3%	-60%	-88%	-88%	-86%	-2.7%	-6.3%	-19%
	R^2	0.64	0.37	0.44	0.36	0.15	0.56	0.56	0.29	0.43
N1	NSE	-194	-15.5	0.32	-5.35	-13.4	-12	-3.72	-7.36	-6.17
	Pbias	1369%	350%	-42%	217%	287%	337%	120%	118%	191%
	R^2	0.36	0.41	0.47	0.39	0.42	0.45	0.46	0.37	0.42
N2	NSE	-326	-15	-0.28	-33.1	-3.65	-29	-14.9	-0.95	-6.95
	Pbias	1712%	319%	-50%	491%	64%	450%	258%	9.1%	179%
	R^2	0.4	0.56	0.12	0.38	0.54	0.46	0.35	0.62	0.48

Figure 4.5. *Efficiency coefficients of the monthly discharge simulated by using different forcing datasets compared to the observed discharge. (RCMs and the initial and boundary conditions: KNU-3:RegCM4-HIS; NIMR-1: HadGEM3-RA-EVA1. : NSE<0 : 0≤NSE <0.5 : NSE ≥0.5).*

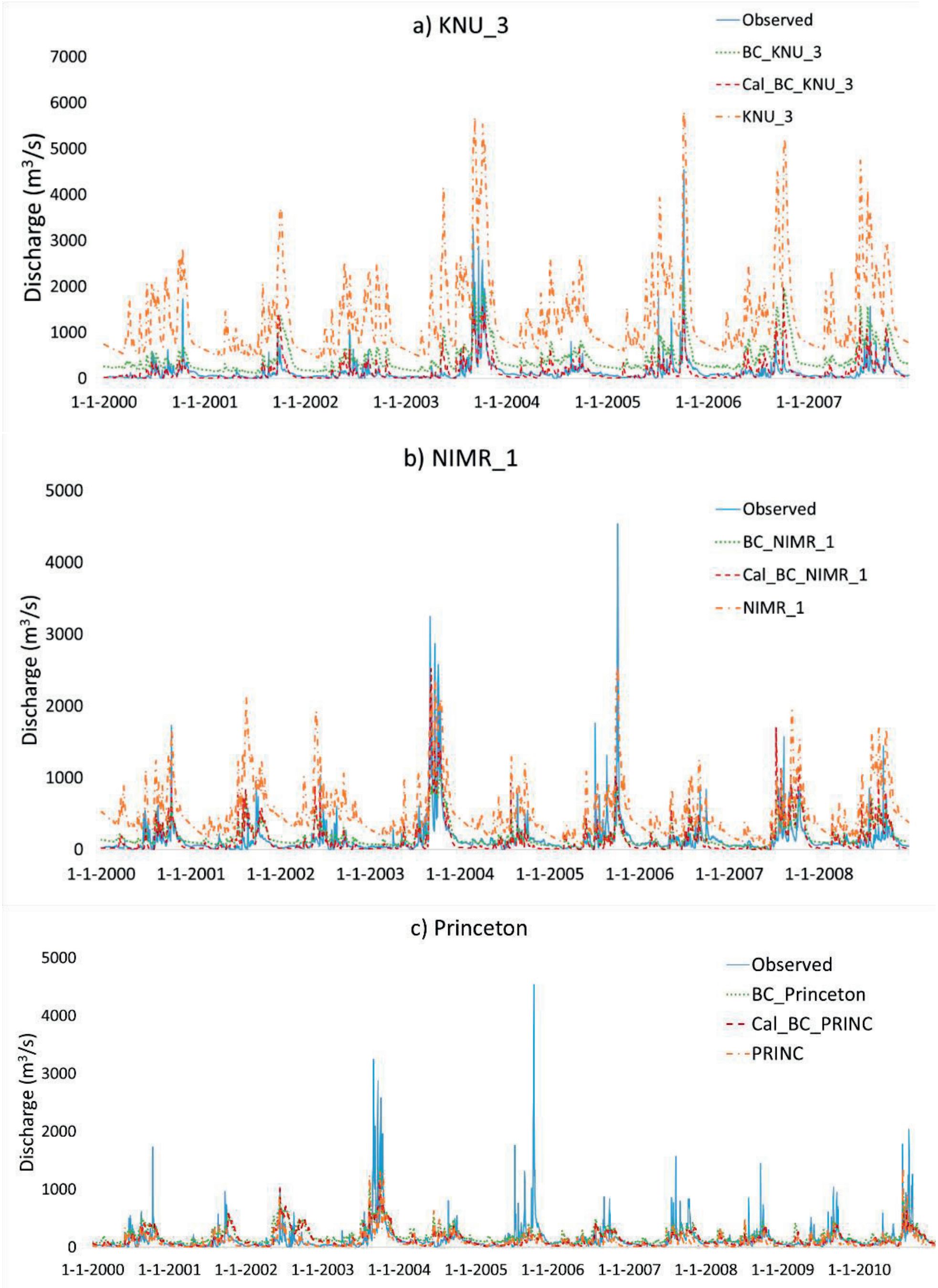

Figure 4.6. *Hydrographs of the discharge at station M1 driven by the original, bias-corrected and calibrated-bias corrected datasets for the (a) KNU-3, (b) NIMR and (c) Princeton datasets (Orange dotted line: Original datasets; Green dotted line: bias corrected datasets; Red dotted line: calibrated-bias corrected datasets; Blue line: observed discharge data).*

4.3.2 Precipitation data from reanalysis

4.3.2.1 Precipitation

The efficiency coefficients of the daily, monthly, 3-day averaged and 5-day averaged precipitation in all the forcing datasets compared to the observations suggested an overestimation of the precipitation in all the datasets except for YSU-2 and SWAT. Although the Princeton dataset managed to grasp the monthly pattern of the precipitation (NSE=0.66, R^2=0.71), the daily simulation was rather poor (NSE=0.00, R^2=0.14)(Fig. 4.7).

	Monthly			Daily			3-day			5-day		
	NSE	Pbias	R^2	NSE	Pbias	R^2	NSE	Pbias	R^2	NSE	Pbias	R^2
Princeton	0.66	2.0%	0.71	-0.87	1.9%	0.01	-0.57	1.9%	0.05	-0.40	1.9%	0.10
SWAT	0.19	-22%	0.42	0.00	-22%	0.14	-3.24	-66%	0.04	-4.58	-66%	0.04
KNU-1	-0.88	84%	0.56	-0.95	84%	0.16	-0.86	84%	0.27	-0.84	84%	0.32
KNU-2	-0.32	29%	0.25	-1.00	28%	0.00	-1.11	28%	0.01	-1.03	28%	0.03
KNU-3	0.24	36%	0.58	-0.32	36%	0.16	-0.16	36%	0.29	-0.08	36%	0.34
NIMR-1	-0.09	46%	0.53	-0.52	46%	0.06	-0.39	46%	0.16	-0.33	46%	0.22
NIMR-2	0.05	18%	0.35	-0.60	18%	0.00	-0.61	18%	0.02	-0.57	18%	0.04
YSU-1	-0.20	5.3%	0.40	-1.06	5.4%	0.02	-0.99	5.4%	0.06	-0.95	5.3%	0.09
YSU-2	-0.73	-21%	0.13	-0.90	-21%	0.00	-0.94	-21%	0.01	-0.95	-21%	0.02
YSU-3	-0.54	30%	0.40	-1.22	30%	0.03	-1.22	30%	0.07	-1.22	30%	0.09

Figure 4.7 *Efficiency coefficients between the precipitation of the observations and from different forcing datasets averaged over the 29 stations. (RCMs and the initial and boundary conditions: KNU-1: RegCM4-EVA1; KNU-2: RegCM4-EVA2; KNU-3:RegCM4-HIS; NIMR-1: HadGEM3-RA-EVA1; NIMR-2: HadGEM3-RA-HIS; YSU-1: YSU-RSM-EVA1; YSU-2: YSU-RSM-EVA2; YSU-3: YSU-RSM-HIS. : NSE<0 : 0≤NSE <0.5 : NSE ≥0.5).*

The spatial pattern of the average precipitation over the whole period from all datasets also suggests that the Princeton dataset has the best spatial representation of both the rainfall gradient and quantity (compare Fig. 4.8a and 4.8b, while SWAT data had a clear underestimation of about 30% and KNU-1 an overestimation of almost 90% of the precipitation over the whole basin (Fig. 4.8). SWAT data also failed to grasp the northwest-southeast rainfall gradient (Fig. 4.8c).

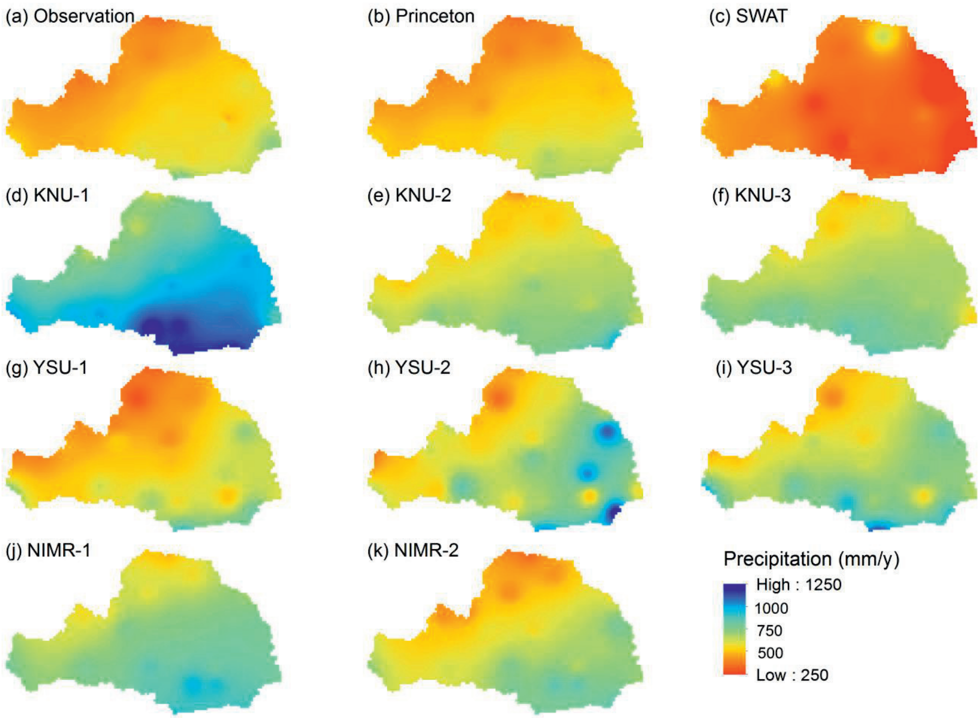

Figure 4.8 *Spatial distribution of average precipitation between observations and difference forcing datasets.*

4.3.2.2 Rain days

Besides the total quantity of the precipitation, most forcing datasets overestimated the number of days with precipitation. Fig. 4.10a shows the days with rainfall from different forcing datasets without correction. In comparison with the observation data, the forcing datasets mostly tended to generate rainfall for more days in the month, especially in the summer season (June-September). The Princeton dataset is the only one that underestimated the number of rainy days, although the Pbias of 1.9% in Table 6 suggested a slight overestimation of the precipitation per rain day. The YSU-RSM regional model (YSU-1, YSU-2, YSU-3) seems to generate less rain days when the 0.01 mm daily precipitation were disregarded (Fig. 4.10b). Most forcing datasets managed to estimate relatively correct rainfall days when disregarding all days with less than 0.1 mm precipitation except for NIMR-2, which means that most datasets overestimated precipitation by adding a small amount of rainfall to more days. From Fig. 4.9 we can conclude that the bias correction improved the simulation of precipitation in KNU-3 and NIMR-1 datasets, however the performance is still rather poor for both monthly and daily simulation. Meanwhile, the bias correction of the Princeton dataset diminished the performance probably by cutting the peaks in the rainfall simulation. Therefore, bias correction of the precipitation can hardly improve the quality of the data.

	NSE	Pbias	R^2	NSE	Pbias	R^2	NSE	Pbias	R^2
	Bias corrected KNU-3			Bias corrected NIMR-1			Bias corrected Princeton		
Monthly	0.31	0.6%	0.52	0.09	8.7%	0.49	0.52	10%	0.73
Daily	-0.37	0.6%	0.11	-0.70	8.7%	0.05	-0.93	10%	0.02
	KNU-3			NIMR-1			Princeton		
Monthly	0.01	31%	0.53	-0.09	46%	0.54	0.70	1.1%	0.74
Daily	-0.68	31%	0.11	-0.52	45%	0.06	-0.84	1.1%	0.02

Figure 4.9 *Efficient coefficients of the before and after bias corrected rain gauge data from the forcing datasets against the 29 observation meteorological data. (: NSE<0 : 0≤NSE <0.5 : NSE ≥0.5).*

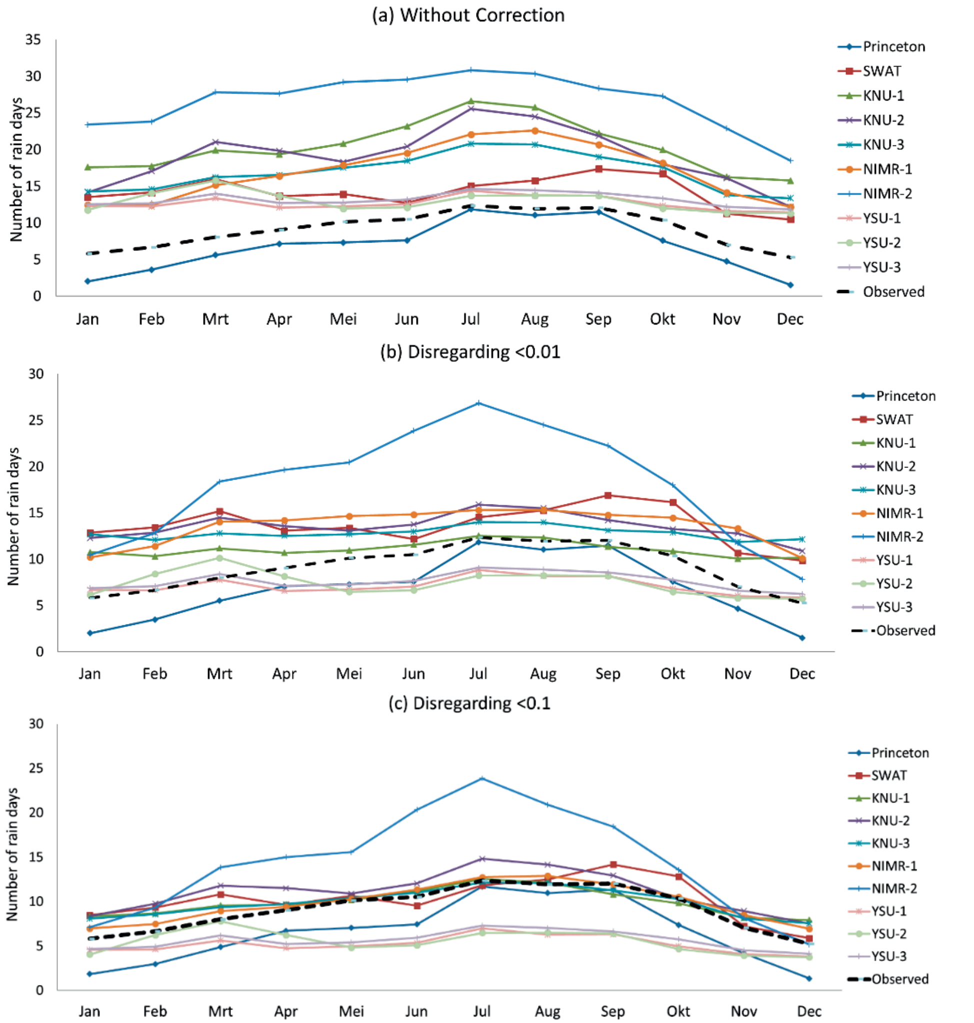

Figure 4.10. *Rain days of observed and different forcing datasets regarding (a) no correction; (b) treating all daily precipitation < 0.01 as 0; (c) treating all daily precipitation <0.1 as 0 (The dashed line indicates the average number of rain days in the observed data for each month of the year).*

4.3.3 Temperature analysis

The pattern of the maximum temperature in the study area was better represented in the Princeton dataset, while the SWAT model has a slight overestimation of the western part and an underestimation in the East (Fig. 4.12). Regarding the CORDEX-EA datasets, all datasets showed an underestimation of the maximum temperature for about 5.5˚C on average. Among all CORDEX-EA datasets, NIMR-1 data had the best simulation with an NSE of 0.70 (Fig. 4.11).

All KNU datasets overestimated the minimum temperature on average. All other datasets tended to generate an average correct pattern with high NSE and R^2 as shown in Fig. 4.11. However, they failed to represent the spatial difference between the north and the south of the basin. The average difference between the north and the south is more than 5˚C in the observed temperature, while the difference in all the CORDEX datasets is on average 2˚C. With the underestimation in the maximum temperature and overestimation of the minimum temperature, the temperature difference (ΔT), which is essential to calculate the evapotranspiration, showed a very bad performance (Fig. 4.11).

		Princeton	SWAT	KNU-1	KNU-2	KNU-3	NIMR-1	NIMR-2	YSU-1	YSU-2	YSU-3
Tmax	NSE	0.79	0.65	0.48	-0.08	0.04	0.7	0.26	0.06	-0.68	0.13
	Bias*	-0.67	-1.02	-5.59	-7.64	-8.66	-2.85	-3.77	-7.83	-9.81	-7.26
	R^2	0.84	0.89	0.88	0.69	0.89	0.88	0.65	0.83	0.73	0.83
Tmin	NSE	0.84	0.74	0.67	0.64	0.82	0.8	0.57	0.72	0.4	0.72
	Bias*	0.57	-0.94	3.9	1.73	0.72	-1.08	-2.27	0.61	-1.52	1.18
	R^2	0.86	0.91	0.87	0.75	0.89	0.88	0.78	0.85	0.78	0.86
ΔT	NSE	-0.13	-0.2	-4.37	-4.57	-4.26	-0.21	-0.99	-3.51	-3.56	-3.5
	R^2	0.14	0.29	0.34	0	0.35	0.27	0.01	0.1	0	0.1

Figure 4.11 *Efficiency coefficients of the daily observed maximum (Tmax), minimum (Tmin) temperature and temperature difference (ΔT) based on different forcing datasets compared with the observed data (very good NSE in bold) (RCMs and the initial and boundary conditions: KNU-1: RegCM4-EVA1; KNU-2: RegCM4-EVA2; KNU-3:RegCM4-HIS; NIMR-1: HadGEM3-RA-EVA1; NIMR-2: HadGEM3-RA-HIS; YSU-1: YSU-RSM-EVA1; YSU-2: YSU-RSM-EVA2; YSU-3: YSU-RSM-HIS. *Bias: the average absolute difference between the reanalysis temperature compared to the observed temperature, unit: ˚C. : NSE<0 : 0≤NSE <0.5 : NSE ≥0.5).*

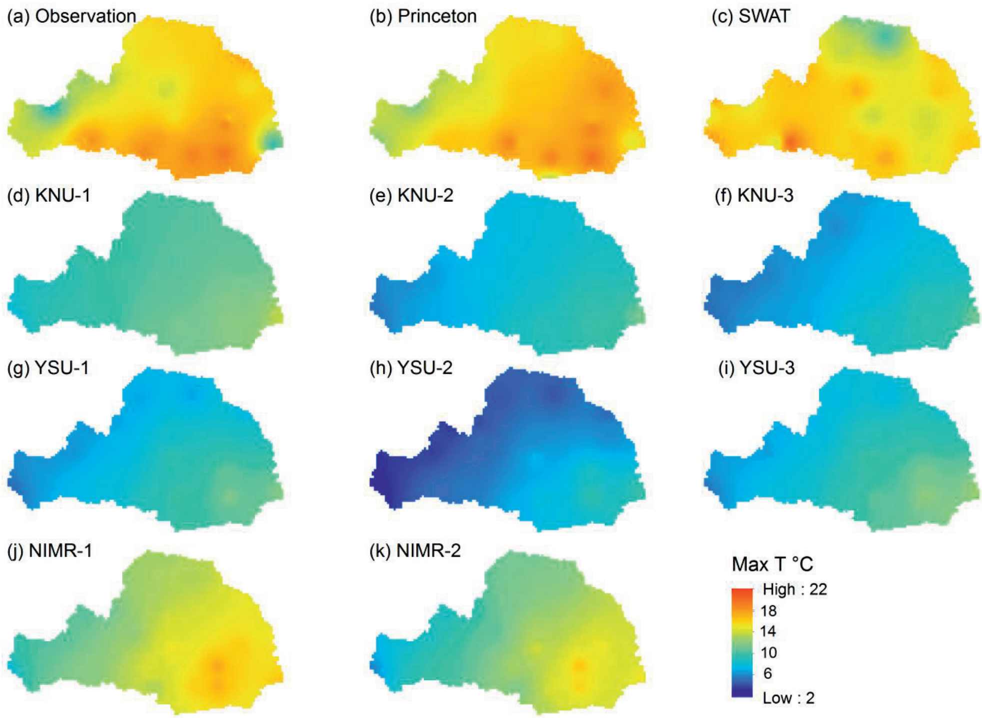

Figure 4.12 *Spatial distribution of the averaged maximum temperature of the available period for (a) Observation, (b) Princeton, (c) SWAT, (d) KNU-1, (e) KNU-2, (f) KNU-3, (g) YSU-1, (h) YSU-2, (i) YSU-3, (j) NIMR-1, (k) NIMR-2 datasets, respectively.*

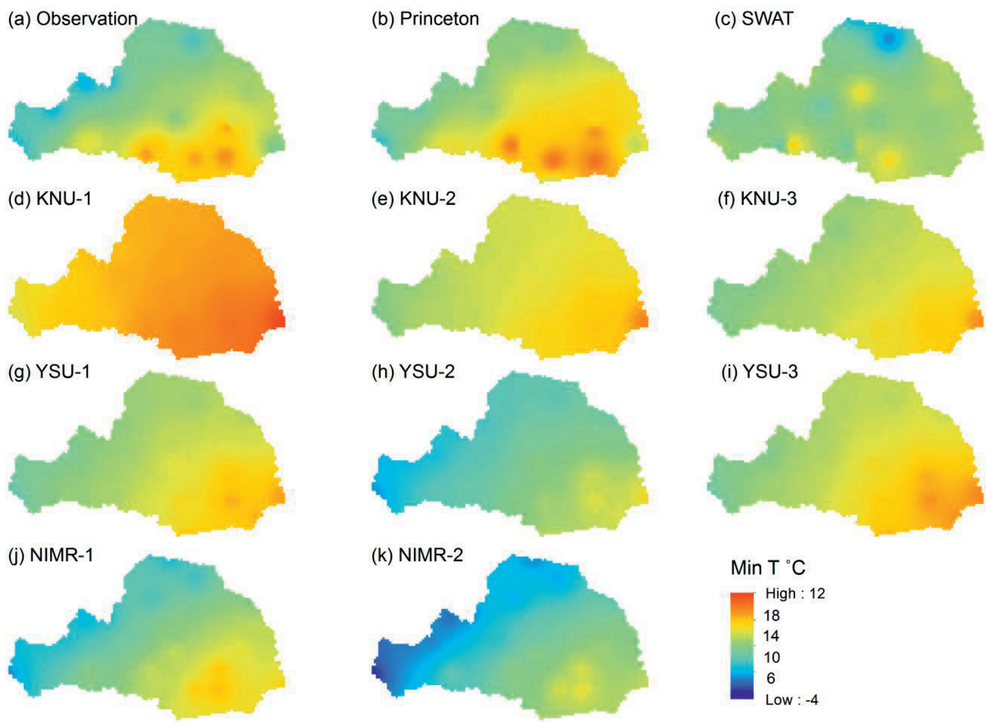

Figure 4.13 *Spatial distribution of the averaged minimum temperature of the available period for (a) Observation, (b) Princeton, (c) SWAT, (d) KNU-1, (e) KNU-2, (f) KNU-3, (g) YSU-1, (h) YSU-2, (i) YSU-3, (j) NIMR-1, (k) NIMR-2 datasets, respectively.*

4.3.4 Evapotranspiration analysis

The simulation of the potential reference evapotranspiration by the LISVAP model driven by different reanalyses in general showed an underestimation compared to the evapotranspiration calculated from the observed data except for the SWAT dataset. The simulation of the HadGEM3-RA-EVA (NIMR-1), Princeton and SWAT datasets are very good according to the criteria of (Moriasi et al., 2007). Both datasets from the HadGEM3-RA regional model gave a good simulation of the evapotranspiration. This may due to the good representation of both the maximum and minimum temperature simulated by the HaDGEM3-RA regional model (Fig. 4.11). Although both the maximum and minimum temperature were underestimated by the HadGEM3-RA model, the temperature difference which is essential for the calculation of the evapotranspiration is well simulated. The same observation can be found for the SWAT dataset, the underestimation of both the maximum and the minimum temperature eliminated the bias for the temperature difference.

Therefore, the evapotranspiration calculated from the SWAT dataset has the best simulation.

	Huaxian			Xi'an			Tongguan		
	NSE	Pbias	R^2	NSE	Pbias	R^2	NSE	Pbias	R^2
KNU-1	-0.44	-64.1%	0.92	-0.44	-64.4%	0.92	-0.42	-63.6%	0.93
KNU-2	-0.60	-65.1%	0.66	-0.62	-65.6%	0.65	-0.58	-64.6%	0.66
KNU-3	-0.51	-66.3%	0.92	-0.53	-66.8%	0.91	-0.48	-65.7%	0.92
NIMR-1	0.81	-15.7%	0.88	0.78	-18.9%	0.88	0.83	-13.9%	0.88
NIMR-2	0.58	-16.6%	0.68	0.55	-20.9%	0.67	0.60	-14.6%	0.68
YSU-1	-0.10	-54.3%	0.81	-0.12	-54.9%	0.81	-0.08	-53.6%	0.82
YSU-2	-0.10	-54.5%	0.77	-0.10	-54.8%	0.77	-0.08	-53.8%	0.77
YSU-3	-0.06	-53.3%	0.83	-0.08	-54.1%	0.83	-0.03	-52.5%	0.84
Princeton	0.87	-5.6%	0.88	0.86	-7.8%	0.87	0.88	-3.9%	0.88
SWAT	0.95	-0.3%	0.96	0.95	2.8%	0.96	0.95	1.0%	0.96

Figure 4.14 *Efficiency coefficients based on the evapotranspiration simulated by different forcing datasets compared to the evapotranspiration from the baseline run at Huaxian, Xi'an and Tongguan (RCMs and the initial and boundary conditions: KNU-1: RegCM4-EVA1; KNU-2: RegCM4-EVA2; KNU-3:RegCM4-HIS; NIMR-1: HadGEM3-RA-EVA1; NIMR-2: HadGEM3-RA-HIS; YSU-1: YSU-RSM-EVA1; YSU-2: YSU-RSM-EVA2; YSU-3: YSU-RSM-HIS. : NSE<0 : 0≤NSE <0.5 : NSE ≥0.5).*

4.4 Discussion

This study investigated the performance of using reanalyses and CORDEX-EA forcing datasets to drive the hydrological model LISFLOOD for discharge simulation in the Wei River Basin in China. The purpose of this study was to evaluate whether these freely available global datasets can be directly used for data scarce areas for hydrological extremes analysis (flooding) and a potential driving force for climate change projections. The results revealed that none of the ten datasets evaluated in this study can be directly used as the driving force for the LISFLOOD model for flood analysis in the study area. Although RegCM4-HIS, HadGEM3-RA-HIS and Princeton datasets are able to capture the monthly discharge pattern, the daily bias in the datasets compromise the daily performance of the model.

Besides the studies that have evaluated the application of other region-specific CORDEX data worldwide, among which mostly suggested that bias correction is necessary to improve the quality of the output from CORDEX simulations (Casanueva et al., 2016; Choudhary et al., 2018; Tramblay et al., 2013; Yira et al., 2017), there are studies implying that the complexity of the East Asian monsoon system makes the representation of East Asia climate a challenge for climate models (Tang et al., 2017; Zhou et al., 2016). The limitations of CORDEX-EA data regarding daily maximum temperature (Wang et al., 2018;. Pereira et al., 2013) result also in the fact that the climate projection WRF model is not able to simulate extreme precipitation. The difference in the results among the application of the CORDEX-

EA datasets is the result of different driving GCMs, technical details, calculation algorithm of RCMs.

Compared to the CORDEX-EA datasets, CSFR reanalysis has been applied to catchments worldwide, which has proven to give a better simulation of streamflow than conventional data gauges in several regions in the world, especially when the observation gauges are missing from a given area of interest, or when the gauge data are not reliable (Dile and Srinivasan, 2014; Essou et al., 2016). These results are different from the findings of our study. This may be explained by the fact that our study region is a semi-arid area, especially the northern catchments, while the other regions have mostly temperate or tropical climate. The only semi-arid region examined was Tesuque Creek in the USA (Fuka et al., 2014), which gave an obvious lower NSE compared to other study regions. The errors in the datasets are enlarged when rainfall is rather little compared to a large amount of rainfall, because the processes such as evaporation and infiltration respond more sensitively to the errors. The difference also lies in the scarcity of the observational gauging stations. Although the meteorological stations in our study area are sparsely distributed compared to the large catchment area, it is better than having only one or two meteorological stations in the whole study area, or the surrounding areas. Besides the good report of the application of CSFR reanalysis data (Sperna Weiland et al., 2012) found that, on a global scale, CFSR reanalysis data gives an underestimation of PET which results in an overestimation of discharge for arid and dry basins, which is coherent with our findings.

In this study we concluded that the simulations for the main station are mostly satisfactory while for all southern and northern catchments these are rather poor. This may partly be due to the reason that spatial rainfall variabilities are smoothened in large catchments (Beven, 2012). Reanalysis outputs are often biased especially due to the relatively coarse grid resolution (Essou et al., 2017). The complexity of terrain, availability of rain gauge data for bias correction and the temporal resolution considered are the main factors influencing the quality of the global precipitation data, especially on a spatial scale (Koutsouris et al., 2017). This study has revealed a large bias in the datasets between the arid and humid region especially demonstrated by applying the hydrological model. There is clearly an overestimation of the discharge in the northern catchments which is located in the arid region, and an underestimation of the discharge in the southern catchments in the humid region. With good simulations of evapotranspiration, the spatial bias of the precipitation data seems to be the cause for these results. With a notable overestimation of the days with rainfall in most models, we decided to test the number of rainy days discarding the 0.01 and 0.1 mm rainfall records, as such events are hardly detectable by commonly used rain gauge tipping bucket devices.

Although the correlation statistics for the temperature analysis are good in all datasets (R^2>0.6), the low NSE and the spatial pattern suggests that underestimation or overestimation has occurred. Zhao et al. (2018) tested the temperature variable in the CFSR dataset for the whole of China. They found coherency between the CFSR dataset and the observations for the seasonal pattern. However, the temperatures of western China were mostly overestimated by the CFSR dataset, which is in line with our results. Although the simulation of the evapotranspiration suggested a good estimation of the temperature difference in most datasets, the absolute bias actually revealed both an underestimation or overestimation of the maximum and minimum temperature. Therefore, the prediction of the temperature needs to be improved specifically on the accuracy of the maximum and minimum temperature.

With the evaluation of the datasets with regard to precipitation, temperature and evapotranspiration differences against observed data, this study indicates that the Princeton dataset represents the precipitation and temperature in both temporal and spatial scale the best. The SWAT model underestimates the precipitation amount by overestimating the number of rainy days. The CORDEX-EA regional model overestimates both the precipitation amount and the number of rainy days. Regarding the temperature data accuracy, the CORDEX-EA regional model generally underestimated the maximum daily temperature while Princeton and SWAT data performed well. The accuracy of the minimum daily temperature from all datasets are relatively good. With these results, we would like to recommend the forcing dataset developers to take into account and address and improve the abovementioned inconsistencies and inaccuracies in future work.

4.5 Conclusion

This studies investigated the possibility to use globally freely available meteorological reanalyses and CORDEX-EA datasets to drive LISFLOOD model for the Wei River Basin in China with the main conclusions listed below:

- The Princeton dataset represented the spatial and temporal pattern of climate variables in the study area the best, and as such can be directly used as input for hydrological models in a data scarce area.
- CORDEX-EA datasets cannot be directly applied to drive a hydrological model without bias correction for the study catchment.
- Bias correction needs to be done separately for arid and humid climates.
- The daily simulation results driven by the evaluated datasets are not good enough for flood analysis even though the bias-corrected and calibrated results are reasonable on a monthly scale.

- We recommend a detailed analysis of the quality of freely available global datasets before using them for hydrological modelling.

Acknowledgements

We would like to thank the China Meteorological Data Service Centre for providing the meteorological data from The Dataset of Daily Values of Climate Data from Chinese Surface Stations. We highly appreciate the support from JEONG for getting access to the CORDEX – EA data portal. J.P. Nunes was supported by a research grant from the Fundação para a Ciência e a Tecnologia (IF/00586/2015).

5. Assessing the impact of human interventions on floods in the Wei River Basin in China using the LISFLOOD model

Floods are extreme hydroclimatic events that may threaten and impact societies and ecosystems. During the last decades, the Wei River Basin in China changed substantially, due to population growth and human interaction affecting land use and soil and water resources. As a result, floods are common in the Wei River Basin, and effects of human interventions need further attention to assess related impacts. A model-based scenario analysis has been performed to compare three groups of contrasting scenarios with a business as usual condition. The results of the scenarios are presented for three strategically important cities located on the floodplain. In general, the construction of reservoirs could have an effect on reducing peak river flows, decreasing flood return periods, and increasing low flows. The land use of the year 2000 has led to a larger runoff in comparison with the year 1980 due to a substantial loss of forest area in the basin. Water transfer could increase low flow substantially for the three respective cities. This study has demonstrated the possibility to apply the LISFLOOD model for flood analysis and management at the catchment scale.

Based on:

L. Gai, J.P. Nunes, J.E.M. Baartman, H. Zhang, F. Wang, A. de Roo, C.J. Ritsema, V. Geissen. 2019. Assessing the impact of human interventions on floods and low flows in the Wei River Basin in China using the LISFLOOD model. Science of The Total Environment 653: 1077-1094.

5.1 Introduction

The typical flood generation mechanism involves intense or prolonged rainfall (meteorological flood) that exceeds soil infiltration or soil storage capacity. The excess water leads to increased and often rapid streamflow (hydrological flood), which can lead to out-of-bank flow that may damage the socioeconomic system (socioeconomic flood) (Garner et al., 2015). However, human interventions that aim to secure sufficient water resources for agricultural, domestic and industrial usage influence streamflow characteristics. Thus, meteorological anomalies no longer necessarily lead to hydrological extremes only.

Changes in land use affect the partitioning of precipitation through the vegetation and soil into the water balance components, including evapotranspiration, precipitation and land-surface temperature (Yira et al., 2016). The substantial effects of land use changes on key elements of the hydrological cycle have been well documented around the world (Stonestrom et al., 2009; De Roo et al., 2001; Wijesekara et al., 2012; Wagner et al., 2013; Wang et al., 2014; Awotwi et al., 2015; Tan et al., 2015; Yira et al., 2016; Chang and Feng, 2017; Rogger et al., 2017). Besides land use changes, about 70% of the rivers globally are intercepted by large reservoirs, which significantly decrease the river's vulnerability towards meteorological extremes and human's independency towards natural availability of water resources (Ran and Lu, 2012). Reservoirs constitute essential components of the hydrologic cycle because of their ability to retain, store and evenly release water as well as their ability to slow down water movement (still-water characteristics) (Lehner and Döll, 2004; Hanasaki et al., 2006). Studies have been done on single reservoir operation on catchment management (Anghileri et al., 2016; Chiew et al., 2003; Das et al., 2016; Uysal et al., 2016). A few studies started to pay attention to the impact of reservoir functionality on water resources on the large catchment scale (Bai et al., 2015; Anghileri et al., 2016; Ehsani et al., 2016; Lv et al., 2016). With good reservoir management, the lack of water during the dry seasons can be compensated by the surplus water collected during the rainy seasons.

This study intended to be the first application of the LISFLOOD model in China to investigate the impact of land use changes, reservoir constructions and water diversion plans on flood variations. Three categories of scenarios of integrated water and land management were created and evaluated to gain a better understanding of their impact on flood management compared with a business as usual situation.

5.2 Methodology

5.2.1 Study Area

The Wei River in China is the largest tributary of the Yellow River. It flows east across the Loess Plateau into the Yellow River with a total length of 818 km. The Wei River Basin (103–111˚E, 33–38˚N) covers three provinces in the central northern China and has a total catchment area of 134, 800 km^2 (Fig. 5.1). The continental summer monsoon climate controls the whole catchment and brings an average annual precipitation of about 570 mm in the basin. The Wei River is the "Mother River" of the Guanzhong Plain, which is the most important agricultural and industrial area in central northern China. The Guanzhong plain is also the floodplain of the Wei River Basin, extending West to Baoji and East to the Yellow River. Xi'an city, which was the capital of more than ten dynasties in the Chinese history, is becoming the cultural, industrial and economic centre of central-western China, and located in the centre of the floodplain. The "Grain for Green" project was launched by the Chinese Government in 1999, aiming at converting farmlands on the slopes into forests and grasslands (Deng et al., 2014; Jian et al. 2015). The land use and river channel have been altered also, especially in the northern part of the Wei River.

5.2.2 LISFLOOD model

The LISFLOOD model was initially developed specifically for flood and drought forecasting as well as to assess the effects of river regulation measures, land-use changes and climate changes in large and trans-national catchments (De Roo et al., 2001; van der Knijff et al., 2010). LISFLOOD is a spatially distributed and physically-based model, capable to be applied to a wide range of spatial and temporal scales (Pappenberger et al., 2011; Thielen et al., 2009; Thiemig et al., 2015). LISFLOOD model input includes topographic, soil, land use, river channel, meteorology and reservoir information (see Supplementary material Table S.1 for more detailed input data requested for LISFLOOD model). The application of the LISFLOOD model consists of three parts: the LISVAP model (Van der Kniff, 2008), the LISFLOOD model (Burek etl al., 2013), and the LISFLOOD calibration model.

The LISVAP model is a pre-processor used to calculate potential evapo(transpi)ration grids which are then used as input to LISFLOOD. The process in the LISFLOOD model includes snow melt, infiltration, interception of rainfall, leaf drainage, evaporation and water uptake by vegetation, surface runoff, preferential flow, soil moisture distribution, drainage to the groundwater, sub-surface as well as groundwater flow, reservoirs and river channel routing (Burek et al., 2013; van der Knijff et al., 2010). Reservoirs are simulated as points in the

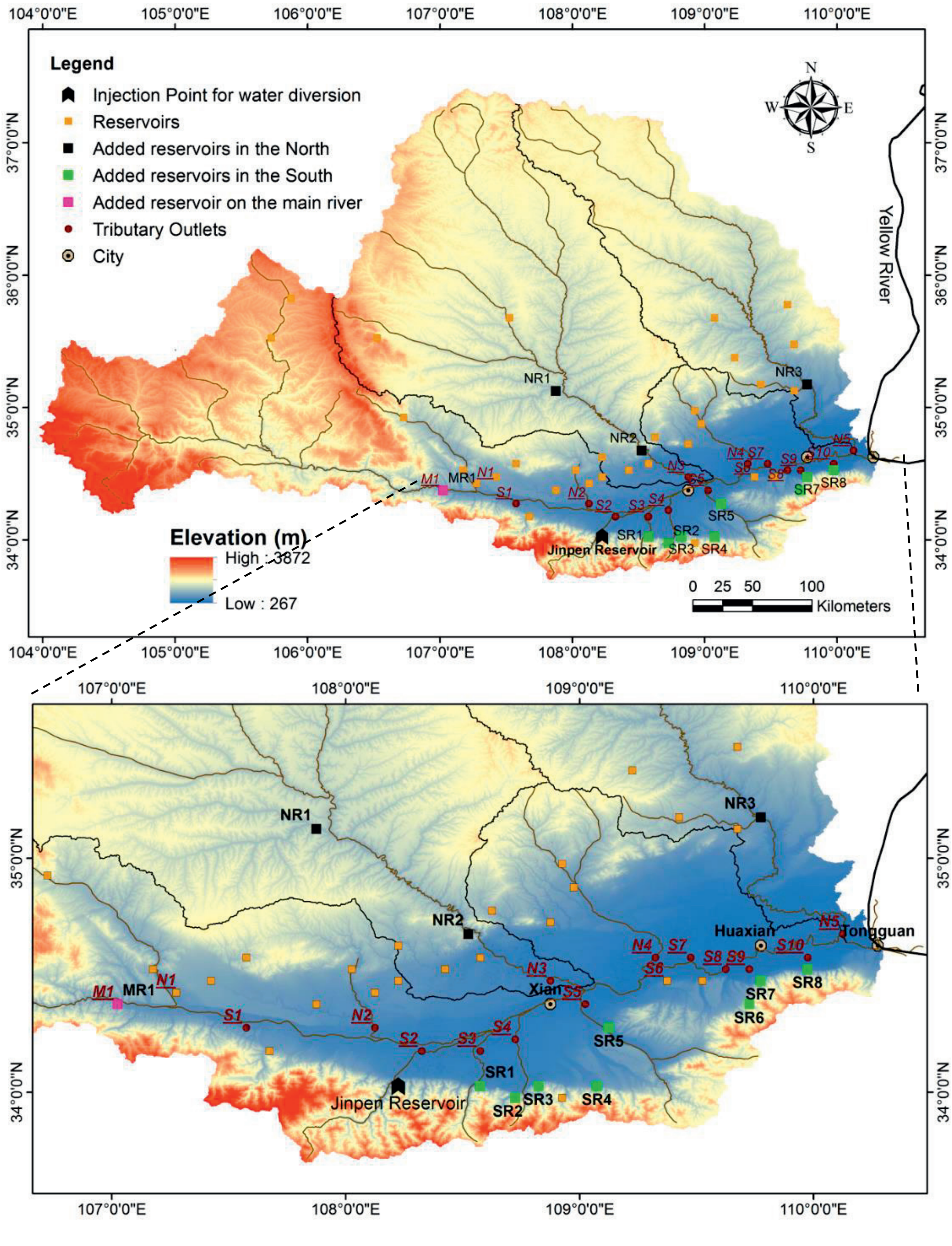

Figure 5.1 *Location of the 1) outlets of all tributaries (dark red dots); 2) the reservoirs (yellow squares: existing reservoirs in the basin; green squares: added reservoirs in the southern catchments; black squares: added reservoirs in the northern catchments; pink squares: added reservoir on the main stream); 3) the injection point of the water diversion plan (Jinpen Reservoir).*

channel network and their inflow equals the channel flow upstream of the reservoir, while the outflow of the reservoirs are estimated using a number of parameters as explained in Chapter 3 of this thesis. The LISFLOOD calibration tool calibrates the simulated discharge against the observations from the hydrological stations in multiple catchments using a multi-objective generic algorithm in Python programming language. In this study, we first calibrated the simulated daily discharge against the observed discharge from seven hydrological stations using the LISFLOOD reservoir module for the years 2000-2010. A Pareto optimal solution was obtained after the calibration using the Nash–Sutcliffe model efficiency coefficient (NSE) as the single objective function. A baseline run of the model was conducted by applying the Pareto optimal parameters and with the data processing procedures explained in Chapter 3. The baseline run is defined as the Business As Usual (BAU) scenario in this Chapter.

5.2.3 Scenario Analysis

Based on the result of the previous chapters, we identified the most influencing factors to the flood discharge in the basin and created nine different scenarios categorised into three groups accordingly, including the BAU scenario (Table 5.1). All scenarios are evaluated for the period of 2000-2010 to be consistent with the model baseline run.

Table 5.1 *Summary of the scenarios*

Scenario Group	Scenario name	Description	Land Use Map	Reservoir Construction	Water Transfer
Natural condition group	S1-BAU	Business As Usual	2000	No additional reservoir	No transfer
	S2-NR	Remove all existing reservoirs	2000	No Reservoirs	No transfer
	S3-L80	Land Use 1980	1980	No additional reservoir	No transfer
Reservoir construction	S4-RS	Additional reservoirs in southern catchments	2000	South	No transfer
	S5-RN	Additional reservoirs in northern catchments	2000	North	No transfer
	S6-RM	Additional reservoir on the main stream	2000	Main stream	No transfer
	S7-RAll	Additional reservoir in all catchments	2000	South+North+Main stream	No transfer
Water transfer	S8-W5	Water diversion Plan	2000	No additional reservoir	Pipeline transfer of 0.5 billion m^3/year
	S9-W15	Water diversion Plan	2000	No additional reservoir	Pipeline transfer of 1.5 billion m^3/year

5.2.3.1 Natural condition scenarios

The first group of scenarios was considered as the natural condition group. The first scenario constructed under the current land use (land use map of the year 2000) and reservoir conditions, defined as Business as Usual (S1-BAU), is also the baseline run of the LISFLOOD model with the calibrated and validated parameters as conducted in Chapter 3. The second scenario considered the condition without any reservoirs meaning disregarding all reservoirs in the basin (S2-NR). The third scenario was evaluated under the land use map of the year 1980 instead of the land use of 2000 to evaluate the flood discharge regime before the large human land use interventions (S3-L80).

There were large changes in land coverage between 1980 and 2000 (Fig. 5.2). An obvious decrease in forest area due to deforestation can be noted from 1980 to 2000 (Figs. 5.2a and 5.2b). However, in the middle of the Beiluo River Basin (North-East of the Wei River Basin), a specific region was regreened due to afforestation demonstration activities during the 90s. Sealed area (Figs. 5.2c and 5.2d) represents the area with impervious surfaces, such as roads, which increased from 1980 to 2000 mainly as the result of urbanization. The sealed area, treated as impervious media, has a direct effect on runoff generation in the LISFLOOD model. For the impervious areas, LISFLOOD assumes that there is no soil moisture storage nor groundwater storage. Due to the massive change from forest land to farmland in the 1980s, the ratio of grassland and arable land increased substantially, as can be seen in Figs. 5.2e and 5.2f.

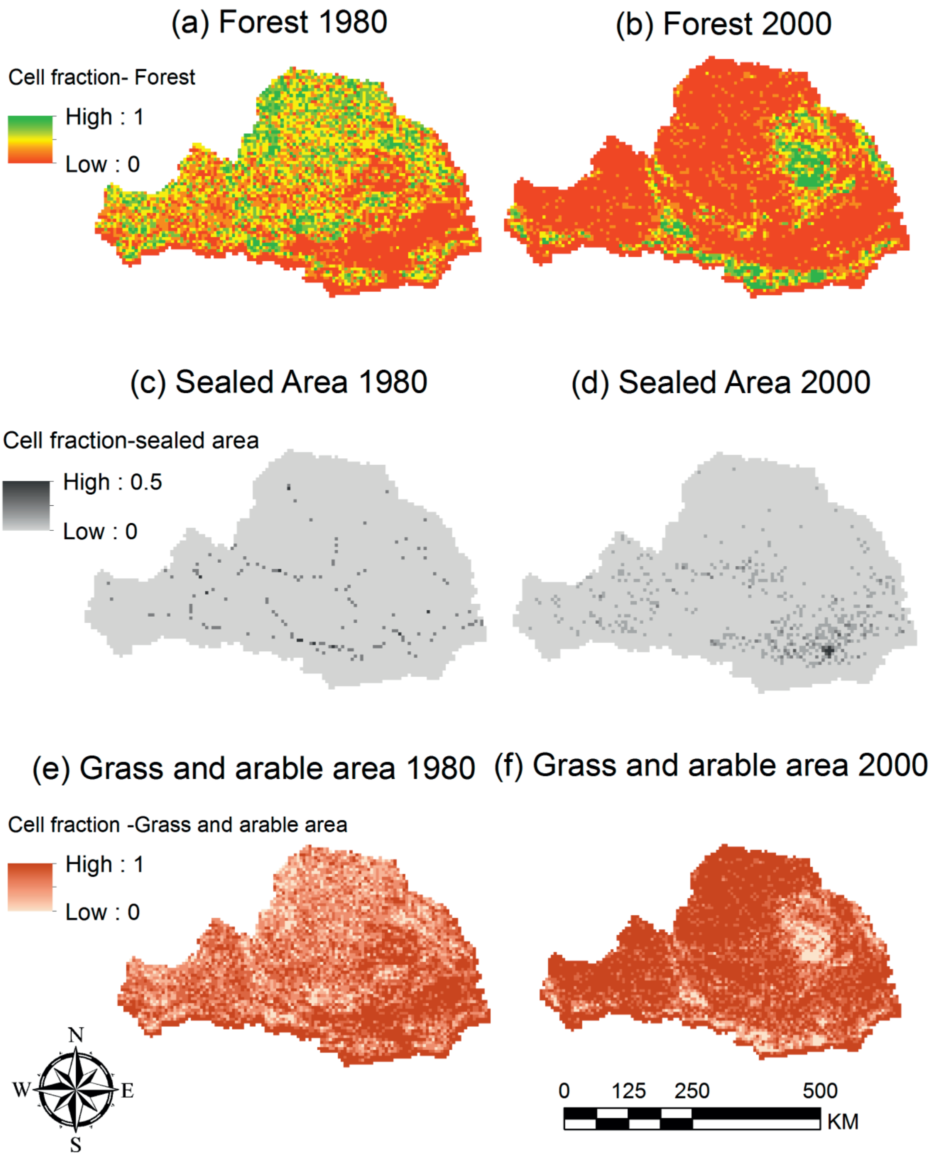

Figure 5.2 *Maps of cell fraction (1=100% cover) of different land use type used in the LISFLOOD model of the years 1980 and 2000. "Sealed area" refers to the area with impervious surface, while "Other area" includes farmland and grassland. The fraction is calculated as the percentage of a certain type of land use in the 0.05 degree cell.*

5.2.3.2 Reservoir construction scenarios

The second group of scenarios was created by identifying the largest contributing tributaries and proposing additional reservoirs for the corresponding catchments. Four reservoir construction scenarios were proposed: additional reservoirs planned for the 1) southern region (S4-RS), 2) northern region (S5-RN), 3) the mainstream (S6-RM), and 4) a combination of the previous three (S7-RAll). Planned reservoirs were designed to be located at the inlet point of the corresponding catchments into the floodplain. The storage capacity of the planned reservoirs was estimated based on the correlation between catchment area and storage capacity of the existing reservoirs in the basin. The reservoir on the main river was planned behind the existing Baojixia Dam (Fig. 5.1). Table 5.2 shows detailed information of all the proposed reservoirs in the basin.

5.2.3.3 Water transfer scenarios

The third group of scenarios was developed based on the water transfer plan that most likely will be carried out in the Wei River Basin (Wang et al., 2006). The plan was designed to address the demand for water for both domestic and industrial use in the Guanzhong Plain. With the installation of a pipeline from an adjacent catchment (Ziwu River Basin), from south of the Qinling Mountains to the Jinpen reservoir in one of the southern tributaries in the Wei River Basin, a total of 0.5 billion m^3 (S8-W5) and 1.5 billion m^3 (S9-W15) of additional water is planned to be transfered to the study area by 2020 and by 2030, respectively. With the proposed design of 70 m^3/s flow rate of the pipeline, 83 and 248 consecutive days of continuous injection flows will be needed to fulfil the 0.5 and 1.5 billion m^3 demand. Based on the principle that water injection occurs in the low flow days, the S8-W5 scenario assumes a constant injection of 70 m^3/s of water from the 10th of November every year to the 31st of January of the next year. The duration of the S9-W15 scenario injection plan is from 1st of October until the 5th of June of the next year.

From all of the discharge results, three points along the mainstream were chosen to be the sample points for flood analysis due to different interests:

- Xi'an City: capital city of the province, strategically important, densely urbanized and densely populated;
- Huaxian City: the most downstream gauged river discharge station of the Wei River Basin whose result can be validated by observed discharge; and
- Tongguan City: the outlet of Wei River into the Yellow river, which is a monitoring station for back water effects from the Yellow River, important for regional flooding.

The daily discharges of the three locations was also estimated by the LISFLOOD model. The 99%, 90% and 5% percentile of the river discharge was calculated to identify the peak and low flows.

Table 5.2 *Properties of the added reservoirs positioned as in Fig. 5.3*

New Reservoir number	Longitude	Latitude	Catchment Area (km^2)	Mean Discharge (m^3/s)	Max Discharge (m^3/s)	Region	Estimated Max Capacity MiM^3	Annual discharge MiM^3	Water retention capacity (years)
1	107.04	34.38	31464	12.91	200.36	Main	2,467.8	407.5	6.06
2	107.92	35.11	3792	2.43	77.85	North	541.1	76.8	7.04
3	108.5	34.71	42144	22.40	396.96	North	2,970.8	706.9	4.20
4	109.77	35.18	25344	12.64	389.23	North	2,103.1	398.8	5.27
5	108.54	34.02	408	2.13	191.34	South	82.7	67.3	1.23
6	108.71	33.98	288	2.21	81.62	South	60.5	69.8	0.87
7	108.81	34.03	264	2.91	106.09	South	55.8	91.8	0.61
8	109.07	34.02	168	0.46	21.10	South	36.5	14.4	2.53
9	109.11	34.28	2376	13.01	433.85	South	197.0	410.6	0.48
10	109.72	34.39	120	0.15	6.40	South	26.4	4.6	5.70
11	109.75	34.46	72	0.34	7.76	South	16.1	10.7	1.50
12	109.96	34.52	384	0.92	23.71	South	78.4	29.0	2.70

5.3 Results

5.3.1 Scenario analysis

5.3.1.1 Natural condition scenarios

Fig. 5.3 shows the results of the scenario runs of S1 to S3, for the period of 2000-2010. S2-NR, which is the no reservoir scenario, led to the highest peak flow in all three cities and the lowest low flow in both Huaxian and Tongguan cities, confirming the importance of the reservoirs' regulation on flood control in the catchment. Scenario S2-NR did not seem to contribute to the lowest flow in Xi'an city (Fig. 5.3a), in contrast with the downstream cities of Huaxian and Tongguan; however, this can be explained by the fact that the outlets of both large northern tributaries are located downstream of Xi'an, where the regulation effects of the reservoirs are more obvious. Scenario S2-NR represents the simulated streamflow without the reservoirs, while scenario S1-BAU represents the streamflow with the reservoirs. The hydrograph comparison between the observed streamflow and the streamflow simulated under both S1-BAU and S2-NR scenarios at Huaxian (HM1) station is shown in Fig. 5.4. The S2-NR simulation leads to a lower base flow and high peak flow than the S1-BAU scenario. This is consistent with the reservoirs' regulation function. The Nush-sutcliff coefficient value of the daily discharge simulated under S2-NR scenario against the observed discharge is 0.56 and that of the S1-BAU scenario is 0.69.

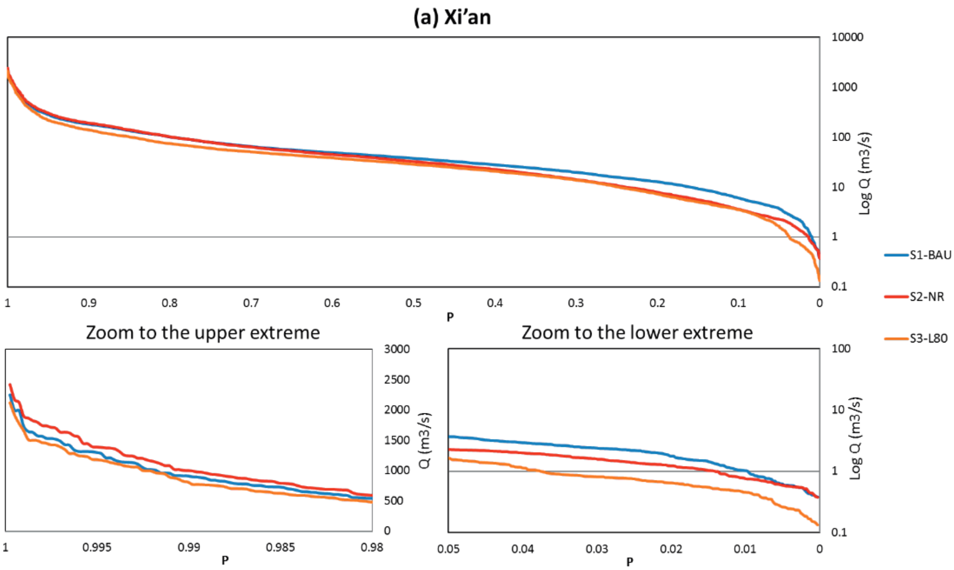

Figure 5.3 *To be continued on next page*

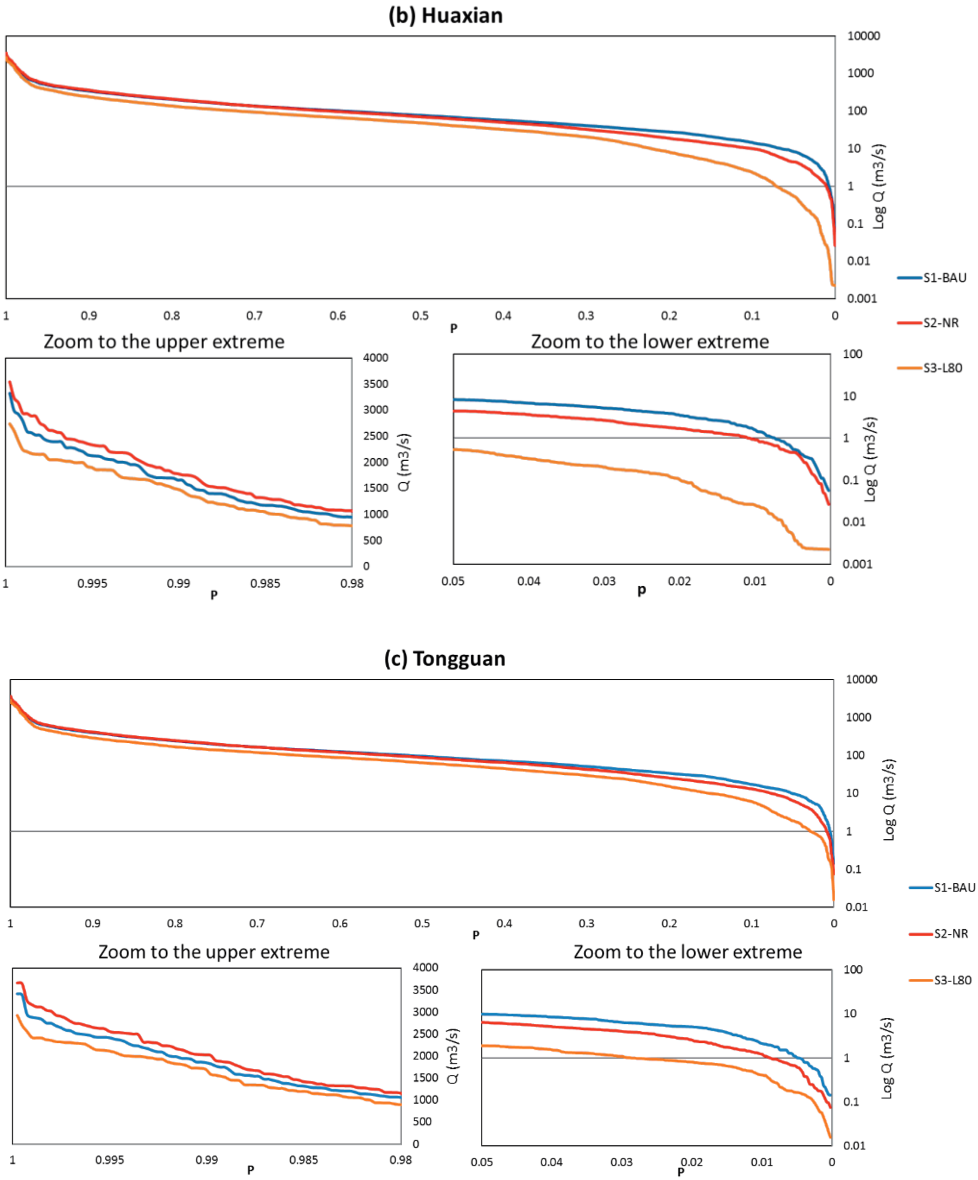

***Figure 5.3** Flow Duration Curves of the three stations (a: Xi'an, b: Huaxian, c: Tongguan) for scenarios concerning the natural conditions (S1-BAU: business as usual, S2-NR: remove all the existing reservoirs, S3-L80: land use as it was in 1980): the whole FDC, zoom to the upper extreme (high flows), and zoom to the lower extreme (low flows), (P: probability of exceedance).*

Compared to the land use in 1980 (Scenario S3-L80), the current land use (2000) has greatly increased the base flow of the basin. The lowest base flow under the current land use of Huaxian, Xi'an and Tongguan city are 25 times, 3 times and 9 times of those under land use of 1980, respectively. The impact of the land use can also be demonstrated by increasing the peak flow of the aforementioned three cities by 21%, 6% and 17% (Table 5.3), respectively.

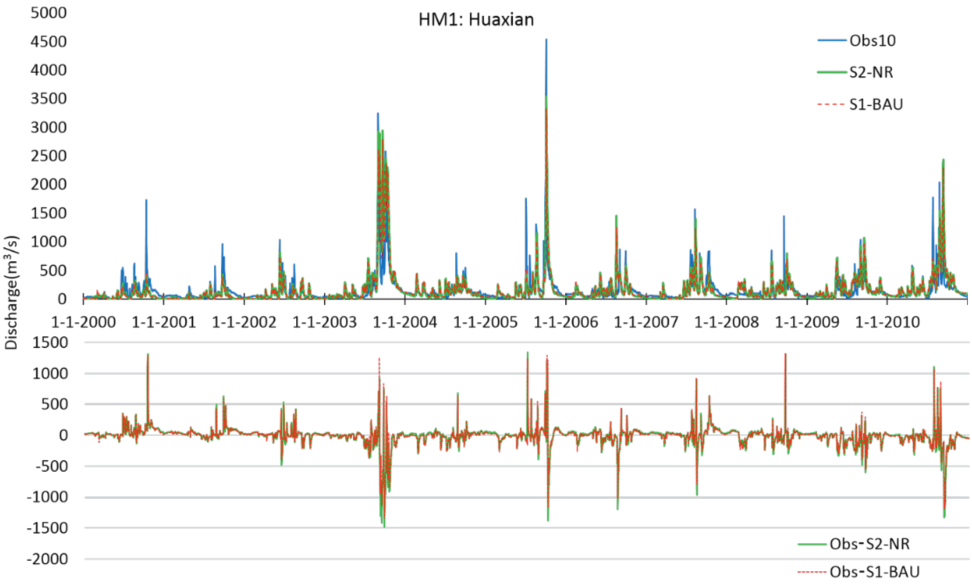

Figure 5.4 *Hydrograph of the discharge from the observed data, simulated by S1-BAU scenario and S2-NR scenario at HM1: Huaxian station (upper part), and the hydrograph of the difference between the observed data against S1-BAU and S2-NR scenario respectively (lower part).*

5.3.1.2 Reservoir construction scenarios

The scenarios with additional reservoirs changed both the peak flow and the low flow of the catchment (Fig. 5.5, Table 5.3). The construction of reservoirs in the northern catchments S5-RN scenario reduced the peak flow for all three stations by 31% on average, and increased the lowest flow of Huaxian and Tongguan by 62 and 40 times, respectively. However, this scenario has no effect on Xi'an city regarding increasing low flows (Fig. 5.5a), again owing to the location of Xi'an city being upstream of the outlets of the northern tributaries. S5-RN scenario has the largest effect on the peak flow control, the S7-RAll scenario has the best regulation effect on increasing low flows in all of the cities (Fig. 5.5). The effect of constructing reservoirs in the south (S4-RS) is more pronounced for reducing the peak flow in Xi'an city compared to that of Huaxian and Tongguan. However, the effect of S7-RAll becomes more similar to that of the S5-RN scenario as cities move closer to the outlet of the whole basin, which reflects the importance of the northern tributaries' contribution. The construction of the reservoirs in the southern catchments (S4-RS) has a much larger effect on regulating both the flood and the low flow for Xi'an city than for Huaxian and Tongguan city. The 0.1 quantile flow – an indicator of low-flow - of Xi'an city increased by 50% for S4-RS, while that of Huaxian and Tongguan city only increased by 20% each. The 0.99 quantile flow –an indicator of floods - for Xi'an city was reduced by 8% compared to 4% for Huaxian city and 3% for Tongguan city.

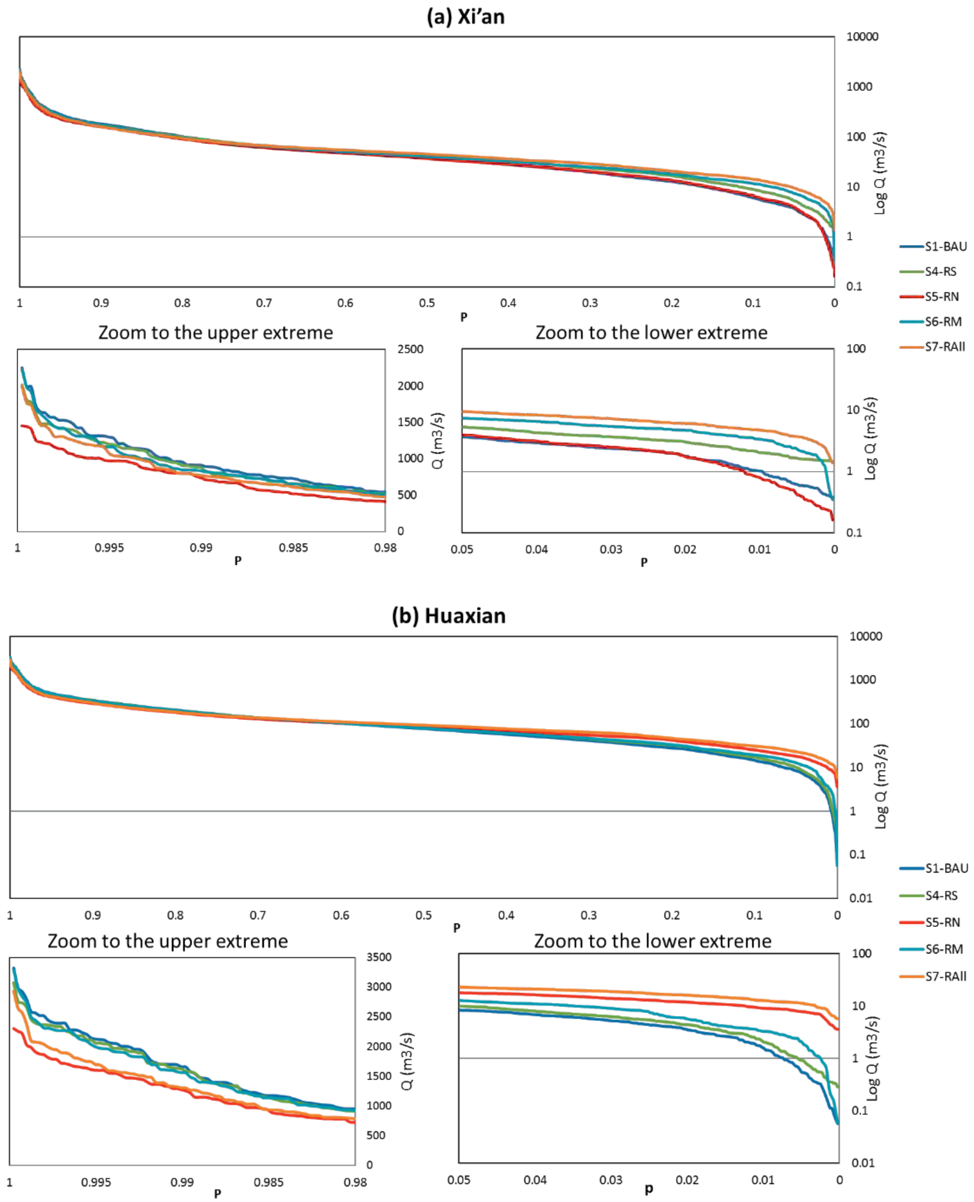

Figure 5.5 To be continued on next page.

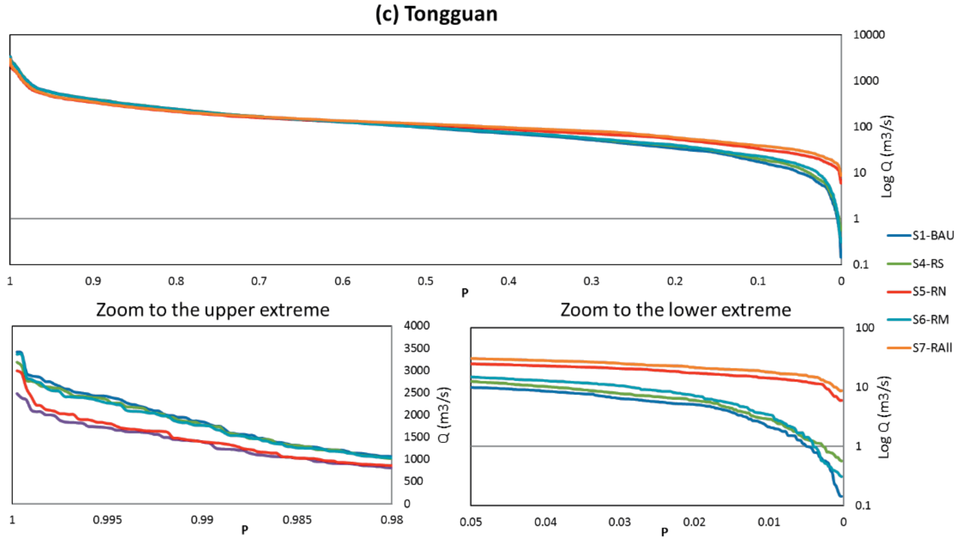

Figure 5.5 *Flow Duration Curves of the three stations (a: Xi'an, b: Huaxian, c: Tongguan) for scenarios concerning reservoir constructions (S1-BAU: business as usual, S4-RS: additional reservoirs in the South, S5-RN: additional reservoirs in the North, S6-RM: additional reservoirs on the main stream, S7-RAll: combination of RS+RN+RM): the whole FDC, zoom to the upper extreme (high flows), and zoom to the lower extreme (low flows), (P: probability of exceedance).*

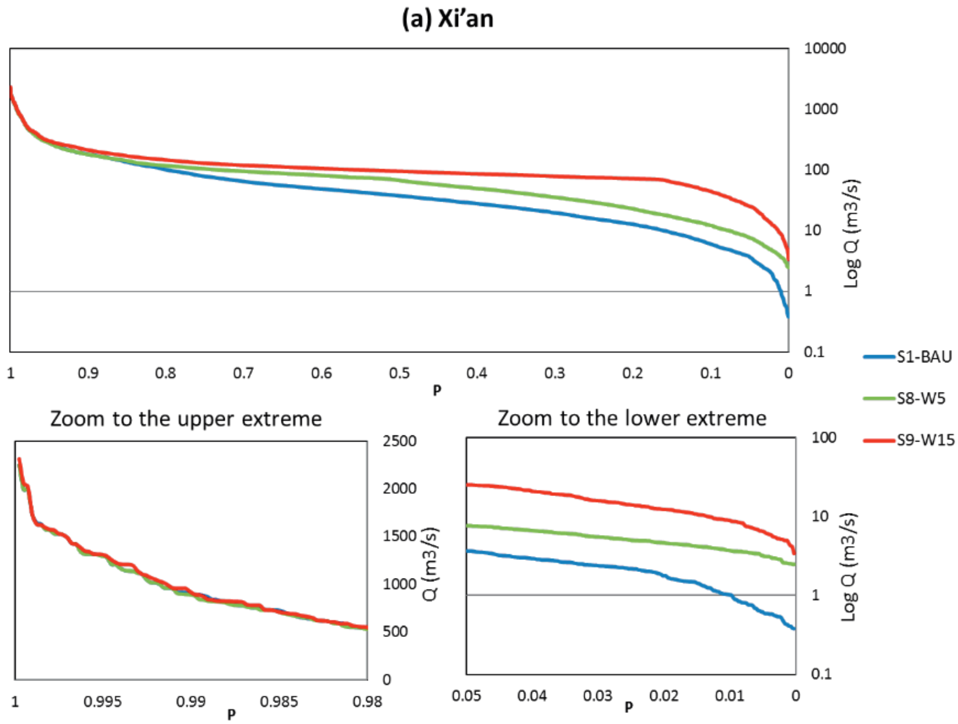

Figure 5.6 *To be continued on next page.*

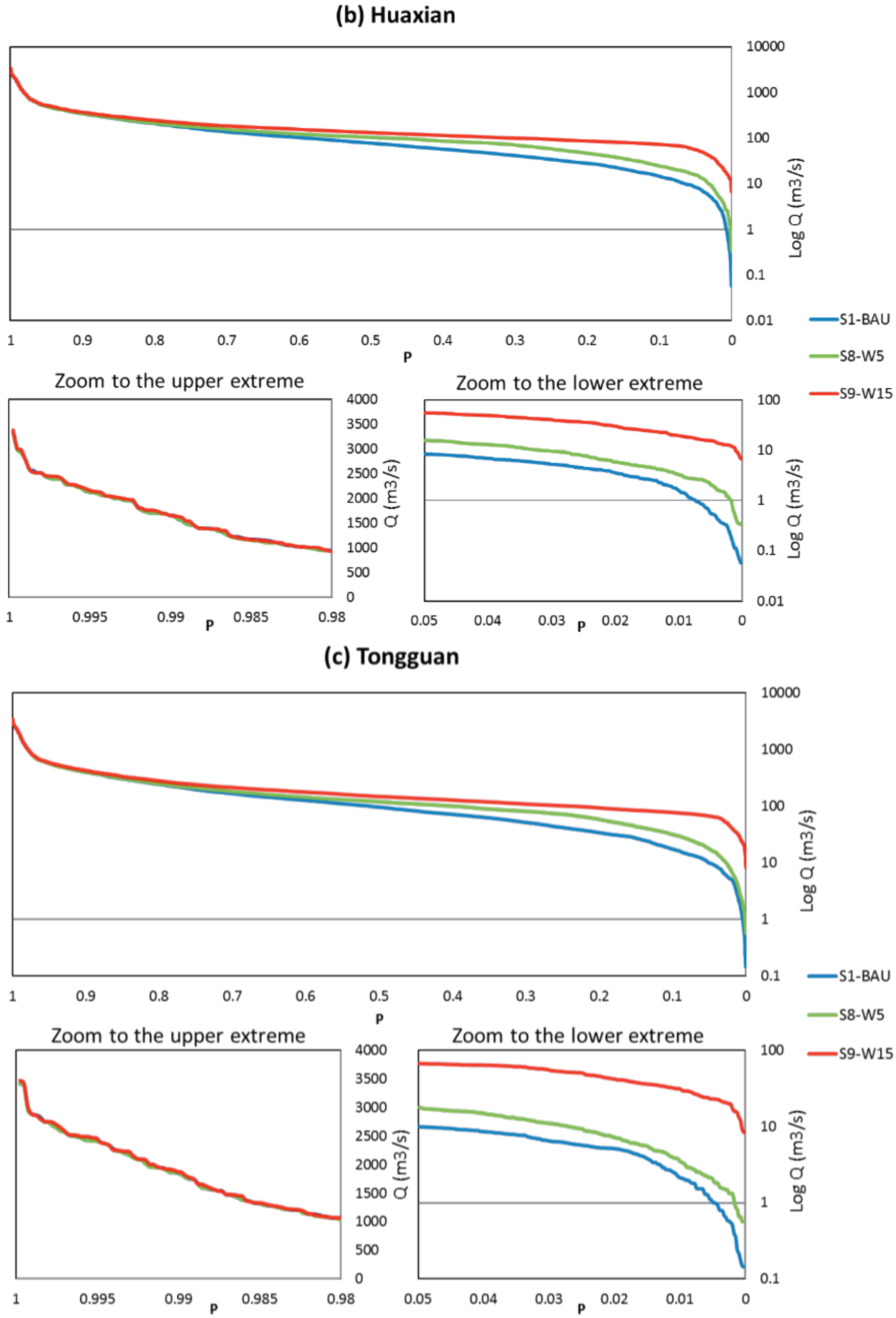

Figure 5.6 *Flow Duration Curves for the three stations (a: Xi'an, b: Huaxian, c: Tongguan) for the scenarios concerning water transfer plans (S1-BAU: business as usual, S8-W5: annual water transfer of 0.5 billion m*^{3}*, S9-W15: annual water transfer of 1.5 billion m*^{3}*): the whole FDC, zoom to the upper extreme (high flows), and zoom to the lower extreme (low flows), (P: probability of exceedance).*

5.3.1.3 Water transfer scenarios

Fig. 5.6 shows the results of the scenarios S1, S8 and S9. The effect of the water transfer plan on the change of peak flow (S8-W5 and S9-W15) can be neglected (<0%), which can be explained by the flood regulating function of the reservoirs. However, the inflow of water has a large effect on increasing the low flow of Xi'an, Huaxian and Tongguan city by 8 times, 111 times, and 59 times for the annual injection of 1.5 billion m^3 of water (Fig. 5.6, Table 5.3). The return periods of the peak flows simulated by all the scenarios for Huaxian city are also listed in Table 5.3, concluded from the S1-BAU flood frequency analysis.

Table 5.3 *Result of flood analysis for all scenario simulated for 2000-2010 with scenario results presented as the change compared to the S1-BAU baseline run (S1-BAU: business as usual, S2-NR: remove all the existing reservoirs, S3-L80: land use as it was in 1980, S4-RS: additional reservoirs in the South, S5-RN: additional reservoirs in the North, S6-RM: additional reservoirs on the main stream, S7-RAll: combination of RS+RN+RM, S8-W5: annual water transfer of 0.5 billion m^3, S9-W15: annual water transfer of 1.5 billion m^3).*

	S1-BAU	S2-NR	S3-RS	S4-RN	S5-RM	S6-RAll	S7-L80	S8-W5	S9-W15
				Xi'an					
Peak flow (m3/s)	2250.2	+7.6%	-10.5%	-35.4%	-1.1%	-11.6%	-5.6%	0.0	+2.8%
0.99 Quantile *	895.2	+10.7%	-7.1%	-20.4%	-8.4%	-15.1%	-13.9%	-2.1%	0.0
0.9 Quantile *	180.8	+5.9%	-4.8%	-12.6%	-6.0%	-11.4%	-23.2%	-0.6%	+17.2%
0.1 Quantile *	6.0	-40.0%	+48.3%	+11.7%	+93.3%	+137%	-4**1.7**%	+103%	+642%
Mean Q (m3/s)	82.4	+2.2%	-1.0%	-13.7%	-1.5%	-2.4%	-19.4%	+19.2%	+57.5%
Days (d) **	41	+8	-4	-15	-8	-12	-6	-2	0
Low flow (m3/s)	0.38	-2.6%	+287%	-57.9%	-7.9%	+266%	-65.8%	+553%	+797%
				Huaxian					
Peak flow (m3/s)	3322.5	+6.6%	-7.4%	-30.7%	-1.0%	-11.7%	-17.7%	0.0	+1.7%
0.99 Quantile *	1643.7	+6.9%	-3.7%	-24.0%	-5.9%	-21.2%	-12.4%	-0.9%	+0.1%
0.9 Quantile *	343.5	+6.4%	-2.2%	-14.8%	-4.0%	-12.0%	-29.6%	+0.4%	+7.4%
0.1 Quantile *	14.7	-31.3%	+17.7%	+70.1%	+31.3%	+110%	-83.7%	+67.3%	+395%
Mean Q (m3/s)	155.7	+1.7%	-0.5%	-9.6%	-0.8%	-3.5%	-28.7%	+10.1%	+30.4%
Days (d) **	41	+4	-4	-24	-7	-19	-8	-1	0
Low flow (m3/s)	0.06	-50.0%	+383%	+5933%	0.0%	9533%	-100%	+450%	11133%
Return Period Peak flow (y)	23	+7	-7	-16	-2	-9	-12	0	0
				Tongguan					
Peak flow (m3/s)	3414.1	+7.2%	-6.8%	-27.4%	-1.5%	-12.4%	-14.4%	0.0	+1.7%
0.99 Quantile *	1815.8	+9.9%	-3.1%	-24.5%	-3.5%	-23.6%	-12.9%	+0.1%	+2.3%
0.9 Quantile *	400.5	+4.7%	-1.8%	-14.9%	-2.8%	-12.8%	-27.6%	+0.1%	+7.0%
0.1 Quantile *	17.5	-23.4%	+16.0%	+93.1%	+33.1%	+122%	-64.6%	+81.7%	+343%
Mean Q (m3/s)	182.2	+1.5%	-0.5%	-8.7%	-0.7%	-3.6%	-25.7%	+8.7%	+26.0%
Days (d) **	41	+4	-2	-27	-4	-22	-7	0	0
Low flow (m3/s)	0.14	-42.9%	+307%	+4186%	+121%	6164%	-85.7%	+300%	+5879%

* : 0.99 Quantile: discharge of 99% quantile, unit: m^3/s; 0.95 Quantile: discharge of 90% quantile, unit: m^3/s; 0.1 Quantile: discharge of 10% quantile, unit: m^3/s.

** : Days: the number of days that exceed the 99% quantile of the S1-BAU scenario.

5.3.2 Contribution analysis

Under different scenarios, the contribution of tributaries (with the tributary's outlets shown in Fig. 5.1) on the floods of 22nd September 2003 and 4th October 2005 have also changed, as shown in Fig. 5.7. In general, the proposed reservoirs decreased the contribution of the corresponding tributaries to flood rates. The two water diversion plans have increased the contribution of the S2 tributary to the flood because of the additional flow. In comparison to S1-BAU, the no reservoir scenario (S2-NR) has shown an obvious contribution of the N1 tributary to the flood on both days, which is currently well regulated by 2 reservoirs on this tributary. The reservoirs in the South scenario (S4-RS) showed a decreased effect of the contributions from all southern tributaries except for S2, as no reservoir was proposed for this tributary in any of the scenarios. The same trend can be found for all the tributaries with a proposed reservoir regarding all catchments. In general, the S2 tributary stood out as the tributary with either the largest or the second largest contribution (after N3), since each scenario weakened the contribution of different tributaries. A similar conclusion can be drawn for the flood on 4th October 2005.

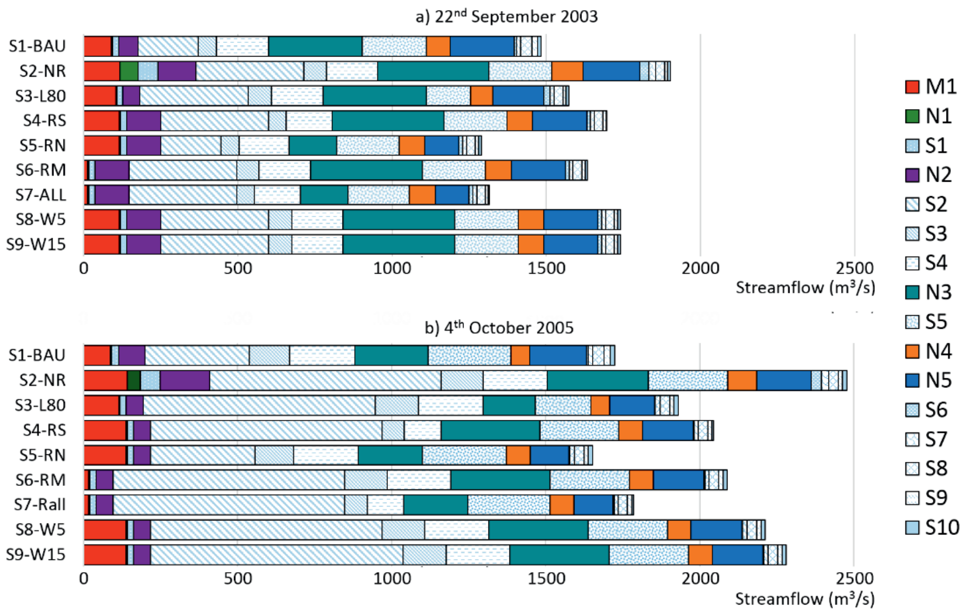

Figure 5.7 *Bar charts of streamflow composition of the tributaries under different scenarios for the floods on 22nd September 2003 and 4th October 2005, respectively (S1-BAU: business as usual, S2-NR: remove all the existing reservoirs, S3-L80: land use as it was in 1980, S4-RS: additional reservoirs in the South, S5-RN: additional reservoirs in the North, S6-RM: additional reservoirs on the main stream, S7-RAll: combination of RS+RN+RM, S8-W5: annual water transfer of 0.5 billion m^3, S9-W15: annual water transfer of 1.5 billion m^3).*

5.4 Discussion

In this study, the LISFLOOD model was applied for the first time to the Wei River Basin in China in order to analyse the flood and low flow characteristics under human intervention scenarios. Three types of scenarios were analysed for their effect on the peak and low flows in the river basin: the construction of reservoirs, land use changes and water diversions. Apart from the studies that focused more on the effect of land use changes on general streamflow patterns (Chang et al., 2015; Li et al., 2007; Shi et al., 2013; Zhang et al., 2016a; Zhang et al., 2011; Zuo et al., 2016), several studies have recently started to observe the effect of land use changes on floods in Chinese river basins (Chang and Feng, 2017, Lei et al., 2016; Zhang et al., 2016b). However, reservoirs and water diversions were often not included in the hydrological regimes' assessments but treated as a single factor that was studied separately (Assani et al., 2006; Bai et al., 2015; Lv et al., 2016; Romano et al., 2009; Sun and Feng, 2013; Wu and Chen, 2012). Therefore, this study has been the first that integrated all of the above factors into one assessment for flood analysis using an advanced modelling approach.

The scenarios concerning the construction of the reservoirs clearly demonstrated the impact of reservoirs on decreasing peak flow and increasing base flow (Sun and Feng, 2013). The impact of constructing reservoirs in the southern catchments had a larger impact on the water regulation in Xi'an city than in Huaxian and Tongguan city, despite the smaller catchment areas compared to the northern catchment. On one hand, the total capacity of the reservoirs constructed upstream of Xi'an city is much bigger than those that are upstream of Huaxian and Tongguan city (Table 5.2), which would result in a better regulation of the flood and low flow. On the other hand, the channel flow propagation also diluted the effect from upstream cities to downstream cities. Due to the high water demand from socio-economic and environmental needs, 171 large- and medium-sized reservoirs with a total water storage volume of around 33.6 km^3 were constructed in the Yellow River Basin by the year 2007 (Ran and Lu, 2012). The purpose of most reservoirs built in the Yellow River Basin has evolved from solely power generation into multi-use objectives, such as water supply, flood control, ecological prevention and sediment deposition. Globally, reservoirs have lost their storage capacity due to sedimentation at around 0.5-1% per year, while Chinese reservoirs have lost about 19% of their storage capacity after 20 years of operation (Ran et al., 2013). The flood (non-damage) storage of the reservoirs are set at 97% of the total storage in the LISFLOOD model and normal storage varies from 57% in the northern catchments to 46% in the mainstream. This means that the reservoirs located in the two northern catchments have a relatively small buffer capacity for flood control, which corresponds with the aforementioned facts of multi-functional reservoirs and the loss of capacity due to sedimentation. However, due to the lack of information concerning the loss of the storage capacities of the reservoirs in the study area, it is difficult to improve the reservoir parameters. In this study, the proposed construction of the three big dams in the northern catchments will be able to reduce the peak flow by 31% on average for the three cities, which demonstrates the flood control capacity of newly constructed large reservoirs. The construction of the northern reservoirs is not only more effective in flood control but may also have higher environmental and economic benefits than constructing more reservoirs in the southern catchments and on the main river.

The big impact of forestation on the hydrological regime is widely acknowledged (Cuo, 2016, Lacombe, 2016, Yang et al., 2010). The big differences between the two land use maps used in this study are the forested areas and the impervious areas. The average forest fraction of the total land use decreased from 0.35 in the year 1980 to 0.15 in 2000, while the average fraction of the impervious area increased from 0.006 to 0.02. Contrary to the fact that the streamflow of the study area has seen a large reduction since the 1980s, found in many studies (Gao et al., 2013; Li et al., 2016; Zhao et al., 2015), the streamflow during our research increased when replacing the 1980's land use map with the 2000's map. This result confirmed the fact that forest affects watershed hydrology by producing less runoff and more evapotranspiration (Li et al., 2009). The LISFLOOD model assumes direct surface runoff from impervious area without any soil or groundwater storage. With more forest area and less impervious area in 1980, the average runoff of the catchment was less than under the 2000 land use condition. With the implementation of the "Grain for Green" project in 1999 (Deng et al., 2014), which aims at converting farmland into woodland on the Loess Plateau, and the continuous expansion of the urban area due to population growth in the Wei River Basin, runoff of the Wei River may decrease at the end (Zhao et al., 2014; Li et al., 2018). On the one hand, reduced (flood) peak flow is to be expected, on the other hand, the decrease of the low flow may have impacts on ecosystems and might lead to water scarcity. Therefore, an integrated assessment of the flood and base flow control should always be included when analysing land use plans in future studies.

With the tributary contribution analysis, along with the proposed reservoir construction plans, water diversion plans and climate change scenarios for flood control, nature-based solutions have been recently proposed by several studies. These plans indend to address the environmental and social challenges by using nature itself, which includes flood regulation, groundwater and soil moisture regulation and biodiversity support (Metcalfe et al., 2017, Thorslund et al., 2017). The use of hydrological modelling approaches, such as the LISFLOOD model in this study, is highly recommended to evaluate the effect of such nature-based solutions in flood and base flow control under climate change conditions in future studies.

5.5 Conclusions

Based on the executed scenario analysis with the LISFLOOD model for the Wei River Basin, the following conclusion can be drawn from this study:

- The construction of reservoirs in the northern catchment is more effective for overall flood control
- Deforestation and urbanization have led to an increase in runoff
- Construction of reservoirs in the Wei River Basin may only reduce the occurrence of floods to a certain extent, but will certainly increase low flows downstream
- Water transfer plans will increase the low flow of the basin substrantially, but will not lead to an increase in floods in the Wei River basin.

6. Synthesis

6.1 General conclusions

This thesis focused on flood analysis of the Wei River Basin in China using the following steps: i) identify the influencing factors of the historical floods, ii) application of hydrological modelling for flood analysis, iii) assessing the feasibility to use global freely available meteorological datasets for flood discharge simulation, and iv) evaluation of scenario impacts on floods and low-flow discharge. The main findings of the study are depicted in Fig 6.1. To summarise, the main results of this study are:

- Flood occurence during the last 60 years in the Wei River was mainly influenced by the dam construction periods and the discharges from the northern loess and southern mountainous regions.
- The LISFLOOD model showed a good performance for the discharge simulation at the main outlet of the basin, and therefore can be applied for scenario analysis regarding flood management.
- Open source meteorological datasets cannot be directly used as input for the LISFLOOD model to simulate flood discharge.

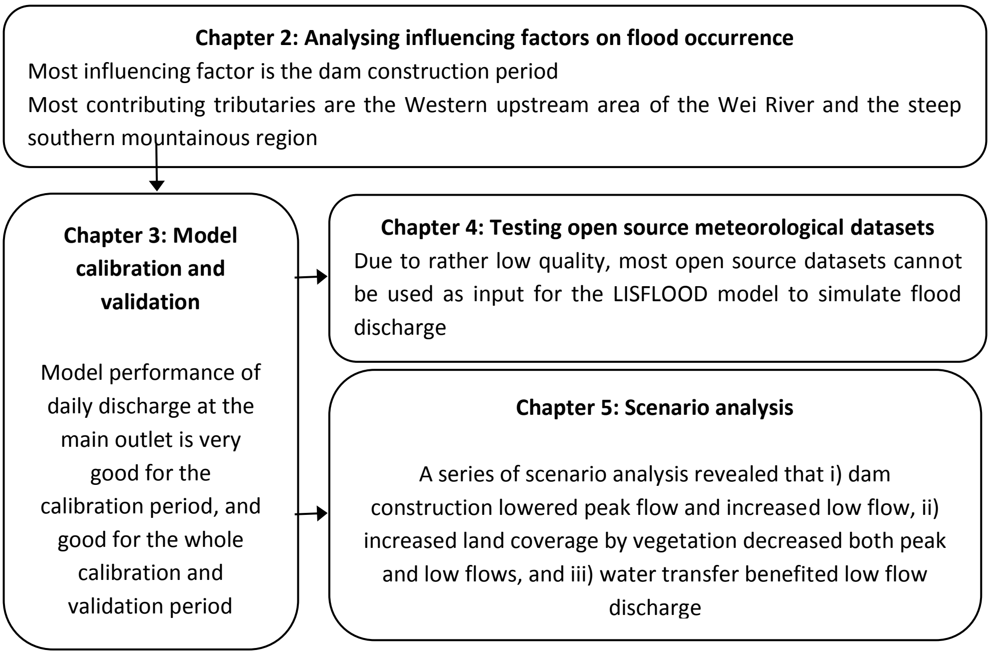

Figure 6.1 *Synopsis of the overall structure and finding of this thesis (calibration period: 2000-2007, whole period: 2000-2010).*

The insights gained from this study are directly applicable to improve flood control practices in the study area, and also can be transmitted to other river basins in China for technical support and decision making processes:

- The framework approach for flood analysis developed in this study is able to identify the causes of historical flood occurrence and related factors, using a conditional inference tree analysis. By answering the questions in a logical order of Why-Where-When-How, this approach is capable of facilitating exploratory analysis to better understand flood occurrence in complex environments.
- The LISFLOOD model is capable of simulating discharge at the main outlet of the basin rather well, both on daily and monthly basis.
- The upstream areas South of the Wei River contribute the most to the discharge at the outlet of the Wei River Basin, as well as causing related floods. The upstream loess areas North from the Wei River also contribute to discharge at the outlet of the basin, however to a lesser extent due to existing dams and reservoirs in this region.
- The construction of reservoirs in the loess northern areas is more effective than in other regions for overall flood control. Deforestation and urbanization across the basin increased peak flow.
- Water transfer plans, such as the South - North Water Transfer project, aim at fulfilling the water usage demands in the Guanzhong Plain located in the study area, and will increase low flow discharges without increasing flood peak discharge.
- The currently global freely available meteorological datasets should be carefully examined before being used as input data for hydrological modelling, because daily estimates of both precipitation and temperature are rather poor, especially for the northern arid loess region in the Wei River Basin.

6.2 General Discussion

This study has unravelled the factors causing the floods in the Wei River China in the years between 1950-2010 with a framework approach based on Conditional Inference Tree analysis (Hothorn et al. 2006). Being the first application of the LISFLOOD model in the region for daily flood discharge study under both climate and anthropogenic changes, the research has advanced the scientific understanding of the flood analysis for the particular study area. The effort lies mostly in the repeated validation of the methodology to build up a reliable and accurate technical base. The framework approach can be applied in other catchments for flood factor analysis also to understand complex conditions causing flood occurrence. The hydrological model for flood discharge simulation can be further applied in other catchments for integrated flood and water resources management. The lessons learnt during this research through the cross-validation of the processes as well as the scientific advancement in the field of flood analysis are discussed below from four different angles.

6.2.1 Epistemology versus ontology

6.2.1.1 Factors influencing flooding

As listed in the introduction, the factors influencing flood occurrence were categorized into meteorological, biophysical and anthropogenic factors. In Chapter 2, a framework approach was developed to evaluate the importance of these factors based on the application of Conditional Inference Tree analysis. Our results show that the most influential factors for flooding in the study area over the last 60 years were related to the elevation of the Tongguan outlet station and the precipitation of the southern region. Several studies have made the effort to understand the cause of individual flood occurrence. For instance, Jiang et al. (2004) and Xing et al. (2004) have both characterized the Tongguan elevation and the flood discharge from the southern tributaries as the leading two reasons of the 2003 floods. Pang (2007) also concluded that the precipitation in the southern tributaries that drain into the Wei River upstream of Huaxian City is the main factor causing the flood in 2005. However, these studies did not identify the most influential tributary contributing to each flood event. With the help of the modelling approach used in this study, it was possible to explore the importance of each tributary to each flood occurrence. Without tackling the most troublesome tributary causing the flood in the area, it is difficult for policymakers to design adequate and implement flood mitigation or adaptation measures. Therefore, this study is the first to use both statistical and modelling approaches for better system understanding and related flood mitigation.

6.2.1.2 Application of the CORDEX datasets

There is a common perception that the CORDEX datasets, resulting from regional climate models, are by far the most reliable climate projections that can be applied to drive diverse models for future predictions (Alfieri et al., 2015; Aich et al., 2016; Osuch et al., 2017). However, our study has suggested that due to the heterogeneity of different regions, the simulation of the regional climate models may lead to large bias. Studies about different aspects of the meteorological variables also suggested biases and high uncertainties in the current CORDEX-EA datasets (Park et al., 2016; Myoung - Jin et al., 2017; Wang et al., 2018). Therefore, without a proper evaluation of the precision of the CORDEX datasets for the study area under consideration, these datasets should be used with special care.

6.2.1.3 Floods in arid regions

The location of our study area is in the semi-arid region of the loess plateau in China. The northern part of the respective basin, which has an arid climate, covers 54% of the total area. The flood plain lies in the valley between the northern loess and southern mountain range. The common perception is that the basin suffers more drought and water scarcity than floods (Huang et al., 2015b; Huang et al., 2015c; Zhang et al., 2018). However, both historical records and this study have shown that floods are severe in this area. In particular the southern mountain range, characterised by steep slopes and relief, contributes significantly to flood development. Huang et al. (2015a) have investigated the spatial difference in precipitation patterns between the northern and the southern regions of the Wei River Basin and demonstrated the importance of recognizing the impact of the two distinct areas on the overall water regime. A better understanding of the large contribution from a small fragment of the basin on flood occurrence can also support better implementation of alert and management practices.

6.2.2 Modelled versus observed

6.2.2.1 Model data

In Chapter 3, the calibration and validation of the LISFLOOD model made use of interpolated observed meteorological gauging station data. While in Chapter 4, freely available meteorological reanalyses and regional climate model datasets were used as input for the LISFLOOD model. Usually, the ground observation data is criticized because of scarce spatial distribution, human-induced uncertainty and discontinuity in time, being rather unreliable as input data for hydrological models (Xu et al., 2013; Fuka et al., 2014; Zeng et al., 2018). However, in our study, the observed meteorological datasets performed better than global reanalyses and regional climate model datasets even with use of virtual precipitation points. Huang et al. (2015a) have investigated the anomaly and irregularity of daily precipitation in the Wei River Basin, confirming the importance of good quality rainfall data for flood analysis. Peng et al. (2014) applied the TOPMODEL for the lower reach of the Wei River basin, including the southern mountain range, with an intensive distribution of 27 rainfall gauges resulting in comparable simulated and observed discharges for two hydrological gauging stations. This indicates that a good spatial distribution of state-of-the-art rainfall gauges may lead to an improvement of model performance.

Another point worth mentioning is that the local gauge data for the northern part of the basin resulted in relatively better model results than by using the global reanalysis datasets. There is a clear difference between simulations under observed meteorological data versus the global reanalyses data regarding model evaluation coefficient values (Chapter 3 compared to Chapter 4). Another reason for unsatisfactory results of simulated discharges relates to the quality of the soil data. With the absence of local data, the global Soilgrid dataset was used together with pedotransfer functions developed for American soils (Saxton et al., 1986) for calculation of soil water distribution parameters. Although we acknowledge that the flood peak results are less sensitive to soil related processes, the low flow discharges can be highly influenced by the improvement of either the local or the global soil data.

6.2.2.2 Model performance

Modelled discharge is often different from observed discharge simply because the model is not perfect. Among the studies concerning the application of hydrological models in the Wei River Basin, Shen et al. (2015) achieved a good agreement at Xianyang hydrological station for the monthly discharge using the VIC model. Zuo et al. (2015a) and Li et al. (2016) have also obtained good simulation results for monthly discharge in the Wei River basin by applying the SWAT model. However, none of the studies has conducted or reported a long-term daily discharge simulation for the period after the year 2000. Despite the rather unsatisfactory daily validation results, the 2003 and 2005 floods were successfully simulated, and the contribution analysis has confirmed the cause of both flood events. The LISFLOOD model has been used elsewhere also, for instance for pan-African catchments with most of the KGE scores greater than 0.5, an indication of good model performance (Thiemig et al., 2015). It also has been applied to the Elbe river basin in central Europe with an average NSE score for the calibration period of 0.66 (van der Knijff et al., 2010). While in our study, four out of seven hydrological gauging stations has reached a KGE score of greater than 0.65, indicating very good simulation results, the other stations have a KGE score greater than 0.5, which is still good. To conclude, the LISFLOOD model performed well in combining with existing input data, to simulate daily discharge in the Wei River basin.

As indicated by (Zajac et al., 2017), the reservoir simulation in the LISFLOOD model might need improvements due to large parameter uncertainty in the reservoir simulation. Despite the existing differences between simulated and observed discharge, conclusions of the study are not affected because the uncertainty in reservoir simulation is rather small compared with the total reservoir storage capacity.

Due to the lack of data and limitation of the model structure, we could not simulate the sedimentation process which might be important for flood occurrence also. It was observed in the data, that the trend of the peak discharge of all flooding events remained stable while the peak discharge depth was increasing in time. Most likely, this is the result of rising of the river bed, as demonstrated in several other studies focussing on the morphology of the Wei River (Wu et al., 2004; Wang et al., 2007; Zheng et al., 2015). Therefore, without knowledge on the sedimentation processes in the catchment, it is difficult to predict the exact flood occurrence, even if discharge is accurately simulated. Furthermore, flood magnitude may have a great influence on the sediment yield (Hu et al., 2019) and hence the formation of the river bed, which in return will affect the flood inundation (Wu et al., 2004; Jin et al., 2012). The interaction and the feedback mechanism among these components and processes needs a better understanding.

6.2.3 Local versus global

6.2.3.1 Local and global datasets

Freely available datasets for describing the biophysical conditions of the basin were used as input for the LISFLOOD model, such as elevation, soil and vegetation parameters and a river channel network, together with the observed meteorological gauging station data. The results of the calibration and validation of the model were satisfactory (Chapter 3). However, the use of global freely available meteorological forcing data (CORDEX-EA and reanalyses) together with the same biophysical condition datasets appeared not to be successful (Chapter 4). This means that the current global freely available datasets can be used for hydrological model calibration and validation, but not with regard to climatic and/or meteorological input data. This was demonstrated also in the application of the LISFLOOD in the Elbe river basin (Thielen et al., 2009).

With respect to the freely available meteorological datasets, efforts has been undertaken aiming at both improving the accuracy of the current methodologies and developing new downscaling methods (Kanamaru and Kanamitsu, 2007; Cha and Lee, 2009; Maraun et al., 2010; Hong and Chang, 2012; Srivastava et al., 2015; Tang et al., 2017). Compared to a relatively wide application and investigation of the CORDEX and reanalyses datasets to other parts of the world (Smith and Kummerow, 2013; Tramblay et al., 2013; Abiodun et al., 2016; Aich et al., 2016; Essou et al., 2016; Osuch et al., 2017; Roudier et al., 2016), the studies concerning the future climate change projections in East Asia or China are still limited with higher uncertainties (Park et al., 2016; Myoung - Jin et al., 2017; Gu et al., 2018; Wang et al., 2018).

6.2.3.2 Wei River basin in a global perspective

The current study indicates that it is important to first identify differences among sub-basins, and calibrate and validate the hydrological processes separately. In the Wei River Basin, large spatial differences exist between northern and southern regions, leading to specific hydrological regimes and flood characteristics. Gaba et al. (2017) has applied a lumped model for comparing 20 catchments under different conditions, and the results indicated high differences between individual catchments. Hattermann et al. (2005) applied the distributed hydrological model SWIM for several mesoscale and macroscale catchments in Germany with different sub-basin characteristics, and the result also demonstrated the importance to divide the processes and parameterization across the different sub-basins.

Water resources distribution in China is considered to be the most dependent on human activities in the coming century (IPCC, 2013). In this study, we examined the impact of human interventions in the river basin, ranging from vegetation change, urban expansion to water diversion plans. The “Green for Grain” project and the “South Water to North” water diversion projects are both large examples of human intervention on the biophysical environment. Therefore, the effort of this study was amongst others to seek for and apply a powerful simulation tool accounting both for biophysical processes and effects of human interactions upon river discharge and flood generation. LISFLOOD appeared to be an adequate tool for that purpose.

6.2.4 Past versus future

6.2.4.1 Climate change

Precipitation is a key driver for flood generation. It is expected that climate change will increase the number of extreme events at both global and regional scales (Lehner et al., 2006; Kundzewicz et al., 2010; Wilby and Keenan, 2012; Montanari et al., 2013). Studies has suggested a hotter and wetter trend in East Asia in terms of climate projections (Freychet et al., 2015; Park et al., 2016). Flood risks in China under climate change has been explored by Zuo et al. (2015b), indicating a higher risk of extreme events, both floods and droughts, in the Wei River basin, using statistically downscaled global climate model projections. However, an in depth study about the future risks of floods under climate change, based on daily discharge simulation, should be conducted also, preferably by using accurate projections of future meteorological conditions.

6.2.4.2 Dam construction

Dam construction period is the largest influencing factor influencing the flood occurrence. In Chapter 5, impacts of dams and reservoirs have been assessed on flood discharge. In particular, the dam constructions in the northern territory affected flood peak discharges at the basin outlet. The no reservoir scenario indeed showed an increase in general discharge, and higher peak discharges and lower low flows. In general, the reservoirs decreased the contribution of the corresponding tributaries to the total river discharge. This finding is in line with other studies concerning the water regulation function of the dams and sluices (Wang and Xia, 2010; Bai et al., 2015). Studies has investigated a smart cascade reservoir functionality on the regulation of the streamflow (Zhou et al., 2014b; Bai et al., 2015; Feng et al., 2018), which can be applied in future to optimize catchment flood management using an hydrological modelling approach.

6.2.4.3 Land use change

During the last decades, the land use changes in the study area are mainly reforestation and urban expansion (Chapter 5). With more sealed area as the result of urban expansion, discharge is expected to increase. With less forest, evapotranspiration is expected to decrease, thus also leading to more discharge. Our study investigated the land use change of 2000 in comparison with the year 1980, as a more recent land use map was not available. However, since the “Grain for Green” afforestation project, launched in the river basin in the 1990s, the landscape regreened up to 2005 according to vegetation cover studies (Wang et al., 2017; Zheng et al., 2019). As a result, the river discharge decreased since then. Moreover, water extraction increased as a result of domestic, industrial and agricultural use, which will also affect river discharge. At present, it is not possible to clearly understand which of these processes dominate, as this will depend on future landscape and water management decisions for the region also. This emphasises the importance of using a powerful management tool to support decision making at the catchment scale.

6.2.4.4 Water transfer project

Defined as a strategic programme, the China’s South - North Water Transfer project is by far the largest water supply infrastructure of the world, which will result in large social, environmental and ecological impacts (Zhu et al., 2008; Chen et al., 2013; Webber et al., 2015; Ma et al., 2016; Pohlner, 2016; Zhuang, 2016). As part of the current study, the water transfer plan scenario was evaluated and provided insights into the impact on discharge of the recipient basin, which has not been done before. Due to the regulation function of the water receiving reservoir, the flood discharge is not expected to increase. However, the base flow downstream of the reservoir is expected to increase, which is in line with other studies concerning the improvement of water quantity and quality of water receiving basins (Chen et al., 2008; Dadaser-Celik et al.; 2009, Zhuang, 2016). The water transfer plan is designed to be used for domestic and industrial water consumption purposes in the Guanzhong Plain, required due to both rapid economic and population growth (Fan et al., 2014). Therefore, the water extractions to be expected in the basin will compromise the inflow into the basin led by the water transfer plan.

6.3 Implications and recommendations

6.3.1 For researchers

6.3.1.1 Fundamental research

As verified in this study, especially in Chapters 3 and 4, as well as indicated by (Beven, 2012; Zeng et al., 2018), the distribution and data quality from local rain gauges is of vital importance for the accurate simulation of surface discharge. Like all other big data solutions, hydrological modelling needs to be supported by large amounts of data to reach an optimal accuracy and a realistic representation of the system. This finding implies that, for some regions, a significant scientific advancement can be achieved simply by installing a good amount of gauge stations with a proper representation of the spatial distribution of rainfall. As indicated in Chapter 4, the accuracy of RCM simulations is essential for flood discharge prediction, which is the fundamental base for flood mitigation and adaptation under climate change circumstances. Besides meteorological data, the quality of data for all other natural conditions that may directly or indirectly influence the flood regime is also important due to feedback mechanisms within the water cycle (Andréassian et al., 2004; Bormann et al., 2005; Bormann et al., 2007; Brulebois et al., 2015; Luo et al., 2017). For instance, our study applied globally available soil and topographical data directly without validation, under the assumption that the global datasets are sufficiently accurate and that runoff process are less sensitive to these parameters. However, the uncertainty associated with this remains unknown. Publicly available and region-specific data sources with trustworthy quality are fundamental conditions for any research. We would like to suggest that researchers in related fields spend efforts to improve the quality of field data they collect and to increase sharing.

6.3.1.2 Hydrological modelling

Although model developers are currently focusing on the trade-off between model complexity and accuracy, both the increase of model complexity and generic calibration approaches can be facilitated in the future with the fast development in computational ability. Therefore, more efforts should be put on system optimization of hydrological models, such as integrating more processes in the model while keeping the possibility for the user to choose the modules to be included in the simulation based on system complexity, processes to be studied, or data availability. As an example, Amatya and Harrison (2016) have indicated that the estimation of evaporation of different land use types may differ, depending on the equation used. In the LISFLOOD model, it is therefore possible to choose between the Penman–Monteith and the Hargreaves equation to calculate evaporation. Another aspect to be improved in hydrological models is the spatial resolution which could be increased with higher computational ability in the future, since higher spatial resolutions can better represent hydrological connectivity (Nunes et al., 2018).

To facilitate flood mitigation and adaptation, more relevant concepts and processes can be included in the model structure. For instance, instead of assuming complete impermeability for built-up areas, in simulations, improvements are needed to resemble reality, for instance to account for effects of nature based solutions for urban flood control (Thorslund et al., 2017; Chan et al., 2018; Mei et al., 2018; Lee and Huang, 2018; Van Coppenolle et al., 2018).

6.3.1.3 Flood prediction

The LISFLOOD model is currently applied as the base model for the Global Flood Awareness System (GloFAS, Alfieri et al., 2013), which is a good practice of model application. Concerning flood predictions, studies are mainly performed to assess future effects resulting from natural changes and human activities (Bell et al., 2009; Zhou et al., 2014a; Apurv et al. 2015; Aich et al., 2016; Alfieri et al., 2017). The application of climate projections for future flood prediction is of great importance, and the flood characteristics are more sensitive to daily or even hourly meteorological processes, rather than to monthly or seasonal processes. However, the climate projections from CORDEX-EA in our study area are rather coarse, and therefore more efforts should be undertaken to improve the simulation accuracy of climate projections. Another factor that greatly influence the flooding regime is topography, which determines the routing of runoff and flood water (Stockdon et al., 2006). Remote sensing techniques are appropriate for accurate estimation of the earth surface elevation, and to predict source points for overflows (Feng et al., 2012). Complexing factors are related to the river channel topography (Horritt and Bates, 2002), and estimates of sediment transport and deposition (Hu et al., 2019). The interaction and feedback mechanisms among these components require a better understanding.

6.3.2 For policy makers

Apart from better understanding of the flood related processes and factors, the insights gained in this study are also relevant for policy makers, for instance with regard to the overall effect of multiple dam systems in complex river systems, and for flood mitigation and adaptation purposes.

6.3.2.1 Flood mitigation and adaptation

Decision making can be based on a joint understanding of the processes of flood generation, discharge, and propagation from upstream to downstream, especially in cross-boundary river basins. In China, the majority of the rivers drain through several provinces or different administrative regions, and therefore the result of this study is important for those large river basins and their management. Instead of acting independently towards a certain local flood warning, which usually happens in the downstream floodplain, flood discharge can be better mitigated by actions from upstream management authorities, such as water storage in reservoirs, diverting flood water into large riparian areas, or taking advantage of the time lag between the upstream and the downstream flood peak for proper and timely evacuation plans. Spatially distributed flood models like LISFLOOD could play an important role with this respect.

6.3.2.2 Water resources management

In a broader context, river discharge is the carrier for sediment, pollutants and nutrients, which is of vital relevance to aquatic life, human health, and food production (Batalla and Vericat, 2009; Taylor et al., 2011; Bierkens, 2015). The transport of sediment greatly influences the formation of the geomorphology of the river, and in return the flood regime. The transport of pollutants in the river and related floods might impact ecosystems and endanger food production (Yang et al., 2015; Ouyang et al., 2017; Franqueville et al., 2018; Bento et al., 2019; Yang et al., 2019). The amount of water trasported in the river channel is also crucial for aquatic life and energy (Marquès et al., 2013). Therefore, the accurate simulation and prediction of the hydrological regime of complex river systems is vital for multiple purposes, including decision making processes.

The demand for natural resources and the need for sufficient food and others have altered the structure of human society, particularly being reflected by changes in for instance land use and construction of infrastructures, affecting courses of rivers and related flood and drought regimes (Istomina and Dobrovoski, 2016). Although dams have clear and positive effects on flood control, it is also argued that dam construction is not always economic and ecologically sustainable. A more comprehensive and integrated cross-disciplinary assessment for dam construction, especially for dams hydropower functions, is needed for future decision making. Meanwhile, nature-based solutions are proposed as a more environmental friendly and sustainable approach for flood mitigation, often receiving support from relevant stakeholders (Metcalfe et al., 2017; Thorslund et al., 2017).

6.3.2.3 Public awareness

Public campaigns are needed to inform the general public about the principles and potential risks of floods, in particular in flood-prone areas. Governmental authorities can play a key role in this process, and use can be made by different means to inform inhabitants. For this purpose both traditional (newspapers, radio, television) and more innovative social media can be used to inform the general public and/or specific target groups. In addition, national natural disaster plans are essential, both from a prevention as well as a remediation point of view. Good examples can for instance be found at the website of the Environmental Protection Agency in the USA (www.epa.gov/natural-disasters), addressing a range of different natural disasters, including flooding.

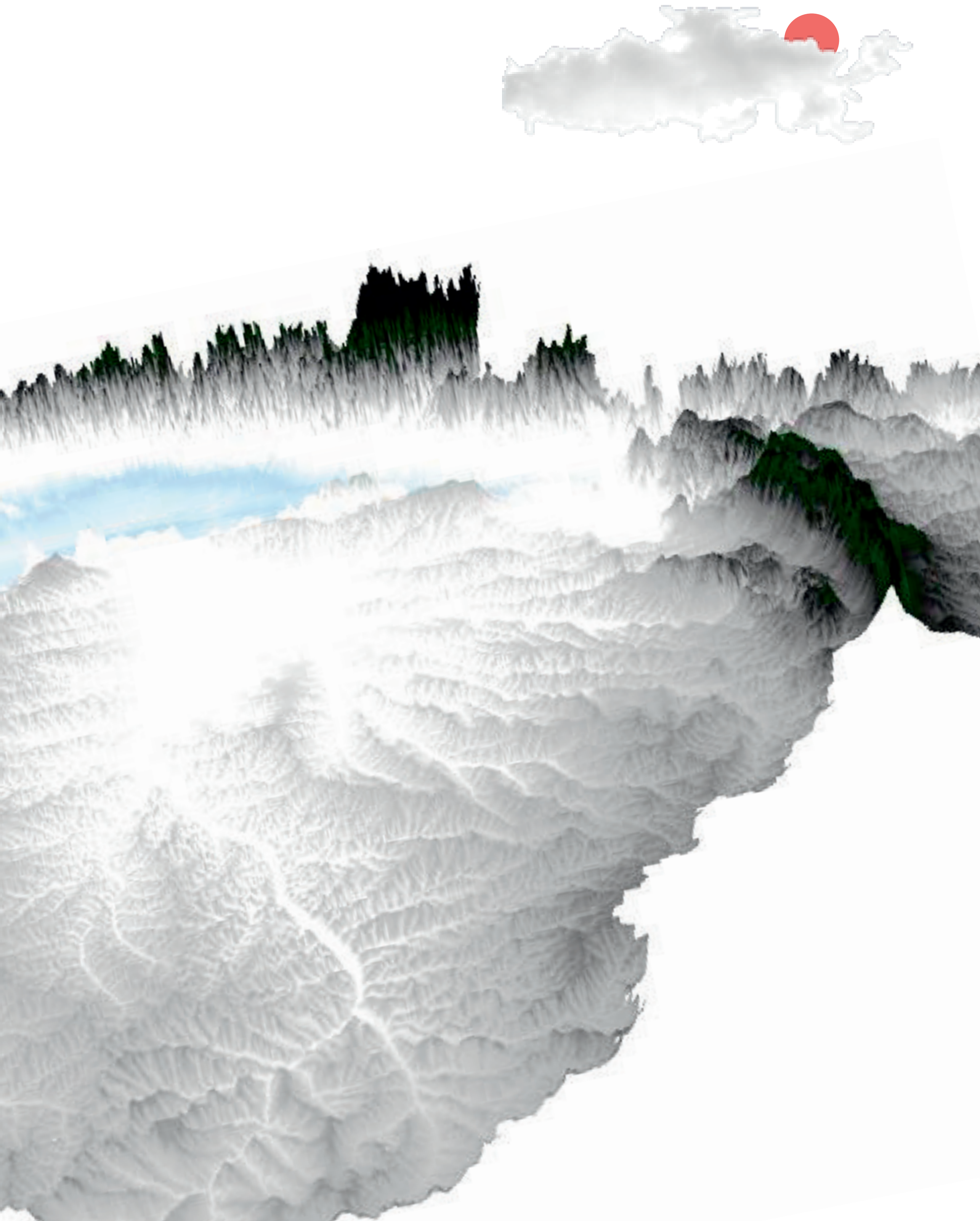

Supplementary Material

S.1 LISVAP model

The LISVAP model is a pre-processor used to calculate potential evapo(transpi)ration grids which are then used as input to LISFLOOD. Calculation of reference potential evapotranspiration and evaporation are simplified by only using the maximum, minimum and average daily temperatures:

$$ET0 = \frac{\Delta R_{na} + \gamma EA}{\Delta + \gamma} \tag{S.1}$$

Where $ET0$ is the potential evapotranspiration rate from a closed vegetation canopy (mm day^{-1}), R_{na} is the net absorbed radiation (mm day^{-1}), EA is the evaporative demand of the atmosphere (mm day^{-1}), Δ is the slope of the saturation vapour pressure curve (mbar °C^{-1}) and γ is the psychrometric constant (mbar °C^{-1}).

The net absorbed radiation is calculated as

$$R_{na} = \frac{(1-\alpha)R_{gd} - R_{nl}}{L} \tag{S.2}$$

Where R_{gd} is the incoming solar radiation (J m^{-2} day^{-1}), R_{nl} is the net long-wave radiation (J m^{-2} day^{-1}), α is the albedo (reflection coefficient, equals to 0.23) of the surface, and L is the latent heat of vaporization (MJ kg^{-1}): L=2.501-2.361-10^{-3} T_{av}.

For the incoming solar radiation,

$$R_{g,d} = R_{a,d} A_h \sqrt{(T_{\max} - T_{\min})} + B_h \tag{S.3}$$

Where $R_{a,d}$ is the Angot radiation (J m^{-2} day^{-1}), A_h: Empirical constant (°C $^{-0.5}$) and B_h: Empirical constant (J m^{-2}d^{-1}),

For the net long-wave radiation:

$$R_{nl} = f\varepsilon'\sigma(T_{av} + 273)^4 \tag{S.4}$$

Where σ is the Stefan Boltzmann constant (4.90×10^{-3}) (J m^{-2} K^{-4} day^{-1}), f is the adjustment factor for cloud cover (-), and ε' is the net emissivity between the atmosphere and the ground (-).

S.2 LISFLOOD model

The detailed processes included in the LISFLOOD model are snow melt, infiltration, interception of rainfall, leaf drainage, evapo(transpi)ration, surface runoff, preferential flow, exchange of soil moisture between the two soil layers and drainage to the groundwater, sub-surface and groundwater flow, and flow through river channels. LISFLOOD model input includes topographic, soil, land use, river channel, meteorology and reservoir information, as listed in Table S.1.

Table S.1 *Important LISFLOOD model inputs*

Map name	Unit	Range	Description
Topography			
Ldd.map	Flow direction	1-9	Local drain direction 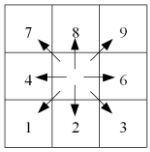
Gradient.map	m/m	>0	Slope gradient
Elvstd.map	m	>0	Standard deviation of elevation
Land Use			
Fracwater.map	-	0-1	Fraction of inland water area for each cell
Fracsealed.map	-	0-1	Fraction of impermeable surface for each cell
Fracforest.map	-	0-1	Forest fraction for each cell
Fracother.map	-	0-1	Other land use fraction for each cell
Soil			
Thetas.map	-	0-1	Saturated volumetric soil moisture content
Thetar.map	-	0-1	Residual volumetric soil moisture content
Lambda.map	-	0-1	Pore size index (λ)
Alpha.map	-	0-1	Van Genuchten parameter (α)
Ksat.map	cm/day	1-100	Saturated conductivity
Channel			
Chan.map	-	0-1	Boolean 1 for channel pixels and Boolean 0 for all others
Changrad.map	m/m	>0	Channel gradient
ChanMan.map	-	>0	Manning's roughness coefficient for channels
ChanLeng.map	m	>0	Channel length
Chanbw.map	m	>0	Channel bottom width
Meteorology			
p.	mm/day	>0	Map stacks of daily precipitation
Ta.	˚C	-50 - +50	Map stacks of average daily temperature
Tn	˚C	-50 - +50	Map stacks of minimum daily temperature
Ts	˚C	-50 - +50	Map stacks of maximum daily temperature
Es	mm/day	>0	Daily potential evaporation rate of bare soil

E0	mm/day	>0	Daily potential evaporation rate of free water surface
Et	mm/day	>0	Daily potential evapotranspiration rate of reference crop
		Definition of input/output	
Outlets.map	-	>0	Nominal map with locations at which discharge time series are reported
Sites.map	-	>0	Nominal map with locations at which time series of intermediate state and rate variables are reported
		Reservoir	
Res.map	-	>0	Reservoir locations
Rtstor.txt	m^3	>0	Reservoir storage capacity
Rclim.txt	-	>0	Conservative storage limit
Rnlim.txt	-	>0	Normal storage limit
Rflim.txt	-	>0	Flood storage limit
Rminq.txt	m^3/s	>0	Minimum outflow
Rnormq.txt	m^3/s	>0	Normal outflow
Rndq.txt	m^3/s	>0	Non-damaging outflow

S.3 The LISFLOOD calibration tool

The LISFLOOD calibration tool uses a multi-objective generic algorithm to calibrate the simulated streamflow against the observations from the hydrological stations for multiple catchments scripted in Python programming language. It loops through all the sub-basins in an ascending order of the catchment area to calibrate LISFLOOD for each interstation region using the defined objective genetic algorithm. In our study, a single objective function, which is the Nash-Sutcliffe model efficiency coefficient, was used for all the calibration. The model performance coefficient to evaluate the goodness of fit between the simulated and observed discharge in the model are listed below:

Nash–Sutcliffe model efficiency coefficient (*NSE*)

$$NSE = 1 - \frac{\sum_{t=1}^{T}(Q_m^t - Q_o^t)^2}{\sum_{t=1}^{T}(Q_o^t - \overline{Q_O})^2} \tag{S.5}$$

Where：
Q_o is the mean of observed discharges (m^3/s)
Q_m is simulated discharge (m^3/s)
Q_o^t is observed discharge at time t (m^3/s)
Q_m^t is modelled discharge at time t (m^3/s)

KGE is a decomposition of *NSE* which gives equal weighting to linear correlation (*r*) (dimensionless), bias ratio (β) and variability (γ) (Gupta, 2009) with the optimal value of 1:

$$KGE = 1 - \sqrt{(r-1)^2 + (\beta - 1)^2 + (\gamma - 1)^2} \qquad \text{(S.6)}$$

$$\beta = \frac{\mu_S}{\mu_O} \qquad \text{(S.7)}$$

$$\gamma = \frac{CV_S}{CV_O} = \frac{\sigma_S/\mu_S}{\sigma_O/\mu_O} \qquad \text{(S.8)}$$

Where:
CV is the coefficient of variation (-) between the simulated (CV_s) and observed (CV_o) discharge (-)
β is the bias ratio between average values for simulated (μ_s) and observed (μ_o) discharge (-)
γ is the variability ratio between the standard deviation of modelled (σ_s) and measured (σ_o) discharge (-)

The percent bias (*Pbias*) measures the average tendency of the simulations to be larger or smaller than the observations, where positive values indicate an overestimation and negative values indicate an underestimation bias.

$$Pbias = 100\,\frac{\sum_{i=1}^{N}(S_i - O_i)}{\sum_{i=1}^{N} O_i} \qquad \text{(S.9)}$$

Where:
S_i: Simulated discharge (m^3/s)
O_i: Observed discharge (m^3/s)
N: Number of records (-)

The Pearson linear correlation coefficient (*r*) measures the strength of the linear correlation between the simulated and observed values, where 1 indicates a total positive linear correlation and -1 means a total negative linear correlation:

$$r = \frac{\sum_{i=1}^{n}(S_i - \mu_S)(O_i - \mu_O)}{\sqrt{\sum_{i=1}^{n}(S_i - \mu_S)^2}\sqrt{\sum_{i=1}^{n}(O_i - \mu_O)^2}} \qquad \text{(S.10)}$$

Where:
S_i: Simulated discharge(m^3/s)
O_i: Observed discharge (m^3/s)
μ_s: mean simulated discharge (m^3/s)
μ_o: mean observed discharge (m^3/s)

Literature cited

Abdulkareem J, Sulaiman WNA, Pradhan B, Jamil NR. Relationship between design floods and land use land cover (LULC) changes in a tropical complex catchment. Arabian Journal of Geosciences 2018; 11: 376.

Abedini M, Md Said MA, Ahmad F. Integration of statistical and spatial methods for distributing precipitation in tropical areas. Hydrology Research 2013; 44: 982-994.

Abiodun BJ, Abba Omar S, Lennard C, Jack C. Using regional climate models to simulate extreme rainfall events in the Western Cape, South Africa. International Journal of Climatology 2016; 36: 689-705.

Ahn SR, Jeong JH, Kim SJ. Assessing drought threats to agricultural water supplies under climate change by combining the SWAT and MODSIM models for the Geum River basin, South Korea. Hydrological Sciences Journal 2015: 1-14.

Aich V, Liersch S, Vetter T, Fournet S, Andersson JCM, Calmanti S, van Weert FHA, Hattermann FF, Paton EN. Flood projections within the Niger River Basin under future land use and climate change. Science of The Total Environment 2016; 562: 666-677.

Alfieri L, Bisselink B, Dottori F, Naumann G, de Roo A, Salamon P, Wyse K, Feyen L. Global projections of river flood risk in a warmer world. Earth's Future 2017; 5: 171-182.

Alfieri L, Burek P, Dutra E, Krzeminski B, Muraro D, Thielen J, Pappenberger F. GloFAS - global ensemble streamflow forecasting and flood early warning. Hydrol. Earth Syst. Sci. 2013; 17: 1161-1175.

Alfieri L, Burek P, Feyen L, Forzieri G. Global warming increases the frequency of river floods in Europe. Hydrol. Earth Syst. Sci. 2015; 19: 2247-2260.

Amatya DM, Harrison CA. Grass and forest potential evapotranspiration comparison using five methods in the Atlantic Coastal plain. Journal of Hydrologic Engineering 2016; 21: 05016007.

Andréassian V, Perrin C, Michel C. Impact of imperfect potential evapotranspiration knowledge on the efficiency and parameters of watershed models. Journal of Hydrology 2004; 286: 19-35.

Anghileri D, Voisin N, Castelletti A, Pianosi F, Nijssen B, Lettenmaier DP. Value of long-term streamflow forecasts to reservoir operations for water supply in snow-dominated river catchments. Water Resources Research 2016; 52: 4209-4225.

Apurv T, Mehrotra R, Sharma A, Goyal MK, Dutta S. Impact of climate change on floods in the Brahmaputra basin using CMIP5 decadal predictions. Journal of Hydrology 2015; 527: 281-291.

Archfield SA, Steeves PA, Guthrie JD, Ries III KG. Towards a publicly available, map-based regional software tool to estimate unregulated daily streamflow at ungauged rivers. Geosci. Model Dev. 2013; 6: 101-115.

Arnell NW, Gosling SN. The impacts of climate change on river flood risk at the global scale. Climatic Change 2016; 134: 387-401.

Arnold JG, Srinivasan R, Muttiah RS, Williams JR. Large area hydrologic modeling and assessment part I: Model development 1. Journal of the American Water Resources Association 1998; 34: 73-89.

Assani AA, Stichelbout É, Roy AG, Petit F. Comparison of impacts of dams on the annual maximum flow characteristics in three regulated hydrologic regimes in Québec (Canada). Hydrological Processes 2006; 20: 3485-3501.

Auger JD, Birkel SD, Maasch KA, Mayewski PA, Schuenemann KC. An ensemble mean and evaluation of third generation global climate reanalysis models. Atmosphere 2018; 9: 236.

Awotwi A, Yeboah F, Kumi M. Assessing the impact of land cover changes on water balance components of White Volta Basin in West Africa. Water and Environment Journal 2015; 29: 259-267.

Bai L, Shi C, Li L, Yang Y, Wu J. Accuracy of CHIRPS Satellite-Rainfall Products over Mainland China. Remote Sensing 2018; 10: 362.

Bai T, Wu L, Chang J-x, Huang Q. Multi-objective optimal operation model of cascade reservoirs and its application on water and sediment regulation. Water Resources Management 2015; 29: 2751-2770.

Bastola S, Misra V. Evaluation of dynamically downscaled reanalysis precipitation data for hydrological application. Hydrological Processes 2014; 28: 1989-2002.

Batalla RJ, Gómez CM, Kondolf GM. Reservoir-induced hydrological changes in the Ebro River basin (NE Spain). Journal of Hydrology 2004; 290: 117-136.

Batalla RJ, Vericat D. Hydrological and sediment transport dynamics of flushing flows: Implications for management in large Mediterranean rivers. River Research and Applications 2009; 25: 297-314.

Beck HE, van Dijk AIJM, Levizzani V, Schellekens J, Miralles DG, Martens B, de Roo A. MSWEP: 3-hourly 0.25° global gridded precipitation (1979-2015) by merging gauge, satellite, and reanalysis data. Hydrology and Earth System Sciences 2017; 21: 589-615.

Beldring S, Engeland K, Roald LA, Sælthun NR, Voksø A. Estimation of parameters in a distributed precipitation-runoff model for Norway. Hydrol. Earth Syst. Sci. 2003; 7: 304-316.

Beldring S, Engen-Skaugen T, Førland EJ, Roald LA. Climate change impacts on hydrological processes in Norway based on two methods for transferring regional climate model results to meteorological station sites. Tellus A 2008; 60: 439-450.

Bell VA, Kay AL, Jones RG, Moore RJ, Reynard NS. Use of soil data in a grid-based hydrological model to estimate spatial variation in changing flood risk across the UK. Journal of Hydrology 2009; 377: 335-350.

Benali A, Carvalho AC, Nunes JP, Carvalhais N, Santos A. Estimating air surface temperature in Portugal using MODIS LST data. Remote Sensing of Environment 2012; 124: 108-121.

Bento CPM, van der Hoeven S, Yang X, Riksen MMJPM, Mol HGJ, Ritsema CJ, Geissen V. Dynamics of glyphosate and AMPA in the soil surface layer of glyphosate-resistant crop cultivations in the loess Pampas of Argentina. Environmental Pollution 2019; 244: 323-331.

Berger KP, Entekhabi D. Basin hydrologic response relations to distributed physiographic descriptors and climate. Journal of Hydrology 2001; 247: 169-182.

Berz G, Kron W, Loster T, Rauch E, Schimetschek J, Schmieder J, Siebert A, Smolka A, Wirtz A. World map of natural hazards – A global view of the distribution and intensity of significant exposures. Natural Hazards 2001; 23: 443-465.

Best J. Anthropogenic stresses on the world’s big rivers. Nature Geoscience 2019; 12: 7-21.

Beven KJ. Rainfall-runoff modelling: The Primer, 2nd Edition: Wiley-Blackwell, 2012.

Beven KJ, Kirkby MJ. A physically based, variable contributing area model of basin hydrology. Hydrological Sciences Bulletin 1979; 24: 43-69.

Bieger K, Hörmann G, Fohrer N. Using residual analysis, auto- and cross-correlations to identify key processes for the calibration of the SWAT model in a data scarce region. Adv. Geosci. 2012; 31: 23-30.

Bierkens MFP. Global hydrology 2015: State, trends, and directions. Water Resources Research 2015; 51: 4923-4947.

Blank L, Blaustein L. A multi-scale analysis of breeding site characteristics of the endangered fire salamander (Salamandra infraimmaculata) at its extreme southern range limit. Hydrobiologia 2014; 726: 229-244.

Blöschl G, Gaál L, Hall J, Kiss A, Komma J, Nester T, Parajka J, Perdigão RAP, Plavcová L, Rogger M, Salinas JL, Viglione A. Increasing river floods: fiction or reality? Wiley Interdisciplinary Reviews: Water 2015; 2: 329-344.

Boé J, Terray L, Habets F, Martin E. Statistical and dynamical downscaling of the Seine basin climate for hydro-meteorological studies. International Journal of Climatology 2007; 27: 1643-1655.

Bormann H, Breuer L, Gräff T, Huisman JA. Analysing the effects of soil properties changes associated with land use changes on the simulated water balance: A comparison of three hydrological catchment models for scenario analysis. Ecological Modelling 2007; 209: 29-40.

Bormann H, Faß T, Giertz S, Junge B, Diekkrüger B, Reichert B, Skowronek A. From local hydrological process analysis to regional hydrological model application in Benin: Concept, results and perspectives. Physics and Chemistry of the Earth 2005; 30: 347-356.

Braatne J, Rood S, Goater L, Blair C. Analyzing the impacts of dams on riparian ecosystems: A review of research strategies and their relevance to the Snake River through Hells Canyon. Environmental Management 2008; 41: 267-281.

Bradshaw CJA, Sodhi NS, Peh KSH, Brook BW. Global evidence that deforestation amplifies flood risk and severity in the developing world. Global Change Biology 2007; 13: 2379-2395.

Brath A, Montanari A, Moretti G. Assessing the effects on flood risk of land-use changes in the last five decades: An Italian case study. IAHS-AISH Publication 2003: 435-441.

Braud I, Vich AIJ, Zuluaga J, Fornero L, Pedrani A. Vegetation influence on runoff and sediment yield in the Andes region: Observation and modelling. Journal of Hydrology 2001; 254: 124-144.

Brocca L, Melone F, Moramarco T. On the estimation of antecedent wetness conditions in rainfall–runoff modelling. Hydrological Processes 2008; 22: 629-642.

Brocca L, Melone F, Moramarco T. Distributed rainfall-runoff modelling for flood frequency estimation and flood forecasting. Hydrological Processes 2011; 25: 2801-2813.

Brown AE, Western AW, McMahon TA, Zhang L. Impact of forest cover changes on annual streamflow and flow duration curves. Journal of Hydrology 2013; 483: 39-50.

Brulebois E, Castel T, Richard Y, Chateau-Smith C, Amiotte-Suchet P. Hydrological response to an abrupt shift in surface air temperature over France in 1987/88. Journal of Hydrology 2015; 531: 892-901.

Burek P, Van der Knijff JM, De Roo A. LISFLOOD-Distributed Water Balance and Flood Simulation Model - Revised User Mannual. JRC Technical Reports. European Commission Joint Research Centre, Institute for Environment and Sustainability, Luxembourg: Publications Office of the European Union, 2013, 2013.

Cançado V, Brasil L, Nascimento N, Guerra A. Flood risk assessment in an urban area: Measuring hazard and vulnerability. 11th International Conference on Urban Drainage, Edinburgh, Scotland, UK, 2008.

Casanueva A, Kotlarski S, Herrera S, Fernández J, Gutiérrez JM, Boberg F, Colette A, Christensen OB, Goergen K, Jacob D, Keuler K, Nikulin G, Teichmann C, Vautard R. Daily precipitation statistics in a EURO-CORDEX RCM ensemble: added value of raw and bias-corrected high-resolution simulations. Climate Dynamics 2016; 47: 719-737.

Cha DH, Lee DK. Reduction of systematic errors in regional climate simulations of the summer monsoon over East Asia and the western North Pacific by applying the spectral nudging technique. Journal of Geophysical Research: Atmospheres 2009; 114.

Chan FKS, Griffiths JA, Higgitt D, Xu S, Zhu F, Tang Y-T, Xu Y, Thorne GR. “Sponge City” in China—A breakthrough of planning and flood risk management in the urban context. Land Use Policy 2018; 76: 772-778.

Chang C, Feng P. The impact of land use/land cover changes and hydraulic structures on flood recession process. Journal of Water and Climate Change 2017; 8: 375-387.

Chang J, Wang Y, Istanbulluoglu E, Bai T, Huang Q, Yang D, Huang S. Impact of climate change and human activities on runoff in the Weihe River Basin, China. Quaternary International 2015; 380–381: 169-179.

Chen G, Iwasaki T, Qin H, Sha W. Evaluation of the warm-season diurnal variability over East Asia in recent reanalyses JRA-55, ERA-Interim, NCEP CFSR, and NASA MERRA. Journal of Climate 2014; 27: 5517-5537.

Chen G, Wang Y, Liu D, Liu S. Detection of basin runoff variation based on moving correlation coefficient method. Journal of Natural Disasters 2016; 25: 11-18.

Chen H, Chen G, G. Ding. Rigional flood hazard risk assessment based on GIS (in Chinese). Yangtze River 2003; 36: 49-51.

Chen Y, Pang Z, Chen Y, Li W, Xu C, Hao X, Huang X, Huang T, Ye Z. Response of riparian vegetation to water-table changes in the lower reaches of Tarim River, Xinjiang Uygur, China. Hydrogeology Journal 2008; 16: 1371-1379.

Chen Z, Wang H, Qi X. Pricing and water resource allocation scheme for the South-to-North water diversion project in China. Water Resources Management 2013; 27: 1457-1472.

Cheng Q-B, Reinhardt-Imjela C, Chen X, Schulte A, Ji X, Li F-L. Improvement and comparison of the rainfall–runoff methods in SWAT at the monsoonal watershed of Baocun, Eastern China. Hydrological Sciences Journal 2016; 61: 1460-1476.

Chiew FHS, McMahon TA. The applicability of morton's and penman's evapotranspiration estimates in rainfall-runoff modeling1. JAWRA Journal of the American Water Resources Association 1991; 27: 611-620.

Chiew FHS, Zhou SL, McMahon TA. Use of seasonal streamflow forecasts in water resources management. Journal of Hydrology 2003; 270: 135-144.

Chifflard P, Kranl J, Strassen Gz, Zepp H. The significance of soil moisture in forecasting characteristics of flood events. A statistical analysis in two nested catchments. 2018; 66: 1-11.

Choi W, Nauth K, Choi J, Becker S. Urbanization and rainfall–runoff relationships in the Milwaukee River Basin. Professional Geographer 2016; 68: 14-25.

Choudhary A, Dimri AP, Maharana P. Assessment of CORDEX-SA experiments in representing precipitation climatology of summer monsoon over India. Theoretical and Applied Climatology 2018; 134: 283-307.

Costa MH, Botta A, Cardille JA. Effects of large-scale changes in land cover on the discharge of the Tocantins River, Southeastern Amazonia. Journal of Hydrology 2003; 283: 206-217.

Cuo L. Land use/cover change impacts on hydrology in large river basins: A review. Terrestrial Water Cycle and Climate Change (eds Q. Tang and T. Oki), 2016.

Dadaser-Celik F, Coggins JS, Brezonik PL, Stefan HG. The projected costs and benefits of water diversion from and to the Sultan Marshes (Turkey). Ecological Economics 2009; 68: 1496-1506.

Dalrymple T. Flood Frequency analysis US Geological Survey Water Supply Paper 1960; 1543A.

Dankers R, Christensen OB, Feyen L, Kalas M, de Roo A. Evaluation of very high-resolution climate model data for simulating flood hazards in the Upper Danube Basin. Journal of Hydrology 2007; 347: 319-331.

Das M, Ghosh SK, Chowdary VM, Saikrishnaveni A, Sharma RK. A probabilistic nonlinear model for forecasting daily water level in reservoir. Water Resources Management 2016; 30: 3107-3122.

Davies T, Cullen MJP, Malcolm AJ, Mawson MH, Staniforth A, White AA, Wood N. A new dynamical core for the Met Office's global and regional modelling of the atmosphere. Quarterly Journal of the Royal Meteorological Society 2005; 131: 1759-1782.

de la Paix MJ, Lanhai L, Xi C, Ahmed S, Varenyam A. Soil degradation and altered flood risk as a consequence of deforestation. Land Degradation and Development 2013; 24: 478-485.

De Roo A, Odijk M, Schmuck G, Koster E, Lucieer A. Assessing the effects of land use changes on floods in the meuse and oder catchment. Physics and Chemistry of the Earth, Part B: Hydrology, Oceans and Atmosphere 2001; 26: 593-599.

Dee DP, Uppala SM, Simmons AJ, Berrisford P, Poli P, Kobayashi S, Andrae U, Balmaseda MA, Balsamo G, Bauer P, Bechtold P, Beljaars ACM, van der Berg L, Bidlot J, Bormann N, Delsol C, Dragani R, Fuentes M, Geer AJ, Haimberger L, Healy SB, Hersbach H, Holm EV, Isaksen L, Kallberg P, Kohler M, Matricardi M, McNally AP, Monge-Sanz BM, Morcrette JJ, Park BK, Peubey C, de Rosnay P, Tavolato C, Thepaut JN, Vitart F. The ERA-Interim reanalysis: configuration and performance of the data assimilation system. Quarterly Journal of the Royal Meteorological Society 2011; 137: 553-597.

Delgado JM, Apel H, Merz B. Flood trends and variability in the Mekong river. Hydrol. Earth Syst. Sci. 2010; 14: 407-418.

Deng L, Shangguan Z, Sweeney S. “Grain for Green” driven land use change and carbon sequestration on the Loess Plateau, China Scientific Reports 4: 7039.

Dile YT, Srinivasan R. Evaluation of CFSR climate data for hydrologic prediction in data‐scarce watersheds: an application in the Blue Nile River Basin. JAWRA Journal of the American Water Resources Association 2014; 50: 1226-1241.

Du S, Shi P, Van Rompaey A, Wen J. Quantifying the impact of impervious surface location on flood peak discharge in urban areas. Natural Hazards 2015; 76: 1457-1471.

Duan Z, Liu J, Tuo Y, Chiogna G, Disse M. Evaluation of eight high spatial resolution gridded precipitation products in Adige Basin (Italy) at multiple temporal and spatial scales. Science of The Total Environment 2016; 573: 1536-1553.

Eisner S, Flörke M, Chamorro A, Daggupati P, Donnelly C, Huang J, Hundecha Y, Koch H, Kalugin A, Krylenko I, Mishra V, Piniewske M, Samaniego L, Seidou O, Wallner M, Krysanova V. An ensemble analysis of climate change impacts on streamflow seasonality across 11 large river basins. Climatic Change 2017; 141: 401-417.

Essou GRC, Brissette F, Lucas-Picher P. Impacts of combining reanalyses and weather station data on the accuracy of discharge modelling. Journal of Hydrology 2017; 545: 120-131.

Essou GRC, Sabarly F, Lucas-Picher P, Brissette F, Poulin A. Can precipitation and temperature from meteorological reanalyses be used for hydrological modeling? Journal of Hydrometeorology 2016; 17: 1929-1950.

Ewea HA, Elfeki AM, Al-Amri NS. Development of intensity–duration–frequency curves for the Kingdom of Saudi Arabia. Geomatics, Natural Hazards and Risk 2017; 8: 570-584.

Fan L, Liu G, Wang F, Ritsema CJ, Geissen V. Domestic water consumption under intermittent and continuous modes of water supply. Water Resources Management 2014; 28: 853-865.

Feng L, Hu C, Chen X, Cai X, Tian L, Gan W. Assessment of inundation changes of Poyang Lake using MODIS observations between 2000 and 2010. Remote Sensing of Environment 2012; 121: 80-92.

Feng Y, Brubaker KL, McCuen RH. New view of flood frequency incorporating duration. Journal of Hydrologic Engineering 2017; 22: 04017051.

Feng Y, Zhou J, Mo L, Yuan Z, Zhang P, Wu J, Chao W, Wang Y. Long-Term Hydropower Generation of Cascade Reservoirs under Future Climate Changes in Jinsha River in Southwest China. Water 2018; 10: 235.

Fohrer N, Haverkamp S, Eckhardt K, Frede HG. Hydrologic response to land use changes on the catchment scale. Physics and Chemistry of the Earth, Part B: Hydrology, Oceans and Atmosphere 2001; 26: 577-582.

Franqueville D, Benhamou C, Pasquier C, Hénault C, Drouet J-L. Modelling reactive nitrogen fluxes and mitigation scenarios on a landscape in Central France. Agriculture, Ecosystems & Environment 2018; 264: 99-110.

Freychet N, Hsu H-H, Chou C, Wu C-H. Asian Summer Monsoon in CMIP5 Projections: A Link between the Change in Extreme Precipitation and Monsoon Dynamics. Journal of Climate 2015; 28: 1477-1493.

Fuka DR, Walter MT, MacAlister C, Degaetano AT, Steenhuis TS, Easton ZM. Using the Climate Forecast System Reanalysis as weather input data for watershed models. Hydrological Processes 2014; 28: 5613-5623.

Gaba C, Alamou E, Afouda A, Diekkrüger B. Improvement and comparative assessment of a hydrological modelling approach on 20 catchments of various sizes under different climate conditions. Hydrological Sciences Journal 2017; 62: 1499-1516.

Gai L, Baartman JEM, Mendoza-Carranza M, Wang F, Ritsema CJ, Geissen V. A framework approach for unravelling the impact of multiple factors influencing flooding. Journal of Flood Risk Management 2018; 11:111-126.

Gai L, Nunes JP, Baartman JEM, Zhang H, Wang F, de Roo A, Ritsema CJ, Geissen V. Assessing the impact of human interventions on floods and low flows in the Wei River Basin in China using the LISFLOOD model. Science of The Total Environment 2019; 653: 1077-1094.

Gao J, Nickum JE, Pan Y. An assessment of flood hazard vulnerability in the Dongting Lake Region of China. Lakes & Reservoirs: Research & Management 2007; 12: 27-34.

Gao L, Bernhardt M, Schulz K. Elevation correction of ERA-Interim temperature data in complex terrain. Hydrol. Earth Syst. Sci. 2012; 16: 4661-4673.

Gao L, Hao L, Chen X-W. Evaluation of ERA-interim monthly temperature data over the Tibetan Plateau. Journal of Mountain Science 2014a; 11: 1154-1168.

Gao P, Geissen V, Ritsema CJ, Mu XM, Wang F. Impact of climate change and anthropogenic activities on stream flow and sediment discharge in the Wei River basin, China. Hydrol. Earth Syst. Sci. 2013; 17: 961-972.

Gao P, Geissen V, Temme AJAM, Ritsema CJ, Mu X, Wang F. A wavelet analysis of the relationship between Loess Plateau erosion and sunspots. Geoderma 2014b; 213: 453-459.

Gao P, Zhang X, Mu X, Wang F, Li R, Zhang X. Trend and change-point analyses of streamflow and sediment discharge in the Yellow River during 1950–2005. Hydrological Sciences Journal 2010; 55: 275-285.

Garner G, Van Loon AF, Prudhomme C, Hannah DM. Hydroclimatology of extreme river flows. Freshwater Biology 2015; 60: 2461-2476.

Giorgi F, Coppola E, Solmon F, Mariotti L, Sylla MB, Bi X, Elguindi N, Diro GT, Nair V, Giuliani G, Turuncoglu UU, Cozzini S, Güttler I, Brien OTA, Tawfik AB, Shalaby A, Zakey AS, Steiner AL, Stordal F, Sloan LC, Brankovic C. RegCM4: model description and preliminary tests over multiple CORDEX domains. Climate Research 2012; 52: 7-29.

Giorgi F, Jones C, Asrar GR. Addressing climate information needs at the regional level: the CORDEX framework. WMO Bulletin 2009; 58: 175-183.

Gu H, Yu Z, Yang C, Ju Q, Yang T, Zhang D. High-resolution ensemble projections and uncertainty assessment of regional climate change over China in CORDEX East Asia. Hydrol. Earth Syst. Sci. 2018; 22: 3087-3103.

Gudmundsson L. Package ‘qmap’, 2016, https://CRAN.R-project.org/package=qmap.

Hargreaves G, Samani Z. Reference crop evapotranspiration from temperature, American Society of Agricultural and Biological Engineers, 1985.

Hanasaki N, Kanae S, Oki T. A reservoir operation scheme for global river routing models. Journal of Hydrology 2006; 327: 22-41.

Hapuarachchi HAP, Wang QJ, Pagano TC. A review of advances in flash flood forecasting. Hydrological Processes 2011; 25: 2771-2784.

Hardie MA, Cotching WE, Doyle RB, Holz G, Lisson S, Mattern K. Effect of antecedent soil moisture on preferential flow in a texture-contrast soil. Journal of Hydrology 2011; 398: 191-201.

Haslinger K, Koffler D, Schöner W, Laaha G. Exploring the link between meteorological drought and streamflow: Effects of climate-catchment interaction. Water Resources Research 2014; 50: 2468-2487.

Hattermann FF, Wattenbach M, Krysanova V, Wechsung F. Runoff simulations on the macroscale with the ecohydrological model SWIM in the Elbe catchment–validation and uncertainty analysis. Hydrological Processes 2005; 19: 693-714.

Hengl T, Mendes de Jesus J, MacMillan RA, Batjes NH, Heuvelink GBM, Ribeiro E, Samuel-Rosa A, Kempen B, Leenaars JGB, Walsh MG, Gonzalez MR. SoilGrids1km - Global soil information based on automated mapping. PlosOne 2014; 9: e114788.

Hirabayashi Y, Mahendran R, Koirala S, Konoshima L, Yamazaki D, Watanabe S, Kim H, Kanae S. Global flood risk under climate change. Nature Climate Change 2013; 3: 816.

Hong S-Y, Chang E-C. Spectral nudging sensitivity experiments in a regional climate model. Asia-Pacific Journal of Atmospheric Sciences 2012; 48: 345-355.

Hong S-Y, Park H, Cheong H-B, Kim J-EE, Koo M-S, Jang J, Ham S, Hwang S-O, Park B-K, Chang E-C, Li H. The Global/Regional Integrated Model system (GRIMs). Asia-Pacific Journal of Atmospheric Sciences 2013; 49: 219-243.

Horritt MS, Bates PD. Evaluation of 1D and 2D numerical models for predicting river flood inundation. Journal of Hydrology 2002; 268: 87-99.

Hothorn T, Hornik K, Zeileis A. Unbiased recursive partitioning: A conditional inference framework. Journal of Computational and Graphical Statistics 2006; 15: 651-674.

Hsu MH, Chiang SH, Chen CF. Analyzing the effects of impervious surface area and rainfall variables on flood hazard in Tainan City, Taiwan. ACRS 2015 - 36th Asian Conference on Remote Sensing: Fostering Resilient Growth in Asia, Proceedings, 2015.

Hu J, Gao P, Mu X, Zhao G, Sun W, Li P, Zhang L. Runoff-sediment dynamics under different flood patterns in a Loess Plateau catchment, China. Catena 2019; 173: 234-245.

Hu S, Qiu H, Yang D, Cao M, Song J, Wu J, Huang C, GAO Y. Evaluation of the applicability of climate forecast system reanalysis weather data for hydrologic simulation: A case study in the Bahe River Basin of the Qinling Mountains, China. Journal of Geographical Sciences 2017; 27: 546-564.

Huang CC, Pang J, Zha X, Su H, Jia Y, Zhu Y. Impact of monsoonal climatic change on Holocene overbank flooding along Sushui River, middle reach of the Yellow River, China. Quaternary Science Reviews 2007; 26: 2247-2264.

Huang CC, Pang J, Zha X, Zhou Y, Su H, Wan H, Ge B. Sedimentary records of extraordinary floods at the ending of the mid-Holocene climatic optimum along the Upper Weihe River, China. The Holocene 2012; 22: 675-686.

Huang S, Chang J, Huang Q, Chen Y. Identification of abrupt changes of the relationship between rainfall and runoff in the Wei River Basin, China. Theoretical and Applied Climatology 2015a; 120: 299-310.

Huang S, Hou B, Chang J, Huang Q, Chen Y. Spatial-temporal change in precipitation patterns based on the cloud model across the Wei River Basin, China. Theoretical and Applied Climatology 2015b; 120: 391-401.

Huang S, Huang Q, Chang J, Chen Y, Xing L, Xie Y. Copulas-based drought evolution characteristics and risk evaluation in a typical arid and semi-arid region. Water Resources Management 2015c; 29: 1489-1503.

Huang S, Huang Q, Chang J, Leng G, Xing L. The response of agricultural drought to meteorological drought and the influencing factors: A case study in the Wei River Basin, China. Agricultural Water Management 2015d; 159: 45-54.

Hundecha Y, Bárdossy A. Modeling of the effect of land use changes on the runoff generation of a river basin through parameter regionalization of a watershed model. Journal of Hydrology 2004; 292: 281-295.

Huo S, X. Jiang., Y. Zhao, S. Xu. Characteristic analysis of autumn rainstorm flood of 2003 in WeiRiver (in Chinese). Hydrology and Earth System Sciences 2004; 24: 58-61.

IPCC. Climate Change 2013: The Physical Science Basis. Contribution of Working Group I to the Fifth Assessment Report of the Intergovernmental Panel on Climate Change. In: [Stocker TF, D. Qin, G.-K. Plattner, M. Tignor, S.K. Allen, J. Boschung, A. Nauels, Y. Xia, V. Bex and P.M. Midgley (eds.)]. editor, Cambridge University Press, Cambridge, United Kingdom and New York, NY, USA, 1535 pp., 2013.

Islam MM, Sado K. Flood hazard assessment in Bangladesh using NOAA AVHRR data with geographical information system. Hydrological Processes 2000; 14: 605-620.

Istomina MN, Dobrovoski SG. Floods of the world: Quantitative analysis of natural characteristics and parameters of social-economic damages. Water Resources 2016; 43: 459-471.

Javelle P, Ouarda TBMJ, Lang M, Bobée B, Galéa G, Grésillon J-M. Development of regional flood-duration–frequency curves based on the index-flood method. Journal of Hydrology 2002; 258: 249-259.

Jian S, Zhao C, Fang S, Yu K. Effects of different vegetation restoration on soil water storage and water balance in the Chinese Loess Plateau. Agricultural and Forest Meteorology 2015; 206: 85-96.

Jiang T, Kundzewicz ZW, Su B. Changes in monthly precipitation and flood hazard in the Yangtze River Basin, China. International Journal of Climatology 2008; 28: 1471-1481.

Jiang X, Huo S, Liu L, Sun W, Chen J. Analysis of the characteristics of Wei River flood in 2003 (in Chinese). Yellow River 2004; 26: 24-27.

Jin D, Lin S, Du X, Du X, Luo X, Yang F. Prediction model of tongguan elevation changes in non-flood seasons based on T-S fuzzy reasoning. Advances in Future Computer and Control Systems. 159. Springer Berlin Heidelberg, 2012, pp. 265-272.

Johnstone CP, Lill A, Reina RD. Habitat loss, fragmentation and degradation effects on small mammals: Analysis with conditional inference tree statistical modelling. Biological Conservation 2014; 176: 80-98.

Jonkman SN. Global perspectives on loss of human life caused by floods. Natural Hazards 2005; 34: 151-175.

Jun-ping Y, Yan-sui L. A study on environmental aridity over northern and southern to Qinling Mountains under climate warming. Journal of Geographical Sciences 2001; 11: 193.

Jung C-G, Lee D-R, Moon J-W. Comparison of the Penman - Monteith method and regional calibration of the Hargreaves equation for actual evapotranspiration using SWAT-simulated results in the Seolma-cheon basin, South Korea. Hydrological Sciences Journal 2016; 61: 793-800.

Kanamaru H, Kanamitsu M. Scale-selective bias correction in a downscaling of global analysis using a regional model. Monthly Weather Review 2007; 135: 334-350.

Kavian A, Azmoodeh A, Solaimani K. Deforestation effects on soil properties, runoff and erosion in northern Iran. Arabian Journal of Geosciences 2014; 7: 1941-1950.

Khaleghi MR. The influence of deforestation and anthropogenic activities on runoff generation. Journal of Forest Science 2017; 63: 245-253.

Khelfi MEA, Touaibia B, Guastaldi E. Regionalisation of the “intensity-duration-frequency” curves in Northern Algeria. Arabian Journal of Geosciences 2017; 10: 441.

Kimani MW, Hoedjes JCB, Su Z. An assessment of satellite-derived rainfall products relative to ground observations over East Africa. Remote Sensing 2017; 9: 430.

Kliment Z, Matoušková M. Changes of runoff regime according to human impact on the landscape. Geografie-Sbornik CGS 2006; 111: 292-304.

Kliment Z, Matoušková M. Runoff changes in the Šumava Mountains (Black Forest) and the foothill regions: Extent of influence by human impact and climate change. Water Resources Management 2009; 23: 1813-1834.

Van der Kniff J., Evaporation pre-processor for the LISFLOOD water balance and flood simulation model - revised user manual. In: European Commission D-GJRC, Institute for Environment and Sustainability, Italy, 2008.

Kong D, Miao C, Wu J, Borthwick AG, Duan Q, Zhang X. Environmental impact assessments of the Xiaolangdi Reservoir on the most hyperconcentrated laden river, Yellow River, China. Environ Sci Pollut Res Int 2017; 24: 4337-4351.

Koutsouris A, Seibert J, Lyon S. Utilization of global precipitation datasets in data limited regions: A case study of Kilombero Valley, Tanzania. Atmosphere 2017; 8: 246.

Kron W. Flood Risk = Hazard • Values • Vulnerability. Water International 2005; 30: 58-68.

Kundzewicz ZW, Lugeri N, Dankers R, Hirabayashi Y, Döll P, Pińskwar I, Dysarz T, Hochrainer S, Matezak P. Assessing river flood risk and adaptation in Europe—review of projections for the future. Mitigation and Adaptation Strategies for Global Change 2010; 15: 641-656.

Lacombe G, Ribolzi O, de Rouw, A, Pierret A, Latsachak K, Silvera N, Pham-Dinh R, Orange D, Janeau J-L, Soulileuth B, Robain H, Taccoen A, Sengphaathith P, Mouche E, Sengtaheuanghoung O, Tran Duc T, Valentin C. Contradictory hydrological impacts of afforestation in the humid tropics evidenced by long-term field monitoring and simulation modelling. Hydrology and Earth System Sciences 2016; 20: 2691-2704.

Lauri H, Räsänen TA, Kummu M. Using reanalysis and remotely sensed temperature and precipitation data for hydrological modeling in monsoon climate: Mekong River case study. Journal of Hydrometeorology 2014; 15: 1532-1545.

Lee KT, Huang P-C. Assessment of flood mitigation through riparian detention in response to a changing climate – a case study. Journal of Earth System Science 2018; 127: 83.

Lehner B, Döll P. Development and validation of a global database of lakes, reservoirs and wetlands. Journal of Hydrology 2004; 296: 1-22.

Lehner B, Döll P, Alcamo J, Henrichs T, Kaspar F. Estimating the impact of global change on flood and drought risks in Europe: A continental, integrated analysis. Climatic Change 2006; 75: 273-299.

Lei C, Xu Y, Zhang Q, Wang Y, Li G. Impacts of land-use chang on flood process and frequency of various return periods: a case study of Jiaokou Reservoir watershed in Fenghua River. Shengtai Xuebao/Acta Ecologica Sinica 2016; 36: 5017-5026.

Li C, Tang G, Hong Y. Cross-evaluation of ground-based, multi-satellite and reanalysis precipitation products: Applicability of the Triple Collocation method across Mainland China. Journal of Hydrology 2018a; 562: 71-83.

Li D, Christakos G, Ding X, Wu J. Adequacy of TRMM satellite rainfall data in driving the SWAT modeling of Tiaoxi catchment (Taihu lake basin, China). Journal of Hydrology 2018b; 556: 1139-1152.

Li L-J, Zhang L, Wang H, Wang J, Yang J-W, Jiang D-J, Li J-Y, Qin D-Y. Assessing the impact of climate variability and human activities on streamflow from the Wuding River basin in China. Hydrological Processes 2007; 21: 3485-3491.

Li L, Wu B. Prediction of the bankfull discharge in the lower Wei River. 2010; 50: 852-856.

Li W, Wu B. Analysis of influential factors of bankfull discharge in the lower Wei River. 2011; 19: 28-36.

Li X, Huang C, Pang J, Zha X, Ma Y. Sedimentary and hydrological studies of the Holocene palaeofloods in the Shanxi-Shaanxi Gorge of the middle Yellow River, China. 2014: 1-12.

Li Y, Chang J, Luo L, Wang Y, Guo A, Ma F, Fan J. Spatiotemporal impacts of land use land cover changes on hydrology from the mechanism perspective using SWAT model with time-varying parameters. Hydrology Research 2018; 50:244-261.

Li Y, Chang J, Wang Y, Jin W, Guo A. Spatiotemporal impacts of climate, land cover change and direct human activities on runoff variations in the Wei River Basin, China. Water 2016; 8: 220.

Li Z, Liu W, Zhang X, Zheng F. Impacts of land use change and climate variability on hydrology in an agricultural catchment on the Loess Plateau of China. Journal of Hydrology 2009; 377: 35-42.

Liang L. Analysis of the "05.10" flood characteristics of Wei River (in Chinese). Journal of Northwest Hydroelectric Power 2006; 22: 81-84.

Liang X, Lettenmaier DP, Wood EF, Burges SJ. A simple hydrologically based model of land surface water and energy fluxes for general circulation models. Journal of Geophysical Research: Atmospheres 1994; 99: 14415-14428.

Lindsey SD, Farnsworth RK. Sources of solar radiation estimates and their effect on daily potential evaporation for use in streamflow modeling. Journal of Hydrology 1997; 201: 348-366.

Lindström G, Johansson B, Persson M, Gardelin M, Bergström S. Development and test of the distributed HBV-96 hydrological model. Journal of Hydrology 1997; 201: 272-288.

Liu J, Kuang W, Zhang Z, Xu X, Qin Y, Ning J, Zhou W, Zhang S, Li R, Yan C, Wu S, Shi X, Jiang N, Yu D, Pan X, Chi W. Spatiotemporal characteristics, patterns, and causes of land-use changes in China since the late 1980s. 2014a; 24: 195-210.

Liu S, Gao W, Liang X-Z. A regional climate model downscaling projection of China future climate change. Climate Dynamics 2013; 41: 1871-1884.

Liu W, Chen W, Peng C. Assessing the effectiveness of green infrastructures on urban flooding reduction: A community scale study. Ecological Modelling 2014b; 291: 6-14.

Lohmann D, Raschke E, Nijssen B, Lettenmaier DP. Regional scale hydrology: I. Formulation of the VIC-2L model coupled to a routing model. Hydrological Sciences Journal 1998; 43: 131-141.

Löwe R, Thorndahl S, Mikkelsen PS, Rasmussen MR, Madsen H. Probabilistic online runoff forecasting for urban catchments using inputs from rain gauges as well as statically and dynamically adjusted weather radar. Journal of Hydrology 2014; 512: 397-407.

Luo K, Tao F, Deng X, Moiwo JP. Changes in potential evapotranspiration and surface runoff in 1981–2010 and the driving factors in Upper Heihe River Basin in Northwest China. Hydrological Processes 2017; 31: 90-103.

Lv M, Hao Z, Lin Z, Ma Z, Lv M, Wang J. Reservoir operation with feedback in a coupled land surface and hydrologic model: A case study of the Huai River Basin, China. Journal of the American Water Resources Association 2016; 52: 168-183.

Ma H, Yang D, Tan SK, Gao B, Hu Q. Impact of climate variability and human activity on streamflow decrease in the Miyun Reservoir catchment. Journal of Hydrology 2010; 389: 317-324.

Ma M, Song S, Ren L, Jiang S, Song J. Multivariate drought characteristics using trivariate Gaussian and Student t copulas. Hydrological Processes 2013; 27: 1175-1190.

Ma Y-J, Li X-Y, Wilson M, Wu X-C, Smith A, Wu J. Water loss by evaporation from China's South-North Water Transfer Project. Ecological Engineering 2016; 95: 206-215.

Magilligan FJ, Nislow KH, Renshaw CE. Flow regulation by dams. Treatise on geomorphology. 9, 2013, pp. 794-808.

Mantegna GA, White CJ, Remenyi TA, Corney SP, Fox-Hughes P. Simulating sub-daily Intensity-Frequency-Duration curves in Australia using a dynamical high-resolution regional climate model. Journal of Hydrology 2017; 554: 277-291.

Maraun D, Wetterhall F, Ireson AM, Chandler RE, Kendon EJ, Widmann M, Briene S, Rust HW, Sauter T, Themel M, Venema VKC, Chun KP, Goodess CM, Jones RG, Onof C, Vrac M, Thiele-Eich I. Precipitation downscaling under climate change: Recent developments to bridge the gap between dynamical models and the end user. Reviews of Geophysics 2010; 48: 1-34.

Marquès M, Bangash RF, Kumar V, Sharp R, Schuhmacher M. The impact of climate change on water provision under a low flow regime: A case study of the ecosystems services in the Francoli river basin. Journal of Hazardous Materials 2013; 263: 224-232.

Martínez-Graña AM, Boski T, Goy JL, Zazo C, Dabrio CJ. Coastal-flood risk management in central Algarve: Vulnerability and flood risk indices (South Portugal). Ecological Indicators 2016; 71: 302-316.

Masih I, Maskey S, Uhlenbrook S, Smakhtin V. Assessing the impact of areal precipitation input on streamflow simulations using the SWAT model1. Journal of the American Water Resources Association 2011; 47: 179-195.

Massari C, Brocca L, Barbetta S, Papathanasiou C, Mimikou M, Moramarco T. Using globally available soil moisture indicators for flood modelling in Mediterranean catchments. Hydrol. Earth Syst. Sci. 2014; 18: 839-853.

Matoušková M, Kliment Z, Ledvinka O, Královec V. Application of selected statistical tests to detect changes in the rainfall and runoff regime. Bodenkultur 2011; 62: 95-100.

Mediero L, Garrote L, Martín-Carrasco FJ. Probabilistic calibration of a distributed hydrological model for flood forecasting. Hydrological Sciences Journal 2011; 56: 1129-1149.

Mei C, Liu J, Wang H, Yang Z, Ding X, Shao W. Integrated assessments of green infrastructure for flood mitigation to support robust decision-making for sponge city construction in an urbanized watershed. Science of The Total Environment 2018; 639: 1394-1407.

Merriam-Webster's collegiate dictionary (10th ed.) 1999, Springfield, MA: Merriam-Webster Incorporated.

Merz R, Blöschl G, Parajka J. Spatio-temporal variability of event runoff coefficients. Journal of Hydrology 2006; 331: 591-604.

Metcalfe P, Beven K, Hankin B, Lamb R. A modelling framework for evaluation of the hydrological impacts of nature-based approaches to flood risk management, with application to in-channel interventions across a 29-km^2 scale catchment in the United Kingdom. Hydrological Processes 2017; 31: 1734-1748.

Michaelides S, Levizzani V, Anagnostou E, Bauer P, Kasparis T, Lane JE. Precipitation: Measurement, remote sensing, climatology and modeling. Atmospheric Research 2009; 94: 512-533.

Milewski A, Elkadiri R, Durham M. Assessment and comparison of TMPA satellite precipitation products in varying climatic and topographic regimes in Morocco. Remote Sensing 2015; 7: 5697.

Milly PCD, Betancourt J, Falkenmark M, Hirsch RM, Kundzewicz ZW, Lettenmaier DP, Stouffer RJ. Stationarity is dead: Whither water management? Science 2008; 319: 573-574.

Mo X, Beven KJ, Liu S, Leslie LM, De Roo APJ. Long-term water budget estimation with the modified distributed model – LISFLOOD-WB over the Lushi basin, China. Meteorology and Atmospheric Physics 2005; 90: 1-16.

Mohamed Elmoustafa A. Weighted normalized risk factor for floods risk assessment. Ain Shams Engineering Journal 2012; 3: 327-332.

Montanari A, Young G, Savenije HHG, Hughes D, Wagener T, Ren LL, Koutsoyiannis D, Cudennec C, Toth E, Grimaldi S, Blöschl G, Sivapalan M, Beven K, Gupta H, Hipsey M, Schaefli B, Arheimer B, Boegh E, Schymanski SJ, Di Baldassarre G, Hubert P, Huang Y, Schumann A, Post DA, Srinivasan V, Harman C, Thompson S, Rogger M, Viglione A, McMillan H, Charaklis G, Pang Z, Belyaev V. Panta Rhei—Everything Flows: Change in hydrology and society—The IAHS Scientific Decade 2013–2022. Hydrological Sciences Journal 2013; 58: 1256-1275.

Moriasi DN, Arnold JG, Van Liew MW, Bingner RL, Harmel RD, Veith TL. Model evaluation guidelines for systematic quantification of accuracy in watershed simulations. Transactions of the ASABE 2007; 50: 885-900.

Myoung-Jin U, Yeonjoo K, Jeongbin K. Evaluating historical drought characteristics simulated in CORDEX East Asia against observations. International Journal of Climatology 2017; 37: 4643-4655.

Neupane RP, White JD, Alexander SE. Projected hydrologic changes in monsoon-dominated Himalaya Mountain basins with changing climate and deforestation. Journal of Hydrology 2015; 525: 216-230.

Ngai ST, Tangang F, Juneng L. Bias correction of global and regional simulated daily precipitation and surface mean temperature over Southeast Asia using quantile mapping method. Global and Planetary Change 2017; 149: 79-90.

Ni J, Sun L, Li T, Huang Z, Borthwick AGL. Assessment of flooding impacts in terms of sustainability in mainland China. Journal of Environmental Management 2010; 91: 1930-1942.

Nkemdirim LC. An empirical relationship between temperature, vapour pressure deficit and wind speed and evaporation during a winter chinook. Theoretical and Applied Climatology 1991; 43: 123-128.

Nunes JP, Wainwright J, Bielders CL, Darboux F, Fiener P, Finger D, Turnbull L. Better models are more effectively connected models. Earth Surface Processes and Landforms 2018; 43: 1355-1360.

Onen F, Bagatur T. Prediction of flood frequency factor for Gumbel Distribution using regression and GEP model. Arabian Journal for Science and Engineering 2017; 42: 3895-3906.

Opere A. Floods in Kenya. Developments in Earth Surface Processes. 16, 2013, pp. 315-330.

Osuch M, Lawrence D, Meresa HK, Napiorkowski JJ, Romanowicz RJ. Projected changes in flood indices in selected catchments in Poland in the 21st century. Stochastic Environmental Research and Risk Assessment 2017; 31: 2435-2457.

Ouyang W, Cai G, Tysklind M, Yang W, Hao F, Liu H. Temporal-spatial patterns of three types of pesticide loadings in a middle-high latitude agricultural watershed. Water Research 2017; 122: 377-386.

Pang L. Analysis of rainstorm flood of 2005-10 in Wei River Basin (in Chinese). Journal of China Hydrology 2007a; 27: 86-90.

Pang L. Analysis of the characteristics of rainstorm flood in Wei River Basin in October 2005 (in Chinese). Journal of China Hydrology 2007b; 27: 33, 86-90.

Pappenberger F, Thielen J, Del Medico M. The impact of weather forecast improvements on large scale hydrology: analysing a decade of forecasts of the European Flood Alert System. Hydrological Processes 2011; 25: 1091-1113.

Parajka J, Viglione A, Rogger M, Salinas JL, Sivapalan M, Blöschl G. Comparative assessment of predictions in ungauged basins - Part 1: Runoff-hydrograph studies. Hydrol. Earth Syst. Sci. 2013; 17: 1783-1795.

Park C, Min S-K, Lee D, Cha D-H, Suh M-S, Kang H-S, Hong S-Y, Lee D-K, Baek H-J, Boo K-O, Kwon W-T. Evaluation of multiple regional climate models for summer climate extremes over East Asia. Climate Dynamics 2016; 46: 2469-2486.

Peng D, Xu Z, Qiu L, Zhao W. Distributed rainfall-runoff simulation for an unclosed river basin with complex river system: a case study of lower reach of the Wei River, China. Journal of Flood Risk Management 2014: 1-9.

Peng H, Jia Y, Niu C, Gong J, Hao C, Gou S. Eco-hydrological simulation of soil and water conservation in the Jinghe River Basin in the Loess Plateau, China. Journal of Hydro-Environment Research 2015.

Peng Y, Chu J, Sun X, Zhou H, Zhang X. Flood forecasting that considers the impact of hydraulic projects by an improved TOPMODEL model in the Wudaogou basin, Northeast China. Water Supply 2016; 16: 1467-1476.

Penman HL, Keen BA. Natural evaporation from open water, bare soil and grass. Proceedings of the Royal Society of London. Series A. Mathematical and Physical Sciences 1948; 193: 120-145.

Pereira SC, Carvalho AC, Ferreira J, Nunes JP, Keizer JJ, Rocha A. Simulation of a persistent medium-term precipitation event over the western Iberian Peninsula. Hydrol. Earth Syst. Sci. 2013; 17: 3741-3758.

Pfister L, Kwadijk J, Musy A, Bronstert A, Hoffmann L. Climate change, land use change and runoff prediction in the Rhine-Meuse basins. River Research and Applications 2004; 20: 229-241.

Plate EJ. Flood risk and flood management. Journal of Hydrology 2002; 267: 2-11.

Pohlner H. Institutional change and the political economy of water megaprojects: China's south-north water transfer. Global Environmental Change 2016; 38: 205-216.

Rajib A. Flood Frequency Analysis using RWater. Data and model driven hydrology education. 2018, Purdue University-Main Campus, 2018.

Ran L, Lu XX. Delineation of reservoirs using remote sensing and their storage estimate: an example of the Yellow River basin, China. Hydrological Processes 2012; 26: 1215-1229.

Ran L, Lu XX, Xin Z, Yang X. Cumulative sediment trapping by reservoirs in large river basins: A case study of the Yellow River basin. Global and Planetary Change 2013; 100: 308-319.

Ravazzani G, Bocchiola D, Groppelli B, Soncini A, Rulli MC, Colombo F, Mancini M, Rosso R. Continuous streamflow simulation for index flood estimation in an Alpine basin of northern Italy. Hydrological Sciences Journal 2015; 60: 1013-1025.

Reisenbüchler M, Bui MD, Skublics D, Rutschmann P. An integrated approach for investigating the correlation between floods and river morphology: A case study of the Saalach River, Germany. Science of the Total Environment 2019; 647: 814-826.

Ren-Jun Z. The Xinanjiang model applied in China. Journal of Hydrology 1992; 135: 371-381.

Requena AI, Flores I, Mediero L, Garrote L. Extension of observed flood series by combining a distributed hydro-meteorological model and a copula-based model. Stochastic Environmental Research and Risk Assessment 2016; 30: 1363-1378.

Requena AI, Ouarda TBMJ, Chebana F. Flood frequency analysis at ungauged sites based on regionally estimated streamflows. Journal of Hydrometeorology 2017; 18: 2521-2539.

Revilla-Romero B, Beck HE, Burek P, Salamon P, de Roo A, Thielen J. Filling the gaps: Calibrating a rainfall-runoff model using satellite-derived surface water extent. Remote Sensing of Environment 2015; 171: 118-131.

Rienecker MM, Suarez MJ, Gelaro R, Todling R, Julio Bacmeister, Liu E, Bosilovich MG, Schubert SD, Conaty A, Silva AD, Gu W, Joiner J, Koster RD, Lucchesi R, Molod A, Owens T, Pawson S, Pegion P, Redder CR, Reichle R, Robertson FR, Ruddick AG, Sienkiewicz M, Woollen J. MERRA: NASA's modern-era retrospective analysis for research and applications. Journal of Climate 2011; 24: 3624-3648.

Rogger M, Agnoletti M, Alaoui A, Bathurst JC, Bodner G, Borga M, Chaplot V, Gallart F, Glatzel G, Hall J, Holden J, Holko L, Horn R, Kiss A, Kohnova S, Leitinger G, Lennartz B, Parajka J, Perdigão R, Peth S, Plavcová L, Quinton JN, Robinson M, Salinas JL, Santoro A, Szolgay J, Tron S, van den Akker JJH, Viglione A, Blöschl G. Land use change impacts on floods at the catchment scale: Challenges and opportunities for future research. Water Resources Research 2017; 53: 5209-5219.

Romano SP, Baer SG, Zaczek JJ, Williard KWJ. Site modelling methods for detecting hydrologic alteration of flood frequency and flood duration in the floodplain below the carlyle dam, lower Kaskaskia River, Illinois, USA. River Research and Applications 2009; 25: 975-984.

Roudier P, Andersson JCM, Donnelly C, Feyen L, Greuell W, Ludwig F. Projections of future floods and hydrological droughts in Europe under a +2°C global warming. Climatic Change 2016; 135: 341-355.

Saad C, El Adlouni S, St-Hilaire A, Gachon P. A nested multivariate copula approach to hydrometeorological simulations of spring floods: the case of the Richelieu River (Québec, Canada) record flood. Stochastic Environmental Research and Risk Assessment 2015; 29: 275-294.

Saha S, Moorthi S, Pan H-L, Wu X, Wang J, Nadiga S, Tripp P, Kistler R, Woollen J, Behringer D, Liu H, Stokes D, Grumbine R, Gayno G, Wang J, Hou Y-T, Chuang Y, Juang H-MH, Sela J, Iredell M, Treadon R, Kleist D, van Delst P, Keyser D, Derber J, Ek M, Meng J, Wei H, Yang R, Lord S, van den Dool H, Kumar A, Wang W, Long C, Chelliah M, Xue Y, Huang B, Schemm J-K, Ebisuzaki W, Lin R, Xie P, Chen M, Zhou S, Higgins W, Zou C-Z, Liu Q, Chen Y, Han Y, Cucurull Lidia, Reynolds RW, Rutledge G, Goldberg M. The NCEP climate forecast system reanalysis. Bulletin of the American Meteorological Society 2010; 91: 1015-1058.

Saini R, Wang G, Pal JS. Role of soil moisture feedback in the development of extreme summer drought and flood in the United States. Journal of Hydrometeorology 2016; 17: 2191-2207.

Saxton KE, Rawls WJ, Romberger JS, Papendick RI. Estimating generalized soil-water characteristics from texture. Soil Science Society of America Journal 1986; 50: 1031-1036.

Schreider SY, Jakeman AJ, Letcher RA, Nathan RJ, Neal BP, Beavis SG. Detecting changes in streamflow response to changes in non-climatic catchment conditions: Farm dam development in the Murray-Darling basin, Australia. Journal of Hydrology 2002; 262: 84-98.

Seiler RA, Hayes M, Bressan L. Using the standardized precipitation index for flood risk monitoring. International Journal of Climatology 2002; 22: 1365-1376.

Shao H, Gao J, Zhang Y. Preliminary assessment of the human and natural contributions to the changes of Weihe River runoff using SWAT model. Journal of Food, Agriculture and Environment 2013; 11: 2629-2633.

Sharifi E, Steinacker R, Saghafian B. Assessment of GPM-IMERG and other precipitation products against gauge data under different topographic and climatic conditions in Iran: Preliminary results. Remote Sensing 2016; 8: 135.

Shaw SB, Marrs J, Bhattarai N, Quackenbush L. Longitudinal study of the impacts of land cover change on hydrologic response in four mesoscale watersheds in New York State, USA. Journal of Hydrology 2014; 519, Part A: 12-22.

Sheffield J, Goteti G, Wood EF. Development of a 50-year high-resolution global dataset of meteorological forcings for land surface modeling. Journal of Climate 2006; 19: 3088-3111.

Shen H, Ren L, Yuan F, Yang X. Comparative assessment of extreme climate variability and human activities on regional hydrologic droughts in the Weihe River basin, North China. Proc. IAHS 2015; 369: 141-146.

Shi H, Shao M. Soil and water loss from the Loess Plateau in China. Journal of Arid Environments 2000; 45: 9-20.

Shi P, Ma X, Hou Y, Li Q, Zhang Z, Qu S, Chen C, Cai T, Fang X. Effects of land-use and climate change on hydrological processes in the upstream of Huai River, China. Water Resources Management 2013; 27: 1263-1278.

Silberstein RP. Hydrological models are so good, do we still need data? Environmental Modelling & Software 2006; 21: 1340-1352.

Simonovic SP. Bringing future climatic change into water resources management practice today. Water Resources Management 2017; 31: 2933-2950.

Siqueira VA, Paiva RCD, Fleischmann AS, Fan FM, Ruhoff AL, Pontes PRM, Paris A, Calmant S, Collischonn W. Toward continental hydrologic–hydrodynamic modeling in South America. Hydrol. Earth Syst. Sci. 2018; 22: 4815-4842.

Smith RA, Kummerow CD. A comparison of in situ, reanalysis, and satellite water budgets over the Upper Colorado River Basin. Journal of Hydrometeorology 2013; 14: 888-905.

Sperna Weiland FC, Tisseuil C, Dürr HH, Vrac M, van Beek LPH. Selecting the optimal method to calculate daily global reference potential evaporation from CFSR reanalysis data for application in a hydrological model study. Hydrol. Earth Syst. Sci. 2012; 16: 983-1000.

Srivastava PK, Islam T, Gupta M, Petropoulos G, Dai Q. WRF dynamical downscaling and bias correction schemes for NCEP estimated hydro-meteorological variables. Water Resources Management 2015; 29: 2267-2284.

Stisen S, Sandholt I, Nørgaard A, Fensholt R, Eklundh L. Estimation of diurnal air temperature using MSG SEVIRI data in West Africa. Remote Sensing of Environment 2007; 110: 262-274.

Stockdon HF, Lillycrop JW, Howd PA, Wozencraft JM. The need for sustained and integrated high-resolution mapping of dynamic coastal environments. Marine Technology Society Journal 2006; 40: 90-99.

Stonestrom DA, Scanlon BR, Zhang L. Introduction to special section on Impacts of Land Use Change on Water Resources. Water Resources Research 2009; 45: 1-3.

Su X, Kang S, Wei XX, DW, Cao H. Impact of climate change and human activity on the runoff of Wei River basin to the Yellow River (In Chinese). Journal of Northwest A & F University 2007; 35: 153-159.

Sun T, Feng ML. Multistage analysis of hydrologic alterations in the Yellow River, China. River Research and Applications 2013; 29: 991-1003.

Talei A, Chua LHC. Influence of lag time on event-based rainfall–runoff modeling using the data driven approach. Journal of Hydrology 2012; 438–439: 223-233.

Tan ML, Ibrahim AL, Yusop Z, Duan Z, Ling L. Impacts of land-use and climate variability on hydrological components in the Johor River basin, Malaysia. Hydrological Sciences Journal 2015; 60: 873-889.

Tang J, Wang S, Niu X, Hui P, Zong P, Wang X. Impact of spectral nudging on regional climate simulation over CORDEX East Asia using WRF. Climate Dynamics 2017; 48: 2339-2357.

Tao L, Dang X. Analysis of the characteristics of rainstorm flood of Wei River in July, 2010 (in Chinese). Shaanxi Meteorology 2011; 4: 30-32.

Taylor J, Lai Km, Davies M, Clifton D, Ridley I, Biddulph P. Flood management: Prediction of microbial contamination in large-scale floods in urban environments. Environment International 2011; 37: 1019-1029.

Thielen J, Bartholmes J, Ramos MH, de Roo A. The European flood alert system – Part 1: Concept and development. Hydrol. Earth Syst. Sci. 2009; 13: 125-140.

Thiemig V, Bisselink B, Pappenberger F, Thielen J. A pan-African medium-range ensemble flood forecast system. Hydrol. Earth Syst. Sci. 2015; 19: 3365-3385.

Thornthwaite CW, Mather JR. The water balance. Centerton: Drexel Institute of Technology, 1955.

Thorslund J, Jarsjo J, Jaramillo F, Jawitz JW, Manzoni S, Basu NB, Chalov SR, Cohen MJ, Creed IF, Goldenberg R, Anna H, Kalantari Z, Koussis AD, Lyon SW, Mazi K, Mard J, Persson K, Pietro J, Prieto C, Quin A, van Meter K, Destouni G. Wetlands as large-scale nature-based solutions: Status and challenges for research, engineering and management. Ecological Engineering 2017; 108: 489-497.

Thumerer T, Jones AP, Brown D. A GIS based coastal management system for climate change associated flood risk assessment on the east coast of England. International Journal of Geographical Information Science 2000; 14: 265-281.

Tian S, Luo W, Jia Z, Butalia RS. Temporal variation of over-bank flooding of Wei River and its impact on a riparian wetland in Xi'an, China. Hydrological Processes 2010; 24: 1296-1307.

Tramblay Y, Ruelland D, Somot S, Bouaicha R, Servat E. High-resolution Med-CORDEX regional climate model simulations for hydrological impact studies: a first evaluation of the ALADIN-Climate model in Morocco. Hydrol. Earth Syst. Sci. 2013; 17: 3721-3739.

Uysal G, Şensoy A, Şorman AA, Akgün T, Gezgin T. Basin/reservoir system integration for real time reservoir operation. Water Resources Management 2016; 30: 1653-1668.

Van Coppenolle R, Schwarz C, Temmerman S. Contribution of mangroves and salt marshes to nature-based mitigation of coastal flood risks in major deltas of the world. Estuaries and Coasts 2018; 41: 1699-1711.

van der Knijff JM, Younis J, de Roo APJ. LISFLOOD: A GIS-based distributed model for river basin scale water balance and flood simulation. International Journal of Geographical Information Science 2010; 24: 189-212.

van Dijk AIJM, Beck HE, Crosbie RS, de Jeu RAM, Liu YY, Podger GM, Timbal B, Viney NR. The Millennium drought in southeast Australia (2001–2009): Natural and human causes and implications for water resources, ecosystems, economy, and society. Water Resources Research 2013; 49: 1040-1057.

Venables WN, Ripley BD. Modern applied statistics with S, Fourth edition: Springer (mid 2002), 2002.

Viglione A, Merz B, Viet Dung N, Parajka J, Nester T, Blöschl G. Attribution of regional flood changes based on scaling fingerprints. Water Resources Research 2016; 52: 5322-5340.

Wagner PD, Kumar S, Schneider K. An assessment of land use change impacts on the water resources of the Mula and Mutha Rivers catchment upstream of Pune, India. Hydrol. Earth Syst. Sci. 2013; 17: 2233-2246.

Wan H, C. Huang, J. Pang, X. Zha. Palaeoflood events in the Baojixia Gorges of the Weihe River (in Chinese). Journal of Shaanxi Normal University (Natural Science Edition) 2010; 38: 76-82.

Wang H, Sun F, Xia J, Liu W. Impact of LUCC on streamflow based on the SWAT model over the Wei River basin on the Loess Plateau in China. Hydrol. Earth Syst. Sci. 2017; 21: 1929-1945.

Wang G, Xia J. Improvement of SWAT2000 modelling to assess the impact of dams and sluices on streamflow in the Huai River basin of China. Hydrological Processes 2010; 24: 1455-1471.

Wang J, Hong Y, Gourley J, Adhikari P, Li L, Su F. Quantitative assessment of climate change and human impacts on long-term hydrologic response: a case study in a sub-basin of the Yellow River, China. International Journal of Climatology 2010; 30: 2130-2137.

Wang P, Tang J, Sun X, Liu J, Juan F. Spatiotemporal characteristics of heat waves over China in regional climate simulations within the CORDEX-EA project. Climate Dynamics 2018.

Wang R, Kalin L, Kuang W, Tian H. Individual and combined effects of land use/cover and climate change on Wolf Bay watershed streamflow in southern Alabama. Hydrological Processes 2014; 28: 5530-5546.

Wang S, Fu B, Piao S, Lü Y, Ciais P, Feng X, Wang Y. Reduced sediment transport in the Yellow River due to anthropogenic changes. Nature Geoscience 2015; 9: 38.

Wang W, Li H-Y, Leung LR, Yigzaw W, Zhao J, Lu H, Deng Z, Demisie Y, Blöschl G. Nonlinear filtering effects of reservoirs on flood frequency curves at the regional scale. Water Resources Research 2017; 53: 8277-8292.

Wang X, Wu , J. Lv, X. Wang, W. Xu. Analysis of a flood-causing heavy rainstorm in 2005 in Weihe and Hanjiang Valley (in Chinese). Journal of Catastrophology 2007a; 22: 7-13.

Wang Y, Zhang M, Gong H, Zhang S. Planning for Key Management of Weihe River Basin (in Chinese). Yellow River 2006; 28: 63-64.

Wang ZY, Wu B, Wang G. Fluvial processes and morphological response in the Yellow and Weihe Rivers to closure and operation of Sanmenxia Dam. Geomorphology 2007b; 91: 65-79.

Webber M, Li MT, Chen J, Finlayson B, Chen D, Chen ZY, Wang M, Barnett J. Impact of the Three Gorges Dam, the South–North Water Transfer Project and water abstractions on the duration and intensity of salt intrusions in the Yangtze River estuary. Hydrol. Earth Syst. Sci. 2015; 19: 4411-4425.

Wei X, Zhang M. Quantifying streamflow change caused by forest disturbance at a large spatial scale: A single watershed study. Water Resources Research 2010; 46: W12525.

Wijesekara GN, Gupta A, Valeo C, Hasbani JG, Qiao Y, Delaney P, Marceau DJ. Assessing the impact of future land-use changes on hydrological processes in the Elbow River watershed in southern Alberta, Canada. Journal of Hydrology 2012; 412–413: 220-232.

Wilby RL, Keenan R. Adapting to flood risk under climate change. Progress in Physical Geography: Earth and Environment 2012; 36: 348-378.

Wilson DJ, Western AW, Grayson RB. A terrain and data-based method for generating the spatial distribution of soil moisture. Advances in Water Resources 2005; 28: 43-54.

Winsemius HC, Aerts Jeroen CJH, van Beek Ludovicus PH, Bierkens Marc FP, Bouwman A, Jongman B, Kwadijk JCJ, Ligtvoet W, Lucas PL, van Vuuren DP, Ward PJ. Global drivers of future river flood risk. Nature Climate Change 2015; 6: 381.

Wohlfart C, Kuenzer C, Chen C, Liu G. Social–ecological challenges in the Yellow River basin (China): a review. Environmental Earth Sciences 2016; 75: 1-20.

Worqlul AW, Maathuis B, Adem AA, Demissie SS, Langan S, Steenhuis TS. Comparison of rainfall estimations by TRMM 3B42, MPEG and CFSR with ground-observed data for the Lake Tana basin in Ethiopia. Hydrol. Earth Syst. Sci. 2014; 18: 4871-4881.

Wu B, Wang G, Wang Z, Xia J. Effect of changes in flow runoff on the elevation of Tongguan in Sanmenxia Reservoir. Chinese Science Bulletin 2004; 49: 1658-1664.

Wu Y, Chen J. An operation-based scheme for a multiyear and multipurpose reservoir to enhance macroscale hydrologic models. Journal of Hydrometeorology 2012; 13: 270-283.

Wu ZY, Lu GH, Wen L, Lin CA. Reconstructing and analyzing China's fifty-nine year (1951–2009) drought history using hydrological model simulation. Hydrol. Earth Syst. Sci. 2011; 15: 2881-2894.

WWAP. UN World Water Development Report. World Water Assessment Programme (WWAP) 2006.

Wyzga B. Impact of the channelization-induced incision of the Skawa and Wisłoka Rivers, southern Poland, on the conditions of overbank deposition. River Research and Applications 2001; 17: 85-100.

Xia J, Li X, Li T, Zhang X, Zong Q. Response of reach-scale bankfull channel geometry to the altered flow and sediment regime in the lower Yellow River. Geomorphology 2014; 213: 255-265.

Xing D, Zhang Y, Su X. Thought About Flood of Weihe River in Shaanxi in 2003 (in Chinese). Journal of Water Resources and Architectural Engineering 2004; 2: 1-4, 28.

Xu CY, Singh VP. Evaluation of three complementary relationship evapotranspiration models by water balance approach to estimate actual regional evapotranspiration in different climatic regions. Journal of Hydrology 2005; 308: 105-121.

Xu H, Xu C-Y, Chen H, Zhang Z, Li L. Assessing the influence of rain gauge density and distribution on hydrological model performance in a humid region of China. Journal of Hydrology 2013; 505: 1-12.

Xu Y, Huang G, Fan Y. Multivariate flood risk analysis for Wei River. Stochastic Environmental Research and Risk Assessment 2015: 1-18.

Yan J. Studies on flood mangement of Wei River Basin, Shaanxi Provice (in Chinese). Shaanxi Shui Li 2008; 3: 17-18.

Yan M-J, He Q-Y, Yamanaka N, Du S. Location, geology and landforms of the Loess Plateau. In: Tsunekawa A, Liu G, Yamanaka N, Du S, editors. Restoration and development of the degraded Loess Plateau, China. Springer Japan, Tokyo, 2014, pp. 3-21.

Yang J, Strokal M, Kroeze C, Wang M, Wang J, Wu Y, Bai Z, Ma L. Nutrient losses to surface waters in Hai He basin: A case study of Guanting reservoir and Baiyangdian lake. Agricultural Water Management 2019; 213: 62-75.

Yang Q, Tian H, Friedrichs MAM, Liu M, Li X, Yang J. Hydrological responses to climate and land-use changes along the north american east coast: A 110-Year historical reconstruction. Journal of the American Water Resources Association 2015a; 51: 47-67.

Yang T, Xu CY, Chen X, Singh VP, Shao QX, Hao ZC, Tao X. Assessing the impact of human activities on hydrological and sediment changes (1953–2000) in nine major catchments of the Loess Plateau, China. River Research and Applications 2010; 26: 322-340.

Yang W, Zhang L, Shan L, Chen X, Chen S. Response of extreme hydrological events to climate change in the water source area for the middle toute of South-to-North sater diversion project. Advances in Meteorology 2016; 2016: 15.

Yang X, Wang F, Bento CPM, Meng L, van Dam R, Mol H, Liu G, Ritsema CJ, Geissen V. Decay characteristics and erosion-related transport of glyphosate in Chinese loess soil under field conditions. Science of The Total Environment 2015b; 530-531: 87-95.

Ye X, Zhang Q, Liu J, Li X, Xu C. Distinguishing the relative impacts of climate change and human activities on variation of streamflow in the Poyang Lake catchment, China. Journal of Hydrology 2013; 494: 83-95.

Yihdego Y, Webb J. An empirical water budget model as a tool to identify the impact of land-use change in stream flow in Southeastern Australia. Water Resources Management 2013; 27: 4941-4958.

Yin L, P. Xiao, J. Zhao, X. Zhang. Study on flood change of Weihe River over the past 70 years (in Chinese). Journal of Anhui Agri. Sci. 2010; 38: 11995-11997.

Yin S, Huang C, Zha X. On extreme flood disasters and global climate change: A case study of floodings of Hanjing River and Weihe River. 2012; 21: 41-48.

Yira Y, Diekkrüger B, Steup G, Bossa AY. Modeling land use change impacts on water resources in a tropical West African catchment (Dano, Burkina Faso). Journal of Hydrology 2016; 537: 187-199.

Yira Y, Diekkrüger B, Steup G, Bossa AY. Impact of climate change on hydrological conditions in a tropical West African catchment using an ensemble of climate simulations. Hydrology and Earth System Sciences 2017; 21: 2143-2161.

Yue S. A bivariate gamma distribution for use in multivariate flood frequency analysis. Hydrological Processes 2001; 15: 1033-1045.

Zajac Z, Revilla-Romero B, Salamon P, Burek P, Hirpa FA, Beck H. The impact of lake and reservoir parameterization on global streamflow simulation. Journal of Hydrology 2017; 548: 552-568.

Zeng Q, Chen H, Xu C-Y, Jie M-X, Chen J, Guo S-L, Liu J. The effect of rain gauge density and distribution on runoff simulation using a lumped hydrological modelling approach. Journal of Hydrology 2018; 563: 106-122.

Zeng Y, Chong KY, Grey EK, Lodge DM, Yeo DCJ. Disregarding human pre-introduction selection can confound invasive crayfish risk assessments. Biological Invasions 2015.

Zha X, Huang C, Pang J. Holocene extreme floods and environmental change of Qishuihe River in Western Guanzhong Basin (in Chinese). Acta Geographica Sinica 2007; 62: 291-300.

Zha X, Huang C, Pang J. Palaeofloods recorded by slackwater deposits on the Qishuihe River in the Middle Yellow River. Journal of Geographical Sciences 2009; 19: 681.

Zhang B, Wu P, Zhao X, Gao X, Shi Y. Assessing the spatial and temporal variation of the rainwater harvesting potential (1971-2010) on the Chinese Loess Plateau using the VIC model. Hydrological Processes 2014; 28: 534-544.

Zhang L, Geng J, Fan C. The Comprehensive analysis of flood disasters losses in China from 2000 to 2010. IOP Conference Series: Materials Science and Engineering 2018a; 466: 012023.

Zhang L, Nan Z, Yu W, Ge Y. Hydrological responses to land-use change scenarios under constant and changed climatic conditions. Environmental Management 2016a; 57: 412-431.

Zhang L, Singh VP. Bivariate flood frequency analysis using the copula method. Journal of Hydrologic Engineering 2006; 11: 150-164.

Zhang M, Wei X, Sun P, Liu S. The effect of forest harvesting and climatic variability on runoff in a large watershed: The case study in the Upper Minjiang River of Yangtze River basin. Journal of Hydrology 2012; 464–465: 1-11.

Zhang Q, Li J, Singh VP, Xu C-Y. Copula-based spatio-temporal patterns of precipitation extremes in China. International Journal of Climatology 2013; 33: 1140-1152.

Zhang Q, Sun P, Jiang T, Tu X, Chen X. Spatio-temporal patterns of hydrological processes and their responses to human activities in the Poyang Lake basin, China. Hydrological Sciences Journal 2011; 56: 305-318.

Zhang W, Lou Y, Huang J, Zheng F, Cao Y, Liang H, Shi C, Liu J. Multiscale variations of precipitable water over China based on 1999–2015 ground-based GPS observations and evaluations of reanalysis products. Journal of Climate 2018b; 31: 945-962.

Zhang Y, Feng X, Wang X, Fu B. Characterizing drought in terms of changes in the precipitation–runoff relationship: a case study of the Loess Plateau, China. Hydrol. Earth Syst. Sci. 2018c; 22: 1749-1766.

Zhang Y, Xu Y, Dong W, Cao L, Sparrow MCL. A future climate scenario of regional changes in extreme climate events over China using the PRECIS climate model. Geophysical Research Letters 2006; 33: L24702.

Zhang Y, Zhao Y, Wang Q, Wang J, Li H, Zhai J, Zhu Y, Li J. Impact of land use on frequency of floods in Yongding River Basin, China. Water 2016b; 8: 401.

Zhao G, Mu X, Tian P, Wang F, Gao P. Climate changes and their impacts on water resources in semiarid regions: a case study of the Wei River basin, China. Hydrological Processes 2013; 27: 3852-3863.

Zhao G, Tian P, Mu X, Jiao J, Wang F, Gao P. Quantifying the impact of climate variability and human activities on streamflow in the middle reaches of the Yellow River basin, China. Journal of Hydrology 2014; 519: 387-398.

Zhao J, Huang Q, Chang J, Liu D, Huang S, Shi X. Analysis of temporal and spatial trends of hydro-climatic variables in the Wei River Basin. Environmental Research 2015; 139: 55-64.

Zhao J, Long T, Chen Y. Scale and temporal properties of flood sequence of Guanzhong reach of Weihe River during the last 400 years (in Chinese). Bulletin of Soil and Water Conservation 2010; 30: 5-8.

Zhao S, He W, Jiang Y. Evaluation of NCEP‐2 and CFSR reanalysis seasonal temperature data in China using detrended fluctuation analysis. International Journal of Climatology 2018; 38: 252-263.

Zheng K, Wei J-Z, Pei J-Y, Cheng H, Zhang X-L, Huang F-Q, Li F-M, Ye J-S. Impacts of climate change and human activities on grassland vegetation variation in the Chinese Loess Plateau. Science of The Total Environment 2019; 660: 236-244.

Zheng S, Wu B, Thorne CR, Tan G. Case study of variation of sedimentation in the Yellow and Wei Rivers. Journal of Hydraulic Engineering 2015; 141: 05014009.

Zeng Z, Piao S, Lin X, Yin G, Peng S, Ciais P, Myneni RB. Global evapotranspiration over the past three decades: estimation based on the water balance equation combined with empirical models. Environmental Research Letters 2012; 7: 014026.

Zhou B, Wen QH, Xu Y, Song L, Zhang X. Projected changes in temperature and precipitation extremes in China by the CMIP5 multimodel ensembles. Journal of Climate 2014a; 27: 6591-6611.

Zhou W, Tang J, Wang X, Wang S, Niu X, Wang Y. Evaluation of regional climate simulations over the CORDEX-EA-II domain using the COSMO-CLM model. Asia-Pacific Journal of Atmospheric Sciences 2016; 52: 107-127.

Zhou Y, Guo S, Liu P, Xu C. Joint operation and dynamic control of flood limiting water levels for mixed cascade reservoir systems. Journal of Hydrology 2014b; 519, Part A: 248-257.

Zhu YP, Zhang HP, Chen L, Zhao JF. Influence of the South–North Water Diversion Project and the mitigation projects on the water quality of Han River. Science of The Total Environment 2008; 406: 57-68.

Zhuang W. Eco-environmental impact of inter-basin water transfer projects: a review. Environmental Science and Pollution Research 2016; 23: 12867-12879.

Zou L, Zhou T. Near future (2016-40) summer precipitation changes over China as projected by a regional climate model (RCM) under the RCP8.5 emissions scenario: Comparison between RCM downscaling and the driving GCM. Advances in Atmospheric Sciences 2013; 30: 806-818.

Zuo D, Xu Z, Peng D, Song J, Cheng L, Wei S, Abbaspour KC, Yang H. Simulating spatiotemporal variability of blue and green water resources availability with uncertainty analysis. Hydrological Processes 2015a; 29: 1942-1955.

Zuo D, Xu Z, Yao W, Jin S, Xiao P, Ran D. Assessing the effects of changes in land use and climate on runoff and sediment yields from a watershed in the Loess Plateau of China. Science of The Total Environment 2016; 544: 238-250.

Zuo D, Xu Z, Zhao J, Abbaspour KC, Yang H. Response of runoff to climate change in the Wei River basin, China. Hydrological Sciences Journal 2015b; 60: 508-522.

English summary

Floods are considered to be one of the most destructive natural hazards on Earth. Apart from precipitation as the main driving factor for flood occurrence, there is increased recognition that human activities also largely influence the occurrence and impacts of floods. The Wei River Basin in China has suffered from floods for decades due to its monsoon climate with intensive summer rainfall. With the rapid development of the economy and population growth, land use and the water cycle have been altered due to the demands for resources redistribution. Consequently, the Wei River Basis is under pressure from both climate and anthropogenic changes. This thesis aims to bring a comprehensive understanding of the factors causing flood occurrence in the basin and propose an integrated management tool for flood analysis under the complex environment in the Wei River Basin.

Chapter 1 describes the general factors and processes leading to flood occurrence with respect to meteorological, biophysical and anthropogenic aspects. Chapter 2 starts with the introduction of a framework approach for understanding these factors and their importance regarding contribution to flood occurrence in the Wei River Basin, and then presents the results of our application of this approach. The framework approach uses a set of methods to answer the questions why, where, when, and how flooding occurs and includes Conditional Inference Tree (CIT), cross correlation and double mass curves analyses. The results revealed that the dam construction period was the most important factor (why), and the Western upstream regions of the Wei River contributed the most to the flooding of the downstream floodplain (where). The effect of the periods of dam construction on the time lag change (when) and the precipitation-discharge relationship (how) were also analysed by the cross-correlation analysis and double mass curves analysis, respectively. Being able to bring both numeric and non-numeric factors into the analyses, the CIT analysis proved to be a powerful tool for unravelling complex causes leading to flood occurrence. The insights gained in this chapter can be further applied to understanding of flooding schemes in other regions and to derive targeted flood mitigation measures in the Wei River Basin.

LISFLOOD modelling was then calibrated and validated, the results of which are presented in Chapter 3. The urgent need for the development of an integrated approach to evaluating the impacts of climate change, land use change and river alteration as well on the occurrence of hydrological extreme events drove us to choose a physically-based distributed hydrological model as a solid base for accurate discharge simulation. Using globally available land cover, soil, vegetation as well as geographical datasets, combined

with local observed meteorological gauging data as input, the application of the LISFLOOD model performed well in simulating the discharge at the outlet station on the floodplain. Being a distributed model, LISFLOOD enabled prediction of discharge at the outlets of 17 tributaries draining into the main river. The simulated discharge from these outlets were analysed regarding their contribution to the total runoff as well as for individual flood events. This study is the first application of the LISFLOOD model for a semi-arid region in China for flood discharge analysis, and has shown to be a sophisticated and reliable tool for catchment scale land and water management planning related to flood occurrence and dynamics.

Chapter 4 reports on the evaluation of the usability of various freely available datasets for discharge simulation with LISFLOOD. The quality of the meteorological data inputs into the hydrological model is of vital importance for understanding the hydrological regime as well as for analysis and prediction of hydrological extremes. Many efforts have been made to develop globally freely available meteorological reanalyses data especially for data scarce regions. We evaluated ten globally freely available datasets for discharge simulation by using them as input for the LISFLOOD model and comparing results between and with observed meteorological data and discharge in Chapter 3. The result was rather disappointing and suggested that none of the evaluated datasets can be applied directly for daily discharge simulation by the LISFLOOD model. This is unfortunate as accurate simulation of discharge is essential for flood analysis under climate change circumstances. An in-depth analysis of the performance of precipitation and temperature data against the observations was then conducted in an attempt to improve the simulation of the datasets.

In Chapter 4, we decided to study the impact of anthropogenic changes in the basin on flood peak discharge. This part of the thesis is presented in Chapter 5. It is increasingly recognized that the effects of flood events are greatly influenced by the changes that humans have imposed on the environment and river systems. In the Wei River Basin of China there have been tremendous changes including land use and soil and water alterations under the pressure of population growth and water resource scarcity. To investigate the potential of LISFLOOD for assessing the effects of anthropogenic activities on base flow and peak flow, three categories of scenarios regarding human intervention in the basin were evaluated against a business as usual scenario using the simulated discharge from the LISFLOOD model: 1) natural conditions of the basin, 2) additional reservoirs constructed in different sub-catchments, and 3) water transfer from an adjacent catchment via a pipeline providing a fixed daily inflow. The results of the scenarios are presented for three strategically important cities located on the floodplain. Compared to the business as usual case, the minimum base flow at the three cities increased 54 fold on average with additional dam/reservoir construction, and 41 fold with the pipeline scenario, while with the 1980 land use scenario minimum base flow decreased by 0.8 times. Regarding peak flows, additional reservoirs could reduce them and the water transfer plan would not increase them. The results for the scenarios with the application of the LISFLOOD model cross validated the feasibility of using a modelling approach for catchment flood discharge management as well as providing insight for future policymaking processes.

Last but not the least, Chapter 6 concludes the whole thesis with discussion of the findings from different perspectives as well as provision of outlooks and recommendations regarding the application of hydrological modelling for evaluation of scenarios for regional flood mitigations and related societal impacts. This thesis has increased knowledge and furthered the science regarding flood analysis in the Wei River Basin and how to address the increasing pressure from both climate and anthropogenic changes.

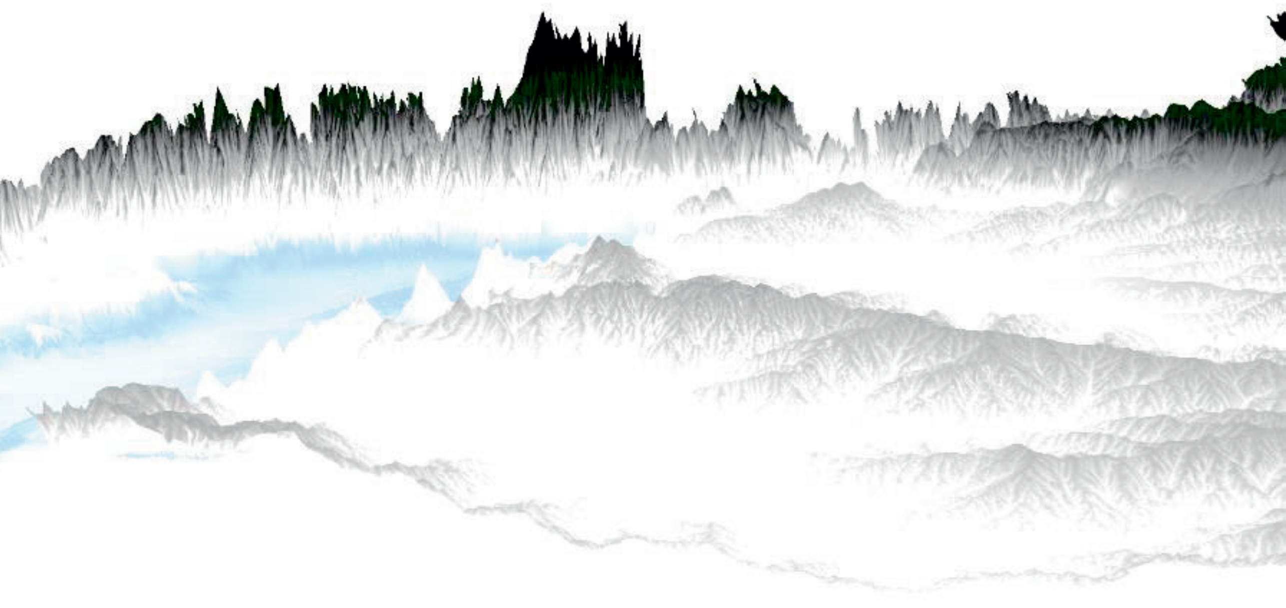

Nederlandse samenvatting

Overstromingen worden gezien als een van de meest verwoestende natuurrampen op aarde. Naast neerslag, dat wordt beschouwd als de belangrijkste factor voor het ontstaan van overstromingen, is er het groeiende besef dat ook menselijke activiteiten een grote invloed hebben op het tot stand komen overstromingen en de impact ervan. Het Wei-stroomgebied in China heeft al tientallen jaren last van overstromingen als gevolg van het moessonklimaat met zijn intensieve regenval gedurende de zomer. Door de snelle ontwikkeling van de economie en de bevolkingsgroei zijn het landgebruik en de kringloop van water veranderd, omdat een herverdeling van middelen noodzakelijk was. Hierdoor staat dit stroomgebied onder grote druk van veranderende klimatologische en antropogene factoren. Dit proefschrift heeft tot doel een beter begrip te krijgen van de factoren die de overstromingen in dit complexe stroomgebied veroorzaken, alsmede een geïntegreerd managementinstrumentarium te introduceren voor het analyseren van overstromingen in het complexe stroomgebied van de Wei.

Hoofdstuk 1 beschrijft de algemene factoren en processen welke leiden tot overstromingen in relatie tot meteorologische, biofysische en antropogene aspecten. Hoofdstuk 2 begint met een plan van aanpak om deze factoren te kunnen begrijpen en wat zij bijdragen in het ontstaan van overstromingen in het stroomgebied van de rivier Wei. Vervolgens worden de resultaten gepresenteerd van deze aanpak. Het plan van aanpak maakt gebruik van een reeks methoden om vragen te kunnen beantwoorden zoals waarom, waar, wanneer en hoe overstromingen ontstaan. De gebruikte methoden zijn onder andere CIT , kruiscorrelatie -, en dubbele massacurves analyses. De resultaten toonden aan dat de tijd die nodig was voor het bouwen van de dam de belangrijkste factor was (waarom) en dat de westelijke stroomopwaarts gelegen regio's van de Wei-rivier het meeste bijdroegen aan de overstroming van de stroomafwaartse uiterwaarden (waar). Het effect van de periodes van damconstructie op veranderingen in het tijdsverloop (wanneer) en het verband tussen neerslag en afvoer (hoe) werden ook geanalyseerd met behulp van kruiscorrelatie en dubbele massa curves. Omdat het mogelijk was om zowel numerieke als niet-numerieke factoren in de analyses te betrekken, bleek de CIT-analyse een krachtig hulpmiddel te zijn voor het ontrafelen van de complexe oorzaken die tot overstroming leidden. De resultaten van dit hoofdstuk kunnen worden toegepast in andere regio’s om hiermee overstromingsgebeurtenissen te begrijpen. Ook kunnen er gerichte maatregelen in het Wei-stroomgebied mee worden afgeleid.

Vervolgens is het LISFLOOD model gekalibreerd en gevalideerd. De resultaten hiervan worden gepresenteerd in Hoofdstuk 3. Er is voor een fysisch en gedistribueerd hydrologisch model gekozen omdat dit een solide basis is voor nauwkeurige afvoersimulaties. Op deze manier kunnen de effecten van klimaatverandering, veranderend landgebruik en wijzigingen van rivierlopen, alsmede het ontstaan van hydrologisch extreme gebeurtenissen worden gesimuleerd. Door gebruik te maken van wereldwijd beschikbare datasets met betrekking tot bodembedekking, bodem, vegetatie en geografie en deze vervolgens te combineren met lokaal waargenomen meteorologische meetgegevens zijn complete invoersets voor LISFLOOD ontstaan. Door het gebruik van deze invoersets werden goede resultaten verkregen bij het simuleren van de afvoer voor het uitlaatstation op de uiterwaarde. Omdat LISFLOOD een gedistribueerd model is konden de afvoeren van de uitlaten van 17 zijrivieren naar de hoofdrivier worden voorspeld. De gesimuleerde afvoeren van deze uitlaat stations werden geanalyseerd met betrekking tot hun bijdrage aan de totale afvoer en hun bijdrage aan de individuele overstromingen. Deze studie is de eerste toepassing van het LISFLOOD-model voor een semi-aride gebied in China. Het is een verfijnd en betrouwbaar hulpmiddel gebleken dat zeer geschikt is voor de planning van maatregelen ten behoeve van waterbeheer in stroomgebieden in relatie tot het ontstaan van overstromingen en de dynamiek ervan.

In Hoofdstuk 4 wordt de bruikbaarheid van verschillende vrij beschikbare datasets voor afvoersimulatie met LISFLOOD geëvalueerd. De kwaliteit van de meteorologische gegevens voor het hydrologische model is van vitaal belang voor het begrijpen van het hydrologische regime en voor de analyse en voorspelling van hydrologische uitersten. Er is veel moeite gedaan om wereldwijd vrij beschikbare meteorologische ge-reanalyseerde gegevens te ontwikkelen, met name voor die regio’s waar weinig data beschikbaar is. We hebben tien wereldwijd vrij beschikbare datasets voor afvoersimulatie geëvalueerd door ze als input voor het LISFLOOD-model te gebruiken en de resultaten van de afvoer zijn zowel onderling als met de waargenomen meteorologische gegevens en afvoeren uit Hoofdstuk 3 vergeleken. Het resultaat was nogal teleurstellend en liet zien dat geen van de geëvalueerde datasets direct kan worden toegepast voor de dagelijkse afvoer-simulatie met het LISFLOOD-model. Dit is jammer omdat nauwkeurige simulatie van afvoer essentieel is voor de analyse van overstromingen onder klimaatverandering. Een grondige analyse van neerslag- en temperatuurgegevens ten opzichte van de waargenomen metingen werd vervolgens uitgevoerd in een poging de simulaties met de gegevens te verbeteren.

In hoofdstuk 5 hebben we de invloed van antropogene veranderingen in het stroomgebied op de piekafvoeren bestudeerd. Men wordt zich er steeds meer van bewust dat de effecten van overstromingen sterk worden beïnvloed door de veranderingen die mensen hebben aangebracht in het milieu en riviersystemen. In China zijn in het stroomgebied van de Wei rivier, door bevolkingsgroei en schaarste van watervoorraden, enorme veranderingen ontstaan in landgebruik en ook in bodem- en watersystemen. Om de potentiele toepassingen van LISFLOOD te onderzoeken wat betreft het effect van antropogene activiteiten op de basis- en piekafvoer, werden drie categorieën van scenario's geëvalueerd en vergeleken met een scenario van 'business as usual'. Deze drie scenario’s zijn: 1) natuurlijke omstandigheden van het bassin, 2) bouwen van extra reservoirs in verschillende deelstroomgebieden en 3) water transporteren via een pijpleiding vanaf een aangrenzend stroomgebied waardoor een vaste dagelijkse instroom mogelijk wordt gemaakt. De resultaten van deze scenario's worden gepresenteerd voor drie strategisch belangrijke steden in de uiterwaarden. In vergelijking met de ‘business as usual’ situatie, was de minimale basisafvoer in de drie steden gemiddeld 54 keer zo groot bij extra dam/reservoir constructies en 41 keer bij het pijpleiding scenario, terwijl met het scenario met landgebruik in 1980 de minimale basisstroom met een factor 0,8 afnam. Extra reservoirs zullen de piekafvoeren verlagen en het water transportplan zal deze niet laten toenemen. De scenario-analyses met behulp van het LISFLOOD model, laten zien dat deze aanpak geschikt is voor het beheersen van stroomgebiedsafvoeren, alsmede het verschaffen van inzichten voor beleidsvormingsprocessen.

Tot slot worden de bevindingen in hoofdstuk 6 samengevat en vanuit verschillende gezichtspunten bediscussieerd. Bovendien wordt er een visie uiteengezet en worden aanbevelingen gedaan voor de toepasbasbaarheid van hydrologische modellen om hiermee scenario's voor het tegengaan van regionale overstromingen te kunnen doorrekenen en de gerelateerde maatschappelijke effecten te kunnen inschatten. Dit proefschrift heeft de kennis en wetenschap vergroot aangaande de analyse van overstromingen in het stroomgebied van de Wei en hoe de toenemende druk van zowel klimaat als antropogene veranderingen aangepakt kunnen worden.

Acknowledgement

My name is the only one that appears on the cover of this thesis, but the work behind this book consists of the efforts and support of many others, one way or another. I would like to take this opportunity to express my appreciations to those who are behind the scene. To be consistent with my reflection on this journey from the beginning to the end, the people acknowledged here are presented mainly in chronological order.

If it were not the "Three Kingdom" game night organized by Hui Zhang and Shiyang Wang, I would not have got to know Dr. Peng Gao. I appreciate that Peng guided me into contact with the SLM group and this PhD position. His open mind and curiosity towards new knowledge were the first lessons I learned. My gratitude then goes to Dr. Fei Wang for his recognition of my ability for starting this PhD research and all the support along the journey, especially with my data acquisition and field works in China. As the project leader of the Chinese part of the China-Netherlands Joint Scientific Thematic Research Programme, Dr. Fei Wang has impressed me with his hard works, dedications and his passion to know the unknowns.

Next, I would like to thank my promotors Prof. Dr. Coen Ritsema and Prof. Dr. Violette Geissen for their guidance throughout the whole journey. From giving me the opportunity to start this PhD, to widening my eyes within but not limited to my own research field, all the way to lead me to be a good researcher and a good person, your view and attitude had a great influence on me. Coen, your wisdom of seeing both the very detail and the big picture, your passion on both professional and personal life, your view into both local and international issues have inspired me and will benefit me my whole life. Violette, thank you for being such a good friend above being my promotor, in those moments when I felt utterly helpless, when I felt proud of succeeding in running the model, when I felt lost in my path, and when I had my happy moment in private life, you are the one that was always there emotionally supporting me. Your sparkles of ideas are like the non-stop fireworks, lighting up the sky of science and people around you in the dark nights. Please keep doing so, so that science will advance, in your and our wished way.

My gratitude also goes to Prof. Dr. Ad de Roo and Dr. Peter Burek and the whole team of the Joint Research Centre of the European Commission in Ispra for my LISFLOOD model capacity building. They led me into the modelling world, which I still love and would like to make a career out of it. Their vision on modelling the world floods and their patience have always been the shining light guided me through those dark nights of modelling.

I am also grateful to the many teachers and friends at the Institute of Soil and Water Conservation, China. I would like to thank Prof. Dr. Rui Li, Director Prof. Dr. Guobin liu and Prof. Dr. Xingmin Mu for their support and supervision during my stay in the institute. Also those students who shared the office with me: Jiao Qiao, Zhang Wenshuai, Jin Kai, Xia Lei, He Yi, Chen Lili, Zhang Tingting, An Chunchun, Yu yipeng, Murati, Guo Minjie, Zheng Ying and Song Guang, I will not forget all those study, seminars, badminton, KTV, movie and game times we enjoyed together.

My sincere gratitude goes next to Dr. Ir. Jantiene Baartman. As my daily supervisor appointed with the special request for helping me with the modelling, Jantiene has supervised me way more than she was appointed for. I do remember those times that I could knock on your door three times a day, and send you my abstract to be submitted the next day and you still commented with the short notice. You were always there, besides the fact that you also had two little daughters, many other PhD students, many projects and education duties. You are the superwomen that I always referred to. Along the journey, your being humble, kind and considerate made me feel you are more like a bigger sister rather than a supervisor.

Apart from all the research conducted in the office, another essential part of this journey are the activities I have done outside the office, which has given me other competences I will benefit the rest of my life. Firstly, I would like to thank Counsellor Qingyu Meng and Senior Secretary Lei Xia and Yiwei Wang from the Embassy of the People's Republic of China in the Netherlands, for giving the opportunity to work in the Association of Chinese Students and Scholars in the Netherlands to connect to many people and organizations. Their care for my study and life has made me felt at home. I would like to thank my colleagues in the association: Jiakun, Wei, Fuyu, Yawen, Jiao, Huatang, Anran, Ding, Guannan, we have grown together working in the same team. Thank you all for your support and comprehension, I appreciate the times that we worked and grew together.

My great thank also goes to Liesbeth van der Linden and Astrid van den Heuvel for leading me into the international environment in Wageningen. Being in the organizing committee of the One World Week of Wageningen for four consecutive years, I got to know the vision of internationalization of Wageningen and I was honored to be working on it. The passion, warmth, open mind and caring from the both of you have made me a more open and expressive person.

Meanwhile, my research got stuck with model calibration. This is the moment when Dr. João Nunes was involved in my supervision team. Although everything started with the “Game of Throne”game, João appeared like a saviour for me. His abundant knowledge on

my study area, hydrological modelling and future research directions have made my work of the last three chapters very smooth and enjoyable. His humorous way of talking, his addiction to games and his love for Chinese food have made us good friends for life. Regarding the model calibation, I woud also like to thank Dr. Hylke Beck for his patient assistant on the calibration scripts and modelling. m

In addition to the above-mentioned names, hereafter comes the special parts that chronological order is not applicable because they are the ones that are always there! First, I would like to thank all the staff and students from the SLM group for all the nice moments we shared together and all your help and support. Thank you, Marnella and Rianne for your patience on my endless requests for the small details, and also to cheer up the group with warm smiling and greetings. You are wonderful secretaries. Thank you Demie for your advice, and help, for the “samendenken” and many tips that you shared with us. I am also grateful to Annelies, Esther, Anita, Geurt and Siawash for your fantastic administration and financial support. Thank you Klaas for your amazing work on revising my reading version of the thesis several times and your amazing graphs, you are the master of art in the group.

My special thanks go to my fellow PhDs in the SLM group known as the “Atlas Gang” although we are not in Atlas anymore. I have developed a lifelong friendship with many of you, on top of that, the international environment has broadened my eyes both professionally and personally. Thank you Kaveh, Mohamed and Celia for making my entrepreneurial dream come true. Thank you Celia for always being there listening to me, for your advice and your wisdom of life, of course many thanks to Bruno too. Thank you Xiaomei for all the support with everything and trust these years. Thank you Vera, João, Ricardo and Nicolas for those endless game days. Our Pokemon team, leader Pavon, Pop and Yueling managed to remain good health while doing PhD. My awesome officemates Vera, Kaveh, Karrar, Xiaomei, Pavon, Pop, Severin, Berhane, Raoul for all the happy and snacky moments. The “Game of Throne” team Vera, Pop, Ricardo, Suhad, João and Jiaoyang has accompanied me for three years. After we moved to Gaia, the Ping Pang group: Vera, Pop, Pavon, Nikola, Darrell, Mirzokhid, Meng, Hao, Meidert, Michel, Carlos have brought a lot of happiness and laughter in the building. The Chinese gang within the gang has seen many people come and go, Hongming, Jinghui, Liangxin, Sha, Miao, Hui, Yu, Jianhong, Meng, Yueling, Yan, Shaoliang, Qian, Jinfeng, Haimei, Jiaoyang, Lihua, Peipei, thank you all for all the happy moments we shared, hotpot, Chinese new year, barbecue, excursion, food hunting, movie night, make up workshops, etc. My sincere thanks go to the lunch group, besides all the names mentioned above, Fabio, Sija, Corjan, Karrar, Rens, Coleen, Marina, Ammar, Diana, Nádia, Renée, Amalia, Tesfaye, Mahrooz, Murilo, Angelica, Marcos, André, Meskerem, Mousumi, Mulatie, Walle and many others are all my teachers in a certain way.

I enjoyed the all the conversations and discussions we had. My knowledge and view of the world came from all of you.

Another special group I would like to thank is the CASSW, which has accompanied me since the beginning. Besides the skills and competencies I have gained, the friendships I gained and the many activities we organized together are of great importance and unforgettable to me: Jing Zhang, Shiyang, Hui, Ronghao, Yuan, Zijing, Tong Zhang, Tingyu, Ziying, Xiaoxiao, Ning, Qizhi, Quanxing, Xu, Yiyun, Zekun, Haoran and many others. And the friends I got to know more or less related to CASSW that gave me support and shared previous moments together: Thank you Zeren and Ron for the wonderful wine tastings and all the dinners together, Yixin and Emily for keeping our dreams in mind and still pursuing it, Na, Jingran, Jing Xiao for sharing with me many details of life, Dandan and Momo for the nice talks and sparkles of ideas, Tianji, Shuwen, Igor for being there and your flexibility to meet up, Lu, Quanxing and Dingming for your wonderful skills of painting, designing and photography that have made my life colourful and joyful.

The friends that are there all along: Christine, Simona, Boudewijn, Danny, Yorick, Sarahi, Victoria, Nyamwaya. Thank you all for your lovely accompanies, the deepest talks and the craziest adventures!

Last but not least, I would like to thank my husband Jan and my family. First, I would like to thank my parents for everything they gave me, which includes but not limited to the support when I decided to go after my dreams, the comfort when I was depressed or frustrated, the personality that could handle all the difficulties and a healthy body that is able to explore the world. I would also like to thank my husband Jan for supporting me in every way. I used the time when you were away to keep learning and working, I used the time when you were around to enjoy life, you have unfolded the world in front of me to explore and made me become the person I wanted to be. I am also grateful that you bring your family to me. Many thanks to the family of my husband, for all those family days, wonderful dinners, relaxing weekends and celebrations, thank you all for taking me into the family and giving me all the warmth as a home far away from home.

Many thanks to all of you!

Lingtong Gai

About the author

Lingtong Gai was born on 14th June, 1988 in Renqiu Hebei, China. After obtained the Bachelor of Engineering Degree in Environmental Engineering and Bachelor of Art Degree in English Libterature in Wuhan University of Science and Techonologty in 2010, the author started the MSc programme in Climate Studies in Wageningen University granted by the WU Fellowship. In Octorber 2012, Lingtong Gai joined the Soil Physics and Land Management Group of Wageningen University to start her PhD study under the project "Development of strategies to improve hydrological and environmental conditions in Wei River catchment, China", which was funded by China-Netherlands Joint Scientific Thematic Research Programme (JTSP) supported by the External Cooperation Program of the Chinese Academy of Sciences and Netherlands Organization for Scientific Research.

Contact: gailingtong@gmail.com

List of publications:

Gai L., Nunes J.P., Baartman J.E.M., Zhang H., Wang F., de Roo A., Ritsema C.J., Geissen V., (2019) Assessing the impact of human interventions on floods and low flows in the Wei River Basin in China using the LISFLOOD model, Science of The Total Environment, 653, pp. 1077-1094.

Gai L., Baartman J.E.M., Mendoza-Carranza M.,Wang F., Ritsema C.J., Geissen V., (2018) A framework approach for unravelling the impact of multiple factors influencing flooding, Journal of Flood Risk Management, 11(2), pp:112-126.

Zhang H., Wei J., Yang Q., Baartman J.E.M., **Gai L.**, Yang X., Li S., Yu J., Ritsema C.J., Geissen V., (2017) An improved method for calculating slope length (λ) and the LS parameters of the Revised Universal Soil Loss Equation for large watersheds, Geoderma, 308, pp. 36-45.

Fan L., **Gai L.**, Tong Y., Li R., (2017) Urban water consumption and its influencing factors in China: Evidence from 286 cities, Journal of Cleaner Production, 166, pp. 124-133.

Zhang H., Yao Z., Yang Q., Li S., Baartman J.E.M., **Gai L.**, Yao M., Yang X., Ritsema C.J., Geissen V., (2017) An integrated algorithm to evaluate flow direction and flow accumulation in flat regions of hydrologically corrected DEMs, Catena, 151, pp:174-181.

Xue S., Yang X., Liu G., **Gai L.**, Zhang C., Ritsema C.J., Geissen V., (2017) Effects of elevated CO2 and drought on the microbial biomass and enzymatic activities in the rhizospheres of two grass species in Chinese loess soil, Geoderma, 286, pp. 25-34.

Yang X., Van der Zee S.E.A.T.M., **Gai L.**, Wesseling J.G., Ritsema C.J., Geissen V., (2016) Integration of transport concepts for risk assessment of pesticide erosion, Science of the Total environment, 551-552, pp. 563-570.

Yang X., Wang F., Bento C.P.M., Xue S., **Gai L.**, van Dam R., Mol H., Ritsema C.J., Geissen V., (2015) Short-term transport of glyphosate with erosion in Chinese loess soil - A flume experiment, Science of the Total environment, 512-513, pp. 406-414.

Co-author affiliations

J.E.M. Baartman	Soil Physics and Land Management Group, Wageningen University, Wageningen, The Netherlands
V. Geissen	Soil Physics and Land Management Group, Wageningen University, Wageningen, The Netherlands
M. Mendoza-Carranza	El Colegio de la Frontera Sur, ECOSUR Unidad Villahermosa, Villahermosa, Mexico
João P. Nunes	CE3C – Centro de Ecologia, Evolução e Alterações Climáticas, Faculdade de Ciências, Universidade de Lisboa, Portugal
C.J. Ritsema	Soil Physics and Land Management Group, Wageningen University, Wageningen, The Netherlands
Ad de Roo	JRC, European Commission, Joint Research Centre, Via Enrico Fermi, Ispra, Italy.
F. Wang	- Institute of Soil and Water Conservation, Chinese Academy of Science and Ministry of Water Resources, Yangling, China - Institute of Soil and Water Conservation, Northwest A&F University, Yangling, China
Hongming Zhang	- Institute of Soil and Water Conservation, Chinese Academy of Science and Ministry of Water Resources, Yangling, China - Institute of Soil and Water Conservation, Northwest A&F University, Yangling, China

Netherlands Research School for the
Socio-Economic and Natural Sciences of the Environment

D I P L O M A

For specialised PhD training

The Netherlands Research School for the
Socio-Economic and Natural Sciences of the Environment
(SENSE) declares that

Lingtong Gai

born on 14 June 1988 in Hebei, China

has successfully fulfilled all requirements of the
Educational Programme of SENSE.

Wageningen, 3 July 2019

The Chairman of the SENSE board

Prof. dr. Martin Wassen

the SENSE Director of Education

Dr. Ad van Dommelen

The SENSE Research School has been accredited by the Royal Netherlands Academy of Arts and Sciences (KNAW)

K O N I N K L I J K E N E D E R L A N D S E
A K A D E M I E V A N W E T E N S C H A P P E N

The SENSE Research School declares that Lingtong Gai has successfully fulfilled all requirements of the Educational PhD Programme of SENSE with a work load of 39.1 EC, including the following activities:

SENSE PhD Courses

- Environmental research in context (2013)
- Workshop Analysing geomorphic coupling and sediment connectivity using digital elevation models (2013)
- Human induced soil degradation (2013)
- Introduction to R (2013)
- Geostatistics (2013)
- Research in context activity: 'Co-organizing SENSE-WIMEK Symposium on Hazard, Risk and Sustainability in the Soil Environment (Wageningen, 14 October 2015)'
- Grasping Sustainability (2016)
- Model training for scenario analysis: river export of nutrients from land to sea (2018)

External training at a foreign research institute

- LISFLOOD model capacity building, EU-Joint Research Centre, Italy (2012)

Management and Didactic Skills Training

- Wageningen Start-up Week (2016)
- Organizing Committee of One World Week Wageningen (2017)
- Organize EU DiverFarming project meeting in The Netherlands (2018)
- Organisation the Chinese New Year Celebration and Sino-Dutch Talent Forum (2016)
- Guest lecturer in the BSc course 'Adaptation to climate change' (2018)
- Guest lecturer in the MSc course 'Erosion Processes and Modelling' (2019)

Oral Presentations

- *Testing LISFLOOD model as a catchment water resources management tool.* Wageningen PhD Symposium 2018, 17 May 2018, Wageningen, The Netherlands
- *Quantitative flood hazard assessment of the impact of human interventions.* Water Science for Impact, 16-19 October 2018, Wageningen, The Netherlands

SENSE Coordinator PhD Education

Dr. Peter Vermeulen

This research was funded by the China-Netherlands Joint Scientific Thematic Research Programme (JSTP) supported by the External Cooperation Program of the Chinese Academy of Sciences (Grant No. GJHZ1018) and the Netherlands Organization for Scientific Research (NWO, OND1339291).

Cover:
"Digital Elevation Model of the Wei River Basin, China"
Designed by Lingtong Gai

Printed by: DigiForce || ProefschriftMaken

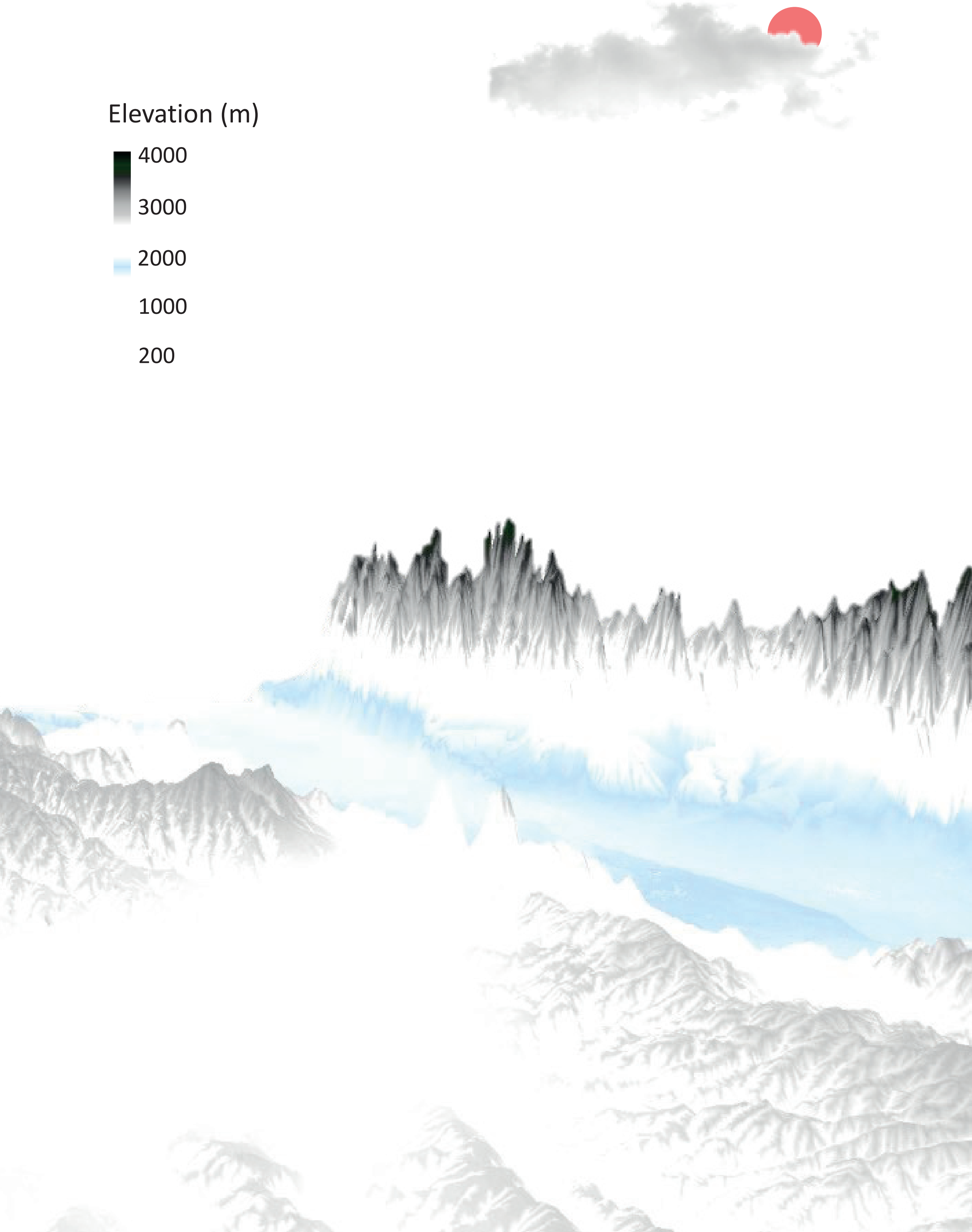
Elevation (m)
4000
3000
2000
1000
200